The Role of Primary Cilia in the Pathogenesis of ADPKD

Philipp Paolo Prosseda

A thesis submitted for the degree of Doctor of Philosophy

August 2016

Supervisors: Prof Albert CM Ong and Dr Andrew Streets
Academic Nephrology Unit
University of Sheffield

ACKNOWLEDGEMENTS

"Variis languoribus et patior mutantur, et nos mutamur in illis"

As the main persons involved in my project, I would like to thank my two supervisors, Professor Albert Ong and Doctor Andrew Streets for their invaluable assistance, encouragement and guidance during the entire course of my PhD. They were the incarnation of what can be defined as hard working scientists and as such, an inspiration on many levels. I thank all members of my family, especially my Parents, who from afar have always given me their unconditional support during the stressful times of my work and life. In addition I would like to thank Kidney Research UK for financial support through a PhD studentship and the Sheffield Area Kidney Association for funding research consumables.

Finally, I would like to express my deepest gratitude to the two most important persons in my life. The constant love and support from my Daughter and from my Wife played a major role in overcoming all the various obstacles during the course of this PhD project. Their firm believe and trust, were more than just a motivational incentive.

Table of contents

Abstract		XI
Abbreviations		XIII
List of figures		XV
Chapter I	**Introduction**	1
1.1	Autosomal Dominant Polycystic Kidney Disease	2
1.2	Genetics of ADPKD	4
1.3	Polycystins	5
	1.3.1 Polycystin-1	6
	1.3.2 Polycystin-1 and cell adhesion	6
	1.3.3 Polycystin-1 Localization and expression	7
	1.3.4 Polycystin-1 and interaction with cellular components	7
	1.3.5 Polycystin-2	8
	1.3.6 Polycystin-2 localization	8
	1.3.7 Polycystin-2 function	9
	1.3.8 The Polycystin-1/Polycystin-2 complex	9
1.4	Primary Cilia	11
1.5	Cell cycle and primary cilium modulation	12
1.6	Molecular control of the cilia development cycle	15
1.7	The role of primary cilia in the pathogenesis of ADPKD	19

Chapter II Materials and Methods 23

2.1 Materials and Reagents 24

2.1.1 Compounds 24

2.1.2 Reagents 25

2.1.3 Cell lines 26

2.1.4 Plasmids 27

2.1.5 1°Antibodies 28

2.1.6 2°Antibodies 28

2.2 Methods 29

2.2.1 Mammalian cell culture 29

2.2.2 Freezing and thawing of cultured cells 29

2.2.3 Specific growth media protocols 30

2.2.4 Primary cilium study 30

2.2.5 Cell fixation and Immunofluorescence 31

2.2.6 Primary cilia treatments 32

2.2.7 Nocodazole resistance assay 32

2.2.8 Measurement of primary cilium number and length 33

2.2.9 Wound healing protocol and cilia orientation measurement 33

2.2.10 Immunohistochemistry 34

2.2.11 Mammalian cell transfection 34

2.4.12 Co-immunoprecipitation 35

2.4.13 GST pull-down assay 36

2.4.14 Protein concentration assay 37

2.4.15 SDS-PAGE 37

2.4.16 Western blot 38

2.4.17 E.coli transformation with plasmid DNA 39

2.4.18 Small-and medium scale purification of plasmid DNA 39

2.4.19 Restriction digestion and agarose electrophoresis 40

2.4.20 Validation of siRNA knockdown by qPCR 41

2.4.21 Special equipment 42

2.4.22 Mycoplasma test 42

2.4.23 Ethic section 42

2.4.24 Statistic section 43

Chapter III Primary cilia formation and regulation in ADPKD 44

3.1 Introduction 45

3.2 Primary cilia formation in baseline models 45

3.3 Primary cilia length regulation 49

3.4 Primary cilia formation in ADPKD models 51

3.5 Primary cilia regulation in ADPKD Models 56

3.6 PKA controls cAMP dependent primary cilia elongation 59

3.7 cAMP treatment induces cilia formation in cycling cells 61

3.8 Effects of cAMP on the cell cycle 63

3.9 Role of AKAPs in primary cilia regulation 65

3.9.1 AKAP350 localizes to the basal bodies at the base of the cilium 65

3.9.2 AKAP inhibition prevents cAMP/PKA cilium elongation 67

3.10 The role PGE2 in primary cilia formation 69

3.10.1 PGE2 induces primary cilia elongation 69

3.10.2 PGE2 dependent cilia elongation acts via EP2 and 4 receptors 69

3.11 Abnormal cilia structure in *PKD1* transgenic cells 73

3.12 Primary cilia number and length in human normal and ADPKD tissue 75

3.13 Primary cilia number and length in normal and *Pkd1* mouse kidneys 78

3.14 PC-1 deficient cells and centrosome number 80

3.15 Cilia length and cell cycle exit 81

3.16 ADPKD primary cilia have orientation defects in wounding assays 83

3.17 Summary and discussion 86

3.17.1 Primary cilia regulators 86

3.17.2 AKAPs localize the cAMP signalling 87

3.17.3 The role of cAMP in cell proliferation 89

3.17.4 PGE2 regulates primary cilia length 89

3.17.5 Ciliary length and defective orientation in cell migration 91

Chapter IV **The role of the cytoskeleton dynamics on primary cilia structure in ADPKD** **95**

4.1 Introduction 96

4.2 Cytoskeletal abnormalities affect normal cilia formation 99

4.2.1 Introduction 99

4.2.2 Actin organisation in normal and ADPKD cells 100

4.2.3 Modulation of Actin polymerisation alters primary cilia length 101

4.2.4 Structural 3D actin analysis in primary cilia vicinity 104

4.3 Microtubules 107

4.3.1 Introduction 107

4.3.2 Microtubule stability affects primary cilia formation 107

4.3.3 ADPKD cells have increased microtubule stability 109

4.3.4 Microtubule/Actin organization controls cilia independently of cAMP/PKA 112

4.4 PI3K is important in ciliogenesis 114

4.5 Rho GTPases modulate primary cilia length 119

4.5.1 Introduction 119

4.5.2 Rac-1 inhibition causes increased cilia elongation in ADPKD models 119

4.5.3 ROCK inhibition normalizes cilia length in ADPKD models 121

4.5.4 Cdc42 inhibition causes increased cilia elongation in ADPKD models 124

4.5.5 Influence of cytoskeleton alterations on primary cilia formation 128

4.6 Sphingolipids affect ciliary length 130

4.7 Summary and Discussion 134

4.7.1 Actin organisation in normal and ADPKD cells 134

4.7.2 The role of microtubules in primary cilium regulation 135

4.7.3 The link between actin and microtubules 136

4.7.4 Polycystin-1 is involved in cytoskeletal organization 138

4.7.5 PI3K is a ciliary length regulator 139

4.7.6 Rho GTPases modulate primary cilia length 142

4.7.7 Sphingolipids (ceramides) and primary cilium formation 144

Chapter V **Cystoproteins interacting proteins involved in primary cilium regulation** **146**

5.1 Introduction 147

5.1.1 Inositol-polyphosphate 5-phosphatase (INPP5E) 147

5.1.2 NPHPs, Gatekeepers of the ciliary compartment 148

5.2 INPP5E 149

5.2.1 INPP5E binds to polycystin-1 PLAT domain 149

5.2.2 INPP5E localization in normal and ADPKD cells 153

5.2.3 INPP5E siRNA reduces ciliary length 155

5.3 Polycystin-2 interacts with NPHPs 157

5.3.1 Polycystin-2 interacts with NPHP3 and NPHP9 157

5.3.2 NPHP2/INVS binds to the polycystin-2/nephrocystins complex 157

5.3.3 Localization of cystoproteins to the primary cilium 160

5.4 Discussion 165

5.4.1 INPP5E interacts with the PLAT domain of polycystin-1 165

5.4.2 NPHP2, 3 and 9 form a complex with polycystin-2 166

5.4.3 INVS siRNA influences polycystin-2 localization 168

Chapter VI Conclusion **170**

Bibliography 178

ABSTRACT

Autosomal Dominant Polycystic Kidney Disease (ADPKD) is the most common inherited kidney disease. Mutations in *PKD1* (85%) or *PKD2* (15%) account for almost all cases of ADPKD. The ADPKD proteins, termed polycystin-1 (PC1) and polycystin-2 (PC2) form a receptor-ion channel complex and in part, co-localise to the primary cilia. Since primary cilia are reported to be structurally normal in ADPKD unlike other ciliopathies, this project sought to test the hypothesis that changes in ciliary dynamics in relation to extracellular or intracellular stimuli might be an unrecognised feature of ADPKD.

Primary cilia assembly and disassembly was assessed in several established cellular models and shown to be synchronised to the cell cycle. In both control and ADPKD cell models, changes in intracellular Ca^{2+} and cAMP were found to similarly regulate ciliary length. Unexpectedly, primary cilia in ADPKD cell models were consistently shorter compared to normal controls; this was confirmed in diseased kidney tissue. Disease cells showed evidence of increased actin and microtubule polymerisation and disorganisation compared to controls. Of significance, the defect in cilia length could be fully restored by cytochalasin D, an inhibitor of actin polymerisation. This effect was independent of cAMP/PKA signalling. Inhibition of Rho GTPases showed differential effects on cilia length between control and disease cells with the most specific difference observed with a Rho inhibitor. Disease cells were less able to reorient cilia towards the migratory axis in wounding assays. Finally, several cystoproteins were shown to bind to either polycystin-1 or polycystin-2 and regulated cilia length (INPP5E) or polycystin-2 localisation to cilia (INVS).

These results indicate that a primary defect in actin organisation may result from polycystin-1 deficiency. Restoring actin dynamics in ADPKD may restore the structure and function of the primary cilium and could offer an alternative treatment strategy for ADPKD.

ABBREVIATIONS

ADPKD	Autosomal dominant polycystic kidney disease
AKAPs	A-kinase anchor proteins
APS	Ammonium persulfate
BBS	Bardet-Biedl syndrome
BSA	Bovine serum albumin
cAMP	Adenosine 3′,5′-cyclic monophosphate (cyclic AMP)
CDK	Cyclin-dependent kinase
cDNA	complementary DNA
CEP	CP centrosomal proteins
CMTC	Cytoplasmic microtubule complex
Co-IP	Co-immunoprecipitation
ddH_2O	double distilled water
DMEM	Dulbecos modified eagle medium
DMSO	Dimethyl sulphoxide
DTT	L-(−)-Dithiothreitol
Dvl	Dishevelled
ECM	Extracellular matrix
EDTA	Ethylenediamine tetra-acetic acid
EGFR	Epidermal growth factor receptor
ER	endoplasmic reticulum
ERK	Extracellular Signal-Regulated Kinase
ESRD	End stage renal disease
FAK	Focal adhesion kinase
FBS	Foetal bovine serum
GPCR	G protein-coupled cell–cell/matrix adhesion receptor
GST	Glutathione S-transferase
HA	Hemagglutinin
HAX1	HCLS1-associated protein X-1
HDAC6	Histone deacetylase 6
HRP	Horseradish peroxidase-conjugated
IFT	Intraflagellar transport
IGF-1	Insulin-like growth factor-1
IGF1R	Insulin-like growth factor
IgG	Immunoglobulin G
IMCD3	Murine inner medullary collecting duct cells
INVS	Inversin
IP	Immunoprecipitation
Kan	Kanamycin
Kb	Kilobase
kDa	Kilo-Daltons
LB	Luria Bertani medium

mDia1	Diaphanous-related formin 1
MKS	Meckel-Gruber syndrome
mM	Millimolar
MTOC	Microtubule-organizing center
MTOC	Microtubule-organizing centre
mTOR	Mammalian target of rapamycin
NaCl	Sodium chloride
NaOH	Sodium hydroxide
NIMA	Never-In-Mitosis NIMA-related kinases (NEK)
NP-40	Nonidet P40
NPHP	Nephronophthisis
OD	Optical density
ORF	Open reading frame
PBS	Phosphate-buffered saline
PC1	Polycystin-1
PC2	Polycystin-2
PCC	Pre-ciliary compartment
PCM1	Pericentriolar material protein 1
PCR	Polymerase chain reaction
PDGF	Platelet-derived growth factor
PGE2	Prostaglandin E2
PKA	Protein kinase A
PKC	Protein Kinase C
PKD	Polycystic kidney disease
PKN	Rho-activated protein kinase N
PTEN	Phosphatase and tensin homolog
PTMs	Post-translational modifications
RNA	Ribonucleic acid
rpm	Revolutions per minute
RT-PCR	Real time PCR
SDS	Sodium dodecyl sulphate
SDS-PAGE	SDS polyacrylamide gel electrophoresis
SHH	Sonic Hedgehog
SphK/ SK1	Sphingosine kinases
STAT	Signal Transducer and Activator of Transcription
TAE	Tris base, acetic acid, EDTA (buffer)
TAZ	Transcriptional coactivator with PDZ-binding motif
TBST	Tris-buffered saline containing 0.2% Tween20
TEMED	N,N,N'N'-tetramethylethylenediamine
Tris	Tris (hydroxymethyl) aminomethane
TRPP	Transient receptor potential polycystic
wt	wild type
YAP	Yes-associated protein

LIST OF FIGURES

Chapter I

Figure 1.1 Artistic representation of a normal and ADPKD kidney

Figure 1.2 Membrane topology of the polycystin-1/polycystin-2 complex

Figure 1.3 Primary Cilia and the Cell cycle

Figure 1.4 Primary cilium regulation

Chapter III

Figure 3.1 Cell Cycle analysis in IMCD, hTERT-RPE and NIH 3T3.

Figure 3.2 Primary cilium assembly and disassembly before, during and after serum removal

Figure 3.3 Primary cilium length can be modulated by cAMP and Ca^{2+} elevation in baseline models

Figure 3.4 Cell cycle profile of cystic and normal human cell lines

Figure 3.5 Primary cilium assembly and disassembly assay in normal and ADPKD models.

Figure 3.6 Number of ciliated cells comparison Healthy v.s ADPKD

Figure 3.7 Effect of calcium increase in ADPKD models

Figure 3.8 Effect of cAMP modulation in ADPKD Models

Figure 3.9 cAMP/PKA elongation is not defective in ADPKD models when modulated directly within the cell

Figure 3.10 Effect of cAMP in non-starved cycling cells

Figure 3.11 Assessment of proliferation profile of cAMP treated cycling cells

Figure 3.12 AKAP350 localizes at the base of the primary cilia

Figure 3.13 AKAP inhibitor ST-Ht31

Figure 3.14 PGE2 induces primary cilium elongation

Figure 3.15 EP receptor agonist in normal and ADPKD cells/EP2 and 4 antagonists in PGE2 treated cells.

Figure 3.16 PGE2-EP2/4 effect is PKA dependent

Figure 3.17 Primary cilium comparison of normal and Transgenic ADPKD models

Figure 3.18 Representative image of primary cilia in human normal and ADPKD (SKI001) tissue

Figure 3.19 Primary cilium analysis in human tissue

Figure 3.20 Mouse tissue of w.t and tamoxifen induced ADPKD models.

Figure 3.21 Analysis of cells with duplicated centrosomes

Figure 3.22 Cilia length and cell cycle exit

Figure 3.23 Primary cilium orientation in migrating normal and ADPKD cells

Figure 3.24 Primary cilium angle of deviation from wound in migrating normal and ADPKD cells

Figure 3.25 Model of primary cilium regulation in ADPKD

Chapter IV

Figure 4.1 Microtubules and Actin

Figure 4.2 Actin organization

Figure 4.3 Effect of Actin depolymerisation on primary cilia

Figure 4.4 Actin organization analysis

Figure 4.5 Representative Z-Stack images of normal and ADPKD actin and primary cilia.

Figure 4.6 SIM 3D images of primary cilia and actin structures

Figure 4.7 Effect of Microtubule depolymerisation

Figure 4.8 Microtubule stabilization affects cilium elongation

Figure 4.9 PKA inhibitor and the microtubulin/actin effect on cilia.

Figure 4.10 PI3K in ciliogenesis

Figure 4.11 PI3K is involved in primary cilia length regulation

Figure 4.12 ADPKD cells are more resistant to PI3K inhibition derived cilia elongation

Figure 4.13 Rac-1 and cilia regulation

Figure 4.14 ROCK and cilia regulation

Figure 4.15 CDC42 inhibition and cilia length

Figure 4.16 Effect of Rho GTPases inhibition on actin structures in normal and ADPKD models

Figure 4.17 Effect of Rho GTPases in ciliogenesis

Figure 4.18 Ceramide-sphingosines

Figure 4.19 SK1 inhibitors or activators in normal and PKD primary cilium formation

Figure 4.20 PI3K pathway

Figure 4.21 Rho GTPases regulation

Chapter V

Figure 5.1 PLAT/INPP5E interaction

Figure 5.2 PLAT Mutants/INPP5E interaction

Figure 5.3 INPP5E localization in different cell lines

Figure 5.4 INPP5E siRNA treatment and ciliary length

Figure 5.5/5.6 NPHP3/NPHP9 and PC2 interaction

Figure 5.7 INVS/PC2 interaction

Figure 5.8 Endogenous polyscytin-2 localization study in primary cilia

Figure 5.9 INVS in primary cilia

Figure 5.10 INVS and primary cilium regulation

Figure 5.11 Polycystin-2/NPHP complex

Chapter VI

Figure 6 Role of cystoproteins in primary cilia/cytoskeletal regulation.

CHAPTER I

Introduction

1.1 Autosomal Dominant Polycystic Kidney Disease

Hereditary cystic kidney diseases comprise a number of monogenic disorders (Bisceglia et al, 2006), which are characterized by the clinical manifestation of multiple bilateral fluid-filled cysts in the kidney (Gabow 1993). For ADPKD, up to date studies show a prevalence of almost 1/2500 people with ADPKD in the European Union, a number which just categorizes it under the threshold for a rare disease according to EU definitions (Willey et al, 2016). However, the prevalence numbers might still be underestimated with a majority of affected individuals remaining undiagnosed during life (Ong et al, 2015).

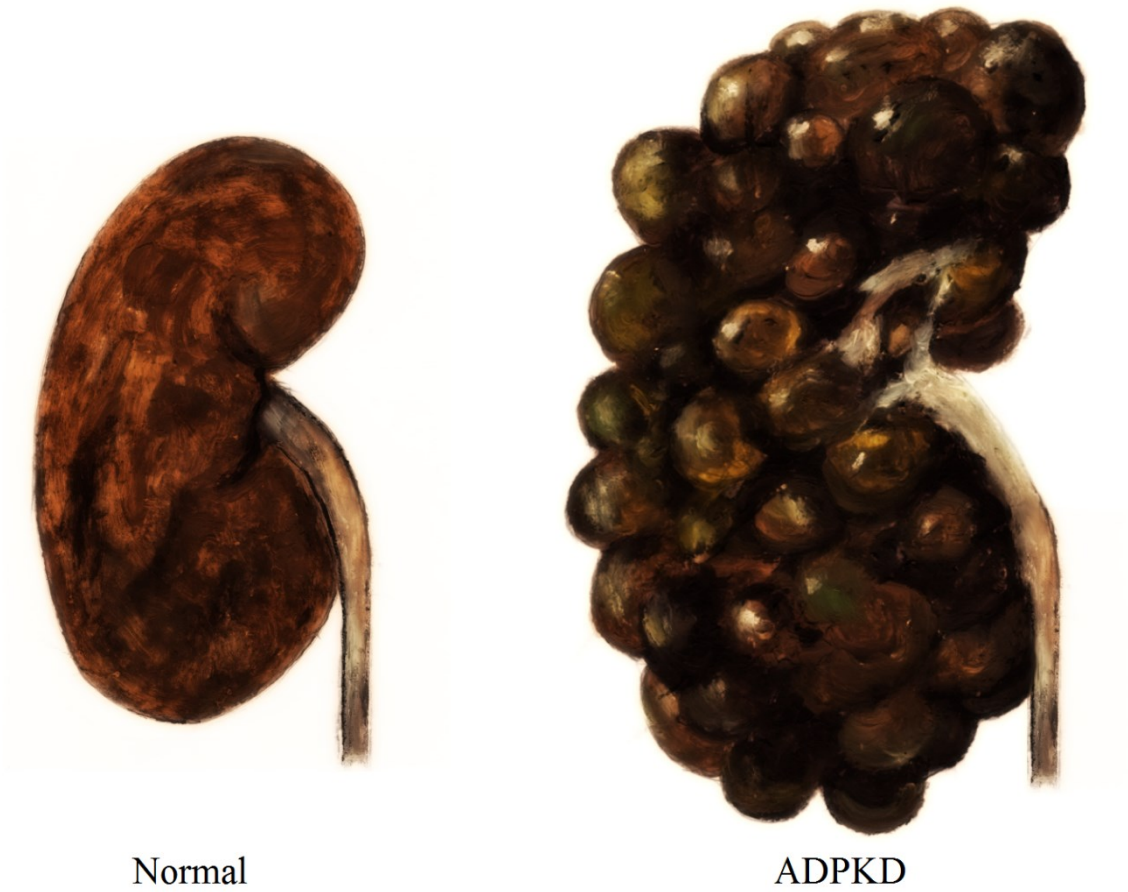

Figure 1.1 Artistic representation of a normal and ADPKD kidney. With disease progression, ADPKD kidneys expand due to the formation of multiple fluid-filled cavities (or cysts) increasing in size to destroy normal tissue until kidney function is completely lost.

Children of a parent with ADPKD have a 50 percent chance of inheriting the disease, reflecting dominant transmission. In general, the disease is of late onset and the clinical manifestations can be variable. Kidney dysfunction is not clinically apparent until the age of 30 to 40 due to compensatory mechanisms from healthy tissue (Grantham 2008; Ong et al, 2015). In cases where the family history is not known, the first diagnosis of ADPKD and the presence of early cysts can be diagnosed incidentally. In the advanced stages, disease progression is more rapid leading to a measurable decline in kidney function. These cysts increase in diameter and number throughout the afflicted person's life and lead to progressive impairment of normal kidney function. At the cellular level, the cystic kidney is characterized by increased proliferation, apoptosis, altered fluid secretion and extracellular matrix deposition. Some of the first symptoms include elevated blood pressure which when left untreated can further damage kidney function and increase the risk of heart disease (Ong et al, 2015).

As a systemic disorder ADPKD is also the cause for other symptoms, including cardiovascular abnormalities and cyst formation in the liver and other organs (Gabow 1993). However the kidney is always affected and becomes enlarged as the direct result of cyst formation and expansion. Common symptoms include urinary tract infections, hypertension, hematuria, nephrolithiasis, acute or chronic flank and abdominal pain (Gabow 1993; Rizk and Chapman 2003). The diagnosis is most commonly made by ultrasound imaging using defined criteria; total kidney volume (TKV) measured by MRI or CT can give an accurate measure of disease burden and has prognostic value (Ong et al, 2015). Currently, symptomatic treatment of symptoms and complications such as the management of high blood pressure, pain or urinary tract, bladder or kidney infections is the main management strategy. Patients with end-stage disease commonly undergo dialysis or renal transplantation (Patel et al, 2009). Recently, a promising new treatment- Tovalptan, a vasopressin V2 receptor antagonist, showed some effect in slowing kidney growth and the associated decline in function (Torres et al, 2012 & 2016).

1.2 Genetics of ADPKD

ADPKD is caused in 85% of cases by mutations in *PKD1* which is located on the short arm of the chromosome 16. Mutations in *PKD2*, mapped on the long arm of chromosome 4, are responsible for the remaining 15% of cases. In both genotypes, the phenotype is clinically indistinguishable, although *PKD2* patients generally have a later onset of end stage renal disease (ESRD) than *PKD1* patients (Gabow 1993; Patel et al, 2009). This overlapping phenotype suggests that both proteins function in the same complex or biochemical pathway, a hypothesis that has been shown experimentally for the ADPKD proteins, polycystin-1 (PC1) and polycystin-2 (PC2) (Grimm et al, 2003; Ong et al, 2005; Torres et al, 2007).

However, regardless of genotype, the onset and progression of ADPKD is more variable than the simplified scheme presented above, making accurate prognostic prediction difficult even within the same family. It is likely that environmental, epigenetic and other genetic factors play a role in modifying disease severity. Somatic mutations have been detected in cystic cells at low frequency but are now not considered necessary for cysts to form through a 'two hit' model.

Genetic screening for *PKD1* or *PKD2* is becoming widely available and is advisable in the absence of family history or where the diagnosis is in doubt. In future, mutation analysis will be an important factor as part of the general assessment of prognosis of disease onset, progression and complications in the individual patient (Braun 2009).

1.3 Polycystins

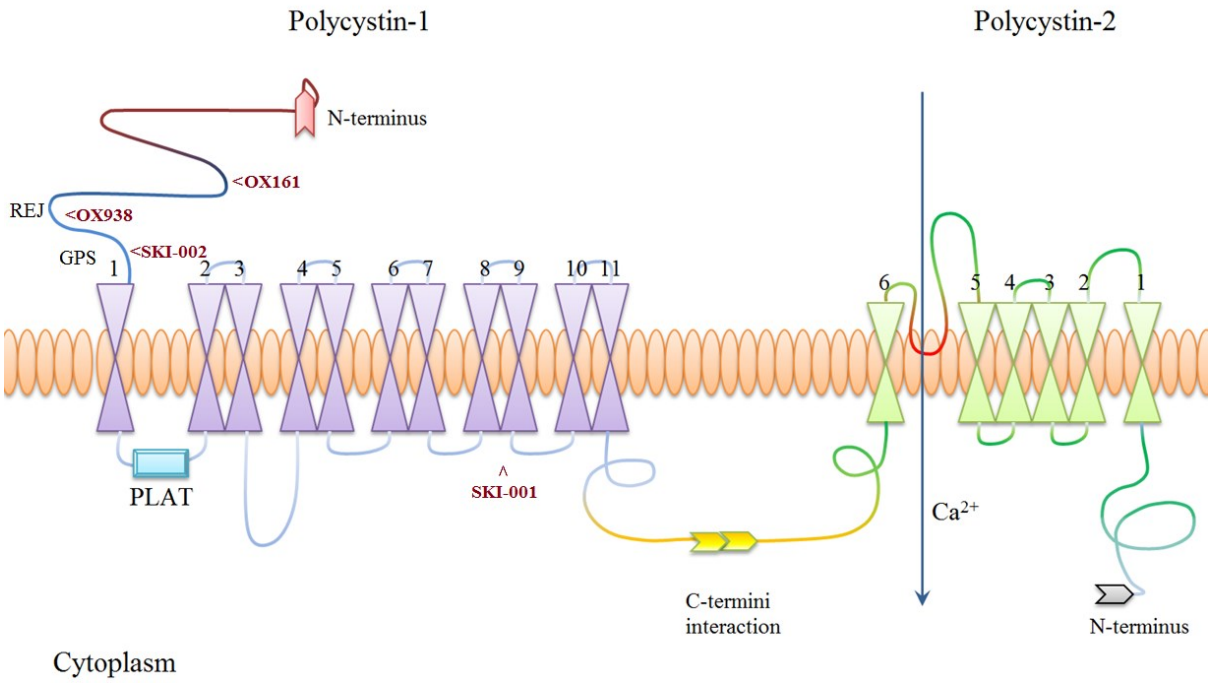

Figure 1.2 Membrane topology of the polycystin-1/polycystin-2 complex

The *PKD1* gene encodes Polycystin-1, a glycoprotein of 4304 amino acid size widely expressed in epithelial cells. The PLAT (Polycystin-1, Lipoxygenase, Alpha-Toxin) domain is located between transmembrane segments 1 and 2 of polycystin-1. The *PKD2* gene encodes polycystin-2, a smaller protein of 968 amino acids expressed in the endoplasmic reticulum and in the cell plasma membrane. The Ca^{2+} channel pore is positioned within transmembrane segments 5 and 6 of polycystin-2. Germline PKD1 mutations of cell lines used in this study are marked in red (Parker, et al 2007).

1.3.1 Polycystin-1

Polycystin-1 is an 11 trans-membrane protein with an extracellular N-terminal domain and a short cytoplasmic C-terminal domain (Tsiokas et al, 1997; Newby et al, 2002). It is a large glycosylated protein with a molecular weight of approximately 460 kDa. The majority of the protein is expressed in the eleven transmembrane domains which share some homology to polycystin-2 and the large N-terminal extracellular domain. These includes various motifs involved in protein to protein interactions and a proteolytic cleavage domain typical of other G protein-coupled cell-receptors (GPCR) regulated by cell/matrix adhesion (Delmas et al, 2002; Parnell et al, 1998; Parnell et al, 2002; Sandford et al, 1999). The C-terminal intracellular domain is characterized by a coiled-coil domain (mediating interaction with polycystin-2), a G-protein binding domain and various predicted phosphorylation sites.
One of the first observations made was its ability to interact with polycystin-2, and its function in tubular morphogenesis (Qian et al, 1997). In addition, studies showed that this interaction upregulated the expression of polycystin-1 (Tsiokas et al, 1997) and induced calcium-permeable whole cell currents (Hanaoka et al, 2000).

1.3.2 Polycystin-1 and cell adhesion

Early studies found that polycystin-1 co-localized and co-precipitated with the cell adhesion molecules E-cadherin and alpha-, beta-, and gamma-catenin (Huan and van Adelsberg 1999), suggesting a role in regulating E-cadherin mediated adhesion and signalling.

Other groups showed that polycystin-1 co-localized with another type of junctional complexes termed desmosomes and to cell-cell contacts in MDCK cells (Scheffers et al, 2000; Bukanov et al, 2002) and that the Ig-like repeats of polycystin-1 might be directly involved in mediating cell adhesion (Ibraghimov-Beskrovnaya et al, 2000; Streets et al, 2003).

Within the cell, the C-terminus of polycystin-1 was shown to interact with cytoskeletal structures such as the intermediate filaments vimentin and cytokeratins (Xu et al, 2001), actin and microtubules (Castelli et al, 2015).

1.3.3 Polycystin-1 Localization and expression

The subcellular localization of polycystin-1 has been an area of controversy and complexity (Ong 2000). Multiple locations have been attributed to polycystin-1 including the plasma membrane, endoplasmic reticulum, primary cilium and the nucleus (following C-terminal cleavage) (Grimm et al, 2003; Nauli et al, 2003; Chauvet et al, 2004). These studies hinted that polycystin-1 could have multiple functions and regulate a number of different signalling pathways in different cellular compartments. Some of the earliest localization studies of Polycystin-1 showed localization to sites of interaction between adjacent cells, which enhanced the role for polycystin-1 in cell-cell interactions. Kidneys and liver cells represent the main pathogenic tissues, where polycystin-1 expression has been reported (Peters et al, 1999). However, polycystin-1 expression was also found expressed in tissues such as epithelia and endocrine cells, not directly reported to be involved in ADPKD. Some examples include pancreatic cells in islets, Leydig cells in the testis or myocardium and myocytes of cardiac valves, cerebral arteries and skeletal muscles (Peters et al, 1999).

1.3.4 Polycystin-1 regulation of different signalling pathways

Despite many studies, the physiological function/s of polycystin-1 and the major signalling pathways regulated by polycystin-1 remain elusive. The C-terminal tail of polycystin-1 has been shown to interact with STAT3 (Talbot et al, 2014) and STAT6 (Low et al, 2006). Furthermore, polycystin-1 was suggested to be involved in the mTOR pathway. It was found that following the mTOR and STAT signalling cascade, a protein named tuberin interacted with the cytoplasmic tail of polycystin-1. Tuberin is an essential inhibitor of the mammalian target of rapamycin (mTOR) kinase, a key mediator in cell proliferation which can be modulated with specific drugs (Shillingford et al, 2006) and whose activation has also been linked to primary cilia (Boehlke et al, 2010). Interestingly, tuberin is also known for its ability to regulate specific GTPases and mTOR FRAP1 kinase activity, thus establishing a potential link between cystoproteins and proliferation or apoptosis mechanisms (Shillingford et al, 2006). In addition to that, potential roles in intermediate filament network regulation, by interaction with vimentin and cytokeratins with the C-terminus and coiled-coil region of polycystin-1 (Xu et al, 2001) further suggested a role of polycystin-1 in regulating cell architecture. Interestingly, studies showed that polycystin-1 is able to interact with a GTPases

protein complex consisting of Arf4, Rab6, Rab11 and GTPase-activating proteins, possibly involved in vesicle budding and Golgi exocytosis (Ward et al, 2011).

Furthermore, it is theorized that polycystin-1 undergoes proteolytic cleavage at different positions, with different possible functions (Lal et al, 2011; Bertuccio et al, 2013). Studies suggested that polycystin-1 was able to transmit messages directly to the nucleus by cleaving and releasing its C-terminal tail, which subsequently activated different signalling process through transport into the nucleus (Chauvet et al, 2004). Other studies suggested a possible cleavage at the GPS domain in synchrony with the REJ domain at the beginning of large N-terminal region of the polycystin-1 protein, and studies showed that mutations preventing this cleavage resulted in an impaired ability to transduce signals and induced tubulogenesis *in vitro* (Qian et al, 2002).

1.3.5 Polycystin-2

Polycystin-2, is characterised by six transmembrane domains with cytoplasmic N and C termini. It is approximately 110 kDa in size and shows significant homology to the transient receptor potential (TRP) channel superfamily: it is also known as TRPP2.

1.3.6 Polycystin-2 localization

Precise localization studies of this protein showed that only a minority (approximately 8%) co-localized with polycystin-1 to the plasma membrane of human and mouse kidney cells, where it could function as a calcium permeable channel (Koulen et al, 2002). In addition, this surface localization was dependent on the co-expression of polycystin-1 (Hanaoka et al, 2000; Newby et al, 2002). Other groups have shown that polycystin-2 can act as a calcium release channel at the endoplasmic reticulum (ER) (Koulen, *et al* 2002) where it has been shown to interact with other resident ER channel proteins such as TRPC1, IP3R and RyR (Anyatonwu et al, 2007; Sammels et al, 2010). In support of a ciliary role, a later study found endogenous polycystin-2 expression in the primary cilium of IMCD3 and MDCK cells (Luo et al, 2003). Expression in tissue of polycystin-2 has been shown in ovary, fetal and adult kidney, testis, and small intestine (Mochizuki et al, 1996).

1.3.7 Polycystin-2 functions

The main proposed function of polycystin-2 encompasses its role as a calcium cation-channel and although the main mechanisms underlying polycystin-2 gating are currently not clear, some evidence suggests gating mechanisms dependent on phosphatidylinositol 4,5-bisphosphate (PIP 2) or the actin organizing diaphanous-related formin 1 (mDia1) interaction (Bai et al, 2008).

An early study showed that polycystin-2 interacted with HAX1, an actin-associated protein through its ability to bind to the F-actin-binding protein cortactin (Gallagher et al, 2000). Other studies suggested that both intracellular domains could associate with alpha-actinins, actin-bundling and actin-binding proteins (Li et al, 2005). In addition, it was shown that polycystin-2 was able to bind indirectly to the actin microfilaments (Li et al, 2003) and that microtubule dynamics were able to regulate polycystin-2 channel functions in renal epithelial cells (Li et al, 2006). Furthermore, polycystin-2 has been shown to directly regulate the cell cycle via modulation of the ID2-CDKN1A-CDK2 pathway, a channel independent function (Li et al, 2005). More recent studies have shown that polycystin-2 was able to interact with different integral membrane receptor proteins including TRPC1, IP3R and RyR and that in the ER, association with these receptors elevated intracellular calcium levels (Anyatonwu et al, 2007; Sammels et al, 2010), while others showed involvement in the regulation of correct left-right patterning (Yoshiba et al, 2012).

1.3.8 The Polycystin-1/Polycystin-2 complex

Since both proteins are expressed on primary cilia of renal tubular epithelial cells, one of the most debated functions of a cilia-localized polycystin-1 and 2 (PC1-PC2) complex is in the flow-activation of polycystin-1 regulating the influx of extracellular calcium through polycystin-2 (Nauli et al, 2003; Mangolini et al, 2016). Recent studies have disputed this finding leaving the physiological ciliary function of the polycystins unclear (Delling et al, 2016). Calcium influx is one of the factors besides growth factors and cAMP which through the extracellular signal-regulated kinase (ERK) pathway governs the proliferative state of renal tubular cells (Yamaguchi et al, 2004). Other important signals include the mammalian target of rapamycin (mTOR) kinase, which was found increased in activity in cysts found in ADPKD tissues. Polycystin-1 may directly or indirectly regulate mTOR or its downstream

effectors (Distefano et al, 2009). However, some evidence points to a homeostatic action of the polycystin-1/2 complex, involving the regulation and balance of cAMP and calcium signalling, which in turn activate intracellular pathways that oppose proliferation signals such as the mTOR and mitogen-activated protein kinase (MAPK) pathways (Franco et al, 2015). Other pathways such as JAK2/STAT1/p21, have also been shown to be regulated by the polycystin-1/ 2 complex (Bhunia et al, 2002).

1.4 Primary Cilia

Primary cilia have been shown to act as an important sensory organ, able to detect extracellular chemical and mechanical signals and transducing them via intracellar signalling pathways to specific coordinated responses which affect proliferation and differentiation (Marshall and Nonaka 2006). The primary cilium is a solitary microtubule-based cytoskeletal organelle that emanates from the surface of most mammalian cell types during growth arrest. The reported length of these organelles is very variable, ranging from 1 1 µm up to 30 µm reported in some kidney epithelial cells (Saggese et al, 2012).

Within the kidney, one of the main roles attributed to primary cilia is as a sensor of extracellular stimuli, including mechanosensation and receptor signalling, and transmitting these signals through intracellular pathways which regulate proliferation and differentiation (Irigoín & Badano 2011). Other roles of primary cilia can be found during embryonic development in cell orientation and differentiation (Goetz and Anderson 2010), in contact inhibition, cancer and directional migration during wound healing (Michaud and Yoder 2006; Schneider et al, 2010).

Changes in the structure or function of the cilium are likely to underlie the development of many cystic diseases such as ADPKD, Nephronophthisis (NPHP) and Bardet-Biedl syndrome (BBS). The structure of a cilium is highly evolutionarily conserved and is formed by a cytoskeletal scaffold arrayed by microtubule triplets termed the axoneme (Plotnikova et al, 2009) (**Figure 1.3**). The ciliary axoneme is composed of nine doublet microtubules. It arises out of the mother centriole (forming the basal body) and is enveloped by the ciliary membrane, a specialised compartment distinct from the apical membrane (Plotnikova et al, 2009). Motile (9+2) cilia are distinguished from the non-motile cilia (9+0) by the presence or absence of a central pair of microtubule doublets, which confer cilia motility (Satir and Christensen 2007). The length of the primary cilium, which is influenced by the assembly and disassembly of ciliary building blocks such as tubulins and other axonemal proteins, has been suggested to critically modulate cilia function by attenuating chemokine and other responses (Wann and Knight 2012). Additional evidence supporting the importance of the role of ciliary organelles has come from the cancer field, where cilia are proposed to function in a surveillance role of proliferation (Seeley et al, 2009; Rocha et al, 2014); thus loss of primary cilium is associated with uncontrolled proliferation, a feature of cyst formation. Interestingly, studies performed on a variety of tumour cells revealed in the majority of cases no cilia development at any stage of the cell cycle, thus suggesting either a loss of cell cycle-

restrictive signals mediated through cilia or that the inability of malignant cells to enter quiescence results in defective cilium development (Seeley et al, 2009; Wheatley 1995). Interestingly, it was found that that loss of intact cilia was able to suppresses cyst growth following inactivation of polycystins, suggesting a still unknown intricate co-regulatory mechanism between the cilia polycystin system (Ma et al, 2013).

1.5 Cell cycle and primary cilium modulation

Most of our current knowledge on primary cilium has been based on structural studies using electron and immunofluorescence microscopy (Jensen et al, 1987; Plotnikova et al, 2009). The processes by which primary cilia are assembled and disassembled during the various stages of the cell cycle remain poorly understood. However, it is broadly accepted that ciliation is a characteristic of cell cycle exit and quiescence, while disassembly of cilia takes place when cells actively re-enter the cell cycle, resulting in their complete absence in mitotic cells (Archer and Wheatley 1971; Paridaen et al, 2013). This is closely linked to other observations that at a specific stage during cell cycle progression, ciliated centrioles i.e. the basal body (which derives from the mother centriole) have to be released to function as a microtubule-organizing centre (MTOC) responsible for the organization of the mitotic spindle apparatus (Plotnikova et al, 2009; Paridaen et al, 2013). Studies in vertebrate cells have shown that the inter-conversion between basal body and MTOC conformations are directly associated to an elongation of primary cilia in quiescent cells or cilium disassembly prior to mitotic entry (Archer and Wheatley 1971; Plotnikova et al, 2009).

In the majority of cells, the assembly of primary cilium occurs in G1 after cytokinesis. During the formation of the primary cilium, the mother centriole that acts as a template for the assembly of the second daughter centriole during S phase of the previous cycle, migrates near the plasma membrane and differentiates into a basal body. From there, the axoneme starts to elongate, still connected to the basal body. The established connection is known as the transition zone where later proteins will traffic in and out from the cilium (Zalli et al, 2012). Thus, in each G1 phase, cells possess both a daughter centriole and a mother centriole where the latter plays a unique role in basal body development via the specific ability to anchor microtubules and thus acts as a microtubule-organizing centre (Piel et al, 2000).

During interphase, both centrioles are located at the centrosomes. In S- phase, both centrioles and DNA undergo replication and towards the end of G2 at the M transition, cilia disassembly begins. Immediately after mitosis, cilia reassemble in G0-G1. The observed length of assembled cilia is typically higher in quiescent rather than cycling cells (Fonte et al, 1971).

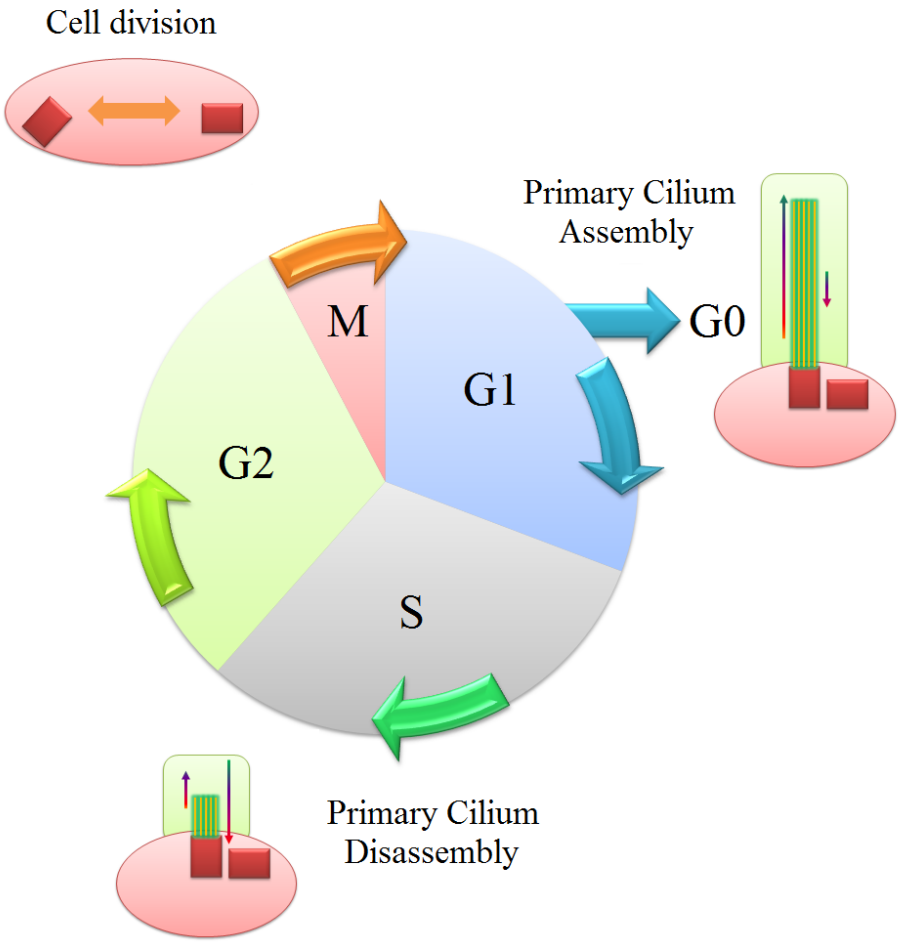

Figure 1.3 Primary Cilia and the Cell cycle. As cells exit mitosis (M), the cell enters the first stage of the interphase. Assembly of primary cilia occurs by an increase of anterograde IFT molecules from the basal body into the cilia tip of the primary cilium, with maximal cilia length during G1-G0 phase. The next stage is represented by the S phase where centrioles and DNA replication initiates. At this point, for some cells an increase of retrograde IFT transport thus cilia disassembly begins, whereas for other cells cilium disassembly begins at the end of the G2 phase with complete disassembly at beginning of the M phase.

1.6 Molecular control of the cilia assembly and disassembly

Studies of cilia development in mammalian cells have uncovered numerous mechanisms involved in the regulation of the primary cilia growth cycle. Besides phosphorylation of different protein kinases -which have been shown to be involved in cilium regulation- including aurora kinases (AurA), mitogen-activated protein (MAP) and never in mitosis A (NIMA) kinases or more novel cyclin-dependent protein kinases (Mahjoub et al, 2005; Cao et al, 2009; Majeed et al, 2012), it has been reported that flagellar length can be influenced by intracellular calcium concentrations and cyclic AMP (cAMP) acting through protein kinase A (PKA) activation (Besschetnova et al, 2010). Cilia elongation is believed to take place via a PKA dependent rise in the amount of anterograde IFT particles involved in the intraflagellar transport (IFT) process (Besschetnova et al, 2010). The IFT process is an essential component for cilia development and maintenance. IFT particles are formed by non-membrane bound protein complexes, which are transported along the axonemal doublet microtubules along the entire cilia length from the base to the tip (Plotnikova et al, 2009). IFT defines an active process where ciliary building blocks can be transported in both directions by IFT particles. These associate with ciliary proteins and represent the executers of anterograde and retrograde ciliary protein transport.

Differences between the velocity of anterograde and retrograde movement can define cilia resorption or extension. This has been shown in studies performed in *Chlamydomonas* where cilium disassembly was augmented when cargo-less IFT particles entered the primary cilium (Pan and Snell 2005; Rosenbaum and Witman 2002). The two-way protein transport is accomplished by two different IFT macromolecular complexes. Complex A, associated with the motor protein dynein, is responsible for retrograde transport from the tip while complex B, connected to kinesin 2, is responsible for anterograde transport from the cell body towards the tip (Plotnikova et al, 2009; Williamson et al, 2012; Huet et al, 2014). The balance between the rate of anterograde and retrograde delivery through these two complexes ultimately influences ciliary assembly and resorption during different stages of the cell cycle (Rosenbaum and Witman 2002). The process initially observed in *Chlamydomonas* is a highly conserved process through evolution as shown by studies performed on mammalian cilia in RPE cells (Pan and Snell 2005; Pugacheva et al, 2007). Mutations in IFT particles or their motor proteins are predicted to negatively affect ciliogenesis. The first example came

from the recognition that the intraflagellar transport 88 protein (also known as Tg737, polaris, or OSM-5), a component of the IFT-B complex resulted in abnormally short flagellar and cilia in *Chlamydomonas*, *C. elegans*, mice and in cyst development and abnormal cell-cycle progression (Haycraft et al, 2001, Taulman et al, 2001, Yoder et al, 2002).

However, a number of mechanisms independent of IFT are also known to influence ciliary dynamics in mammalian cells as indicated in studies on Ptk1 cells, where cilia resorption during mitosis associated this organelle as a component of the cytoplasmic microtubule complex (CMTC) and spindle pole formation regulate cilia dynamics (Rieder et al, 1979). Comparative genomics and proteomic analysis on eukaryotic cilia have identified a variety of proteins localized to the cilium or the basal body which have been shown to negatively affect ciliogenesis and result in cystic diseases including the large families of Bardet-Biedl, Joubert or Meckel-Gruber syndrome genes, (Li et al, 2004; Pazour et al, 2005 Badano et al, 2006), and others, including the primary ciliary dyskinesia and the nephronophthisis genes.

A potential link to ADPKD has been the reported by the association of nephrocystin-1 encoded by the *NPHP1* gene, with polycystin-1 (Wodarczyk et al, 2010). Other links between proteins involved in cilia development and the polycystin proteins are therefore promising candidates to study in the pathogenesis of ADPKD. Recent examples include a variety newly identified CP centrosomal proteins (CEP) that are involved in suppression of cilium protusion (Graser et al, 2007, Spektor et al, 2007, Tsang et al, 2008, Chaki et al, 2012) or the "Never-In-Mitosis" NIMA-related kinases (NRK or NEK) which have been shown to localize to the cilium and shown involvement in cell cycle and primary cilium regulation (Otto et al, 2008; Trapp et al, 2008; White and Quarmby 2008; Hoff et al, 2013). In the latter case, it was specifically shown that mutations in two of the kinases, Nek1 and NPHP9 (Nek8) resulted in the development of cysts in kidneys of mice and humans (Liu et al, 2002; Upadhya et al, 2000; Zalli et al, 2012).

At least two large recent functional genomics screens aimed at the identification of novel modulators of ciliogenesis and cilium length and have highlighted a variety of new candidate genes involved in ciliogenesis and cilia length regulation (Kim et al, 2010; Wheway et al, 2015). Some of the new ciliogenesis regulators hint to mitotic cell cycle regulators such as Cdc27 or Cdc77 or novel centrosome proteins such as CEP120 (Wheway et al, 2015), components of the ubiquitin-proteasome system, G-protein-coupled receptors, pre-mRNA processing factors (Szymanska et al, 2015) or findings, showing that many of the molecular

mechanisms involved in ciliogenesis are also involved in early steps of the autophagic process, with partial inhibition of autophagy and cell-volume regulation in primary cilia ablated models (Pampliega et al, 2013; Orhon et al, 2016). In addition, there is evidence to suggest that endocytic recycling proteins such as EHD1 might also represent an important factor in primary cilia modulation and SHH signalling as shown by studies in *Ehd1* gene knockout in mice (Bhattacharyya et al, 2016).

Interesting are recent ciliary modulating molecules involved in microtubule organization (Miyamoto et al, 2015), vesicle trafficking and actin dynamics (Kim et al, 2010), the latter gaining importance later in our study, were it was shown that actin organization is an important ciliary length regulator possibly disturbed in ADPKD.

Although the clear mechanisms and exact pathways of actin control over ciliogenic processes is still poorly understood and only recently gaining increased importance, some studies suggest that the transcriptional regulators Yes-associated protein (YAP) and transcriptional coactivator with PDZ-binding motif (TAZ), which are the main effectors of Hippo signalling (Hansen et al, 2015; Kim et al, 2015), might play an important role in mediating this control mechanisms.

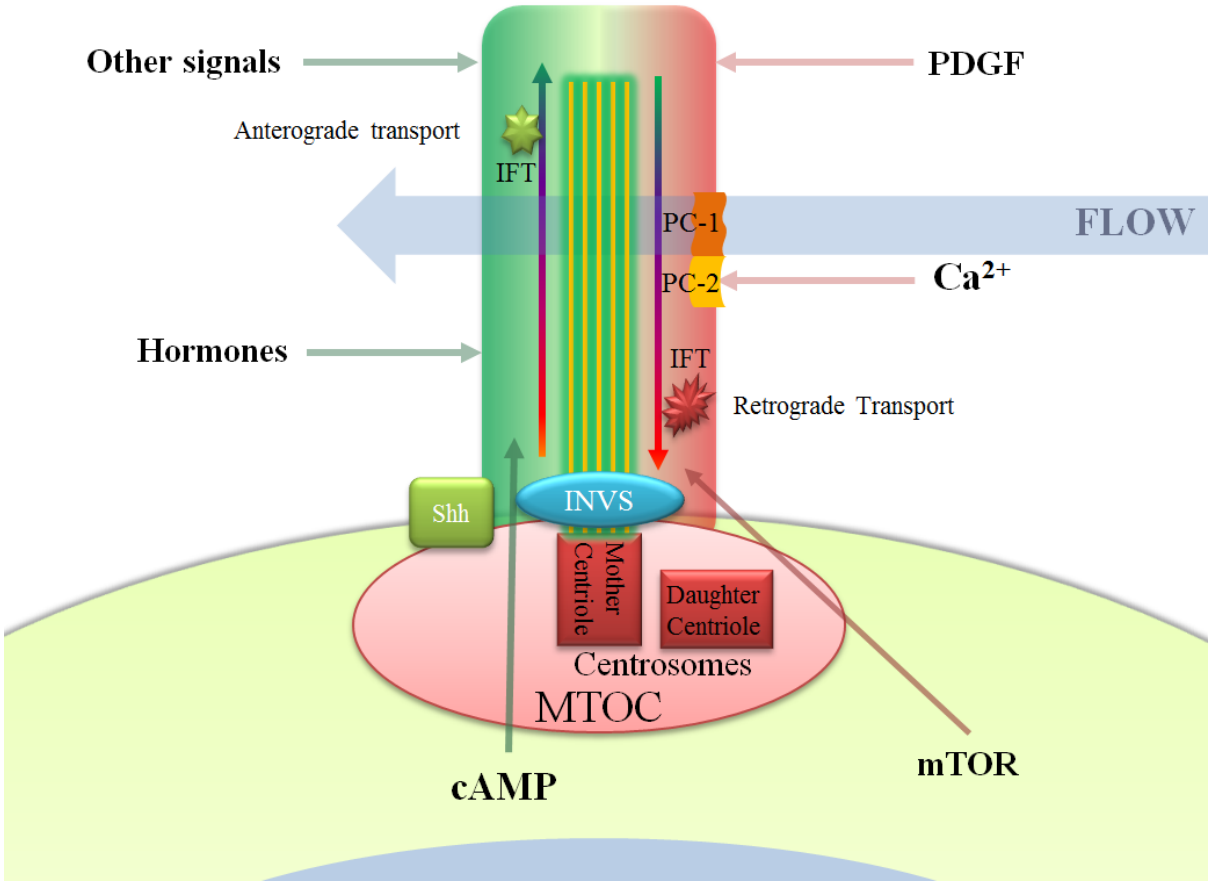

Figure 1.4 Primary cilium regulation. Summary figure of the currently major identified pathways involved in primary cilium dynamics and regulation. ADPKD, and other diseases characterized by the formation of renal cysts are commonly classified into the family ciliopathies. Ciliary proteins or building blocks are transported in both directions by IFT particles, which are the executers of the anterograde and retrograde machinery. The primary cilium formation machinery is influenced by different pathways which are known to affect to various degrees cilia formation and development. Primary cilia are found on the apical surface of the epithelial cells of the renal tubules and collecting ducts. Ciliary IFT Anterograde activating signalling and pathways such as cAMP and PGE2 (Green arrows). Ciliary IFT Retrograde activating or stabilizing signalling and pathways such as PDGF and mTOR (Red arrows) (Yuan et al, 2012).

1.7 The role of primary cilia in the pathogenesis of ADPKD

From its structural conformation it is safe to assume that the main function of primary cilia revolves around cell signalling. Some of the most well-known are summarized in (**Figure 1.4**). The primary cilium is packed with a large amount of different receptors, ion channels and transporter proteins. The formation of a structure such as the cilium, extends these sensing organs far out from the cell similarly to an antenna. This allows for flexibility and an increased overall reach of signal detection in regions accessible to diffusing biological molecules, mechanical forces or other extracellular regulators, without the possible limitations posed by the physical organization of the whole cell. The localization of polycystin-1 and polycystin-2 to the primary cilium was the first link to primary cilia function as potentially relevant to ADPKD pathogenesis. Since cilia have been reported to be structurally normal, it was postulated that a defect in function was the main abnormality. The ability of polycystin-1 to act as a flow-sensor has been supported by studies showing that its extracellular region is endowed with high mechanical strength (Forman et al, 2005). Although studies have shown that an increase of intracellular calcium was specifically mediated by the deflection of the cilia axoneme (Praetorius & Spring 2003) and possibly mediated by the ciliary resident polycystins (Nauli et al, 2003), recent studies have disputed the ability of polycytin-1/2 or primary cilium bending in transducing a flow-sensitive cilia Ca^{2+} current (Delling et al, 2016). In multiple different cell lines including kidney epithelial cells, they showed that intracellular Ca^{2+} was not altered upon mechanical bending of the primary cilia as previously suggested, from which they concluded that a possible ciliary mechanosensation role, if present, was not mediated by Ca^{2+} entry in cilia (Delling et al, 2016).

Alternatively, primary cilia are speculated to be involved in a surveillance task of cell regenerative potential against extensive proliferation, via sequestration of the in cell division required centrioles (Seeley et al, 2009; Rocha et al, 2014). Studies on a PKD mouse model support these findings, showing that wound healing following acute kidney injury modulated cilia length and activates cell cycle processes. Without the normal cilium surveillance, this promoted the uncontrolled proliferation of cells, increasing the overall cystogenic potential and expansion of cysts (Happe et al, 2009; Patel et al, 2009; Verghese et al, 2008 & 2009).

Impaired cilium cell cycle surveillance mechanisms could then lead to unopposed proliferation.

Recent studies have also implicated STAT6 (Low et al, 2006) and mTOR in cilia signalling, the latter through the action of LKB1 (Boehlke et al, 2010); both pathways have also been linked to polycystin-1. Primary cilia have also been associated with growth factor signalling such as the platelet-derived growth factor (PDGF) and thus involved in cell migration and proliferation (Hoch and Soriano 2003). The PDGFRα receptor is upregulated and localizes to primary cilia in growth arrested cultured fibroblasts and is activated through ligand PDGF-AA binding leading to downstream activation of the Akt, ERK1/2- and MEK1/2-pathway (Schneider et al, 2005), thus primary cilia defects are likely to impair these mechanisms.
Interestingly, recent studies hypothesize a possible role of primary cilia as a sensor, which regulates directional cell movement in migrating fibroblasts through the PDGFRα receptor (Christensen et al, 2013). Beside the PDGF receptor, other tyrosine kinases (RTK) are shown to be regulated and mediated via the primary cilia in different cell models, such as the insulin-like growth factor (IGF1R), the epidermal growth factor receptor (EGFR) and the angiopoietin receptor (Tie-2) (Christensen et al, 2012) all of which influence basic cellular functions which might converge in ADPKD pathogenesis.

The primary cilium is also found involved in the *Hedgehog* (Hh) pathway, activation of the latter being mainly depends on cilia integrity (Fliegauf et al, 2007). The Hh-signaling pathway is involved in many developmental mechanisms and cell differentiation and recent studies showed that downregulation of this pathway reduced the renal cystogenic potential of mouse models (Tran et al, 2014), suggesting that enhanced or uncontrolled hedgehog activity may be a feature related to common ADPKD development. In this context, a defect in cilia integrity is able to critically influence Hh-signaling, which depending on defect type either increase or decrease Hh-signaling (Goetz et al, 2010) resulting in according developmental defects for example in neural tube patterning.

Primary cilia seem also to be important in restraining canonical Wnt signalling, important in developmental and homeostatic processes (Gerdes et al, 2007). Downregulation of different genes important in ciliogenesis such as BBS1, BBS4, MKKS or KIF3A in different models resulted in an increased transcriptional activity of canonical Wnt target genes and

accumulation of nuclear β-catenin (Corbit et al, 2008). Interestingly, in context to the β-catenin involvement is that the ciliary resident nephronophthisis protein NPHP2/INVS is able to deactivate β-catenin by a Dishevelled (Dvl) protein mediated transport to the destruction complex, thus INVS impairment results in an abnormal augmentation of nuclear β-catenin accumulation (Otto et al, 2003; Simons et al, 2005), which is a common hallmark of renal cysts (Kheddouci et al, 2001).

New studies have uncovered additional potential roles of primary cilia that could have an implication in the pathogenesis of ADPKD such as Notch-signalling (Ezratty et al, 2012), which is important during renal development and has been shown to be involved in renal cysts formation in mouse cells (Surendran et al, 2010), or the disruption of signalling via the alterations in the composition of the specific and unique primary cilia membrane proteins itself, such as the inositol polyphosphate-5-phosphatase E (INPP5E) (Bielas et al, 2009; Jacoby et al, 2009).

HYPOTHESIS

The major hypothesis of this project was that altered primary cilia formation or regulation might play a critical role in ADPKD pathogenesis. To do this, the following aims were addressed:

Main Aims

- Assess the effect of polycystin-1 and /or polycystin-2 deficiency on ciliogenesis
- Investigate molecular mechanisms underlying the observed defects in ciliogenesis in ADPKD
- Identify novel polycystin-1 or polycystin-2 binding proteins involved in primary cilium structure or function

CHAPTER II

Materials and Methods

2.1 Materials and Reagents

2.1.1 Compounds

BSA A7906	Sigma
Blasticidin	Invitrogen
BM Chemiluminescence Blotting kit	Roche
BSA A7906	Sigma
Cytochalasin-D	Sigma
DAPI	Vector Laboratories
dbc cAMP	Tocris Biosciences
Dimethyl Sulfoxide	Sigma
Dual Colour Precision Plus	Bio-Rad
Dynabeads Protein G	Life Technologies AS
EGF	Sigma
EP-1-4 agonists	Ono
Ep-2, Ep-4 antagonists	Ono
FBS	Biosera
Forskolin	Tocris Biosciences
Glycine	VWR Chemicals
H89 (PKA inhibitor)	LKT laboratories
InCellect AKAP St-Ht31 inhibitor peptide	Promega
Ionomycyn calcium salt	Sigma
ITS	Sigma
L-Glutamine	BioWhittaker® Lonza
LY 294002	Tocris
ML 141	Tocris
Mounting medium	VectaShield®
Nocodazole	Sigma
NSC23766	Tocris
Nu Serum	BD Biosciences
Optimem	Invitrogen

Paraformaldehyde	Sigma
PBS (10X)	BioWhittaker® Lonza
Penicillin and streptomycin	BioWhittaker® Lonza
Phalloidin	Tocris
PKA inhibitor 14-22 amide	Calbiochem
Propidium Iodide P-4864	Sigma
Prostaglandin E2 (PGE2)	Tocris Biosciences
Protein Assay Standards II	Bio Rad
Rapamycin	Sigma
Skim Milk Powder	Oxoid
Taxol	Tocris
Thapsigargin T7458	Invitrogen
Tris Base	Fisher Scientific
Triton X-100	Sigma
TWEEN 20	Sigma
y-27632	Sigma

2.1.2 Reagents

	Compounds
SDS-PAGE Separating Gel (5%)	1.35 ml 30% acrylamide (Biorad®) 2 ml 1.5 M Tris (pH8.8) 4.5 ml dH_2O 80 µl 10 % SDS 80 µl 10 % APS 8 µl TEMED
SDS-PAGE Stacking Gel	0.67 ml 30% acrylamide (Biorad ®) 1.25 ml 0.5 M Tris (pH6.8) 3.05 ml dH_2O 50 µl 10 % SDS 50 µl 10 % APS 10 µl TEMED
Immunoprecipitation (IP) lysis buffer	150 mM NaCl 25 mM $NaPO_4$ pH 7.0 1 % Triton X-100 0.5 % Nonidet-P40 Complete protease inhibitor cocktail (Roche, Burgess Hill, UK) 50 mM NaF 2.5 mM $NaVO_3$

Phosphate buffered saline (PBS)	16 mM Na_2HPO_4 4.6 mM NaH_2PO_4 0.15 M NaCl
Tris buffered saline with tween (TBST)	8 g NaCl 10 ml 2M Tris pH 7.6 2 ml Tween 20 H_2O to 1 litre
Western blot transfer buffer	14.4 g Glycine 3 g Tris 200 ml Methanol H_2O to 1 litre
SDS-PAGE Running Buffer	14.4 g Glycine 3 g Tris 1 g SDS H_2O to 1 litre

2.1.3 Cell lines

Name	Description	Source
NIH-3T3	Mouse embryonic fibroblast cell line	A.Evans (Sheffield, UK)
IMCD3	Murine Inner Medullary Collecting Duct cells	Lorraine Eley (Newcastle, UK)
hTERT-RPE1	Human Retinal Pigment Epithelial cells	A.Fry (Leicester, UK)
HEK293	Human Embryonic Kidney cells	V.Ponnambalam (Leeds, UK)
PTEC DSRED/PC1KO	Proximal Tubule Epithelial cells DS RED control/PC1 KO cells	De Smedt H (Leuven, Belgium)
MEK PC1+/+ / PC1 -/-	Mouse Embryonic Kidney cells PC positive contol/PC1 null cells	S.M.Nauli (Toledo, USA)
MDCKII	Madin-Darby canine kidney	N. Simmons (University of Newcastle
Primary cultures of cystic tubular cells derived from ADPKD human kidneys (Described in detail in (Parker, et al 2007).		
OX161 (8+13)	Germline Mutation exon 15 (E1537X)	The generation of these cell lines has been previously reported (Parker et al, 2007)
OX938	Germline exon 16, 7000dup7	
SKI001	Germline Mutation 3904-4001aaIVS43-2A>G	
SKI002	Germline Mutation 2983-3067aaIVS25-3C>G	
UCL93	Normal cell line	
RFH	Normal cell line	
M7	PKD1 transgenic mouse kidney cells (M7)	The generation of these cell lines has been previously reported (Newby et al, 2002)
M8	non-transgenic mouse kidney cells	

2.1.4 Plasmids

Name	Description
CT2 (GST)	C-terminus polycystin-2 GST
FLAG PC1 HA	HA and FLAG tagged polycystin-1
GFP INVS plasmid	GFP tagged Inversin (*NPHP2*)
HA-INPP5E	Phosphatidylinositol-4,5-bisphosphate 5-phosphatase with an N-terminal HA tag
INPP5E-GFP	Phosphatidylinositol-4,5-bisphosphate 5-phosphatase with an N-terminal GFP tag
INVS-GFP	GFP tagged Inversin (*NPHP2*)
N PC 2 (GST)	N-terminus polycystin-2 GST
NPHP3-FLAG	FLAG tagged *NPHP3*
NPHP3-PKTAG	PKTAG tagged *NPHP3*
NPHP9-FLAG	FLAG tagged *NPHP9*
NPHP9-PKTAG	PKTAG tagged *NPHP9*
PCDNA3	Control Vector
PEBG	Control Vector
YFP-PLAT	PLAT domain with an C-terminal YFP Tag
YFP-PLAT (R3162C) Mutant	PLAT domain with an C-terminal YFP Tag Patient Mutation which prevents phosphorylation by PKA at this site
YFP-PLAT (S3164A) Mutant	PLAT domain with an C-terminal YFP Tag Mutation created in our lab, prevents phosphorylation by PKA at this site
YFP-PLAT (S3164D) Mutant	PLAT domain with an C-terminal YFP Tag Mutation created in our lab, phosphomimetic mutation is always phosphorylated and is the control of the S3164A Mutant

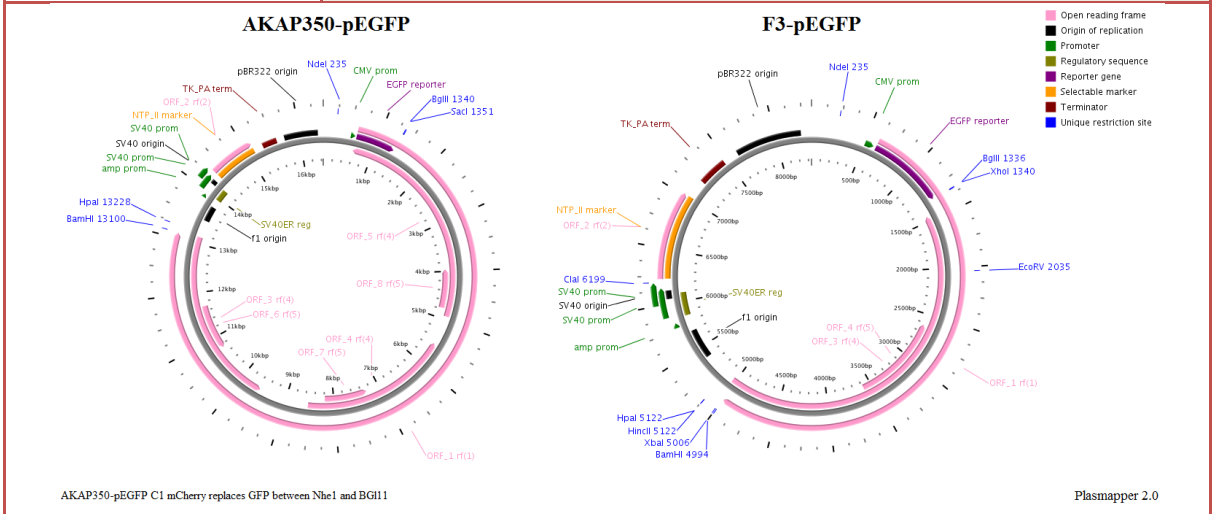

AKAP Plasmids: peGFP AKAP 350, mCherry AKAP 350 and truncated peGFP F3

2.1.5 1°Antibodies

Directed against	*Type*	*Application/ Dilution*	*Source*
HA	Rat	WB/1:1000	Roche Diagnostics Limited, Burgess Hill
HA	Rabbit	WB/1:1000	Abcam
GFP	Rabbit	WB/1:1000	Santa Cruz Biotechnology, Santa Cruz
FLAG	Mouse	WB/1:1000	Sigma
GFP	Mouse	WB/1:1000	Santa Cruz Biotechnology, Santa Cruz
GST	Rabbit	WB/1:1000	Santa Cruz Biotechnology, Santa Cruz
G20	Goat polyclonal IgG (raised against Polycystin-2 of human origin)	WB/1:1000	Santa Cruz Biotechnology, Santa Cruz
7e12	Mouse IgG1 (raised against Polycystin-1 of human origin)	WB/1:1000	Santa Cruz Biotechnology, Santa Cruz
Myc	Rabbit	WB/1:1000	Santa Cruz Biotechnology, Santa Cruz
PkTAG	Mouse	WB/1:1000	
FLAG	Rabbit	WB/1:1000	Sigma
INPP5E polyclonal	Rabbit	IS/1:1000	Proteintech
α-Tubulin	T7451	IS/1:1000	Sigma
γ-Tubulin	T5192	IS/1:1000	Sigma
ARL13b polyclonal antibody (rabbit)	Rabbit	IS/1:500	Proteintech
Ki67	mouse	IS/1:500	Sigma
Aurora A	Sheep	IS/1:1000	LifeSpan BioSciences

2.1.6 2°Antibodies (WB: Western Blot, IS: Immunofluorescence Study)

Type	*Application/ Dilution*	*Source*
Goat anti Rat	WB/1:5000	Santa Cruz Biotechnology, Santa Cruz
Goat anti Mouse IgG1	WB/1:1000	Santa Cruz Biotechnology, Santa Cruz
Goat anti mouse IgG2b	WB/1:5000	Dako
Goat anti Rabbit HRP	WB/1:5000	Santa Cruz Biotechnology, Santa Cruz
Goat anti Rabbit FITC	IS/1:1000	Santa Cruz Biotechnology, Santa Cruz
Goat anti Mouse FITC	IS/1:300	Abcam
Goat Anti-Rabbit Alexa Fluor® 594	IS/1:1000	Invitrogen

2.2 Methods

2.2.1 Mammalian cell culture

Different cell lines were cultured in DMEM-F12 media supplemented with 10% fetal bovine serum and 2mM L-Glutamine or in cell dependent modified media.
All media was provided with a streptomycin and penicillin solution. Cell growth was induced in T25 flasks until confluence and subsequently passaged at higher volumes in T75 flasks in cell dependent temperatures (33 and 37 °C) in 5 % CO_2 incubators.
Growth media was replaced every 2 days and cell passaging was performed once cells reached 90% confluency to ensure the healthy viability of cells. Cells were passaged by removing media, washing with PBS and incubation with Trypsin/EDTA at 37 ºC until cells detached from the flask surface. Trypsin was then neutralized by addition of FBS supplemented media. Cells were spun down and re-suspended in fresh media. The number of cells per volume of the new cell suspension was counted using a haemocytometer and subsequently inoculated at the desired density.

2.2.2 Freezing and thawing of cultured cells

Cryogenic preservation was routinely used for the maintenance of mammalian cells.
Prior to storage in liquid nitrogen at -196°C, cells were grown until confluence in a 75mm flask and subsequently harvested, resuspended in freezing media (DMEM, 20% (v/v) FBS, and 10% (v/v) DMSO). The suspension was then aliquoted into cryogenic vials and gradually frozen to a temperature of -85°C for 24-72 h before transfer to a liquid nitrogen freezer for long term storage.
The process of gentle cell thawing which provides a best recovery rate of cells was initiated by the removal of the vial from liquid nitrogen which was placed in a 37°C water bath for 60-90sec with gentle swirling. Next, the cryoprotective agents were removed by transferring the suspension to a sterile 15ml tube with fresh media, followed by centrifugation at 1000×rpm and removal of the old media. The pellet was resuspended in 10ml fresh medium and then transferred to a suitable flask for normal incubation.
Cells were routinely tested for mycoplasma infections by laboratory managers.

2.2.3 Specific growth media protocols

Culture media of a control non Knock down PTEC cell line (PTEC DS RED) and a Polycistin-1 Knock down PTEC line (PTEC PC1 KD) which was generated using lentiviral vectors (Mekahli et al, 2012). Culture of this cell lines was modified according (Mekahli et al, 2012) and was set up as follows: Growing conditions at 33C°and 5%CO2 with full supplemented DMEM-F12 with addition of insulin (5 g/ml), transferrin (5 g/ml), selenium (5 ng/ml), hydrocortisone (36 ng/ml), epithelial growth factor (10 ng/ml), and tri-iodothyronine (40 pg/ml). Stable selection pressure towards the PC1 KD and DS RED vector is achieved by addition of 10 g/ml Blasticidin previous to each inoculation or cell passage. Starving conditions are set with serum free media at 37 C° and 5% CO2.

The different PKD mutant used in this study are listed in Materials section and were mainly isolated from cysts of PKD patients. As our control, I used the non-cystic epithelial cell line (UCL93-3-6) which was derived from a normal human kidney for clinical indications and was used routinely as our control model for normal kidney cells (Parker et al, 2007).

Growing conditions for these cell lines were at 33C°and 5%CO2 while starving condition were set with serum free media at 37 C° and 5% CO2. Growth medium was DMEM-F12 with 5 % FBS, 1% L-Glutamine and 1% Pen/Strep antibiotics.

2.2.4 Primary cilium study

The beginning of our study was initiated by the inoculation in serum supplemented media of an experimental cell line capable of primary cilium formation. The first phase is characterized by a mitotic cell expansion with low levels of ciliated cells. The subsequent phase begins when cell expansion reached approximately 70-80% confluence. At this point the media was replaced with serum free media for 48 h to allow serum deprivation induced cell cycle exit, thus primary cilia formation. The last phase is induced by reintroduction of serum for a determined amount of time until primary cilia number returns to a comparable level before starvation. During each stage of the analysis, cells were collected, fixed and stained for fluorescence microscopy.

2.2.5 Cell fixation and Immunofluorescence

For immuno-fluorescence studies, different cells were grown on coverslip until reaching confluence. Next, at room temperature growth media was removed and the coverslips are rinsed with PBS prior to an incubation step for 15 min in 4 % paraformaldehyde to achieve cell fixation. Subsequently, cells were briefly permeabilized in a 0.1 % Triton X-100 solution for 2 min. Next, cells were washed three times with a PBS solution and then blocked in a 5% bovine serum albumin (BSA) in the PBS solution for 1 h. The BSA was then removed and after a repeated washing step with PBS, cells were incubated with the primary antibody for 1 h at room temperature or over-night at 4 C°. Finally, after another 3X PBS washing step, cells were incubated with the secondary antibody for 1 h and then the coverslips mounted with Vecta-Shield mounting medium and DAPI on a microscope slide and the edge sealed with DPX resin. A wide variety of poly- and monoclonal antibodies can be used to specifically stain the primary for immunofluorescence microscopy. For the scope of a high quality of primary cilium detection, antibody combinations were adapted and changed according to the cell lines used or the scope of the assay. Antibodies for primary cilium detection included Acetylated tubulin, which is known to stain alpha tubulins present in the primary cilium (Alieva et al, 1999) or ARL13b which was later kept as a standard for its ability to exclusively stain the primary cilium while the Acetylated tubulin in some instances stained also microtubules of the mid-body and some cytoplasmic microtubules. In some instances I also used γ-tubulin, which in interphase marks the position of the centrioles and basal bodies found as two dots at the base of the cilium (Liang et al, 1996). DAPI was used by default to stain for the cell nuclei and enhance cell detection. I was able to detect primary cilia formation after a starvation step which peaked between 48 h and 72 h after induced starvation. I decided to choose the 48 h starvation step for our study, since prolonged periods of starvation in some cases resulted in a general decrease of cell number on the coverslip possibly due to cell death or detachment of the starved cells.

2.2.6 Primary cilia treatments

Different compounds including cAMP or Thapsigargin were tested for their ability to regulate ciliary length. The design of the experiment based on the study of (Besschetnova et al, 2010), were the cilium status was evaluated within 3 h after addition of the bioactive compounds. Treatment with these compounds was carried out with a range of different concentrations and cilium length was measured via immunofluorescence microscopy on Olympus IX71 and length assisted detecting software package, SimplePCI (Hammamatsu).

Initial concentration and optimization studies of new tested compounds used in our experiments ranged above and below concentrations previously used in other studies (Besschetnova et al, 2010). All treatments with inhibitors of ciliary regulators e.g. PKA inhibitors, agents like H89 (50 µM) and 14-22 Amide (20µM) (Farrow et al, 2003) were used for 1 h prior to incubation with ciliary regulating compounds + inhibitors at the same concentration as the pre incubation step. DMSO and dH2O were used to dilute the bioactive compounds and a DMSO control was carried out with no alteration on ciliary length.

2.2.7 Nocodazole resistance assay

Nocodazole resistance assays were performed to test the ability of cells to withstand tubulin depolymerizing agents i.e. nocodazole. The assay consisted of a short treatment (30 min) of normal and ADPKD models with a high concentration of nocodazole (5 µM) followed by consecutive washes with 1% Triton to remove destabilized tubulin. Cells were then stained for α-tubulin and analysis of residual microtubule levels was performed via microscopy imaging. Cells with residual tubulin were counted as resistant and counted against cells without any tubulin.

2.2.8 Measurement of primary cilium number and length

Primary cilia number and primary cilia length was measured with Hamamatsu SimplePCI image analysis software provided with the Olympus fluorescent microscope.

Primary cilia number was measured in 3 individual experiments with an independent coverslip and time point. For each coverslip triplicate, a number of > 100 cells were analyzed. Images were taken at 60x magnification from random coverslip fields. Number of ciliated cells was counted via SimplePCI and correlated to the number of non-ciliated cells.

Primary cilia length was measured in 3 individual experiments as described above. Images were taken at 60x magnification from random coverslip fields. The length of primary cilia was measured with tools provided by SimplePCI software. Functions provided in the SimplePCI software, included precise length analysis tools for straight or curved cilia.

2.2.9 Wound healing protocol and cilia orientation measurement

Cells were plated on coverslips and incubated until reaching confluence. A 200ml sterile pipette tip was used to mark straight scratch from the top to the bottom side of the coverslips. Multiple coverslips were scratched marking different time points ranging from 0h (start time point) to 24h (end time point). Coverslips were collected between this ranges and after paraformaldehyde fixation and antibody staining, prepared for fluorescent microscopy analysis for the visualization of cilia orientation. Antibodies used where DAPI for cell nuclei, acetylated tubulin for primary cilia and gamma tubulin for basal bodies.

Measurement of cilia orientation was achieved via analysing software (Image J). Primary cilia orientation was measured by analysis of the orientation angle after different time points of the migration assay. Using Image J, a leading line was marked on the primary cilium starting from its tip in direction to its base (basal bodies were used as orientation markers). From the base of the cilium, a subsequent line was marked which pointed orthogonally in the direction of the scratch. The angle between the two lines of each cilium was recorded and collected as cilium orientation data for further analysis.

2.2.10 Immunohistochemistry

Staining of paraffin sections: Slides were dewaxed with xylene for 3x for 5 min each.
Rehydration was achieved through alcohol incubation:
100% alcohol for 5 min for 2x each, 95% alcohol 5 min, 70% alcohol 5 min.
Sections were immersed in 500ml trisodium citrate (1.47g pH 6.0) and transferred to a microwave for 10 min at 500W. Subsequently, the slides were cooled in ddH2O.
Slides were blocked for 30 min wirh X0909 protein block (Dako), then primary antibody at 1/100 concentration were added and incubated for 1 h at room temperature.
Slides were washed 2x with PBS for 5 min, then secondary antibody at 1/200 concentration were added for 1 h at room temperature. Slides were washed 2x with PBS for 5 min and then left to dry prior to addition of vectorshield hard set mounting medium with DAPI. Slides were wrapped in foil and incubated O/N

2.2.11 Mammalian cell transfection

24h before transfection, 1-3×10^5 cells were plated in standard growth medium + antibiotics per 35-mm dish (6-well plate) and incubated at 37°C (5% CO2) overnight. Optimal transfection was reached with cells at 70–80% confluence.

Lipofectamine

Lipofectamine® (Invitrogen) is a transfection reagent based on the propriety of its lipid subunits to form artificial vesicles in an aqueous environment composed of a lipid bilayer called liposomes. These liposomes are able to entrap transfection materials and overcome the electrostatic repulsion of the cell membranes. Cell Transfection was usually performed in 12 well plates with a 70% confluent HEK cell monolayer. Before transfection culture media was replaced with Antibiotic/Antimycotic free media to prevent cell death during transfection procedure.
Lipofectamine and 0.5 µg DNA were first added to separate Eppendorf containing 100 µl Optimem each, and gently mixed and incubated at room temperature for 5 min. Subsequently, the DNA/Optimem was added to the Lipofectamine/Optimem solution, gently mixed by pipetting and allowed to interact by an incubation step of 15 min at room temperature. Next,

the solution was added dropwise across the surface of the inoculated plate and gently rocked to allow an even distribution on the cells. Plates with transfected cells were incubated at 37 °C with 5 % CO_2 for 48h before harvesting or further analysis.

GeneJuice

Transfections with GeneJuice® Transfection Reagent (Novagen, USA) were performed according to the manufacturer's instructions. The mechanism of action of this compound is similar to lipofectamine. In a sterile Eppendorf, 100µl of serum-free media (Opti-MEM) was mixed with 3µl of the provided GeneJuice® Transfection Reagent followed by an incubation step of 5 min. As with lipofectamine, 1µg of DNA is then added to the mix and gently mixed by resuspending followed by another incubation step of 15 min. The GeneJuice/DNA solution is then added to the cells and gently rocked to ensure an even distribution. Transfected cells are then incubated at 37°C with 5% CO2 for 24–48.

2.4.12 Co-immunoprecipitation

Co-immunoprecipitation (Co-IP) is a standard method routinely used to analyze putative protein-protein interactions in mammalian cells. As a brief overview: Specific antibodies selected for their ability to target a protein of interest or target protein A are immobilized to a solid support, such as sepharose G beads or magnetic beads. These beads are the inserted in a total cell lysate, were they specifically bind and capture the target protein, leaving all other proteins not specific to the antibody unbound in the solution. When then the protein is precipitated, any other proteins which are able to bind to target protein will co-precipitate and accumulate on the pelleted beads. Any other proteins not precipitated or not able to strongly bind by the immobilized Protein are washed away leaving a pool of potential interacting partners. The bound protein complex is then eluted from the solid support for further analysis by SDS-PAGE and western blotting.

A more detailed description of this method will be described with the example of the *INPP5E*/*PLAT* interaction experiment described in result chapter 5.2

A YFP tagged *PLAT* construct (YFP-*PLAT*) was co-transfected with an HA tagged *INPP5E* construct in HEK293 cells in a 12 well plate. 1600 ng DNA of each of the two constructs was transfected per well. A positive control of YFP tagged *PLAT* (YFP-*PLAT*) and HA-tagged *INPP5E* (HA-*INPP5E*) was also carried out. Negative controls replacing YFP-*PLAT*

constructs with pcDNA3 were also done. Transfected cells were lysed 24h/48h after transfection with 500µl lysis buffer which was added to each tube and incubated at 4°C for 30min in a rotator. The samples were then centrifuged at maximum speed 13,000 rpm for 5 min to pellet the cell debris and subsequently the supernatant was transferred to a new tube for further analysis, i.e. protein concentration measurement as described in (methods section 2.7). All following steps were performed at 4°C on ice and using cooled centrifugation. From the resulting protein lysates 20 µl were removed as a lysate control and stored in ice. Samples (250 µg) were subsequently incubated with GFP or HA tagged primary antibody and incubated at 4°C for 1h in a rotator. *PLAT*-GFP was precipitated with rabbit-GFP while *INPP5E*-HA was precipitated with rabbit HA (2.5 µg antibody per immunoprecipitation).
Simultaneously, a bead equilibration step on Dynabeads® beads was performed by resuspension of 30 µl per sample of beads in 1 ml IP lysis buffer and removal of the supernatant after each centrifugation step. This was repeated for 3X to complete the washing step. After the incubation step the cell lysates were cleared to remove endogenous antibodies. For the immunoprecipitation the protein/antibody sample was incubated at 4 °C for 15 min with 30 µl equilibrated magnetic beads on a rotator. To remove unspecific bindings, samples were subsequently washed 3X by resuspension of samples in 500 µl IP lysis buffer following separation step on a magnet. Next, bead conjugated samples were re-suspended in 20 µl 2X Loading Buffer + ß-Mercaptoethanol and denatured together with total lysate samples in heating block at 37 °C for 30 min. Finally, samples were placed in the magnet separating the beads from the in the supernatant residing protein of interest which was subsequently transferred into a clean microfuge tubes and analysed by SDS-PAGE (methods section 2.8) and western blot (methods section 2.9). The Western blot membranes were probed accordingly with antibodies raised in different species compared to the antibodies used for immunoprecipitation.

2.4.13 GST pull-down assay

The GST pull-down assay is a standard *in vitro* method routinely used to test for direct physical interactions between a GST (Glutathione S-transferase) fusion protein and another protein. For this technique the protein of interest is incubated with the GST fusion protein (for a total amount of 1-2µg each) for 1h with gentle rotation to allow binding. Glutathione Sepharose 4B beads were washed and 40µl added to each sample followed by another hour of

incubation on the rotator at 4°C. Next, centrifugation at 6000rpm for 2min is applied to sediment the beads and the supernatant is discarded. A washing procedure is applied by with 1ml of cold 1×PBS (pH7.3) for 4-6 times to remove unbound proteins. To elute the protein from beads a heating step was performed in reducing sample buffer for 5-10min at 70°C or 1h at 37°C depending on the protein of interest. Then, the samples were spun at 13,000rpm for 1min to pellet the beads and the supernatant transferred to a fresh tube. The sample is mixed with an equal amount of 2× gel loading buffer for further analysis by SDS PAGE and Western blotting.

2.4.14 Protein concentration assay

The assessment of the protein concentration of cell lysates was performed using a Bio-Rad DC protein assay kit according to the manufacturers protocol. A standard curve was first created using a BSA (bovine serum albumin) solution of known concentration and generating dilutions in IP lysis buffer ranging from 0 to 1.4 mg/ml in (protein standards). For the measurement of our proteins of interest, a cell lysate of a transfected cell line had to be produced. To ensure adequate cell yield cells from a PBS pre-washed inoculated 12 well plates were inoculated with IP lysis buffer and then scraped and transferred into relevant labelled microfuge tubes and incubated on a rotator at 4 ºC for 30 min. Subsequently, the tubes were centrifuged at maximum speed to separate the cell debris and then supernatant cell lysates were transferred to new labelled microfuge tubes and either prepared for western blot analysis or further diluted for a protein concentration assay. To measure protein concentration 5 µl of each of the BSA standard dilution and protein samples were carefully pipetted in triplicate in a 96 well elisa plate. Next 25 µl reagent S was added followed by 200 µl reagent B and incubated at 37°C for 15 min. Absorbance was measured at 750 nm and protein concentrations were calculated based on the standard curve.

2.4.15 SDS-PAGE

SDS-PAGE is widely used as a tool to separate proteins according to their size. The running gel was prepared according the recipe (Table below) and cast in a Mini-Protean II™ apparatus and subsequently covered with 100 % ethanol, and allowed to polymerize. After solidification of the running gel, the ethanol was replaced with a stacking gel and fitted with

wells prior to solidification. Next, the prepared gels were placed in the tank and the inner and outer chambers were filled with 1x running buffer. Before loading on the gel, protein samples were incubated for 30 min at 37°C in 2 × SDS-PAGE sample buffer and ß-mercaptoethanol to allow protein denaturation and subsequently loaded alongside Dual Colour Precision Plus molecular weight markers via micropipette. The gel was then run at 100 V for 15 min and the voltage subsequently increased to 200 V until the sample buffer dye had run off the gel. Once electrophoresis is complete, the gel was removed and transferred to PVDF membranes for western blot.

Recipe for separating gel						Recipe for stacking gel
(4 pieces)	5%	7%	10%	13%		4%
dH2O	9ml	8ml	6.3ml	4.7ml		3.05ml
1.5M Tris-HCl (pH8.8)	4ml	4ml	4ml	4ml	0.5M Tris-HCl (pH 6.8)	1.25ml
Acrylamide (30%)	2.7ml	3.7ml	5.4ml	6.9ml		0.67ml
10% SDS	160µl					50µl
10% APS						50µl
TEMED	16µl					10µl

2.4.16 Western blot

Western Blot involves a technique were the separated proteins from a polyacrylamide gel are transferred to a PVDF membrane which is subsequently stained with antibodies for the detection of target proteins. The transfer is performed using a Bio-Rad Mini Trans-Blot cell. To remove the hydrophobic propriety of the PVDF membrane, it is first incubated for 30 seconds in 99.8% Methanol and then washed thoroughly with dH_2O. The gel is subsequently placed on the activated membrane and enclosed in two squares of filter paper and two sponges on each side before soaked in transfer buffer. The assembled gel-membrane is placed

facing the negative side of the rack so that the transfer of the protein occurs in direction membrane. The rack was placed in the BioRad apparatus. A stirrer and a cool pack was subsequently added and finally the machine filled with transfer buffer. The transfer was adjusted according to the size of the protein of interest at 100V for 1 h. Subsequently, the membrane was removed and incubated in 10% milk in TBST for 1 h to block. Next, the membrane is probed with the primary and secondary antibody. First, a washing step was performed on the membrane by shaking 4 times for 20 min in TBST. Then, the primary antibody was diluted in a TBST solution with 5% milk and subsequently added to the membrane in a tray for over-night incubation at 4°C. On the next day, another washing step in TBST is performed, and then the membrane was probed with a HRP conjugated secondary antibody diluted a TBST solution with 5% milk for 1h at R.T. A last washing step in TBST was performed before the membrane is treated with a Biorad Clarity ECL kit.
After treatment with BM kit, the membrane was either brought to a Biorad Chemidoc XL system or exposed to SuperRX Fuji Medical X-Ray Film.

2.4.17 *E.coli* transformation with plasmid DNA

E.coli preparation and transformation with plasmid DNA was performed using a standard transformation protocol.
E coli JM109competent cells stored at -80°C were thawed on ice and 50µl samples were aliquoted in pre-chilled 1.5ml Eppendorf tubes. Next, 50ng of plasmid DNA was added to the 50µl cell samples gently mixed and then left on ice for 30 min. A heat-shock step was induced on the samples, consisting of a brief incubation of the sample at 42°C for 50 seconds followed by rapid cooling on ice for 2 min. Cold SOC medium (450 µl) was then added to the samples and incubated at 37°C for 1 h in a shaker at 200 rpm. The transformation mixture was ultimately plated on LB agar antibiotic selective plates and incubated overnight at 37°C until positive transformed colonies appeared.

2.4.18 Small-and medium scale purification of plasmid DNA

For the preparation of plasmid DNA in small (or medium) scale a Wizard® Miniprep Plus SV DNA purification system (Promega) was used. First, 5-10ml (or 100ml) of overnight culture from a single colony were transferred into 20ml (or 50ml) tubes and centrifuged at 5000rpm

for 5 min at room temperature to pellet cells. The pellet was re-suspended in 250µl (or 3ml) cell resuspension solution (50mM Tris-HCl pH7.5, 10mM EDTA pH8.0, 100g/ml Ribonuclease A). Next, 250µl (3ml) of cell lysis solution (0.2M NaOH, 1% SDS) were added to each sample and subsequently mixed by inverting the tubes four times and incubated at room temperature for 5 min. Then 350µl (3ml) of neutralization solution (760mM (x2) potassium acetate, 2.12M glacial acetic acid) was added to the cell lysate, mixed and then centrifuged at 13,000 rpm for 15 min at room temperature. The supernatant clear lysate was transferred into a spin column (or Midi column mixed with 10ml resin by swirling). The Column was then spun at 13,000 rpm for 1 min to let supernatant pass through the resin layer (or a vacuum was used to pellet the resin in the Midi column). Washes are then performed with 750µl (or 15ml) Column Wash Buffer (60% ethanol, 60mM potassium acetate, 8.3mM Tris-HCl, 0.04mM EDTA) and then the plasmid DNA was eluted with 100µl (300 µl) of nuclease-free ddH2O (preheated to 70°C and centrifugation at 13,000 rpm for 1min and then transferred in a 1.5ml Eppendorf tube at 10,000×g for 2min to remove extra liquid. The purified plasmid DNA was stored at -20°C or below.

2.4.19 Restriction digestion and agarose electrophoresis

Digestion of Plasmid DNA was performed via restriction endonucleases at 37°C for 2 h in an appropriate enzyme buffer. The resulting digestion product was analyzed by agarose gel electrophoresis. Agarose gels were prepared by dissolving agarose in 1×TAE and addition of ethidium bromide at 0.5µg/ml concentration. The DNA samples of interest were mixed with 6×Blue/Orange loading dye and subsequently loaded in the agarose gel wells together with DNA ladder. Electrophoresis was then performed using the Bio-Rad mini-sub cell GT or wide mini-sub cell GT system at a voltage of 5V/cm in running buffer (1×TAE, diluted from 50×TAE stock solution (2M Tris base, 5% (v/v) glacial acetic acid, and 0.05 M ETDA pH 8.0). Visualization and imaging of bands on the gel was performed with the Biorad Chemidoc XL machine.

2.4.20 Validation of siRNA knockdown by qPCR

UCL93 and IMCD3 cells were cultured in 12 well plates to 75% confluency. Isoform-specific siRNA to mouse *inpp5e* (IMCD3) and human *Inversin* (UCL93) was chemically synthesized by Dharmacon or MWG Biotech respectively. A scrambled negative control siRNA was obtained from Dharmacon. Transfection of 10 and 50 nM siRNA into cells was achieved using RNAiMax reagent (Life Technologies). Knockdown was confirmed by Taqman qPCR 72 h post-transfection according to the manufacturer's protocol (Life Technologies). Following RNA extraction, cDNA was synthesised using a high capacity RNA to cDNA kit (Life Technologies). Real time PCR was carried out on an ABI7900 qPCR machine. Normalisation of expression was carried out using specific taqman probes to mouse or human GAPDH. Results presented are representative of 3 replicate experiments. Analysis of gene expression was carried out using DataAssist v3.01 (Applied Biosystems) to calculate 1/ΔCt normalised expression values for each cell line. Data was plotted in Graphpad Prism and p-values >0.05 (adjusted for Benjamini-Hochberg False Discovery Rate) were defined as significant. Relative quantification was also carried out using the comparative Ct (ΔΔCt) method to calculate fold changes in expression between control and siRNA samples.

Cycling conditions for qPCR:

50°C	2 min
95°C	10 min
95°C 60°C	15 sec 1 min **x40**

qPCR reaction mix:

Component	Volume (µl) per reaction
Taqman Universal PCR master mix (2x)	10
Taqman gene expression assay (20x)	1
cDNA template (50ng) + water	9

2.4.21 Special equipment

Super-resolution microscopy also known as structured Illumination Microscopy or (SIM) is a fluorescence light microscopy method which I used in our study for detailed actin structure detection. This microscopy method is designed to record images with a resolution below that of the Abbe diffraction limit, thus removing the limitations imposed by the diffraction of light during the observation of normally not resolvable biological structures via conventional microscopy. The functional basis of the SIM is based on the use of structured spot illumination, which replaces standard uniform illumination. These allows for the generation of multiple different patterns of the same area, which remain within the diffraction limit and can subsequently be reconstructed and merged via programmed software with precise knowledge of pattern location into a final super resolution image. The reconstructed image results in an approximate two-fold improvement compared to diffraction limited imaging (Dempsey et al, 2011). Samples were prepared on high precision coverslips and mounted one per slide to allow placement in the centre of the microscope sample holder due to the super microscope limited travel.

2.4.22 Mycoplasma test

Mycoplasma test were performed by laboratory managers. The test was executed by providing cell culture supernatant into a 2ml centrifugation tube, which was subsequently analyzed with an EZ-PCR Mycoplasma Test Kit from BIOLOGICAL INDUSTRIES (BI) according to the provided protocol. Tests were performed routinely on a monthly basis for all laboratory cell lines.

2.4.23 Ethic section

The research project was approved by the relevant university ethics committee and/or meets the ethical guidelines issued by such and such a learned society.

Where applicable, the origin of cell lines and tissues used this study are protected by confidentiality and anonymity.

The studies in this dissertation were performed in an independent and impartial manner. No conflicts of interest to declare.

2.4.24 Statistic section

Statistical analysis was performed with Graph-pad Prism software.
Statistical test used in this thesis were:
t-test or Student's t-distribution under the null hypothesis which determines if two sets of data are significantly different from each other and in our study was used for direct comparison experiments.
two-way-Anova or two-way analysis of variance (ANOVA) which analyzes the influence of two different categorical independent variables on one continuous dependent variable and in our study was used to test for experiments involving multiple comparisons/treatments.
The significance of the p value in each graph was displayed in symbols described below.

Symbol	Meaning
Ns	$P > 0.05$
*	$P \leq 0.05$
**	$P \leq 0.01$
***	$P \leq 0.001$
****	$P \leq 0.0001$ (For the last two choices only)

Chapter III

Primary cilia formation and regulation in ADPKD

3.1 Introduction

The first studies linking the pathogenesis of ADPKD to primary cilia were based on the ciliary localisation of polycystin-1 (PC1) and polycystin-2 (PC2) (Yoder 2002; Pazour et al, 2002). It was suggested that polycystin-1 and polycystin-2 could transduce a mechanosensitive or ligand activated receptor complex, functionally defective in disease (Ong, 2005). Unlike mutations in other ciliary proteins e.g. Tg737/polaris, cilia were assumed to be structurally normal indicating a functional defect. Recently, data from another ciliopathy i.e. mutations in *Inpp5e*, indicated that cilia could be structurally normal yet disassemble faster than their normal controls (Jacoby et al, 2009).

The main hypothesis of this project is to test the role of primary cilium stability in the pathogenesis of ADPKD. First, a robust assay for primary cilium assembly and disassembly was established. Secondly, the role of key signalling pathways known to be altered in disease especially cAMP and Ca^{2+} on this process was examined.

3.2 Primary cilia formation in baseline models

It is well known that many cells can be induced to exit the cell cycle after short periods of growth factor starvation (Larsson et al, 1985). Several cell lines were initially tested for their ability to exit and enter the cell cycle according to serum stimulation and starvation, a critical precondition for the formation of primary cilia (Plotnikova et al, 2009). These baseline models included a mouse embryonic fibroblast cell line (NIH-3T3), a murine inner medullary collecting duct cell line (IMCD3) and a human retinal pigment epithelial cell line (hTERT-RPE1). The cell cycle profile of these lines was studied during serum stimulation and serum removal. As expected, a significant decrease in G2 phase cells and an increase in G1 phase cells was observed in all three cell lines after serum starvation of 48 h (**Figure 3.1 a, b, c)**. Reintroduction of serum after the starvation step induced a decrease in G1 phase cells and increase in mitotic G2.

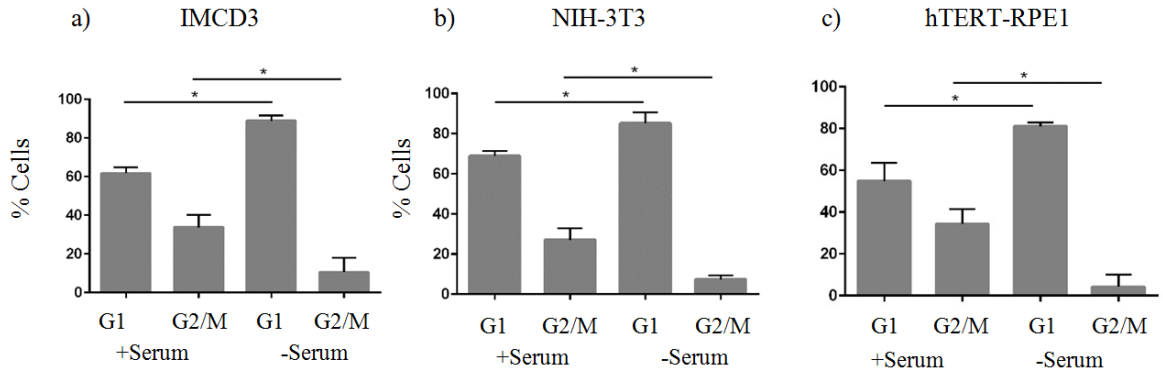

Figure 3.1 Cell Cycle analysis in IMCD, hTERTRPE and NIH 3T3. Flow cytometric analysis of serum starved (a) IMCD3, (b) NIH-3T3, (c) hTERT-RPE1 baseline models results in an increase in G1 phase cells, and a decrease in G2 phase cells. (n=3, Statistical test:paired t- test) (* = $p \leq 0.05$, Error bars indicate mean ± S.E.M).

Primary cilium assembly and disassembly is associated with different phases of the cell cycle (Plotnikova et al, 2009). Cilium formation occurs post-cytokinesis during the G1/G0 phase of the cell cycle and cilium disassembly during the G2–M transition. Optimization experiments were carried out on each cell line to ensure optimal primary cilium detection as described in methods (**chapter 2.2.4)**.

A low percentage of cilia were detected in pre-starved cycling cells: 21% ± SEM in hTERT RPE1, 18% ±SEM in IMCD3, 17.5% ± SEM in NIH 3T3. A significant increase in the number of ciliated cells could be clearly measured in IMCD3, NIH-3T3 and hTERT-RPE1 following a 48 h period in serum free medium **(Figure 3.2)**. This was quantified as a 50% increase in IMCD3 and NIH-3T3 (**b, c)** and a 43% increase in hTERT-RPE1 (**a**) for a total ciliation level of 71% ±SEM, in IMCD3, 73% ±SEM in NIH 3T3 and 64%± SEM in hTERT-RPE1. Following the reintroduction of serum, resorption of cilia between each cell line was variable during the first hours after serum reintroduction. Primary cilium disassembly could be detected as early as 2 h after serum reintroduction and was complete by 24 h. A moderate rate of cilium disassembly ranging from 10 to 20% was measured in hTERT-RPE1 and IMCD3 (**a, c)** cells, while disassembly was more extensive in NIH-3T3 cells with a 36% decrease in ciliated cells **(b)**. Cilium disassembly did not progress in the hTERT-RPE1 and IMCD3 cells at 6 h serum reintroduction but then significantly increased after this period in prolonged periods ranging from 6 to 24 h following serum reintroduction. In the NIH-3T3 cell line, cilium disassembly declined in a slower manner reaching baseline pre-starvation levels at 24 h. This data confirms previous reports that the assembly and disassembly of primary cilia is tightly associated with the cell cycle (Plotnikova et al, 2009).

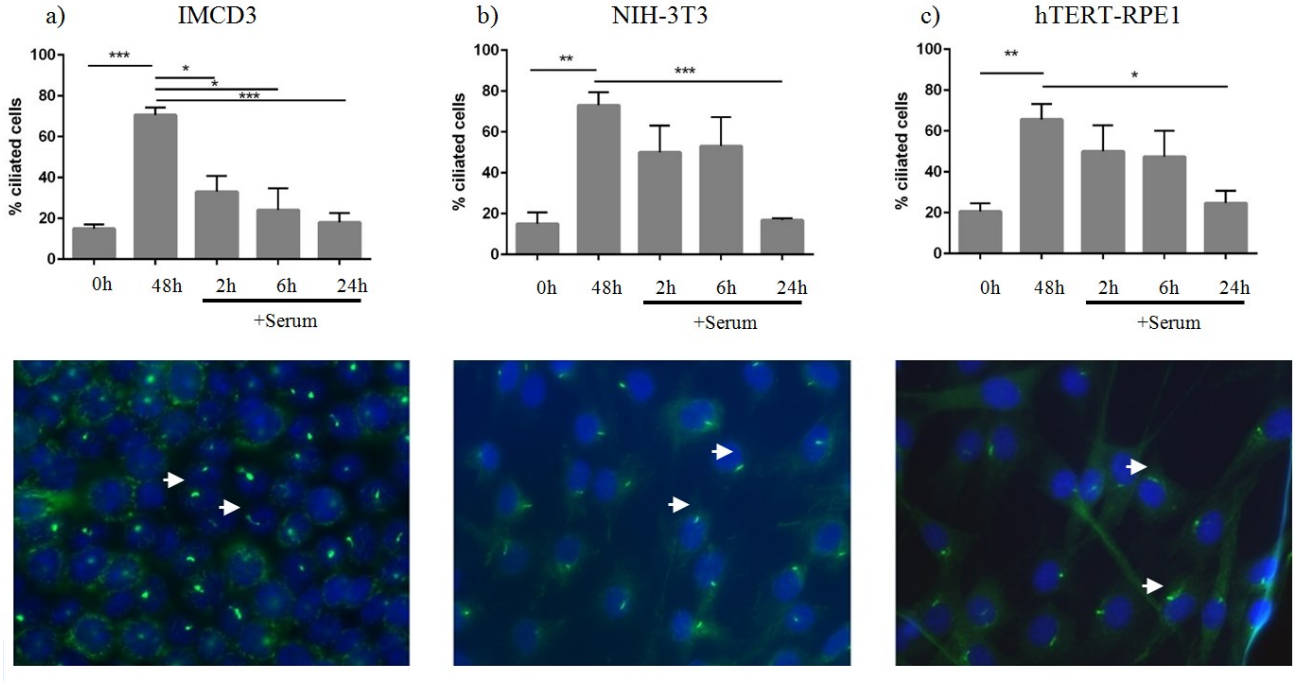

Figure 3.2 Primary cilium assembly and disassembly before, during and after serum removal. Pre-starvation. A low percentage of cilia were detected in pre-starved cells. After 48 starvation, number of ciliated cells significantly increases in **(a)** IMCD3, **(b)** NIH 3T3 and **(c)** hTERT RPE1cells. Re-introduction of serum results in a significant gradual primary cilium disassembly over a period of 24 h in all tested cell lines, comparable to initial pre-starved levels can be detected in all tested cell lines 24 h after serum reintroduction. (n=3, Statistical test:paired t- test) (* = $p \leq 0.05$, Error bars indicate mean ± S.E.M). Representative images of ciliated cells IMCD3, RPE1 and NIH-3T3 at 48h starvation time-point. Magnifications 40X. Cell nuclei (DAPI: Blue) and primary cilia (acetylated tubulin: green) are indicated by the arrows.

3.3 Primary cilia length regulation

Previous reports had suggested that agents acutely increasing cAMP and Ca^{2+} could also alter cilia length (Besschetnova et al, 2010). The effect of increasing cAMP and Ca^{2+} was therefore tested in these baseline models. For cAMP, an increase in intracellular basal cAMP from 1 μM to 10 μM is required to reach the activation threshold for protein kinase A (PKA) (Houslay and Milligan 1997).

Following treatment with compounds that increased the intracellular level of cAMP, a comparable response could be detected in all tested cell lines resulting in a significant increase in primary cilia length (**Figure 3.3**). Comparison of the effect of dibutyryl cAMP (dbcAMP) and forskolin resulted in a similar dose dependent increase in average cilia length, reaching a maximum at 500 μM dbcAMP and 500 μM forskolin, while treatment with Thapsigargin, a compound which release intracellular calcium stores resulted in in a modest decrease in ciliary length in all three cell lines.

In μm n=4	Untreated	dbcAMP 500 μM	Forskolin 500 μM	Thapsigargin 5 μM
IMCD3	2.0 ± 0.1	3.4 ± 0.2	3.7 ± 0.2	0.7 ± 0.2
NIH-3T3	2.15 ± 0.1	3.1 ± 0.1	3.9 ± 0.2	0.5 ± 0.2
hTERT RPE1	2.6 ± 0.2	3.9 ± 0.1	4.2 ± 0.2	0.6 ± 0.2

This data confirms that modulation of intracellular Ca^{2+} and cyclic AMP is able to alter cilium length to various degrees in all three cell lines.

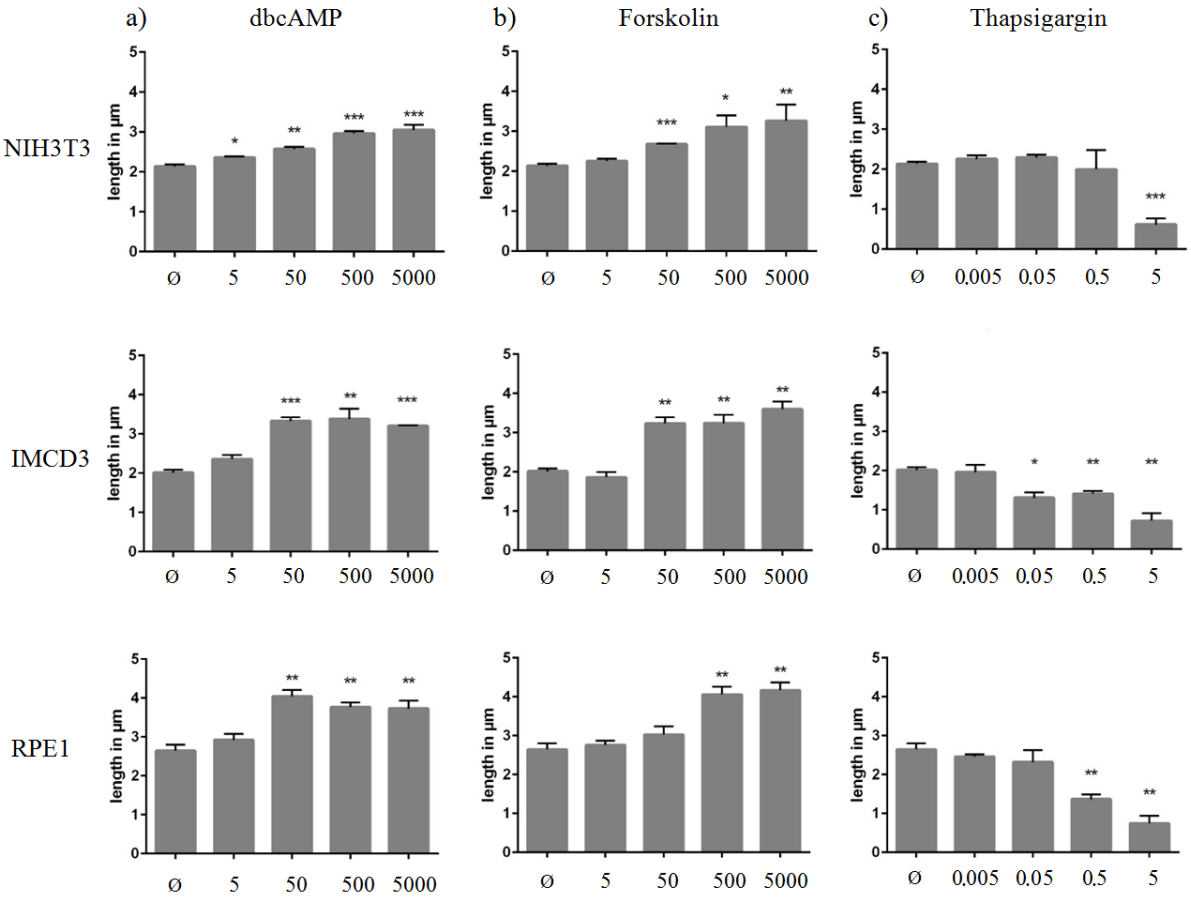

Figure 3.3 Primary cilium length can be modulated by cAMP and Ca^{2+} elevation in baseline models.

a) Increase in intracellular cAMP via dbcAMP or **b)** Forskolin treatment for a treatment period of 3h post-starvation results in a dose dependent primary cilium elongation in all tested baseline models. **c)** Conversely, treatment with Thapsigargin, which releases intracellular Ca^{2+} results in primary cilium shortening at high concentration. (n=3, Statistical test:paired t -test (* = $p \leq 0.05$), Error bars indicate mean ± S.E.M)

3.4 Primary cilia formation in ADPKD models

For the study of primary cilia dynamics in ADPKD models, a number of conditionally immortalised human kidney cell lines normal or deficient in polycystin-1 were studied. Two paired models were mainly studied: UCL93-6-2 (normal human), OX161 (8+13) (*PKD1* mutant) and PTEC-DSRED (control shRNA), PTEC-PC1 KD (shRNA *PKD1* kd). For uncertain reasons, the expression of polycystin-1 in the PTEC-PC1 KD cells showed partial recovery at later passages (**Figure 3.4 e**). These cells were therefore studied at early passages (up to P4) where shRNA kd was maintained.

Serum starvation and temperature switching from 33C° to 37C° induced cell cycle exit similarly in ADPKD cells (**Figure 3.4 b**,**d**) and normal controls (**Figure 3.4 a**,**c**). This was marked by a significant increase in G1 cells and a decrease in S/G2 phase cells. These conditions were therefore used to study primary cilium formation in normal and ADPKD models in subsequent studies.

Similar to the baseline models, both normal and ADPKD models showed a similar pattern of ciliary assembly and disassembly in response to serum removal and reintroduction. (**Figure 3.5 a**, **b**). Comparable results were obtained for PTEC PC1+PC2 KD cells (**Figure 3.5 d**). However, the percentage of ciliated cells (**Figure 3.6 a**, **b**) and the average primary cilium length (**Figure 3.6 c** ,**d**) was significantly decreased in the polycystin-1 deficient models relative to their normal controls.

These unexpected results suggest that polycystin-1 could regulate cilia structure.

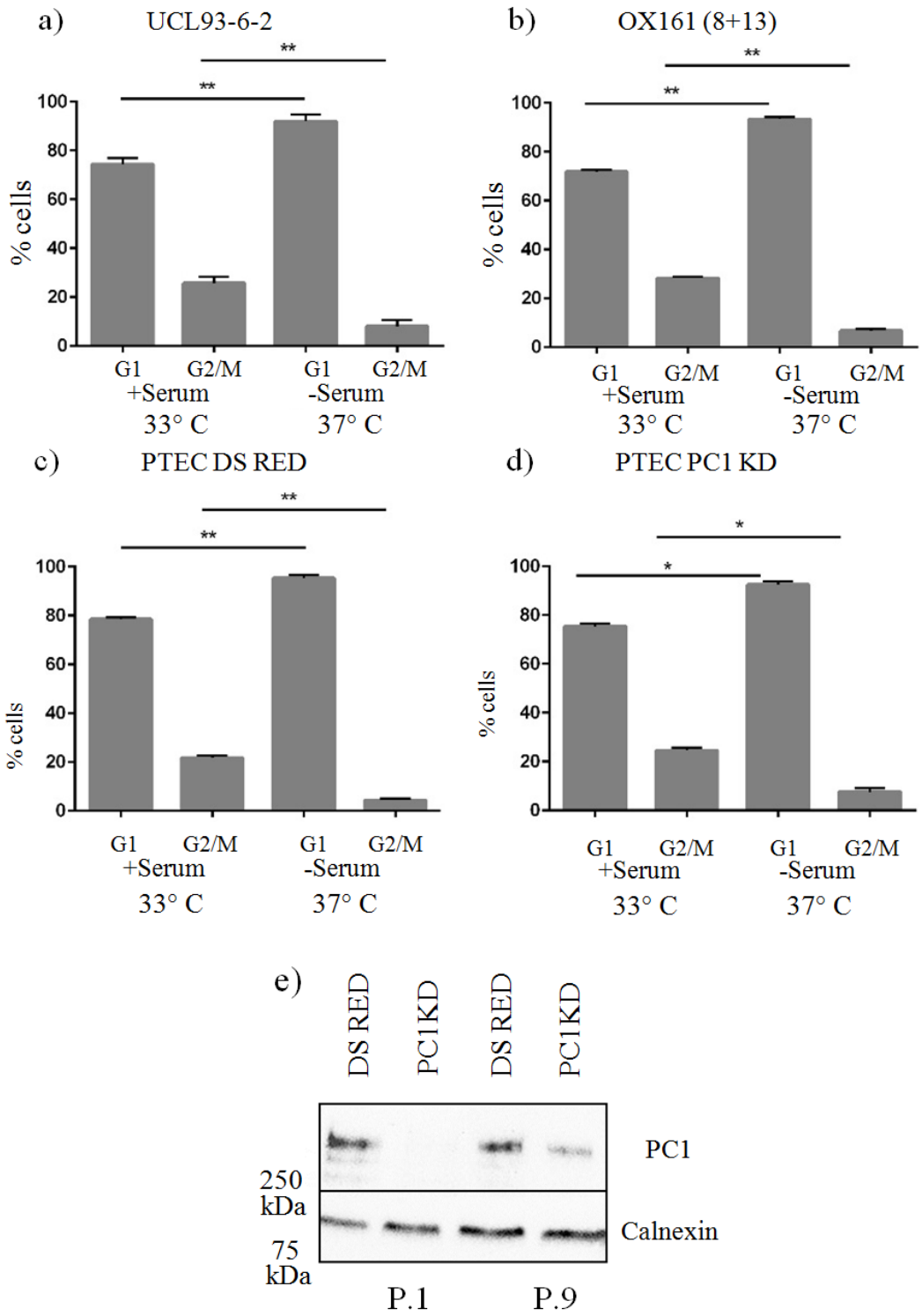

Figure 3.4 Cell cycle profile of cystic and normal human cell lines via serum modulation for 48h and temperature switching from 33C° to 37C°. (n=3, Statistical test:paired t -test (* = p≤ 0.05), Error bars indicate mean ± S.E.M) **(e)** Blot of polycystin-1 in control DSRED and polycystin-1 deficient PTEC Cell lines at early and late passages. Knock down of polycystin-1 is confirmed at passage 2 but returning expression is observed at Passage 9.

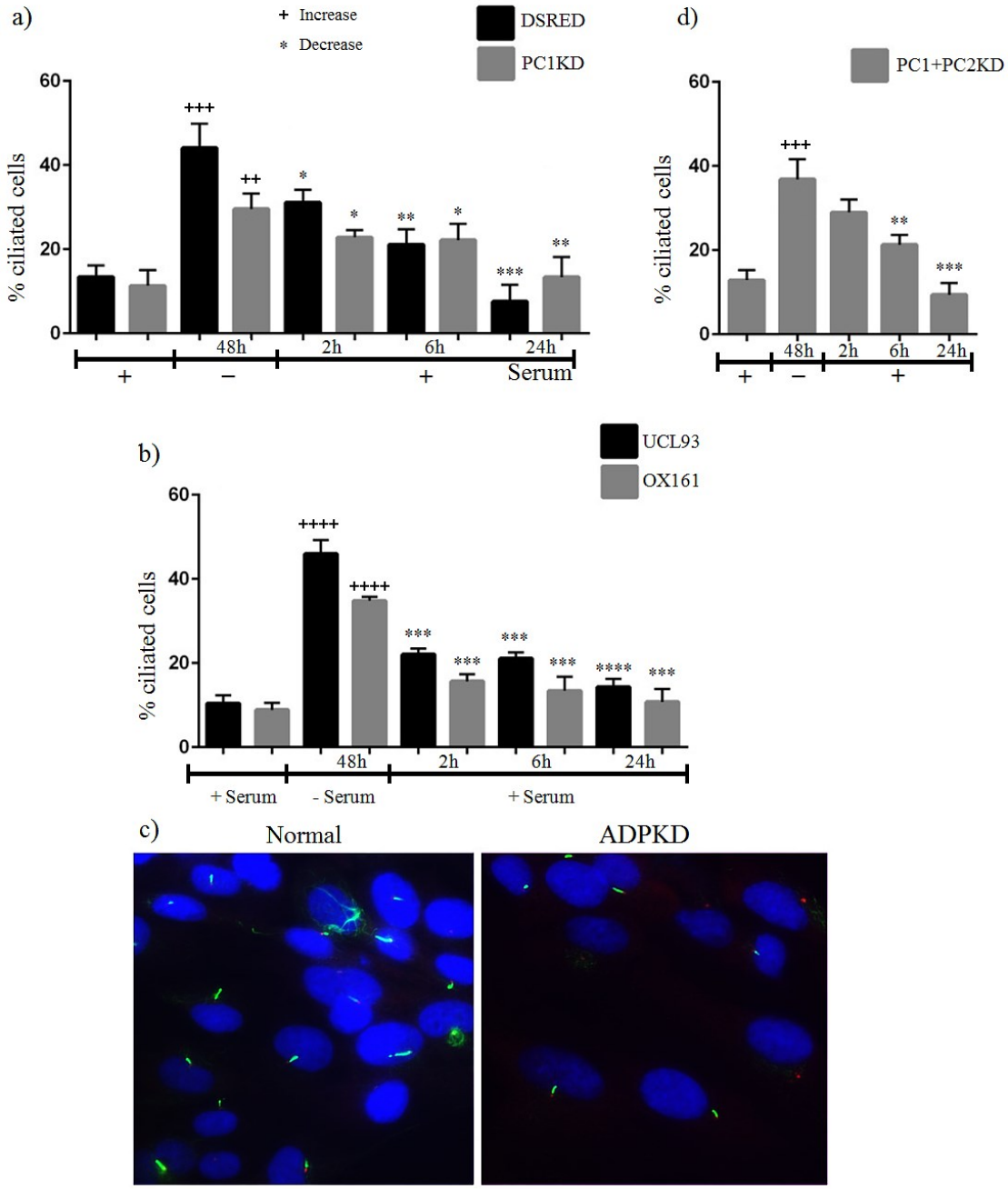

Figure 3.5 (a-b, d) Primary cilium assembly (+) and disassembly (*) assay in normal and ADPKD models. In ADPKD cells and relative control cell lines primary cilia assemble and disassemble according to the cell cycle. Number of primary cilia formed after growth arrest and differentiation is significantly reduced in ADPKD cells, however ratio of cilium disassembly upon cell cycle re-entry is similar in both lines (n=4, Statistical test:paired t- test (* = $p \leq 0.05$), Error bars indicate mean ± S.E.M) (**c) Representative images of primary cilium staining in normal (UCL93) and ADPKD (OX161):** Magnification 60X. Immunofluorescence micrographs of cultured cells stained with antibodies. Cell nuclei are stained in Blue with DAPI and primary cilia in green with acetylated tubulin, basal body with γ-tubulin in red.

f)

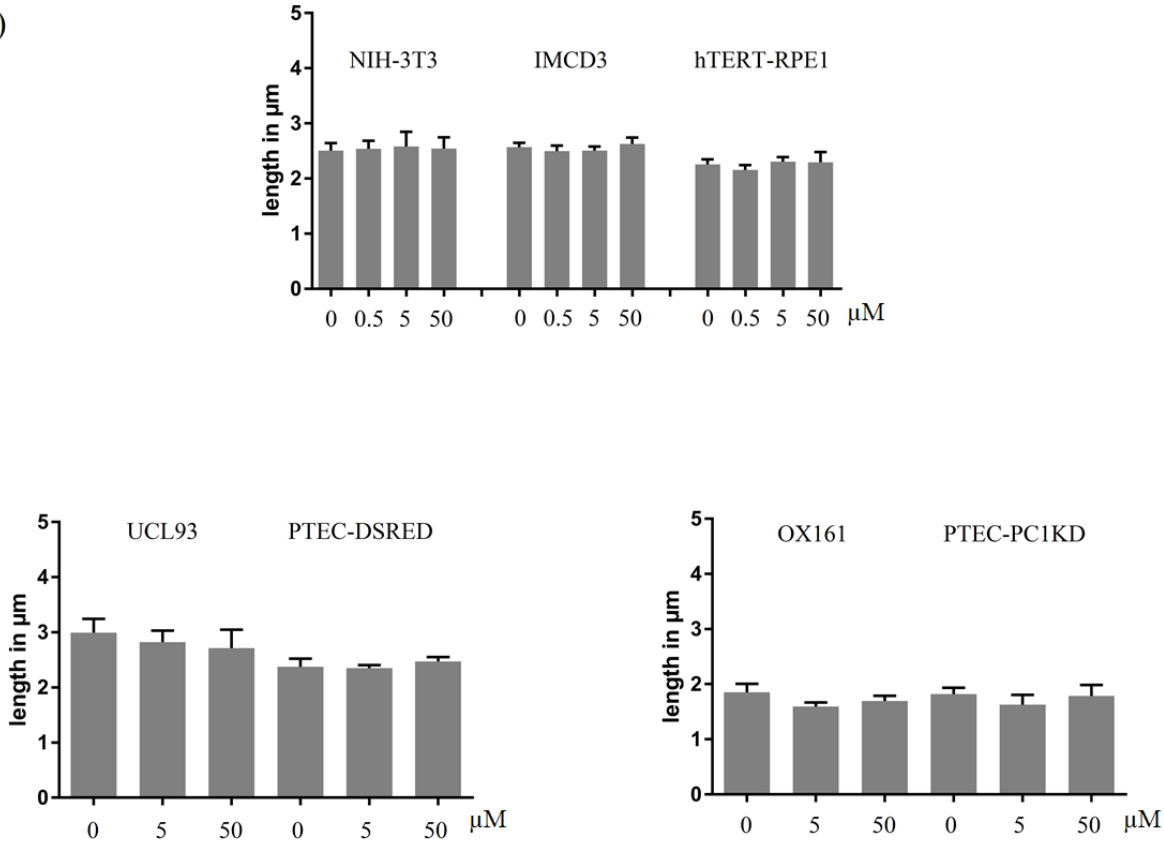

Figure 3.5 f. DMSO treatments at different concentrations. All compound used were either diluted in dH2O or DMSO. Control treatment with DMSO at different concentrations in all tested cell lines did not affect ciliary length as shown in the representative graphs, n=3.

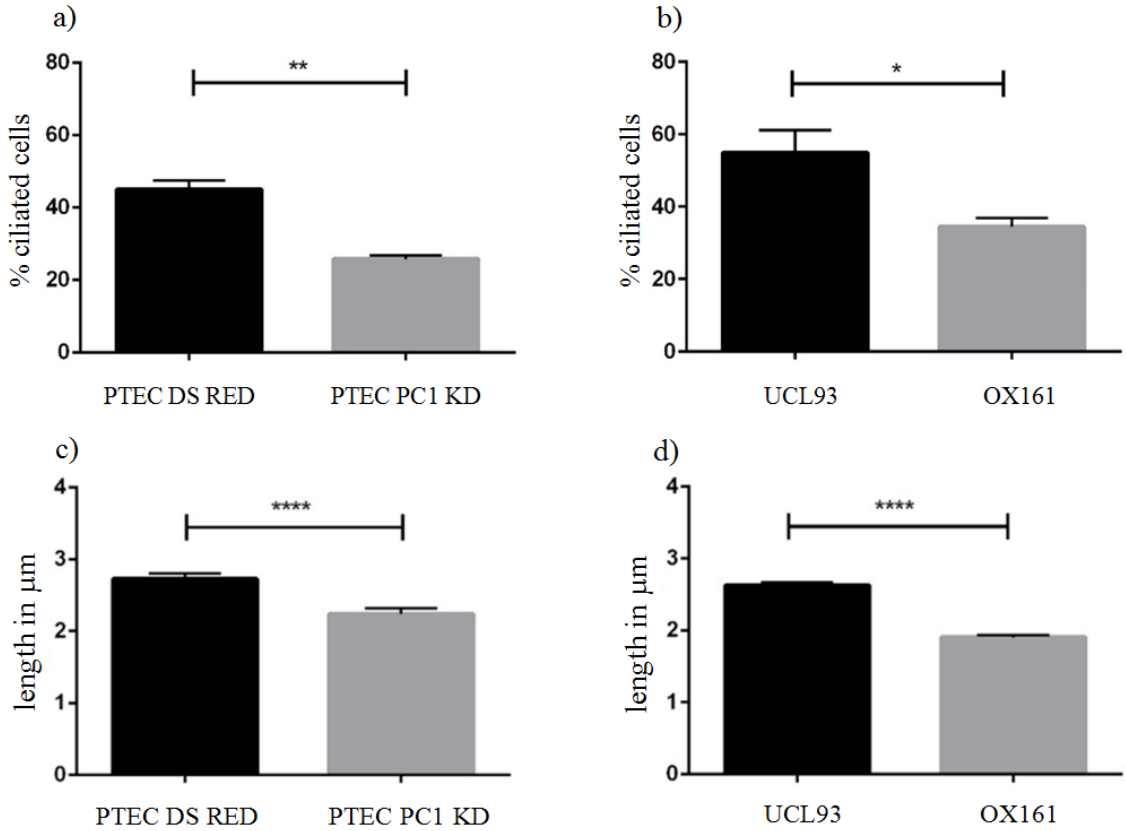

Figure 3.6 (a) (b) Number of ciliated cells comparison Normal v.s ADPKD Number of ciliated cells is decreased in tested ADPKD cells compared to normal control (n=6, 100 cells/N. Statistical test:paired t test (* = p≤ 0.05), Error bars indicate mean ± S.E.M) **(c) (d) Length of Primary cilia comparison Normal vs ADPKD.** Length of primary is decreased in tested ADPKD cells compared to normal control (n=6, 100 cells/N. Statistical test:paired t -test (* = p≤ 0.05), Error bars indicate mean ± S.E.M)

3.5 Primary cilia regulation in ADPKD Models

To test whether polycystin-1 deficiency altered the ciliary response to cAMP and Ca^{2+}, normal and ADPKD cells were studied as described for the baseline models in results **chapter 3.3**.

Treatment with Thapsigargin induced significant cilium shortening in the PC1 KD model **Figure 3.7(a)** and cystic cell line (OX161) **(e)**. Comparison of the % change showed no significant differences between normal and ADPKD models **(b, f).**

Treatment with A23187, a Calcium Ionophore, which facilitates the transport of Ca^{2+} ions across the plasma membrane (Dedkova et al, 2000), also led to significant primary cilia shortening effect in PC1 KD model **(c)** and cystic cell line **(g)**. No significant differences could be detected in % length decrease **(d, h)**.

Treatment with the cAMP analogue dbcAMP increased cilia length in both normal and ADPKD cells **Figure 3.8 (a**, **c**). There was a smaller response to dbcAMP in the ADPKD cells, although this did not reach statistical significance **(b**, **d)**. The reduction in baseline clila length and a reduced response to dbcAMP was consistent in multiple other ADPKD lines (**e, f**) indicating that this is a general feature of polycystin-1 deficiency.

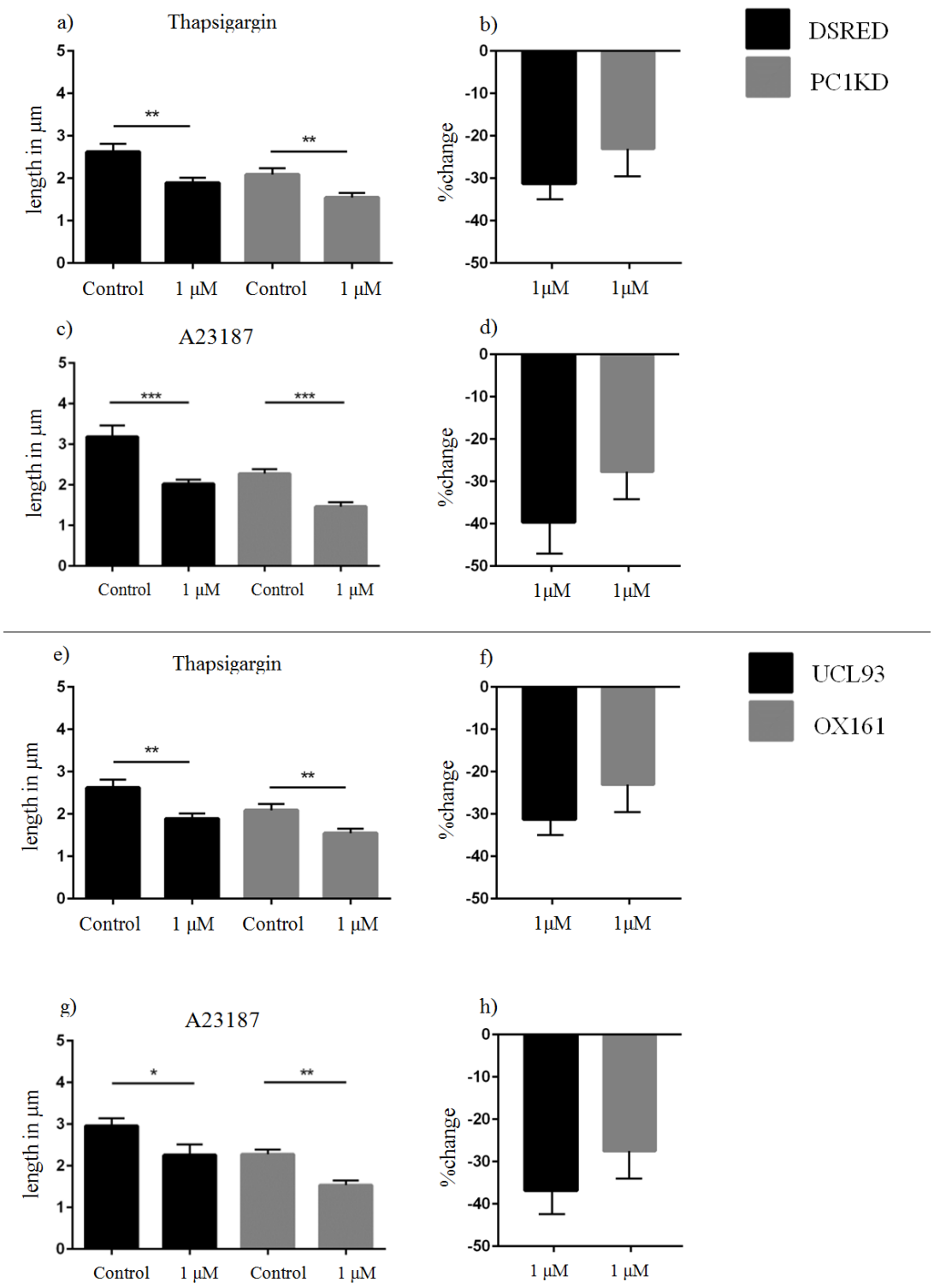

Figure 3.7 Effect of calcium increase in ADPKD models Treatment with agents which result in increase of intracellular Calcium levels result in Significant cilium length reduction in normal and ADPKD models, although there is no statistical difference in length reduction between normal and ADPKD models after normalization, a trend towards ADPKD cells being less responsive is observed. n=3, 100 cells/N. Statistical test:paired t -test (* = p≤ 0.05), Error bars indicate mean ± S.E.M).

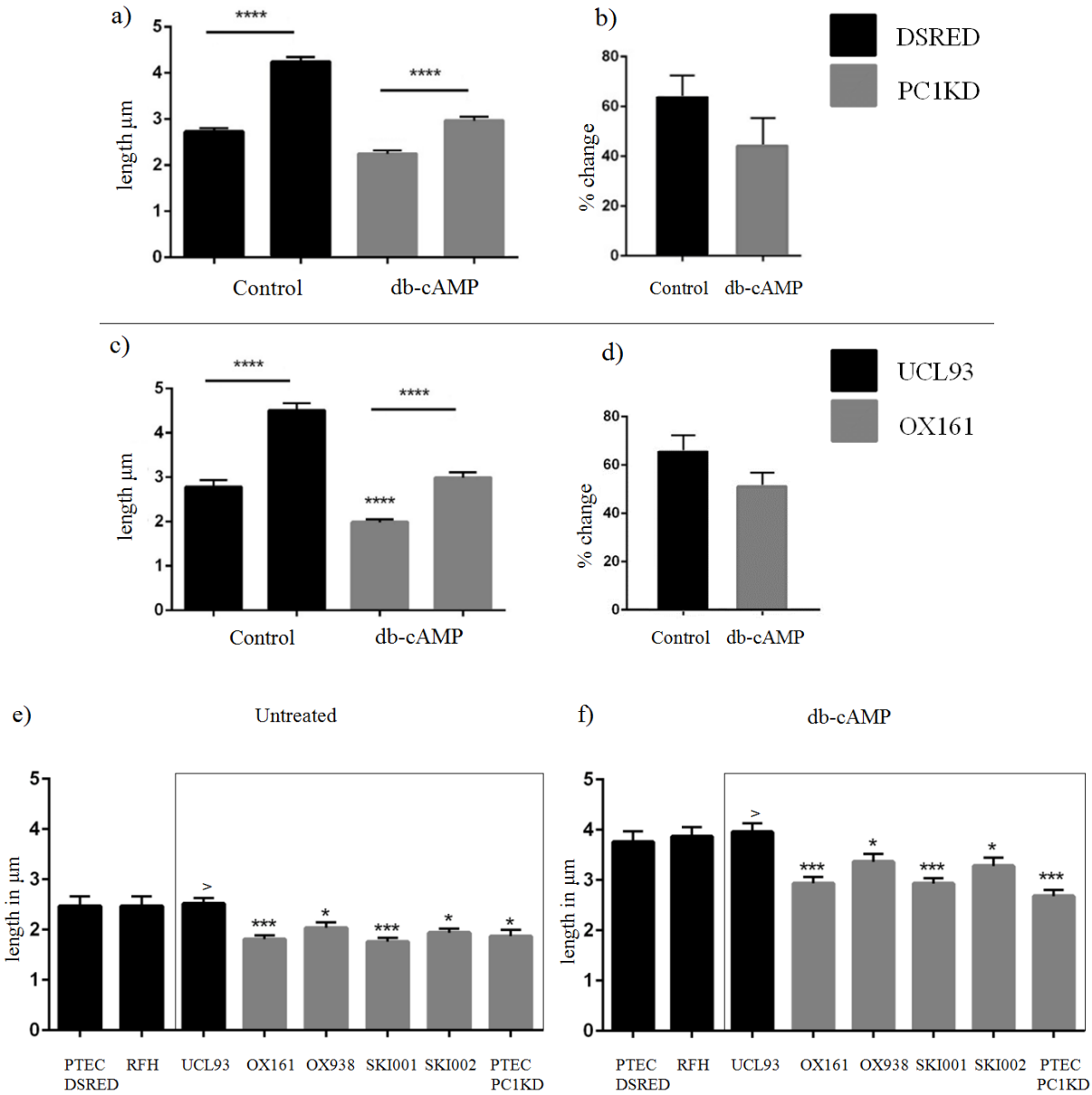

Figure 3.8 Effect of cAMP modulation in ADPKD Models (**1, 2 a**) Treatment with agents which result in increase of intracellular cAMP levels (dbcAMP) results in significant cilium length elongation in normal and ADPKD models. (**1 and 2 b**) Although there is no statistical difference in the length increase between normal and ADPKD models after normalization, again a trend towards ADPKD cells being less responsive is observed, n=6, 100 cells/N. Statistical test:paired t test (* = p≤ 0.05), Error bars indicate mean ± S.E.M). (**3a and 3b)** Primary cilia in untreated ADPKD models are significantly shorter compared with normal UCL93-6-2 the cell line. Treatment with dbcAMP at 500µM results in a significant increase in ciliary length in normal and ADPKD models, the latter reaching approximately the length of untreated normal cells. Primary cilia of ADPKD cells treated with cAMP are significantly shorter than primary cilia of cAMP treated normal cells.N=300 cells. Statistical test:paired t -test (* = p≤ 0.05), Error bars indicate mean ± S.E.M).

3.6 PKA controls cAMP dependent cilia elongation

It is well known that the principal intracellular target for cAMP is PKA (Besschetnova et al, 2011). Using two different compounds to inhibit PKA activation, the ability of cAMP to induce ciliary length increase in our models was investigated using H89 (50 μM) and 14-22 Amide (20μM) (Farrow et al, 2003).

As shown, both PKA inhibitors completely abolished the increase in cilia length following incubation with dbcAMP in both normal **Figure 3.9 (a, c**) and ADPKD cells (**b, e**). This data suggests that the cAMP dependent cilium elongation is acting in a PKA dependent manner and is not altered in ADPKD.

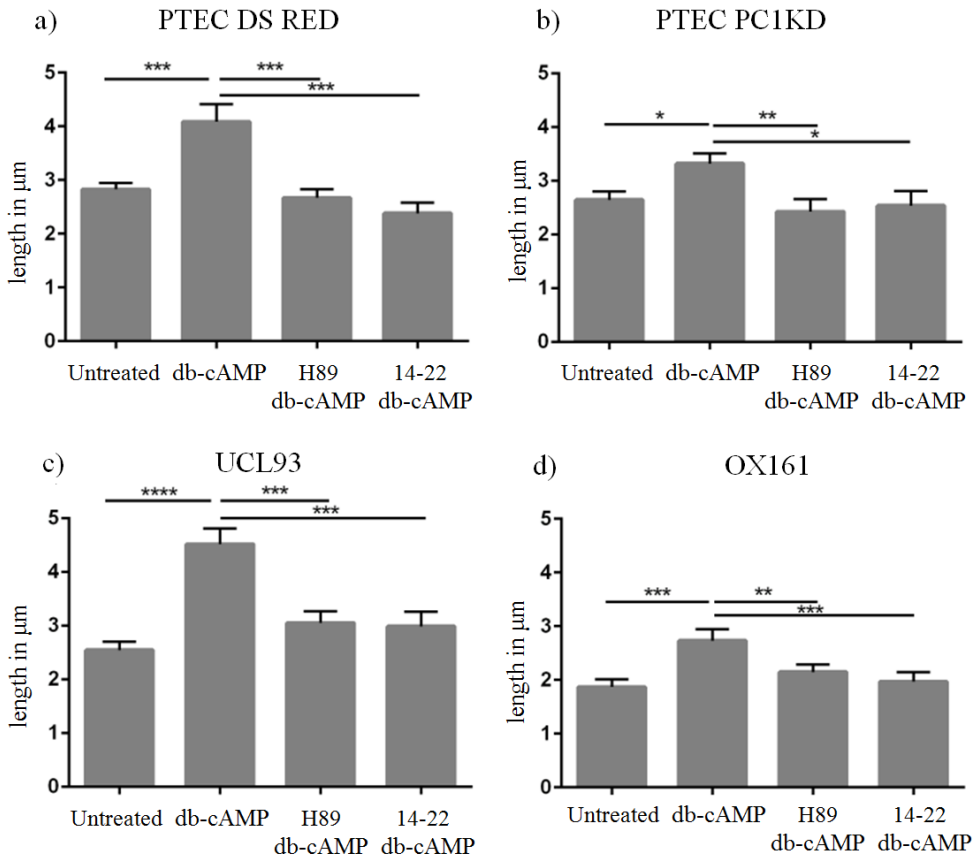

Figure 3.9 cAMP/PKA elongation is not defective in ADPKD models when modulated directly within the cell Treatment for 1 h with H89 or 14-22 amide, two potent PKA inhibitors at 50 µM or at 25 µM respectively, prior to dbcAMP treatment at 500 µM + inhibitors, prevented cAMP dependent primary cilium elongation in both healthy and ADPKD models. (n=3, 100 cells/N. Statistical test:paired t- test (* = p≤ 0.05), Error bars indicate mean ± S.E.M)

3.7 dbcAMP treatment induces cilia formation in cycling cells

To assess how db-cAMP treatment would affect ciliary regulation in regards to formation and length in non-starved cycling cells, both models were treated with db-cAMP for 4 h and cilia length and number was measured. The overall number of ciliated cells was very low in cycling cells, thus a high number of cells (>500) was counted to collect sufficient data for analysis, which converged in approximately 80 to 100 measurable primary cilia per experiment.

Our data showed that db-cAMP treatment significantly increased the number of primary cilia in normal cells while the increase was marginal in ADPKD cells (**Figure 3.10**). Also, formed primary cilia were significantly longer in the normal cell lines. These results suggest that in normal cycling cells, cAMP is able to arrest proliferation and therefore induce cilium formation and lengthening or conversely induce ciliogenesis which then leads to cell cycle arrest (Goto et al, 2013).

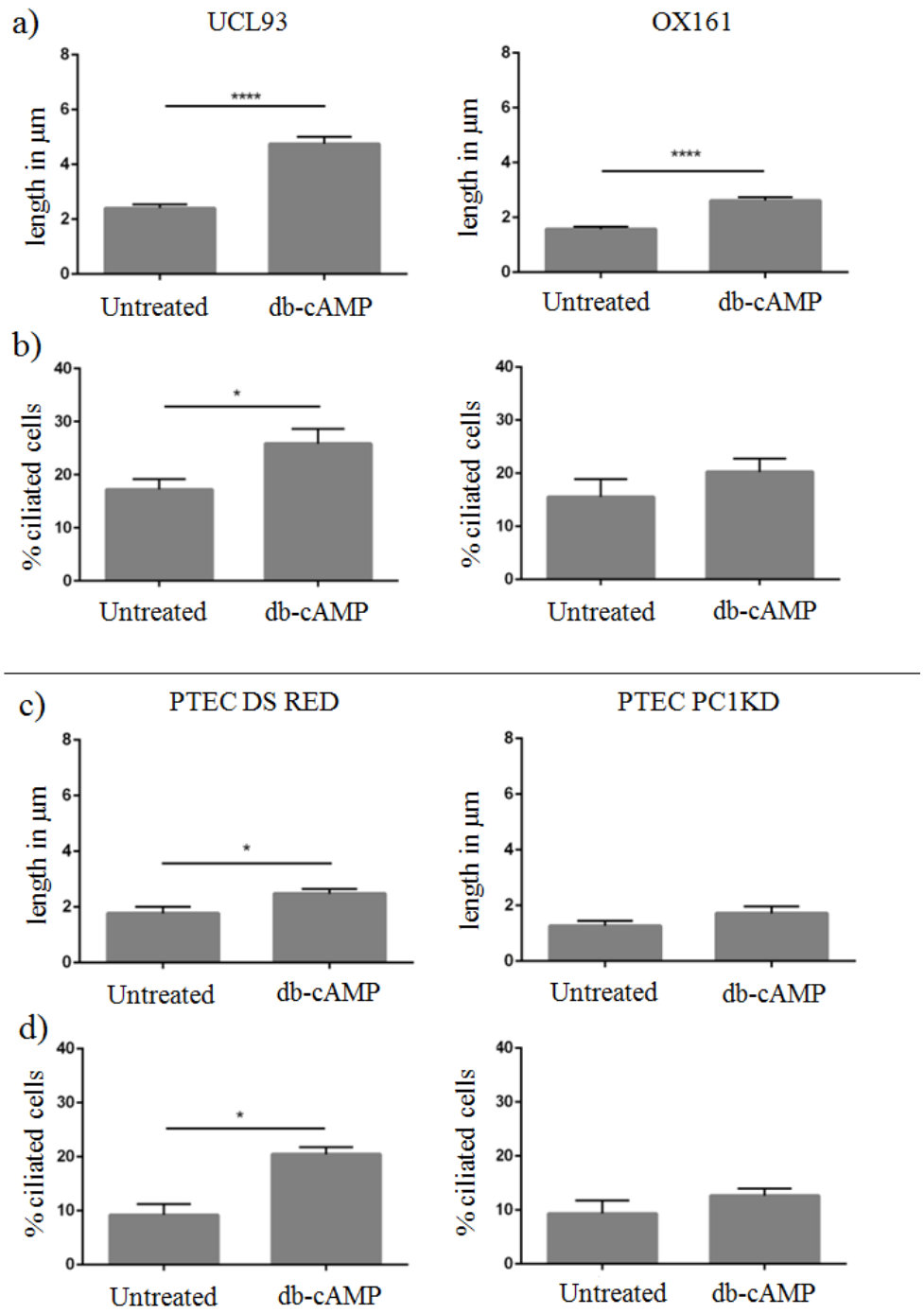

Figure 3.10 Effect of cAMP in non-starved cycling cells. Treatment with 500 µM dbcAMP in cycling cells for 3h results in significant primary cilium elongation in **(a)** normal UCL93 and cystic OX161 and **(c)** in normal PTEC DSRED. **(b) & (d)** The same treatment significantly increased the number of ciliated cells in all normal control lines while no change was detected in ADPKD cells. (n=6, 100 cells/N. Statistical test:paired t- test (* = $p \leq 0.05$), Error bars indicate mean ± S.E.M)

3.8 Effects of cAMP on the cell cycle

To investigate whether cAMP could directly modulate the cell cycle, the cell cycle profile was analysed using different markers of proliferation under the same experimental settings used to study primary cilium elongation. Two markers, Ki67 and phospho-H3 were utilised. The Ki67 protein is present in all interphase phases (G1, S, and G2) of the cell cycle and in mitosis but is absent in quiescent or resting cells in G0 (Gerdes et al*,* 1992). It has a short half-life of 1 h (Heidebrecht et al*,* 1996). Phospho-histone H3 (PH3) on the other hand is a marker for cells undergoing mitosis, a step which is critically important in chromatin remodelling and chromosome segregation and condensation before cell division (James et al, 2012).

Treatment with db-cAMP in normal cells resulted in a significant decrease of Ki67 and PH3 positive cells, suggesting that intracellular cAMP increase induces cell cycle exit in G1/G0 in normal cells **Figure 3.11 (a, c**). In the ADPKD models, this effect could not be detected (**b, d**), suggesting an impairment of this function. The Ki67 results were confirmed in additional normal (RFH) and ADPKD models (SKI001, OX938 and SKI002), showing impaired decline of Ki67 positive cells in ADPKD models (**e**).

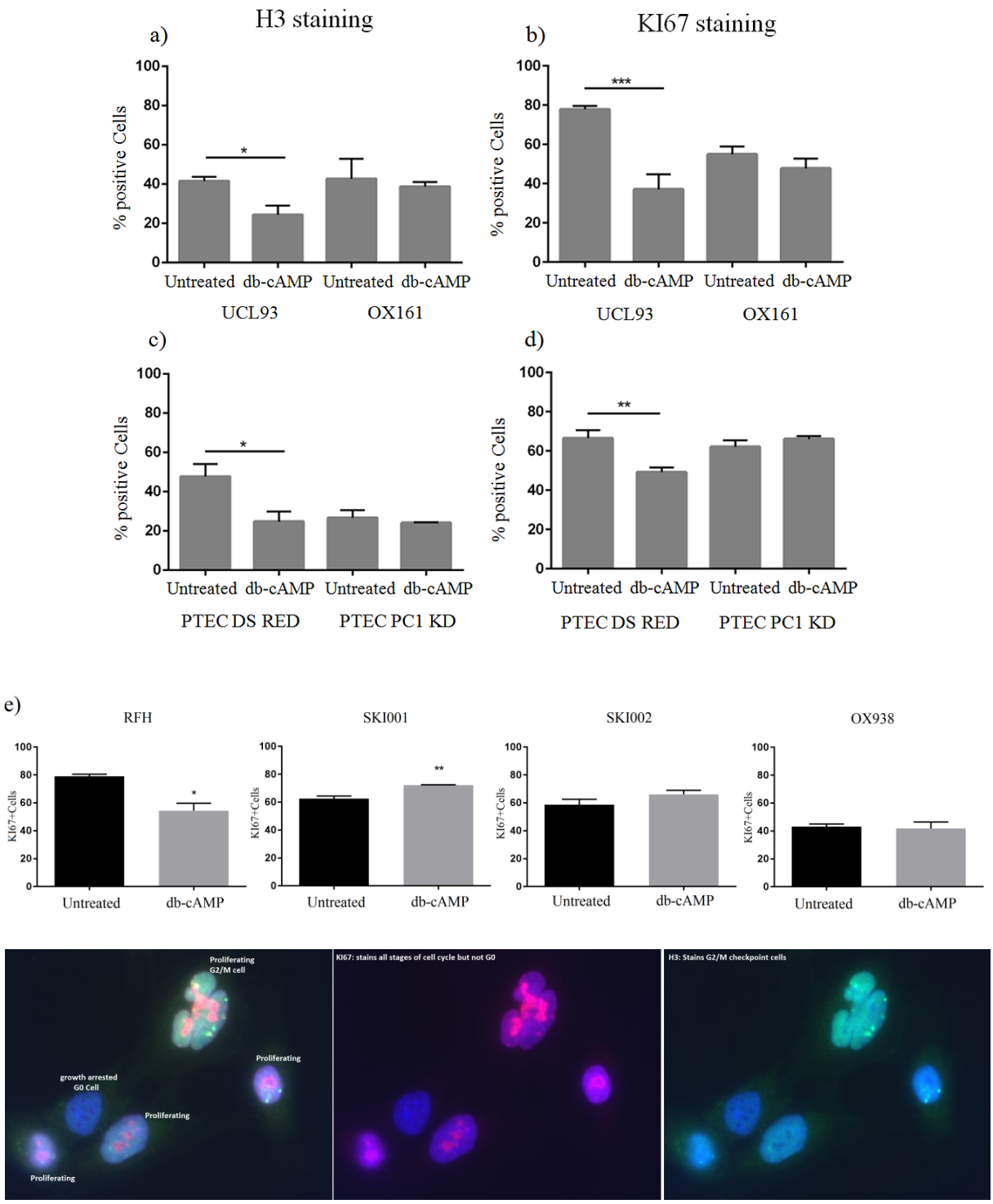

Figure 3.11 Assessment of proliferation profile of cAMP treated cycling cells. **(a-e)** Treatment with dbcAMP in normal cells results in a reduction of proliferation as shown by the significant decrease of proliferation markers KI67 and PH3. In ADPKD models no significant reduction of proliferation markers after cAMP treatment are detected suggesting that the cAMP effect on anti-proliferation in ADPKD cells is disturbed. (n=3, 100 cells/N. Statistical test:paired t- test (* = $p \leq 0.05$), Error bars indicate mean ± S.E.M) **(Bottom).** Representative image of PH3 and KI67 staining in cAMP treated cycling cells, Red: KI67, Green: PH3, Blue: DAPI.

3.9 Role of AKAPs in primary cilia regulation

3.9.1 AKAP350 localizes to the basal bodies at the base of the cilium

Our laboratory was interested in AKAP350 after it was isolated from one of our mass spectrometry screen as a potential binding partner of the polycystin-1 PLAT domain (Streets et al, unpublished). AKAP350 is known under different aliases (e.g. AKAP9, AKAP450) and is reported in the literature as a typical PKA associated adaptor protein which can also associate with other kinases such as Protein Kinase C (PKC) and the Rho-activated protein kinase N (PKN) (Homasany et al, 2005). Co-immunoprecipitation experiments confirmed that PC1-PLAT is able to bind to AKAP 350 and simultaneous localization studies using different fluorescent tagged AKAP 350 constructs in HEK293 cells, revealed partially overlapping co-staining pattern of AKAP 350 with PC1-PLAT (**Figure 3.12a**). Thus polycystin-1 could be an important regulator or effector of PKA signaling at the cilia base.

a)

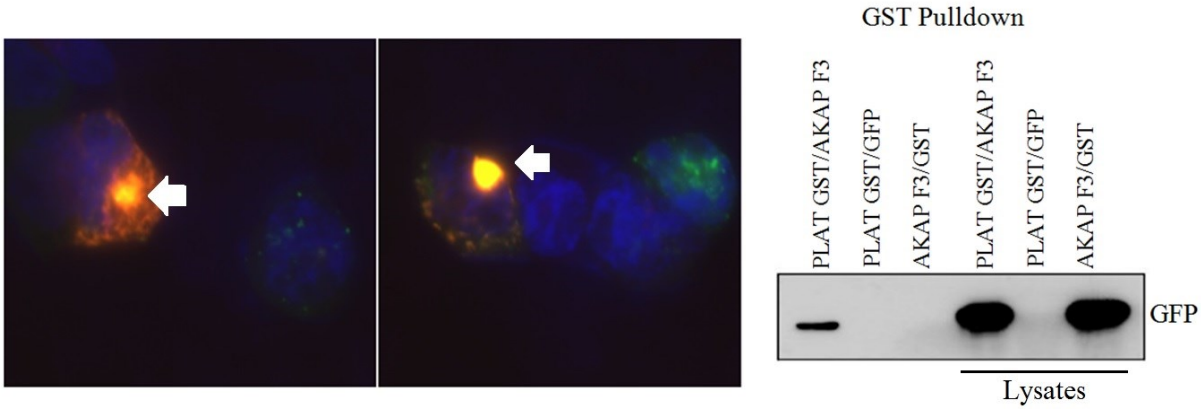

b)

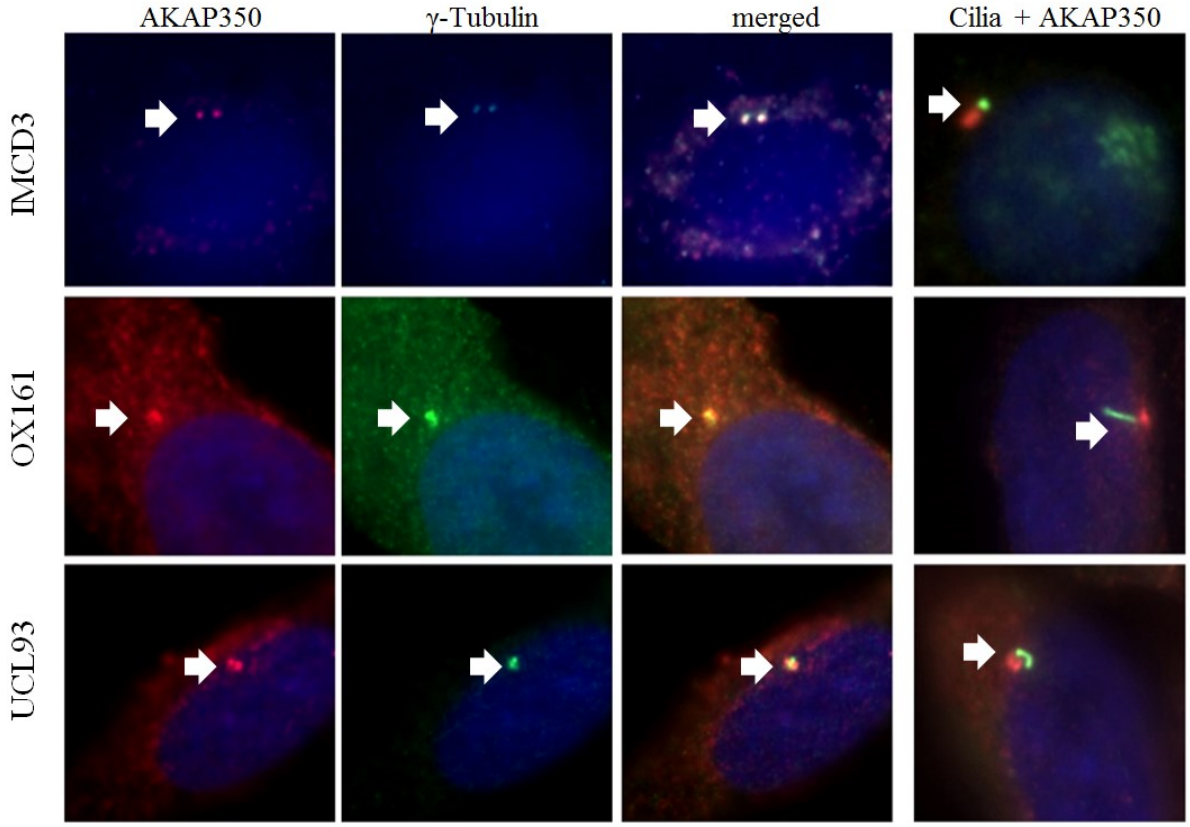

Figure 3.12 AKAP350 localizes at the base of the primary cilia (a) Co-localization: Fluorescent tagged AKAP 350 cherry (Red) constructs with the polycyctin-1 PLAT GFP constructs (Green) shows co-expressed areas in HEK293 cells suggesting co-localization of this proteins. Co-immunoprecipitation: GST-tagged PLAT proteins co-immunoprecipitate GFP tagged AKAP F3 adaptor protein. (**b**) Localization studies of AKAP 350 (Red) in different cell lines shows localization of the adaptor protein to the basal bodies labelled with γ-tub (Green) at the base of the primary cilium (green α-tub). Right Panel; basal bodies labelled with γ-tub (Red) and primary cilia with α-tubulin (Green), Magnification 60X.

In HEK293 cells overexpressing PC1-PLAT and AKAP350 GFP constructs, AKAP350 staining was co-localised to basal bodies **Figure 3.12 (a)**. Using a specific antibody to endogenous AKAP350, co-localization with γ-tubulin was confirmed at the basal bodies in a number of different growth arrested cell lines (**b**). Localization in cycling cells was diffuse and not detectable. Co-staining with α-tubulin as a ciliary marker showed that AKAP350 accumulates at the basal bodies in ciliated cells. This suggested a possible role of this complex during primary cilium formation and that AKAP350 might act as an adaptor protein to localize the cAMP signalling involved in primary cilium elongation to the base of the cilium (**b**). AKAP350 localization to the basal bodies was not prevented in our ADPKD model (OX161) suggesting that AKAP350 localisation was not altered by loss of polycystin-1; however the normal functioning of this complex could still be defective through incorrect or incomplete interaction with other proteins, including polycystin-1.

3.9.2 AKAP inhibition prevents cAMP/PKA cilium elongation

Next, the role of AKAP adaptor proteins in cAMP dependent primary cilium regulation was investigated using a well-recognised pan inhibitor of AKAP binding (InCellect AKAP St-Ht31 inhibitor peptide from Promega). Treatment with ST-Ht31 (50 μM) inhibited cAMP dependent cilium elongation (**Figure 3.13**). This confirmed that AKAPs are involved in PKA/cAMP dependent cilium elongation, thus suggesting that AKAP inhibition prevents the cAMP effect at the ciliary base and that its localization is critical for the ciliary cAMP effect.

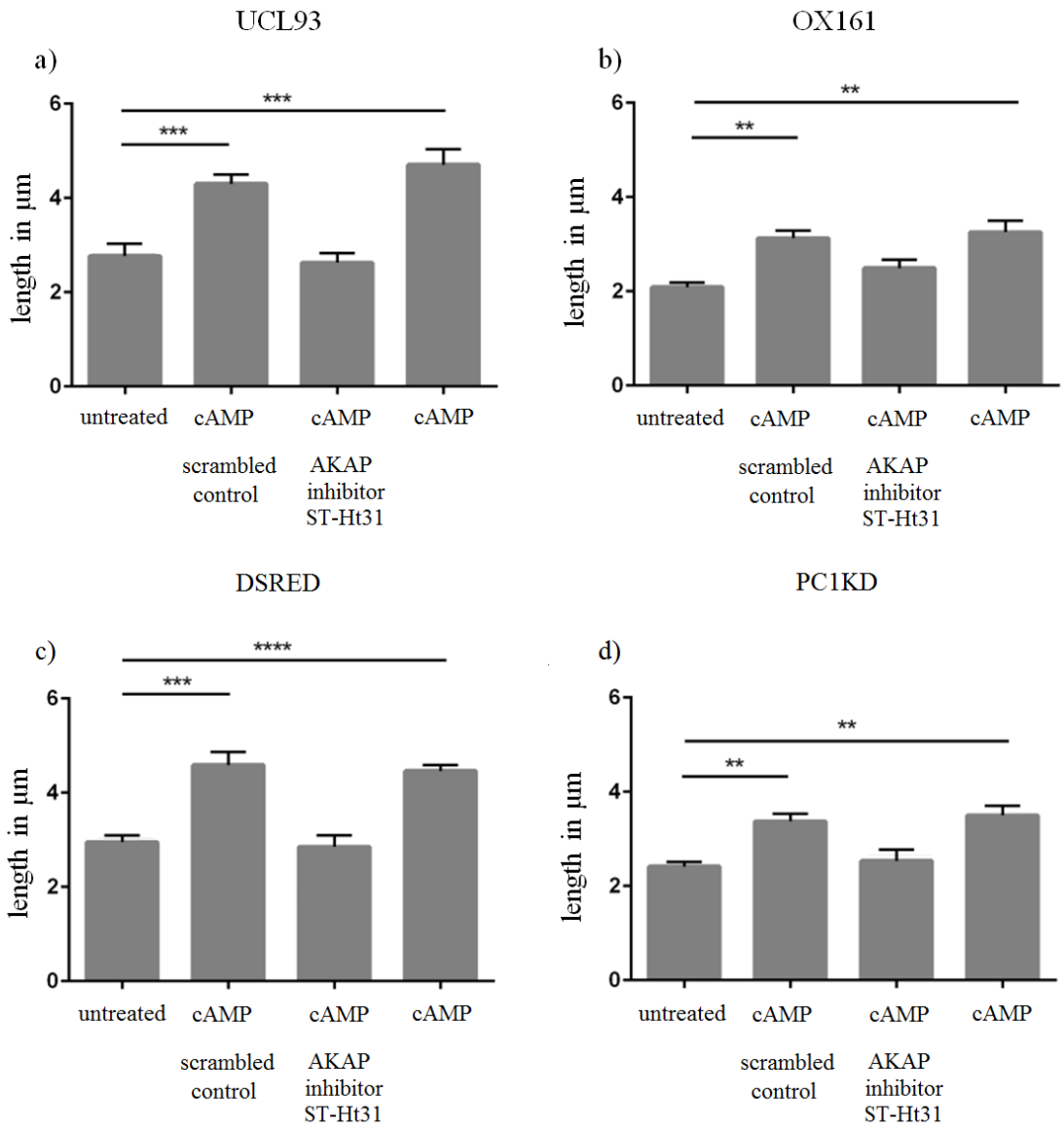

Figure 3.13 AKAP inhibitor ST-Ht31. cAMP dependent cilium regulation is regulated at the base of the primary cilium, a regulation which is confined through AKAP proteins. Pre-treatment with AKAP inhibitor ST-Ht31 at 50 µM concentration in normal **(a)** UCL93, **(c)** PTEC DSRED and ADPKD **(b)** OX161, **(d)** PC1KD cells prior to treatment with 500 µM cAMP prevents cAMP dependent primary cilium elongation suggesting that AKAP proteins are required to confine the cAMP signalling involved in primary cilium elongation at the base of the cilium. (n=3, 100 cells/N. Statistical test:paired t- test (* = $p \leq 0.05$), Error bars indicate mean ± S.E.M)

3.10 The role PGE2 in primary cilia formation

Previous studies have shown that cAMP dependent cysts expansion in kidney epithelial cells can be stimulated by prostaglandin E2 (PGE2), potentially by binding to EP2 receptors (Elberg et al, 2007). The role of PGE2 on cilia length and its action via different receptor subtypes was therefore investigated.

3.10.1 PGE2 induces primary cilia elongation

Incubation of normal and ADPKD models with PGE2 for 3 h resulted in primary cilium elongation at rates similar to that seen with dbcAMP **Figure 3.14 (a-d)**. Thus, PGE2 could represent an endogenous ligand that activates cAMP/PKA regulation of cilia length. Although the maximum extension of cilia length was not reached in the cystic cell line after 3 h treatment, a subsequent test experiment showed similar levels to normal control after prolonged 24 h incubation (**e-f**), suggesting a delayed maximal response to PGE2 treatment.

3.10.2 PGE2 dependent cilia elongation acts via EP2 and 4 receptors

To identify the receptor subtypes involved in the cilia response to PGE2, selective EP agonists were tested in the same assay. These experiments revealed that activation of EP2 and EP4 receptors increased primary cilium length while EP1 or EP3 agonists did not play a primary role in this effect (**Figure 3.15a**).

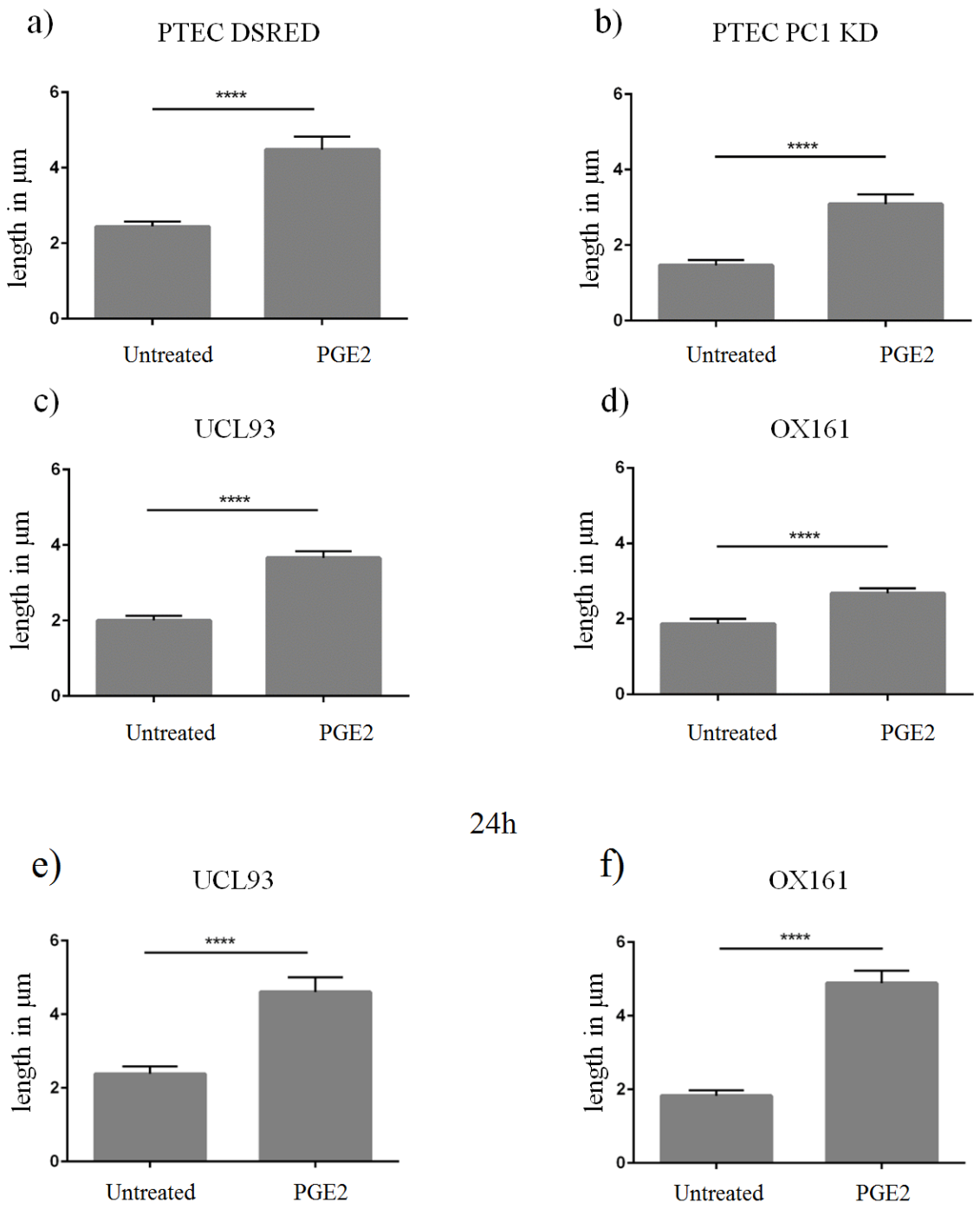

Figure 3.14 PGE2 induces primary cilium elongation. PGE2 stimulation for 3h post-starvation at 100 µM induces significant primary cilium elongation in normal **a)** UCL93, **c)** PTEC DSRED and ADPKD **b)** OX161, **d)** PTEC PC1KD models. PGE2 stimulation for 24 h post-starvation at 100 µM showed similar primary cilium elongation in normal and PKD cells (n=3, 100 cells/N. Statistical test:paired t -test (* = p≤ 0.05), Error bars indicate mean ± S.E.M)

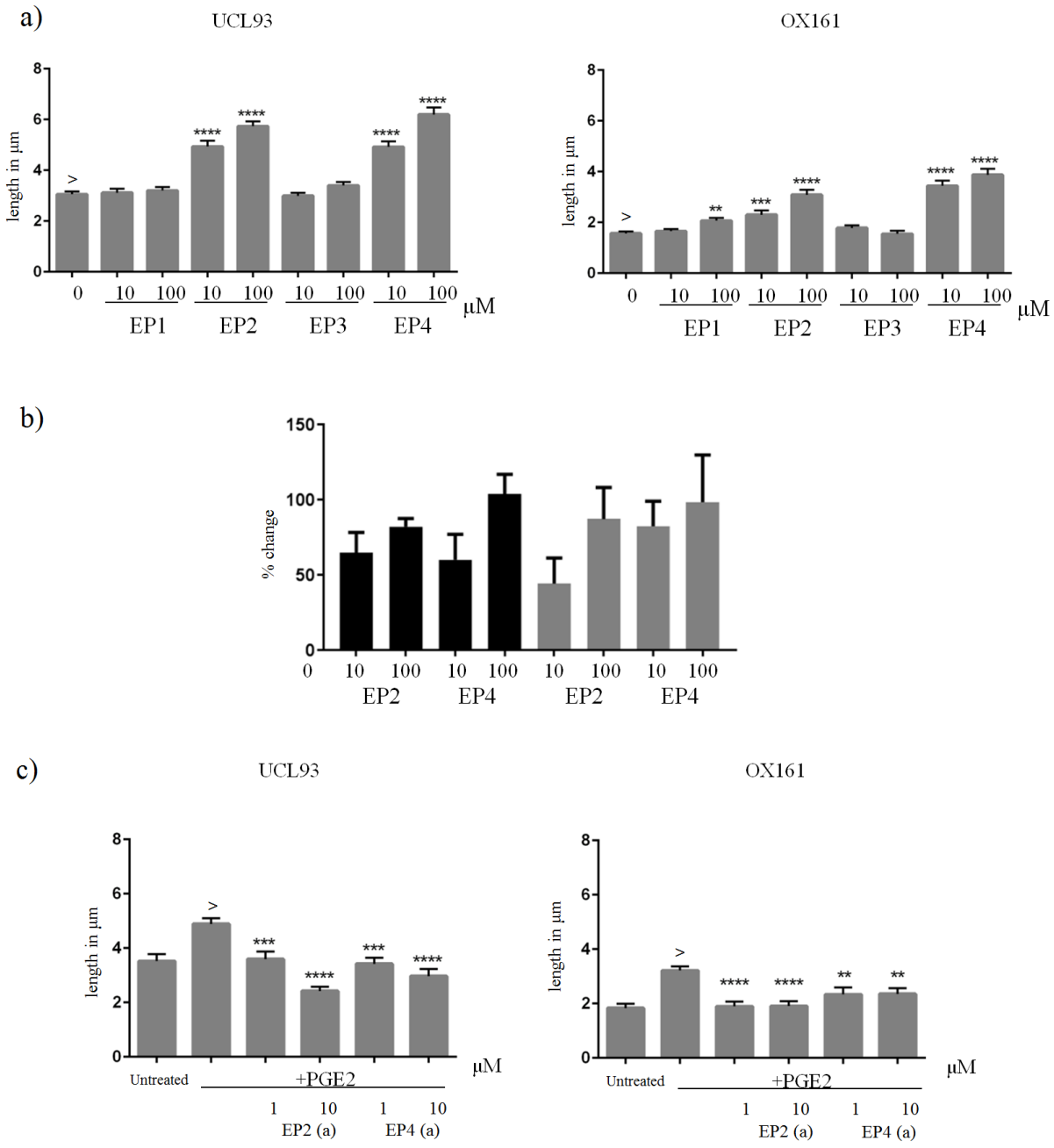

Figure 3.15 (a) EP receptor agonist in normal and ADPKD cells. Treatment with EP2 and EP4 agonists causes significant cilia elongation in normal and ADPKD cells while EP1 and EP3 have no effect, suggesting that EP2 and EP4 receptors are responsible for ciliary length regulation**. (b)** % change of various treatments. **(c) EP2 and 4 antagonists in PGE2 treated cells.** Pre-treatment with EP2 and EP4 antagonists for 1 h prior to treatment with 100µM PGE2, prevents PGE2 dependent cilium elongation in normal and ADPKD cells (n=3, 100 cells/N). Statistical test:paired t -test (* = p≤ 0.05), Error bars indicate mean ± S.E.M)

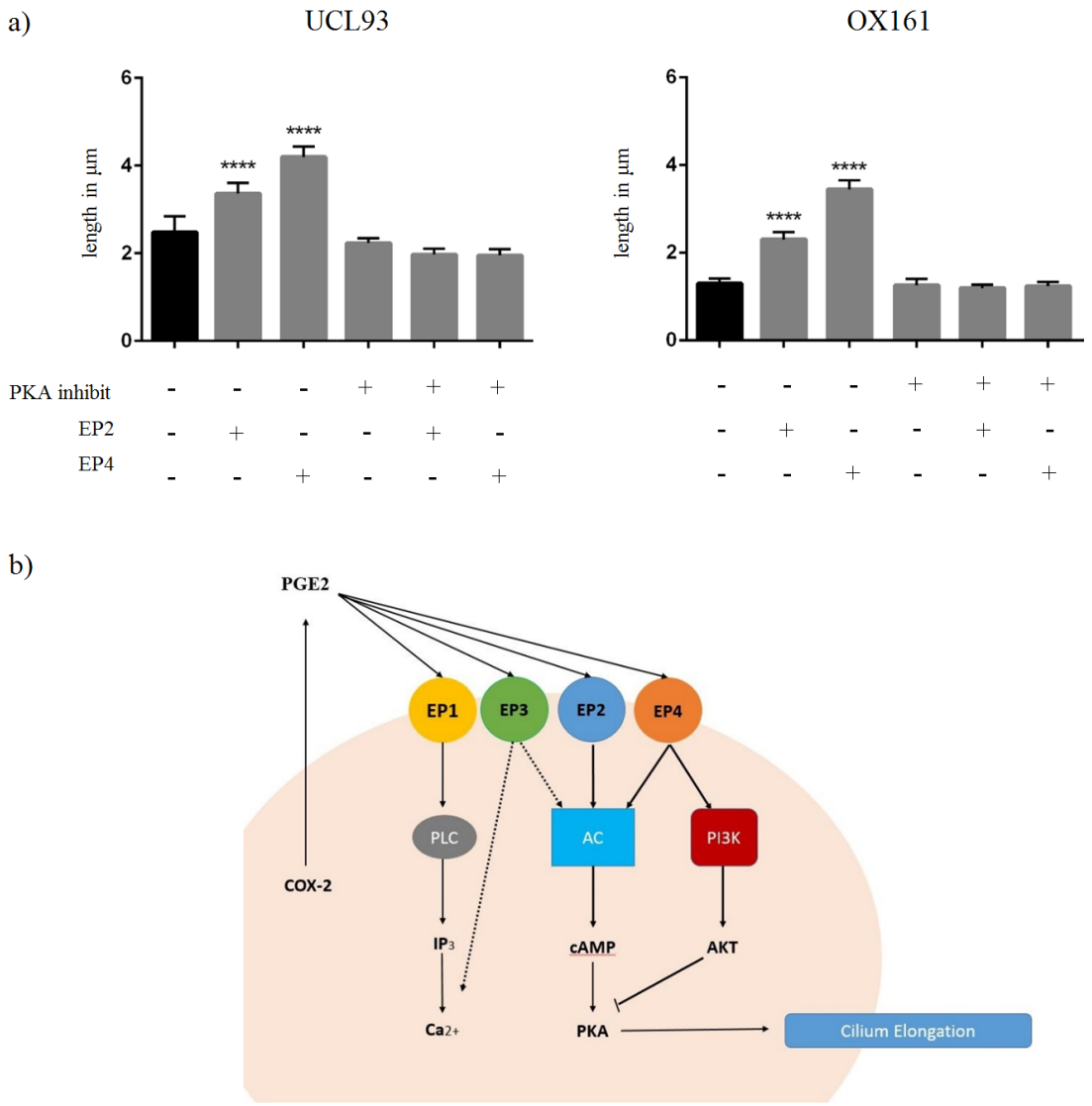

Figure 3.16 PGE2-EP2/4 effect is PKA dependent (a) Pre-treatment with PKA inhibitor at 50 µM, prior to treatment with 10 µM, EP2 or EP4 agonists, prevents EP2/EP4 dependent cilium elongation in UCL93 and OX161 cells. (n=3, 100 cells/N. Statistical test:paired t- test (* = $p \leq 0.0001$), Error bars indicate mean ± S.E.M) **(b)** PGE2 dependent primary cilium regulation model.

As shown with dbcAMP, pretreatment with PKA inhibitors prior to the addition of EP2 or EP4 agonists prevented cAMP dependent cilium elongation **(Figure 3.16)**. To confirm that the EP receptors were actually responsible for PGE2 induced cilium elongation, specific EP2 and EP4 antagonists (Steinwall et al, 2004; Forselles et al, 2011; Xu et al, 2014) were also used. These results show that blocking either EP2 or EP4 was able to fully antagonize the effect of PGE2 on cilium regulation (**Figure 3.15c**). Blockade of EP2 appeared to have a stronger inhibitory effect than EP4 though blocking either subtype was sufficient suggesting possible redundancy in this response. It can be concluded that PGE2 acts through EP2/EP4 receptors to activate PKA/cAMP signalling and increase cilia length. Similar to db-cAMP, the percentage increase in primary cilium length regulation is comparable between normal and ADPKD cells (**Figure 3.15b**).

3.11 Abnormal cilia structure in *PKD1* transgenic cells

To study whether the level of polycystin-1 correlates with cilia length, this study examined *PKD1* transgenic cells (M7) previously generated from a *PKD1* transgenic mouse and compared to cells (M8) derived from a non-transgenic littermate (Newby et al, 2002).

Analysis of primary cilium number and length revealed no significant difference between both lines. However more structurally altered or deformed primary cilia could be detected in the M7 cells (**Figure 3.17**). The deformed cilia were characterized by either double forked ciliary shafts at different heights ranging from the stem to the proximity of the ciliary tip and intertwined sections probably caused by excessive elongation of a not fully developed cilia duct.

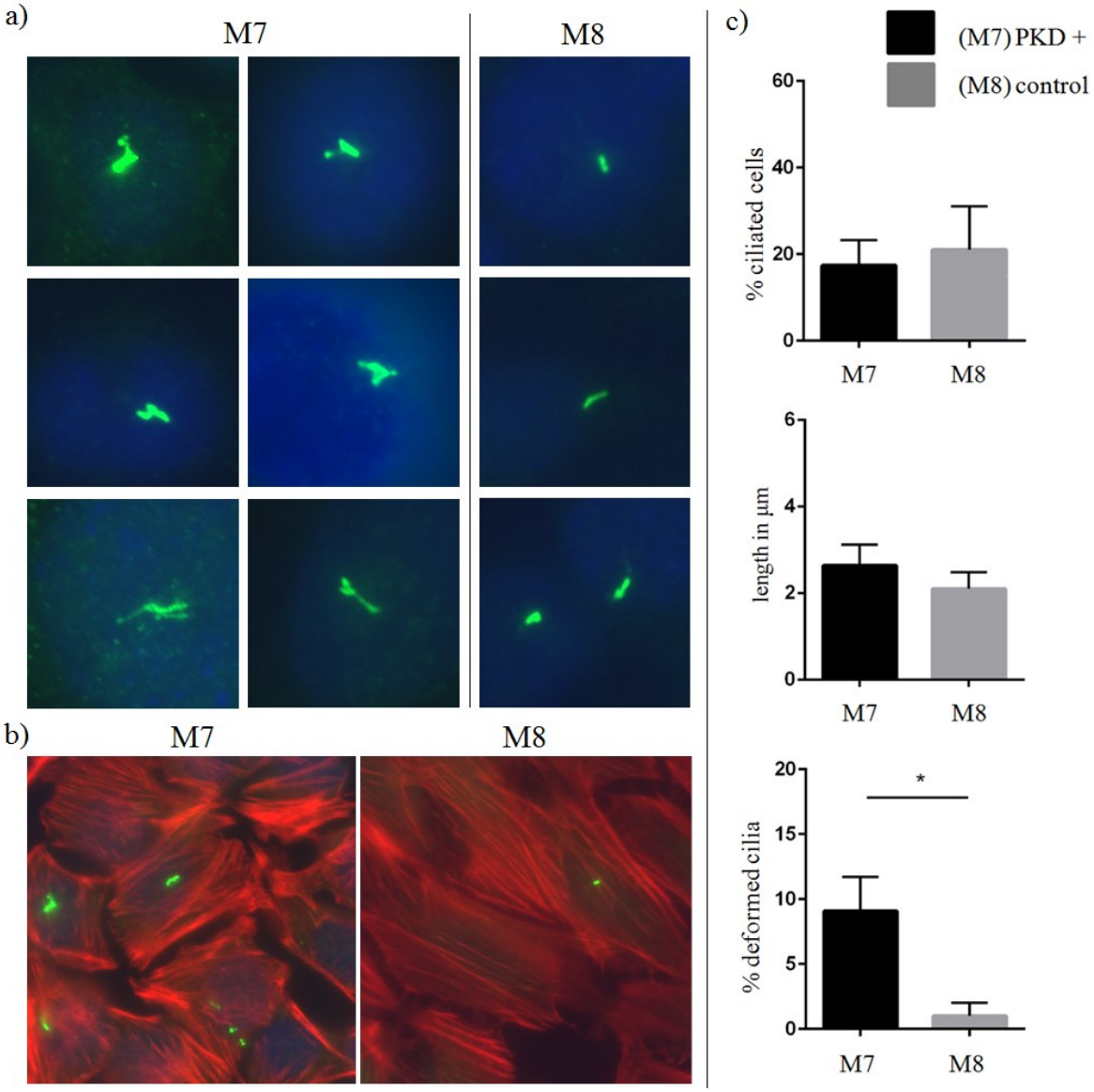

Figure 3.17 Primary cilium comparison of normal and Transgenic ADPKD models

a) Representative images of transgenic ADPKD model (M7) primary cilia in comparison to normal (M8) cilia.

b) Representative images of M7 actin organization in comparison to M8 actin organization.

c) M7 v.s M8 comparison of number of formed primary cilia, primary cilium length and number of deformed primary cilia (n=3, 100 cells/N. Statistical test:paired t- test (* = $p \leq 0.05$), Error bars indicate mean ± S.E.M). Antibody used: DAPI-stained nuclei (Blue), ARL13b stained primary cilia (Green).

3.12 Primary cilia number and length in human normal and ADPKD tissue

To confirm that the changes in primary cilium detected *in vitro* were not related to culture or immortalisation, cilia number in available human and mouse control and ADPKD kidney tissues was measured. Primary cilia were found almost exclusively on the apical surface of tubular epithelial cells.

Initial analysis was performed on fixed kidney sections available from two ADPKD patients (SKI-001 and OX161) from whom cell lines had been derived and stored from our Group and compared to non-cystic human kidney sections. As shown, a significant reduction in cilia length in both SKI001 and OX161 (**Figure 3.19 a, c)** as well as a reduced number of ciliated cells compared to normal controls (**b**, **d**) was observed. These results suggest that the changes observed *in vitro* represent that seen *in vivo.* However, since both tissue and cells represent the advanced stages of disease, it was not possible to be certain if they are primary or secondary changes.

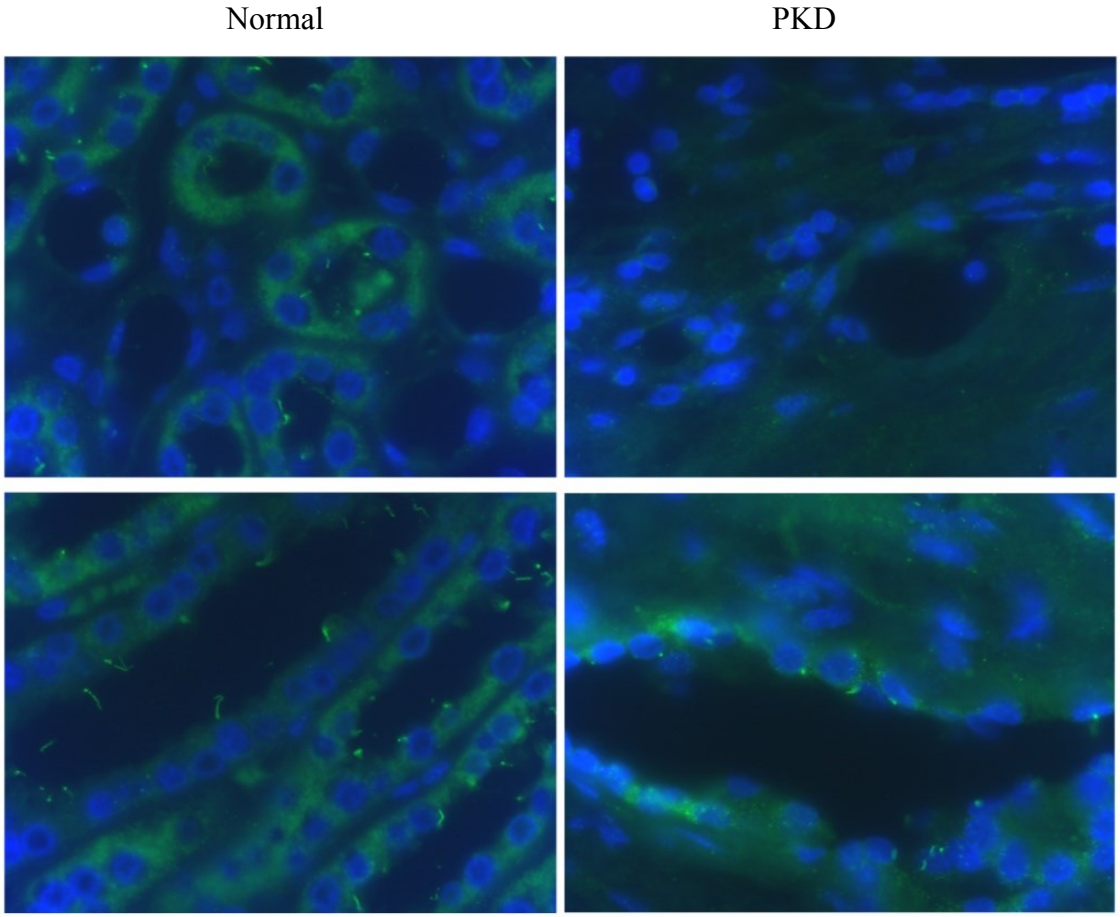

Figure 3.18 Representative image of primary cilia in human normal and ADPKD (SKI001) tissue.
In normal tissue, primary cilia can be detected exclusively protruding from the inner lining of the epithelial cells of the inner lining of renal tubules as seen in parallel and cross section images. In the ADPKD model, renal tubules appear extensively deformed and dilated, with increased disorganization of normal cellular arrangements. Primary cilia appear stubby and are sparsely distributed along dilated tubules and cystic sections of the tissue. Antibody used: DAPI-stained nuclei (Blue), ARL13b stained primary cilia (Green).

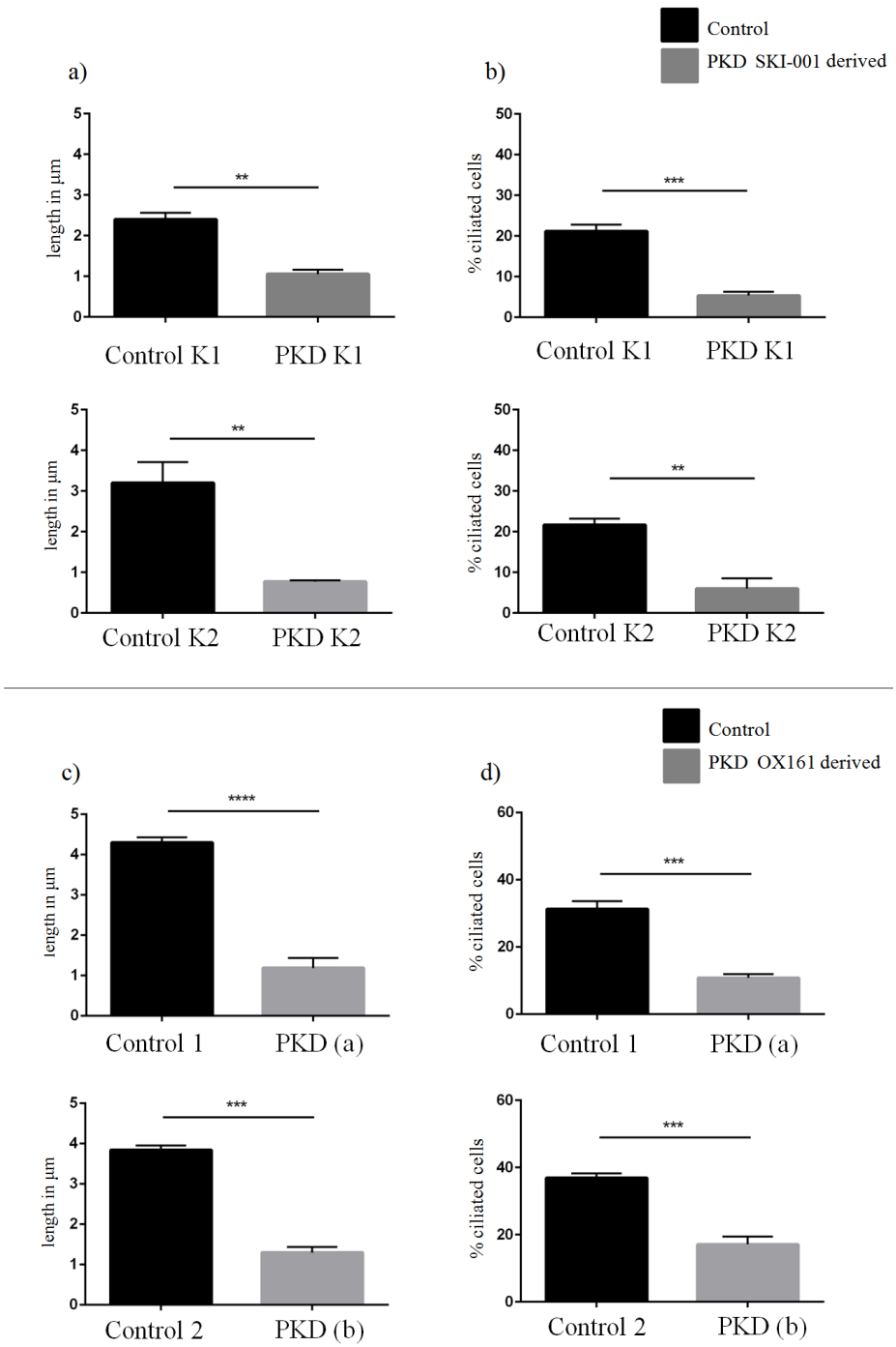

Figure 3.19 Primary cilium analysis in human tissue

a) Number of ciliated cells and **b)** primary cilium length comparison between ADPKD (SKI001) derived V.S normal cells. (Each column represents the result of 3 independent sections (n=3, N=500 to 1000 cells/n) of one test subject. Primary cilia on tubular cells were measured. Test subjects are two different normal controls (control K1 & K2) V.S sections from an ADPKD patient SKI-001) **c)** Number of ciliated cells and **d)** primary cilium length comparison between ADPKD OX161 derived V.S normal cells. (Each column represents the result of 4 independent sections (n=4, N=2000 to 4000 cells/n) of one test subject. Test subjects are two different normal controls (control 1 & 2) V.S sections from an ADPKD patient OX161. (Statistical test: paired t- test (* = $p \leq 0.05$), Error bars indicate mean ± S.E.M).

3.13 Primary cilia number and length in normal and Pkd1 mouse kidneys

To address the limitation of human ADPKD tissues, which could represent end-stage disease, *Pkd1* mouse tissue available from the early stages of disease was studied. Kidney tissue (4 month age) was available from tamoxifen-inducible Ksp-Cre *Pkd1* mice (induced at PN40) and their non-induced controls (Happé et al, 2014).

The results reveal that primary cilium length and number was significantly decreased in different tamoxifen induced *Pkd1* mice (C to G) compared to wild type controls (A to B) (**Figure 3.20 a-b**). The reduction of ciliary length and number although significant, was variable between the different *Pkd1* mice. These results confirm that *Pkd1* kidney mouse tissue is characterised by significant abnormalities in primary cilia expression and length.

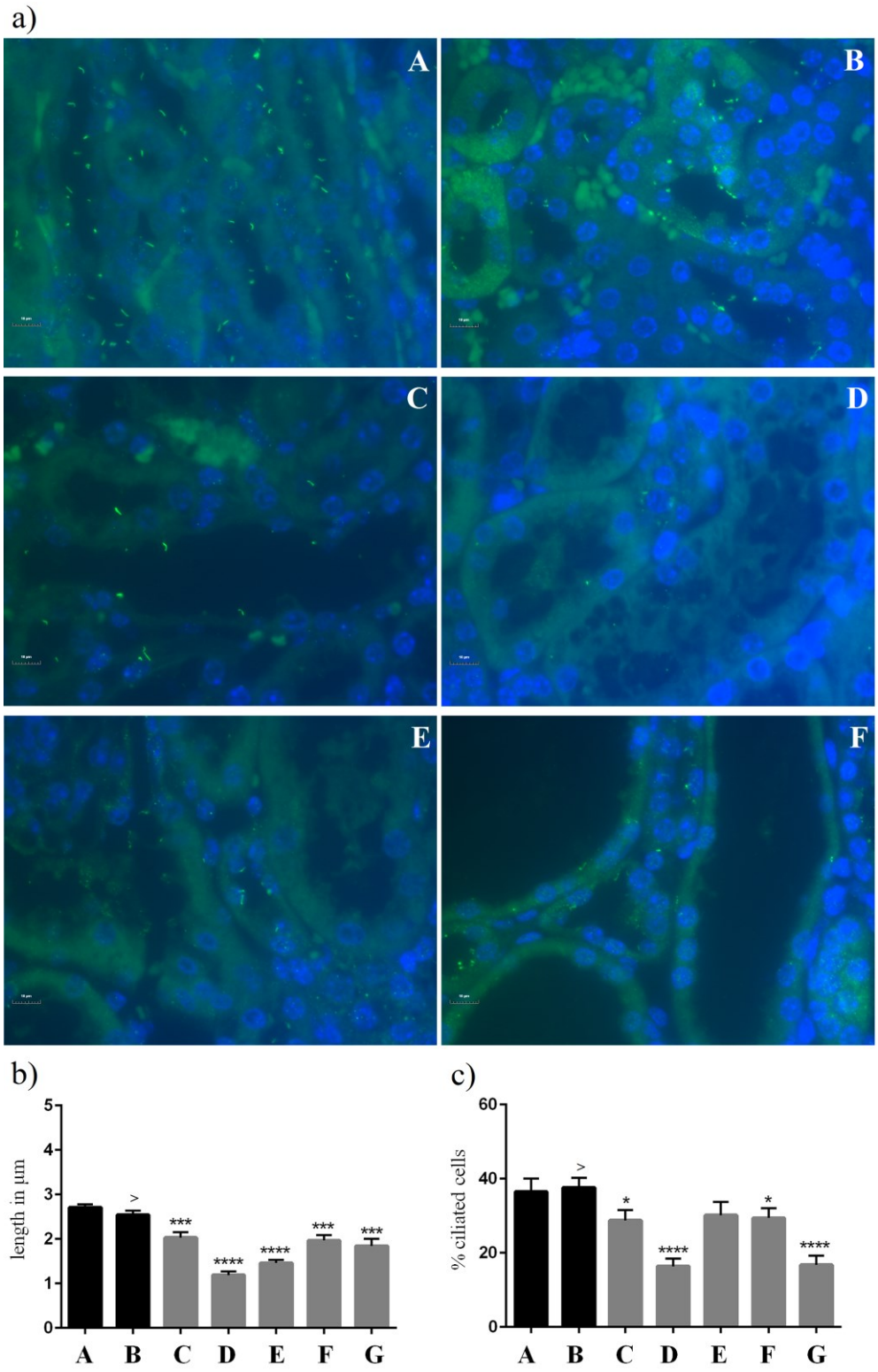

Figure 3.20 Mouse tissue of w.t and tamoxifen induced ADPKD models. a) Representative images of controls (no tamoxifen induction of *PKD1* KO): **A:** EO9-537**, B:** EO9-538**.** *PKD1* KO (tamoxifen induction of *PKD1* KO): **C:** EO9-353**, D:** EO9-355**, E:** EO9-356**, F:** EO9-363. **b)** Primary cilium length and **c)** ciliary number in controls **A, B** and tamoxifen induction of *PKD1* KO **C-G**. (N≈1000 Cells, Statistical test:paired t-test (* = p≤ 0.05), Error bars indicate mean ± S.E.M). Antibody used: DAPI-stained nuclei (Blue), ARL13b stained primary cilia (Green).

3.14 Polycystin-1 deficient cells and centrosome number

Finally, this study found that ADPKD cells were characterized by an increased frequency of cells with extra centrosomes (**Figure 3.21 a, b**), confirming data from a previous study (Lee et al, 2011). Centrosome abnormalities could interfere with mitosis and cilia formation. However the frequency of cells with extra centrosomes was low (less than 10%) suggesting that the reduction in cilia length was unlikely to relate to this.

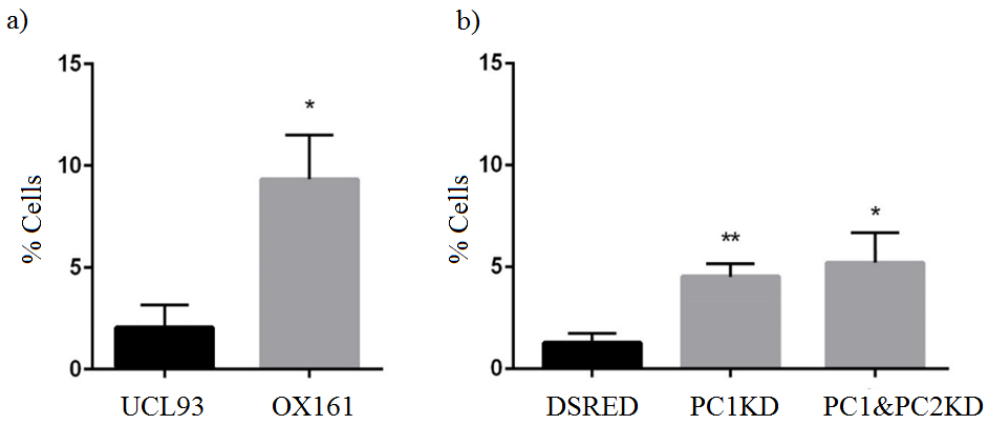

Figure 3.21 Analysis of cells with duplicated centrosomes. I measure a significant increase in cells expressing multiple centrosomes cells in the cystic OX161 **a)** and the PC1KD **b)** lines (n=3, 100 cells/N. Statistical test: paired t- test (* = $p \leq 0.05$), Error bars indicate mean ± S.E.M).

3.15 Cilia length and cell cycle exit

To address whether the shorter cilia in ADPKD observed were caused either by a delayed cilia length increase and/or delayed exit from the cell cycle, quiescent cells were studied for an extended duration of up to 96 h. Analysis by light microscopy showed that the number of attached cells was unchanged up to 72 h but decreased at 96 h probably due to cell detachment (**Figure 3.22 a, b**, **c**). In the control UCL93 cells, cilia length increased further up to 96 h, whereas there was no change for the OX161 ADPKD line. Expression of Ki-67, which marks cycling cells was negative by 48 h (**Figure 3.22 d**) confirming that both cell lines had stopped dividing and were growth arrested by this stage. No normalization of cilia length in the ADPKD models was measured after prolonged starvation times (**Figure 3.22 e**). These results confirm that reduced cilia length in the cystic line was not related to delayed cell cycle exit.

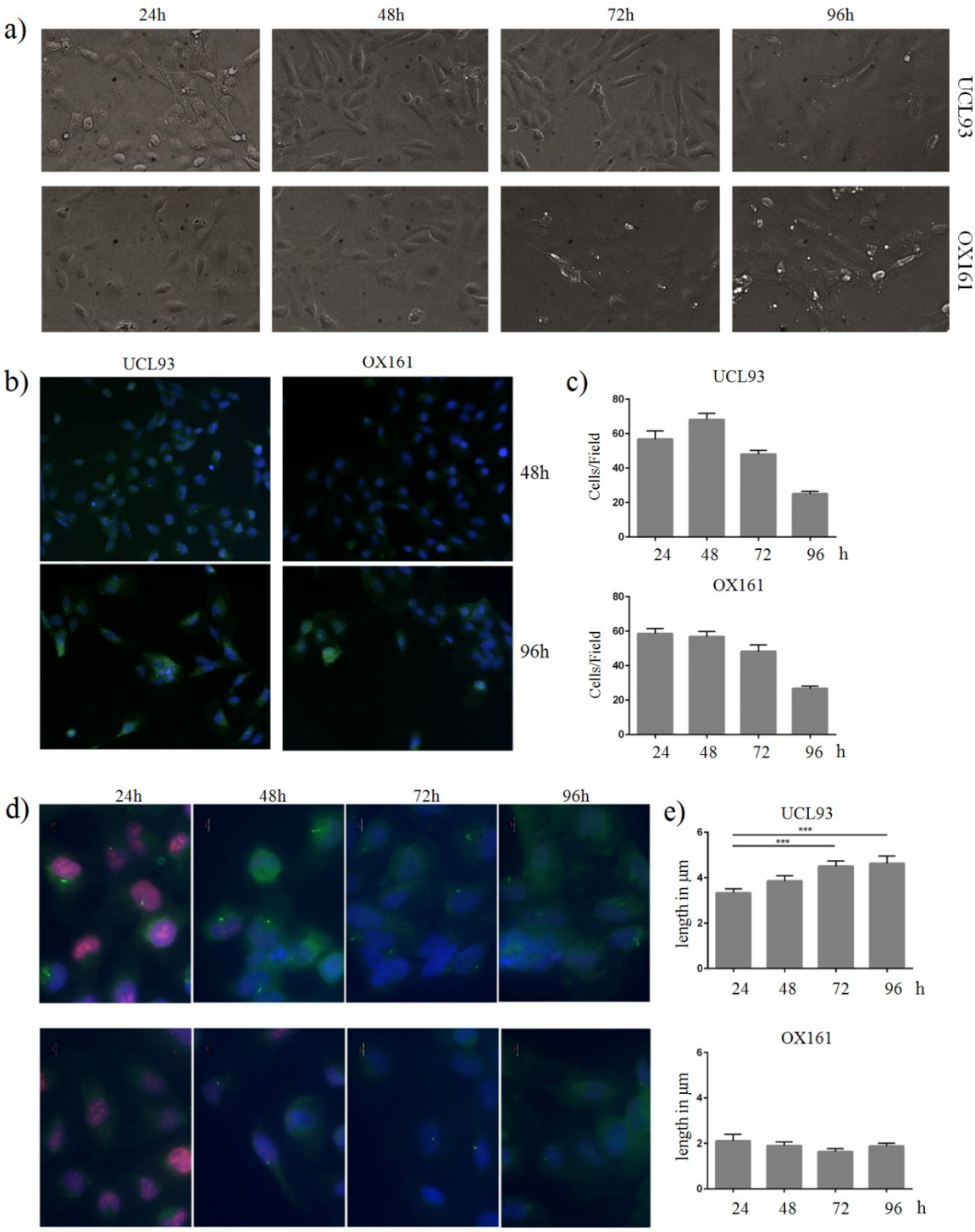

Figure 3.22 a) Cilia length and cell cycle exit Light microscopy images of normal and ADPKD cells over a starvation period of 96 h. **b)** Microscopy images of washed and 4% PFA fixed normal and ADPKD cells at maximum starvation point 96h (Magnification 40X). **c)** Graphic representation of counted cells per field, showing a decline of cell numbers at prolonged starvation periods. **d)** Fluorescent microscopy images with Ki67 proliferation marker shows proliferation decline with increasing starvation time (Magnification 60X). **e)** Prolonged starvation does not normalize ciliary length suggesting that length and number is not reduced due to a delay in cilia formation in PKD. Antibody used: DAPI-stained nuclei (Blue), ARL13b stained primary cilia (Green).

3.16 ADPKD primary cilia have orientation defects in wounding assays

The reduction in cilia length in ADPKD cells led to hypothesis that a possible functional defect in relation to their normal function could exist. One of the defects could be related to directed cell migration and cilia reorientation (Veland et al, 2014). To test this hypothesis, the orientation of cilia in migrating control and ADPKD cells after wounding was examined.

Directly after the scratch assay at time point 0 (t), primary cilia orientation is evenly distributed throughout the whole 180° spectrum with the overall mean hovering around 90° in normal and ADPKD models. After 9 h incubation, a significant reorientation of primary cilia pointing towards the wound scratch (close to 0°) could be measured in the normal cells. However, no significant changes were detected in the ADPKD models suggesting that orientation ability during migration was impaired (**Figure 3.23/24)**.

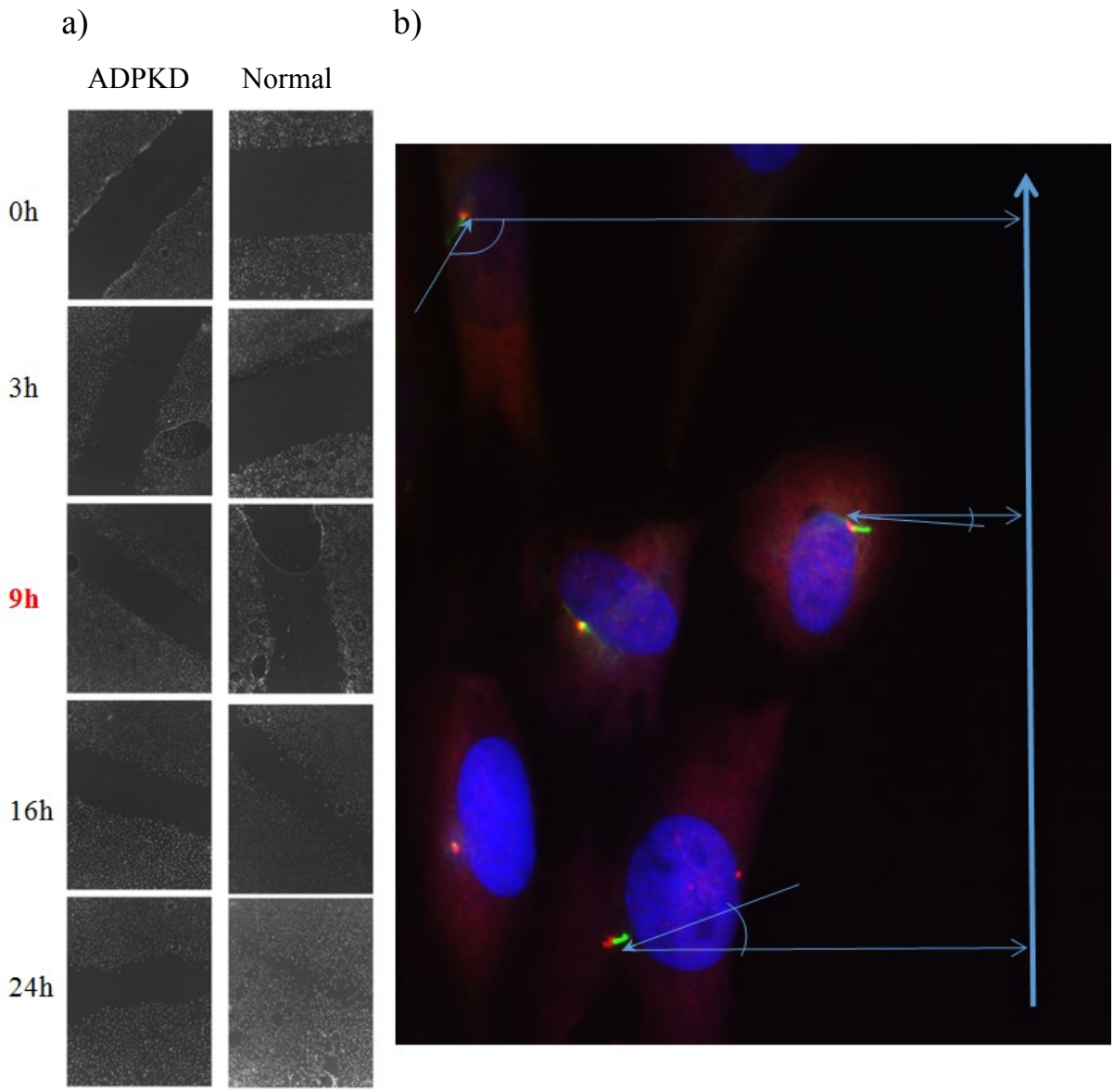

Figure 3.23 Primary cilium orientation in migrating normal and ADPKD cells (a) Time course of migrating normal and ADPKD models shows an optimal target with still clear border detection 9h after scratch assay. **(b)** The orientation of primary cilia towards the scratch is shown in a representative image of migrating normal cells. Measurement was performed by a leading arrow pointing from the cilium tip to the base to the cilium from which a horizontal arrow in direction scratch assay marked the °degree orientation towards the wound. The increase in °degrees from 0° (oriented towards the wound) to higher numbers marked the increase of cilia not oriented towards the wound. Antibody used: DAPI-stained nuclei (Blue), acetylated tubulin stained primary cilia (Green), gamma tubulin stained basal bodies (Red).

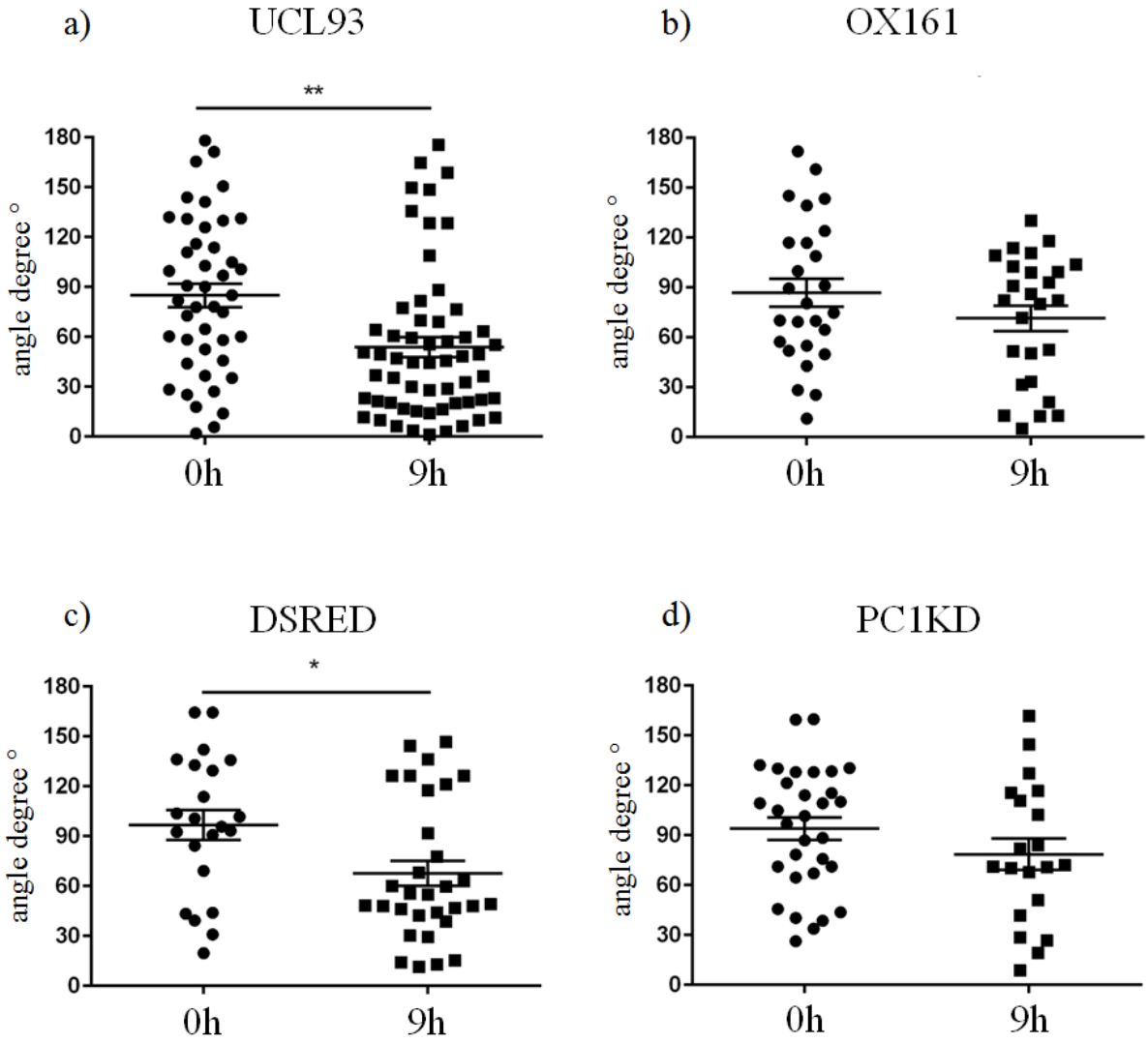

Figure 3.24 Primary cilium angle of deviation from wound in migrating normal and ADPKD cells

For this analysis a primary cilium oriented towards the wound is set at 0° as a standard.

a), c) In normal cells primary cilium orientation switches from a random conformation at time point zero (mean of all measurement combined = 90°) to a marked reorientation towards the wound at time point 9 h, with a significant shift of the 90° mean towards the 0° point (mean 53° UCL93, mean 61° DSRED). In both ADPKD lines a similar but not significant trend is observed, with a majority of cilia still scattered on the complete spectrum of angle orientations. (N=400-500 Cells, Statistical test:paired t- test (* = $p \leq 0.05$), Error bars indicate mean ± S.E.M).

3.17 Summary and discussion

Previous studies have raised concerns about the ability of cells to predictably form primary cilia at different passages or directly after storage (Alieva et al, 1999). However, in our cell line models, the level of ciliation in each cell line within a limited passage range (20 passages) and uniform cell density was found to be stable feature in repeated experiments.

3.17.1 Primary cilia regulators

In this study, no difference in the dynamics of cilia assembly and disassembly ratio were found between normal and ADPKD models in response to serum. However, cilia number and length were consistently decreased in ADPKD models compared to normal controls. This was an unexpected finding.

Further studies confirmed equivalent responses in both normal and disease models to two factors known to affect cilia length i.e. cAMP and Ca^{2+}. Many studies have investigated the role of cAMP and Ca^{2+} in normal cell behaviour (Besschetnova et al, 2010).

Cyclic AMP is a diffusible and ubiquitous second messenger produced in response to hormone action and is known to be involved in the regulation of many biological processes including cell proliferation, differentiation, or growth arrest in different cell types (Dumont et al, 1989). In normal renal epithelial cells, cAMP has an anti-mitogenic effect, while in ADPKD intracellular increases in cAMP have been shown to have a mitogenic effect (Hanaoka et al, 2000). This opposite role of cAMP in ADPKD has been suggested to relate to a disturbed crosstalk of the cAMP and Ca^{2+} pathways (Harris & Torres 2014).

In normal cells, cAMP has been shown to induce PKA dependent inhibition of the MEK/ ERK pathway with inhibition of cell proliferation (Wallace 2011). Ca^{2+} signalling also acts to prevent the activation of the B-Raf kinase upstream of the MEK/ERK pathway; however, the disturbed homeostasis of Ca^{2+} levels in ADPKD, could cause a release of the Akt inhibition of B-Raf, thus resulting in cAMP stimulation of B-Raf, ERK and therefore in cilium shortening and proliferation (Wallace 2011). Thus increases in Ca^{2+} would lead to opposite effects to increases in cAMP (Cooper et al, 1995; Lee et al, 2010). The balance between cAMP and Ca^{2+} in a normal cell is tightly regulated and the conservation of this dynamic

regulation might be critical for fully functional differentiated cells including the maintenance of normal cilia length.

However, the results from this study show that responses in cilia length to increases in intracellular Ca^{2+} or cAMP were no different in normal and ADPKD models, suggesting that these pathways are not defective in ADPKD. These results are in agreement with a previous study in control and a Polycystin-1 or Polycystin-2 deficient MEK and IMCD3 cell models (Besschetnova et al, 2010).

3.17.2 AKAPs localize the cAMP signalling

The ability of cAMP to modulate ciliary length was shown to depend on PKA activation mediated probably through a scaffold and anchoring proteins abbreviated AKAP for A-kinase-anchoring proteins complex at the cilia base. More than 50 different subsets of these AKAP scaffolding proteins have been identified so far, all determined by a common structurally conserved protein kinase A (PKA)-binding domain. AKAPs are able localize signalling to specific subcellular compartments and membrane microdomains. In addition, they have been shown to play an important role in regulating and localizing PKA signalling to specific areas of the cell, and particularly interesting in our case, to the centrosomes at the base of the cilia (Sillibourne et al, 2002). AKAPs proteins target PKA to a variety of distinct subcellular locations, confining enzyme activity at determined cAMP production sites, with the result that only a subset of potential substrates can be phosphorylated (Carnegie et al, 2003). Many localization examples of these large AKAPs complexes to their subcellular target are shown to rely entirely on phosphorylation, and or interaction with other proteins and phospholipids. A few examples include the interaction of AKAP79/150 with PtdIns(4,5)P2 (Dell'Acqua et al, 1998), or the binding of several AKAPs, i.e. AKAP6 (Dodge et al, 2001), AKAP7 (Stefan et al, 2007) and AKAP9 (Taskén et al, 2001) to the (PDE4D3) protein, a member of the family of the Cyclic AMP-dependent phosphodiesterase type D proteins which are elevated in response to cAMP. The PDE enzymes are primary involved in local degradation of cAMP, playing a crucial role in the spatial control of cAMP propagation. In a recent study, the authors investigated the spatial compartmentalization of cAMP to the centrosome via a PKA-PDE4D3-AKAP complex (Terrin et al, 2012).

This study focused on the possible role of AKAP350 which was initially identified as a possible interacting partner of polycystin-1 in MS pull-down assays (unpublished). Co-immunoprecipitation confirmed binding of AKAP350 to polycystin-1 PLAT domain. AKAP350 was shown to localise to centrosomes as previously shown. It is a centrosomal PKA regulator whose activation threshold could be reduced with an increase in auto-phosphorylation (Terrin et al, 2012). Moreover, the binding of PDE4D3 to the AKAP350 complex is entirely regulated by phosphorylation and de-phosphorylation (Takahashi et al, 1999, Tasken et al, 2001). Thus, the close aggregation of PKA and PDE4D3 enzymes via AKAP350 may function as a self-regulating negative feedback system (Dodge et al, 2001). Another study has also shown that cAMP concentrations localised to a specific centrosomal microdomain modulated by PDE4D3 changed during different stages of the cell cycle; disruption of this microdomain stopped cell cycle progression with a resultant accumulation of cells in prophase. The study provided the first tangible evidence that control of cell cycle progression might rely on regulation of centrosomal cAMP/PKA signals (Terrin et al, 2012). PDE4D members are not only involved in PKA, MAP kinases and Erk2 phosphorylation activities but also found to play key roles in regulatory mechanism like protein-protein interactions with cytoskeletal scaffolding proteins at specific targeted locations. In this study however, AKAP350 centrosome localisation was not altered in ADPKD cells suggesting that polycystin-1 binding is not essential for its centrosomal location. However, AKAP350 function may still be abnormal in the absence of polycystin-1, leading to cell cycle dysregulation in response to cAMP. This possibility needs to be tested in future studies.

Impairment of normal centrosome function has been shown together with cilia defects to be involved in both tumorigenesis and ciliopathies (Nigg et al, 2009). The ability of AKAP proteins to localize and modulate the timing of cAMP activation, e.g. through the cell-cycle dependent binding of specific regulatory subunits of PKA, have been so far not only linked to chromatin remodelling during mitosis (Landsverk et al, 2001), but also in more recent investigation to direct or indirect modulation of the Hedgehog and/or RAS/ERK signalling pathways, both involved in cell cycle progression (Waschek et al, 2006). Interestingly, AKAPs have been associated with various cytoskeletal and structural events, including the formation of actin stress fibres via AKAP-Lbc derived activation of the Rho pathway, thus underlining another critically important potential aspect of these proteins as orchestrators of the structural architecture of cells (Diviani et al, 2001; Schmidt et al, 1999).

3.17.3 The role of cAMP in cell proliferation

It is largely accepted that cAMP is associated with regulation of the cell cycle, exerting either an inhibitory or stimulatory effect on proliferation depending on the cell type. The role of cAMP also varies greatly on the cell type or strength of the stimulus (Luciano et al, 1999). This study confirmed two different effects of cAMP. In growth-arrested cells, cAMP increased cilia length independent of the cell cycle. This effect was similar in normal and ADPKD cells. However, in cycling cells, cAMP inhibited the cell cycle in normal but not ADPKD models. Cell cycle exit was confirmed by loss of Ki67 and PH3 expression and associated with ciliation. These results are similar to previous findings in mouse mammary adenocarcinoma cells (Rodriguez-Collazo et al, 2008), which showed that cAMP was able to regulate PH3 by blocking G2 progression as evidenced by mitotic entry inhibition and decreased activity of the CyclinB/Cdk1 kinase. These processes were not only highly sensitive to variations in intracellular cAMP concentration but also dependent on the expression of the catalytic subunit of PKA. The authors conclude that ultimately the loss of mitotic H3 phosphorylation could be caused by either a rather global dephosphorylation of H3 in mitotic chromosomes or the prevention of phosphorylation through a pre-mitotic block to cell cycle progression (Rodriguez-Collazo et al, 2008).

3.17.4 PGE2 regulates primary cilia length

In this study, PGE2 was identified as a potential ligand activating the cAMP/PKA effect on cilia length. A previous study had shown that PGE2 acting via EP2 receptors could increase cAMP and stimulate the formation of cysts, possibly by inhibiting apoptosis (Elberg et al, 2007). For cilia length, PGE2 appears to act not only via EP2 but also via EP4 with some evidence of redundancy. One interpretation of these results could be that the PGE2/EP2-EP4/AC/cAMP signalling cascade, shown to cause primary cilium elongation is potentially necessary for optimal normal cilia length. This could be necessary for normal cilia function e.g. to arrest proliferation and responsiveness to other extracellular stimuli which in turn may regulate cAMP levels (Choi et al, 2011).

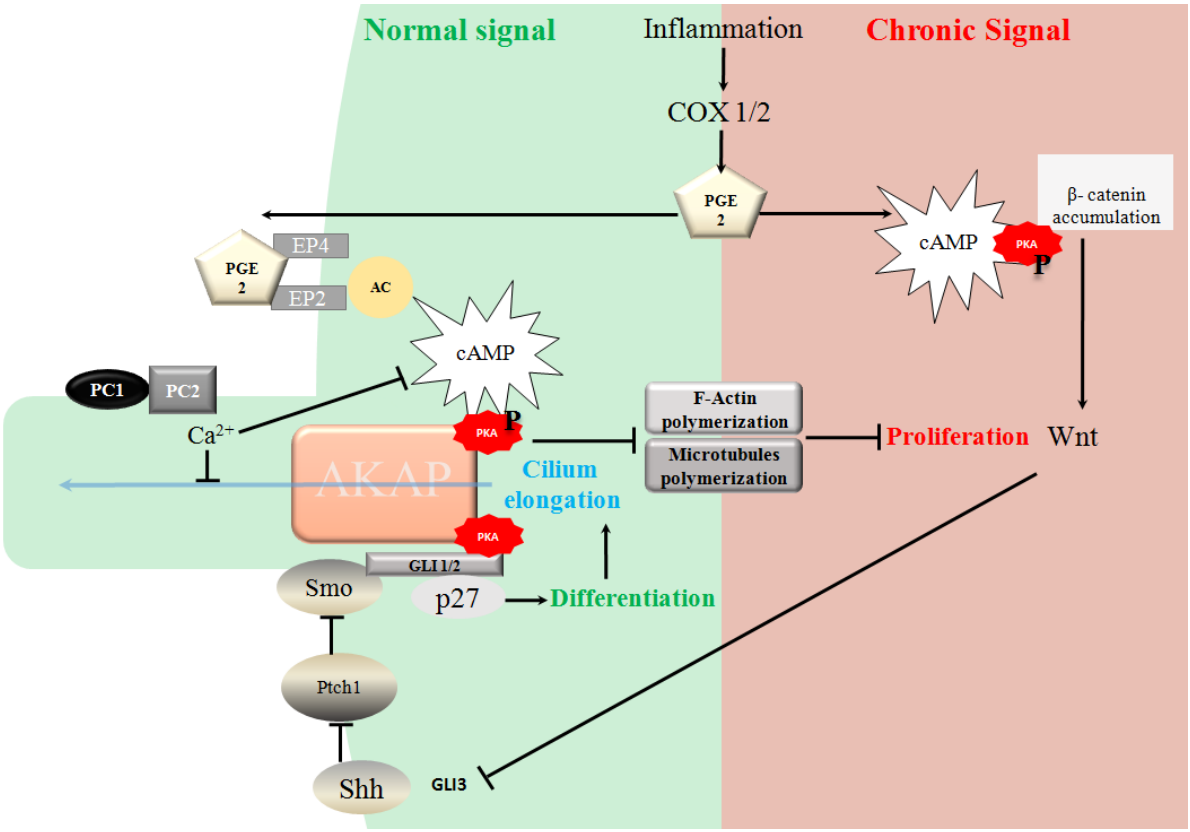

Figure 3.25 Model of primary cilium regulation in ADPKD Normal cAMP signalling results in primary cilium elongation, which is subsequently reverted by feedback mechanism to basal levels in normal cells. In ADPKD cells a prolonged chronic cAMP level might activates alternative pathways e.g lead PKA phosphorylation of Beta catenin, and its subsequent local accumulation which activates the Wnt signalling which cause proliferation (Hino et al, 2005). It has also been shown that the Shh is also antagonized by Wnt activity through the expression of Gli3 (Ulloa et al, 2010), while when the cilium is formed SHH inhibits Ptch1 which in turn inhibits SMO signalling which leads to GLI activation and differentiation pathway.

In the study by Zhang, it was shown that cAMP and PGE2 can be pro or anti-proliferative and that the difference might exclusively rely on the strength and the actual duration of the signal. This biphasic effect was related to the amount and time of PGE2 activation. Stimulating at low concentration resulted in proliferation, while high concentrations were anti-proliferative (Zhang et al, 2014).

3.17.5 Ciliary length and defective orientation in cell migration

In this study, ciliary length in human *PKD1* cystic kidney lines and tissues were consistently shorter than normal controls. This was unexpected since the general consensus in the field is that cilia are structurally normal but functionally defective in ADPKD. However, few studies have addressed this question systematically. A review of published studies have reported no differences (Nauli et al, 2003), shorter cilia in *PKD1* cyst cells (Xu et al, 2007), curved and less ciliated cells in Adipose-derived stem cells (Bodle et al, 2013; Plotnikova et al, 2014), longer cilia in *Pkd1* transgenic mice (Kurbegovic, et al 2010) and longer, but less frequent cilia in dilated collecting ducts tissue of *Pkd1* hypomorphic mice (Hopp et al, 2012). These studies indicate that cilia length and number may be altered in ADPKD cells and tissues, but the mechanism underlying these changes has not been reported. The possibility of delayed cell cycle exit was excluded. The presence of multiple centrosomes was found in a low percentage (<10%) of ADPKD cells as previously reported but could not account for the general reduction in cilia length observed.

The consistent ciliary length defects observed so far led to the hypothesis that a reduction in cilia length could lead to defects in directed cell migration and cilia orientation in ADPKD cells. Normal oriented migration occurs via polarization in response to positional cues, which consist not only of extracellular attractants, but importantly can also be mediated by the disruption or alteration of the contact to neighbouring cells (Etienne-Manneville 2012; Cordeiro & Jacinto. 2013). In regards to our study it is important to note that the primary cilium as a sensory organelle, hosts and coordinates a number of pathways involved in controlling cell migration and orientation such as. TGFβ, PDGF, Hh, Wnt, and RTK signalling (Goetz & Anderson, 2010; Christensen et al, 2012); thus defects in primary cilium formation are likely to impair normal migratory mechanisms.

Previous studies on primary cilium dynamics during migration pointed to a 4 step process (membrane protrusion and adhesion in the direction of movement, contraction, detachment, and retraction of the rear end) which is based on an initial nucleus repositioning followed by the actin cytoskeleton reorganization, which allowed frontal reorientation of the cilia–centrosome axis (Veland et al, 2014). The actual migration process is then subsequently initiated as the primary cilium points towards the movement direction and the actin structures force the membrane in corresponding direction of the signal (Veland et al, 2014).

The clear role of primary cilia in directed cell migration has only recently gained attention and its mechanisms are still poorly understood. However, some studies suggest that the platelet-derived growth factor receptor alpha (PDGFRα), which is localized to the primary cilia might be a key element in ciliary migration mechanisms (Christensen et al, 2013). Sensing of PDGF from a specific direction through the ciliary sensor might activate specific pathways and positional cues that regulate the organization of the cytoskeleton required for actin organization and lamellipodium formation and thus all subsequent migration steps involved in this process.

The reduced ability of ADPKD cells to re-orientate the primary cilium towards the wound suggests that either defects in actin organization or aberrant signals from primary cilium defects in the ADPKD model affect the normal orientation mechanisms of primary cilia during migration.

Recent studies have uncovered a strong link in other ciliopathies, i.e. Nephronophtisis, Bardet–Biedl, Joubert, Meckel–Gruber and Orofacial digital 1 syndromes (Valente et al, 2014) between primary cilia and cell migration in the developing brain.

Normal migration is characterized by microtubules and F-actin organization dependent repositioning of the centrosome between the nucleus and the leading edge (Etienne-Manneville 2013). A seminal study also showed that in confluent 3T3 fibroblasts, orientation of primary cilium appeared random, while in sub-confluent migrating cells, the cilia tended to point in parallel to the 2D layer and in the direction of migration (Albrecht-Buehler, 1977), suggesting that the cilium acted as a sensory organ capable of following or leading the direction of the cell migration path. This observation has been confirmed by many studies showing this unique reorientation effect of cilia i.e. at the wound sites of migrating cells, suggesting that the primary cilium plays a critical role in directed migration and tissue repair (Christensen et al, 2008; Lu et al, 2008; Schneider et al, 2010; McGowan et al, 2013). The

oriented cilium could function as a point of reference for the navigation of cells, such as a sail on a boat, thus steadying a current of environmental synergistic and opposing signals, towards the most favourable direction of migration (IbenRønnVeland et al, 2014).

In support of this, cells with stunted cilia in addition to decreased orientation and directionality were characterized by reduced PDGF-AA dependent cell migration (Schneider et al, 2010; Pedersen et al, 2008). Recent evidence suggesting that primary cilium signalling either induces the transport of polarity proteins along microtubules to the leading edge or directly affects the allocation of microtubule tracks (IbenRønnVeland et al, 2014), although the exact mechanism are still unclear. Other examples for the role of primary cilia in migration include the ciliary PDGFRα, which is involved in PI3K-Akt and Erk1/2-Mek1/2 activation and has been shown to have critical roles in cell polarization of rat kidney epithelial cells (Bisel et al, 2008; 2013) and Wnt/PCP signalling which is also regulated through the primary cilium. The latter acts as a regulator of polarized migration and cell adhesion by regulation of disheveled (Dvl) proteins, which modulate actin and microtubule cytoskeletal rearrangements via Ca^{2+} signalling (Gao & Chen 2010; Amin & Vincan 2012; Wynshaw-Boris, 2012). The role of Wnt/PCP signalling in directional primary cilium dependent migration has implicated Inversin/Nephrocystin-2. The INVS protein is localized to a specific compartment at the base of the cilium termed the INVS compartment (Yamaoka et al, 2009). INVS has been shown to control the switch between canonical and non-canonical Wnt signalling by its ability to degrade Dvl proteins, therefore resulting in βcatenin turnover and PCP (Simons et al, 2005). Invs–/–MEFs are characterized by a reduced polarization and movement ability, marked by dispersed GSK3β-phosphorylated β-catenin localization at the base of the primary cilium, elevated canonical Wnt signalling and defective activation and localization of RhoGTPases to leading edge (Veland et al, 2013). Invs–/–MEFs not only showed defective leading edge and actin targeting and activation of the controller NHE1 (Denker & Barber, 2002), but also failed to upregulate PDGFRα transcription during growth arrest. This then resulted in reduced ciliary PDGFRα accumulation which in turn was characterized by a decreased ability of the cilium to respond to PDGF-AA and thus impaired Akt and Mek1/2-Erk1/2 activation (IbenRønnVeland et al, 2014).

Summary

- Primary cilia assembly and disassembly in response to serum was not altered in ADPKD models compared to controls.
- The average length and number of primary cilia was reduced in ADPKD models compared to controls both *in vitro* and *in vivo*.
- This difference was unrelated to delays in cell cycle exit or changes in centrosome number.
- Cilia length in ADPKD models and controls responded similarly to changes in cAMP and Ca^{2+}.
- The response to db-cAMP in both models was dependent on both PKA activation and AKAP binding.
- AKAP350 co-immunoprecipitated with the polycystin-1 PLAT domain and localised to centrosomes.
- PGE2 could be a physiological ligand for the response to db-cAMP, acting primarily through EP2 and EP4 activation
- ADPKD models showed impaired cell cycle exit in response to db-cAMP compared to controls.
- In wounding assays, re-orientation of cilia towards the wound was defective in ADPKD models compared to controls.

In the next chapter, the potential role of the cytoskeleton in regulating cilia assembly was examined.

Results Chapter IV

The Role of the Cytoskeleton Dynamics on Primary Cilia Structure in ADPKD

4.1 Introduction

Actin filaments and microtubule networks represent important cytoskeletal components in every cell and their dynamic regulation is crucial for many cellular processes including cytokinesis, morphology changes, cell shape and migration. They also exert control over channel and receptor transport, localization and function (Rodriguez et al, 2003; Montalbetti et al, 2007). In this chapter, the potential role of cytoskeletal changes on the regulation of primary cilia length regulation was examined.

Microtubules

Microtubules are cytoskeletal polymers essential for the maintenance of cell shape, division, migration, compartmentalization and ordered intracellular transport powered by motor proteins. A microtubule per se is a cylinder with outer diameter 25 nm formed by 13 laterally bound protofilaments built by heterodimers of globular α- and β-tubulin subunits arranged in a head-to-tail manner (Nogales et al, 1998) (**Figure 4.1**). They are polar structures with two structurally distinct ends, a slow-growing minus end, exposing α-tubulin subunits, and a fast-growing plus end exposing β-tubulin subunits (Nogales et al, 2006). Within the cells the minus ends are stabilized by anchoring in microtubule-organizing centre (MTOCs), whereas plus ends are highly dynamic and switch between phases of growth and shrinkage. Polymerization and depolymerization of microtubules are driven by hydrolysis of GTP on β-tubulin monomer. GTP exchange is necessary for the switch between phases of growth and shrinkage separated by catastrophe (growth to shrinkage transition) and rescue (from shortening to growth). Importantly, this dynamic instability is an essential feature of microtubules that allows them to search through the cell for targets like cell cortex or actin cytoskeleton (Desai et al, 1997). The dynamics of microtubules can be regulated by incorporation of alternative tubulin isotypes (Luduena et al, 2008) or by post-translational modifications (PTMs) of tubulin subunits (mainly acetylation, tyrosination/detyrosination, polyglutamylation, polyglycylation and phosphorylation), and binding of microtubule associated proteins MAPs (Amos et al, 2005; Verhey et al, 2007). Binding of MAPs has been suggested to be largely regulated by PTMs (Nogales 2001).

Microtubule dynamics can be also regulated by a variety of ligands, including microtubule drugs, i.e. docetaxel (taxol) (Jordan et al, 2007). The key regulator of microtubule nucleation

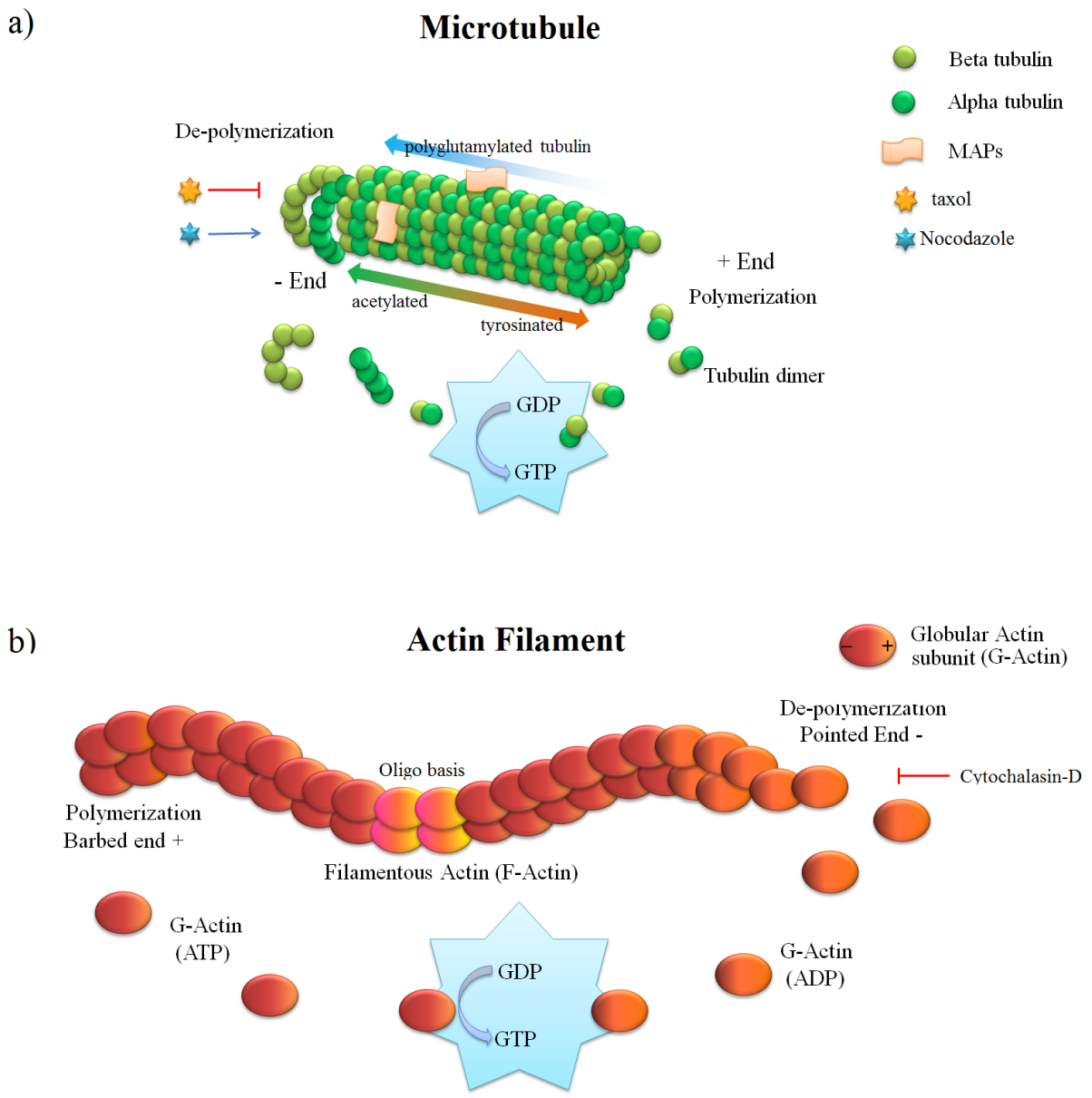

Figure 4.1 Microtubules and Actin a) Microtubule dynamics diagram. α and β tubulin dimers polymerize on the + end of the growing cone while depolymerisation occurs on the – end. Microtubule-associated proteins (MAPs) when not phosphorylated can function as microtubule-stabilizing factors that protect microtubules against depolymerisation (Song and Brady 2015).
PTM such as addition of one or more glutamate (polyglutamylation) or glycine residues (polyglycylation) to the α and β tubulin heterodimers influence microtubule regulation.
b) Actin dynamics diagram Polymerization: actin monomers are added to the barbed end causing actin filament elongation. De-polymerization: Hydrolysis takes place on the pointed other end causing detachment of ADP-actin monomers.

is γ-tubulin (Oakley et al, 1989), a highly conserved minor member of the tubulin family concentrated in MTOCs. γ-tubulin interacts with 6 GCPs (γ-tubulin complex proteins) to create small (γ-TuSC) and large (γ-TuRC) complexes that participate in microtubule nucleation (Teixido et al, 2012). Interestingly, an important role in the regulation of microtubule formation and granule translocation might also be played by Ras guanyl nucleotide releasing proteins (RasGRPs) that activate RhoA via PI3 kinase (Liu et al, 2007) which contributes to a variety of other factors able to regulate the dynamics of microtubule formation. However, the primary determinant of whether microtubules grow or shrink is the rate of GTP hydrolysis, a factor that is both intrinsic and essential to filament assembly (Sharma et al, 2011).

The cilia axoneme comprises a microtubular core comprised of α- and β-tubulin stabilised or destabilized by post-translational modification such as acetylation, glutamylation and polyglutamylation, the latter reported to promote MT severing *in vivo* and *in vitro* (Lacroix et al, 2010, Song and Brady 2015) (**Figure 4.1**). The centrosomes at the cilia base also form the microtubules organizing centre (MTOC). At the start of cell division, the microtubule axoneme of the primary cilium must be completely retracted in order to release the centrioles/centrosome to form the mitotic spindle. As a consequence, it could be said that organization of cilia microtubules is indirectly involved in the regulation of the cell cycle (Pugacheva et al, 2007).

Actin

Actin is a structural related multi-functional protein that is able to forms microfilaments in the cell. It can be present in two forms: G-actin (globular actin) in form of a free monomer or F-actin (filamentous actin) in the form of elongated linear polymer microfilaments. Nucleotide hydrolysis by F-actin regulates the transition between G- and F-actin. The ATP state is more stable than the ADP state.

The polymerization has been described to occur in sequential phases, characterized by an initial lag period where G-actin monomers combine into short, unstable oligomers. A growing phase follows were these oligomer form the basis for the addition of new actin monomers which assemble on both ends of the filament. The last phase is the equilibrium phase were actin monomers are added to the fast-growing barbed end of the elongating filament in the ATP state while hydrolysis takes place on the other end of the filament leading to a faster dissociation rate of ADP-actin monomers from the pointed end. This results in a dynamic

mechanism of actin polymerization/depolymerization also known as actin filament treadmilling (Wegner and Isenberg 1983) with an equilibrium in actin filament structure were no net change in the total mass of filaments can be measured (Uzman et al, 2000).
Ultimately, the form in which actin is organised determines its roles. These include cytokinesis, vesicle and organelle movement, the establishment and maintenance of cell junctions as well as cell shape, mobility and contraction of cells during cell division.
Treadmilling alone does not account for the high dynamic regulatory mechanisms of actin filament formation observed in different in cells. Studies have uncovered a wide variety of different proteins involved in the regulation of actin cytoskeleton dynamics, such as actin monomer sequestering or filament severing and cross-linking proteins (Pollard and Borisy 2003). Interestingly, many promising candidates for the mediation of structural interactions between microtubules and actin filament have been identified in mammalian cells (Mandato et al, 2003).

Recent studies have also suggested a link to primary cilia assembly although the mechanisms underlying these observations have not been clarified (Bershteyn et al, 2010; Sharma et al, 2011).

4.2 Cytoskeletal abnormalities affect normal cilia formation

4.2.1 Introduction

In the previous chapter, it was confirmed that the cAMP/PKA pathway could increase cilia length. However, recent studies have pointed to additional clues, particularly changes in cytoskeletal dynamics which could alter ciliary length. Most of these studies pointed exclusively to cytoskeletal changes and dynamics of tubulin and possibly actin as a main cause for cilia or flagella length (Sharma et al, 2011).

Primary cilia consist of a microtubule core arising from a basal body or mother centriole. The cilia base could be stabilised by polymerised actin filaments. Although microtubule or actin dynamics are shown to be involved in primary cilia regulation in other cells (see chapter 4.2), this effect has not been studied specifically in ADPKD. The following analysis was therefore performed to investigate their potential involvement in primary cilium regulation and in the pathogenesis of ADPKD.

4.2.2 Actin organisation in normal and ADPKD cells

The organisation of F-actin was first compared in normal and cystic cell lines after 48h growth arrest using labelled phalloidin (**Figure 4.2**). Overall F-actin labelling appeared to be more disorganized in both ADPKD models compared to normal controls. Actin fibres appeared generally increased, specifically at the perinuclear regions, the orientation of stress fibers appeared more randomly distributed throughout the cell and a proportion of stress fibers appeared thicker.

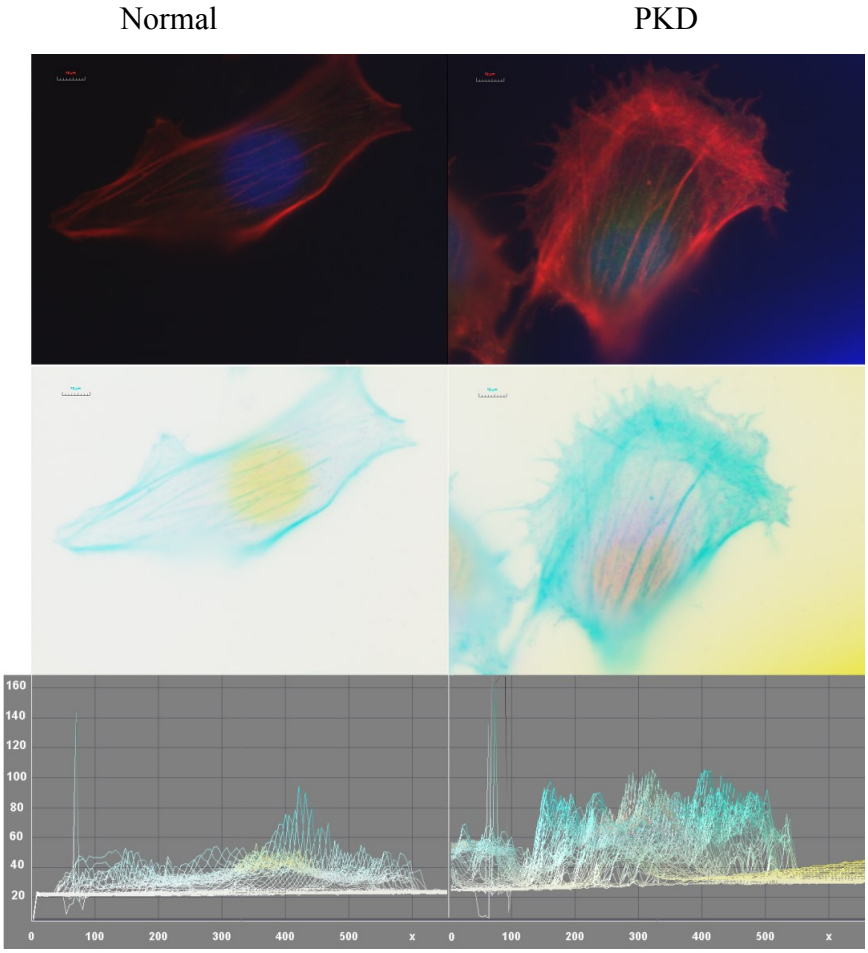

Figure 4.2 Actin organization. Representative image of Actin organization and 3D surface intensity Plot (Fiji) phalloidin labelled F-actin actin structures and stress fibres can be detected in normal and ADPKD models. Subtle differences can be observed in the organization of the cytoskeletal actin structures in the ADPKD model. In particular, actin structure seems less organized and characterized by overlapping structures or bundles of various intensity and thicker non parallel stress fibers. Magnification 60X, Scale bar 10 µm. Antibody used: DAPI-stained nuclei (Blue), Phalloidin stained actin (Red).

4.2.3 Modulation of Actin polymerisation alters primary cilia length

In view of the structural defects in actin organisation observed, it was hypothesised that modulating actin polymerisation could restore cilia length.

Different compounds are known to affect actin polymerization. Cytochalasin D is a cell-permeable and potent inhibitor of actin polymerization. It disrupts actin microfilaments causing arrest of the cell cycle at the G1-S transition. Although the full mechanism of this compound are not clear, the common understanding is that it binds to the plus ends of F-actin polymers blocking further polymerization though actin monomers addition, while simultaneously natural de-polymerization mechanism at the (-) gradually cause loss of the filament (May et al, 1998).

As shown, cytochalasin D treatment induced an increase in cilia length in both normal and ADPKD models. Ciliary length in the ADPKD cells reached the same maximum extension as the normal cells at 1μM concentration (**Figure 4.3 a**, **c**). Comparison of the percentage cilia length increase between normal in ADPKD models revealed a significantly greater ciliary length increase in the disease models (**Figure 4.3 b**, **d**).

The orientation of F-actin fibres was measured by focusing on actin arrangements positioned over the nucleus and measurement of the stress fiber angle relative to a horizontal line. As shown in (**Figure 4.4**), there was a wider spread of actin fibre orientation in the ADPKD cells compared to their controls. The length of the fibres was also significantly shorter.

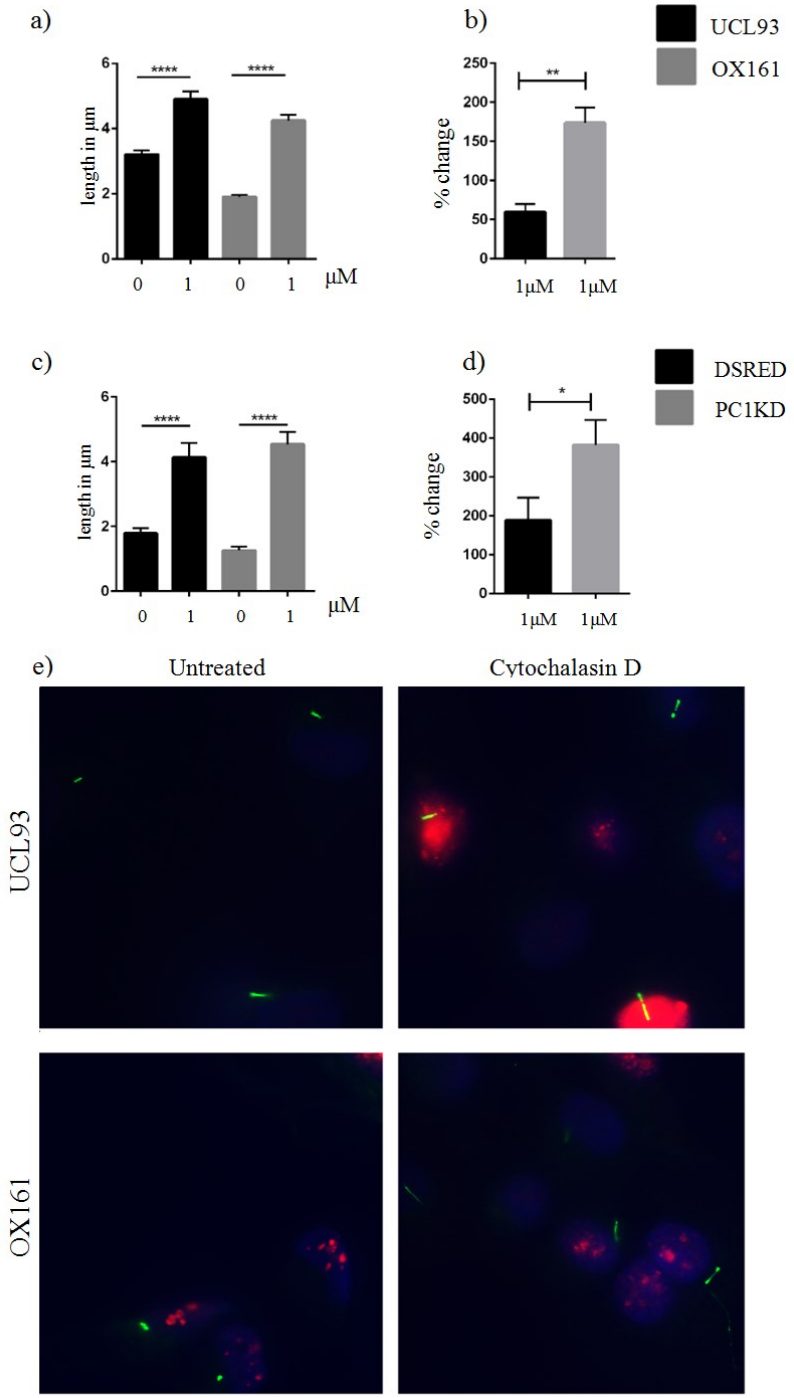

Figure 4.3 Effect of Actin depolymerization on primary cilia. Inhibition of actin polymerization via cytochalasin D results in significant primary cilium elongation in **a)** normal and **c)** ADPKD models. Primary cilium elongation in ADPKD models is significantly increased to the normal control after normalization **b), d)** suggesting that ADPKD cells are more sensible to actin destabilizing agent cytochalasin D (n=3, Statistical test:paired t -test (* = p≤ 0.05), Error bars indicate mean ± S.E.M) **e)** Representative image of cytochalasin D treated/untreated normal and ADPKD cells marked with ARL13b (green) cilia, KI67 proliferation marker (red) and DAPI-stained nuclei (Blue). Magnification 60 X.

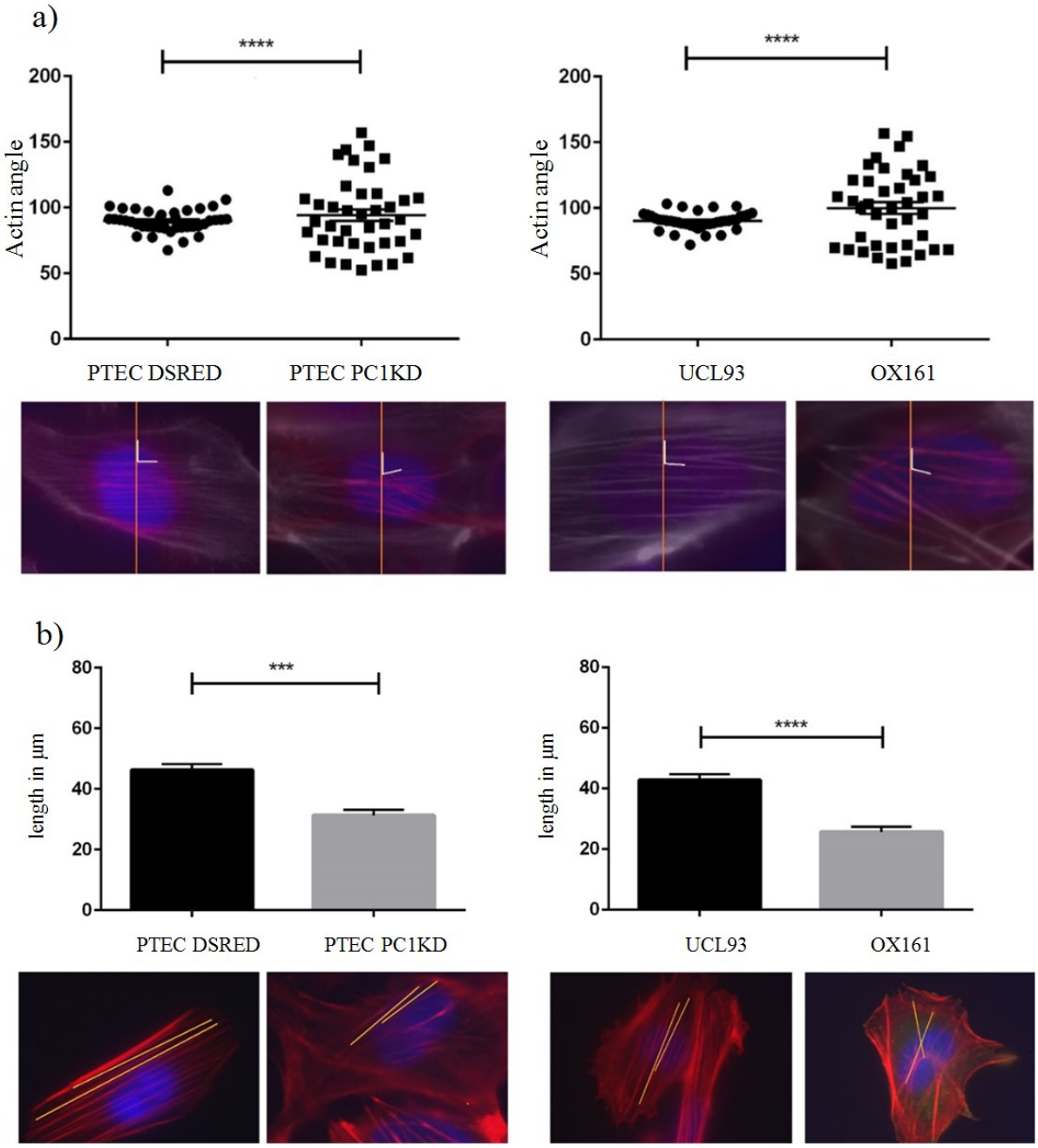

Figure 4.4 Actin organization analysis. Comparison between normal and ADPKD **a)** measurement of stress fiber angle orientation. The amount of parallel running stress fibers is significantly decreased in ADPKD models. **b)** Measurement of stress fiber length shows a significant decrease in the average stress fiber length in ADPKD cells. (N=60 cells, Statistical test:paired t -test (* = $p \leq 0.05$), Error bars indicate mean ± S.E.M). Antibody used: DAPI-stained nuclei (Blue), Phalloidin stained actin (Red).

4.2.4 Structural 3D actin analysis in primary cilia vicinity

To investigate overall 3D actin arrangements in the whole cell especially around the ciliary base, confocal microscopy was performed. F-actin was excluded from the cilia shaft as reported in the literature (Ishikawa et al, 2012; Washburn et al, 2001).
Z-stack fluorescent images showed that in normal cells, most of the detected primary cilia were situated well above the actin stress fiber plane while in ADPKD cells, more actin fibres appeared to be clustered around the cilia base (**Figure 4.5**).

To obtain a more detailed analysis of actin structures and its organisation around the primary cilium, super-resolution light microscopy by SIM (Structured Illumination Microscopy) was performed. This allowed the visualization of images with a resolution below that of the Abbe diffraction limit.

Using super-resolution imaging, most of F-actin in normal cells was localised to the basolateral membrane with little detected in the apical region or membrane (**Figure 4.6 a-c**). In contrast the ADPKD model, F-actin was more randomly distributed within the cell **(Figure 4.6 b**, **d)** and an increase in small actin structures (granules) could be detected around the primary cilium compared to normal control.

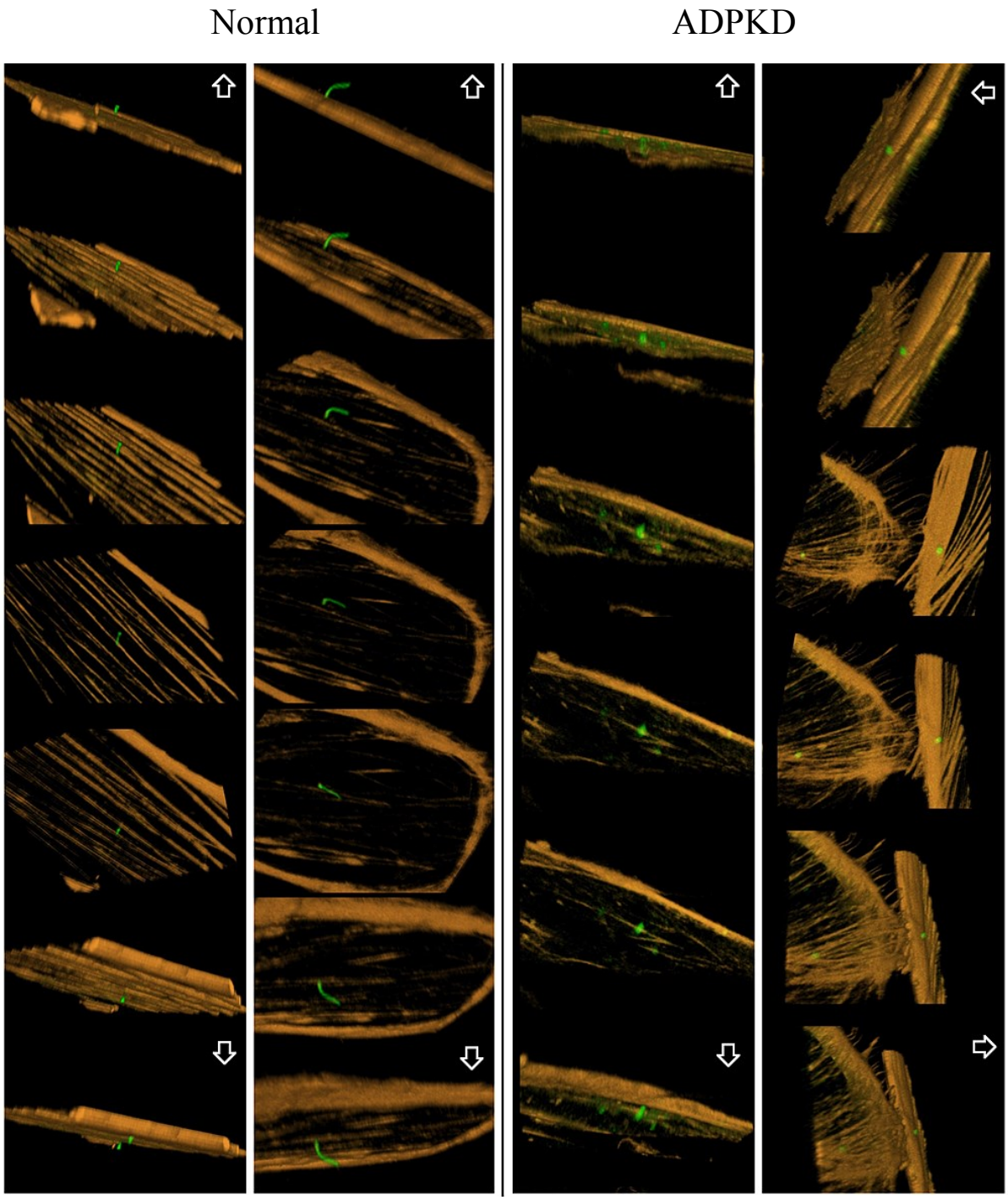

Figure 4.5 Representative Z-Stack images of normal and ADPKD actin and primary cilia. Representative image of Actin structures (Yellow) and primary cilium (Green) from Z-Stack images were used to form a three dimensional representation of structural arrangements in normal and ADPKD cells. Two images of each cell line are provided, which move from one side view to the other over a 180° degree spectrum with sample images. Primary cilia (ARL13b: Green) can be observed protruding to different degrees from actin (Phalloidin: Yellow) structures at the base of the cell.

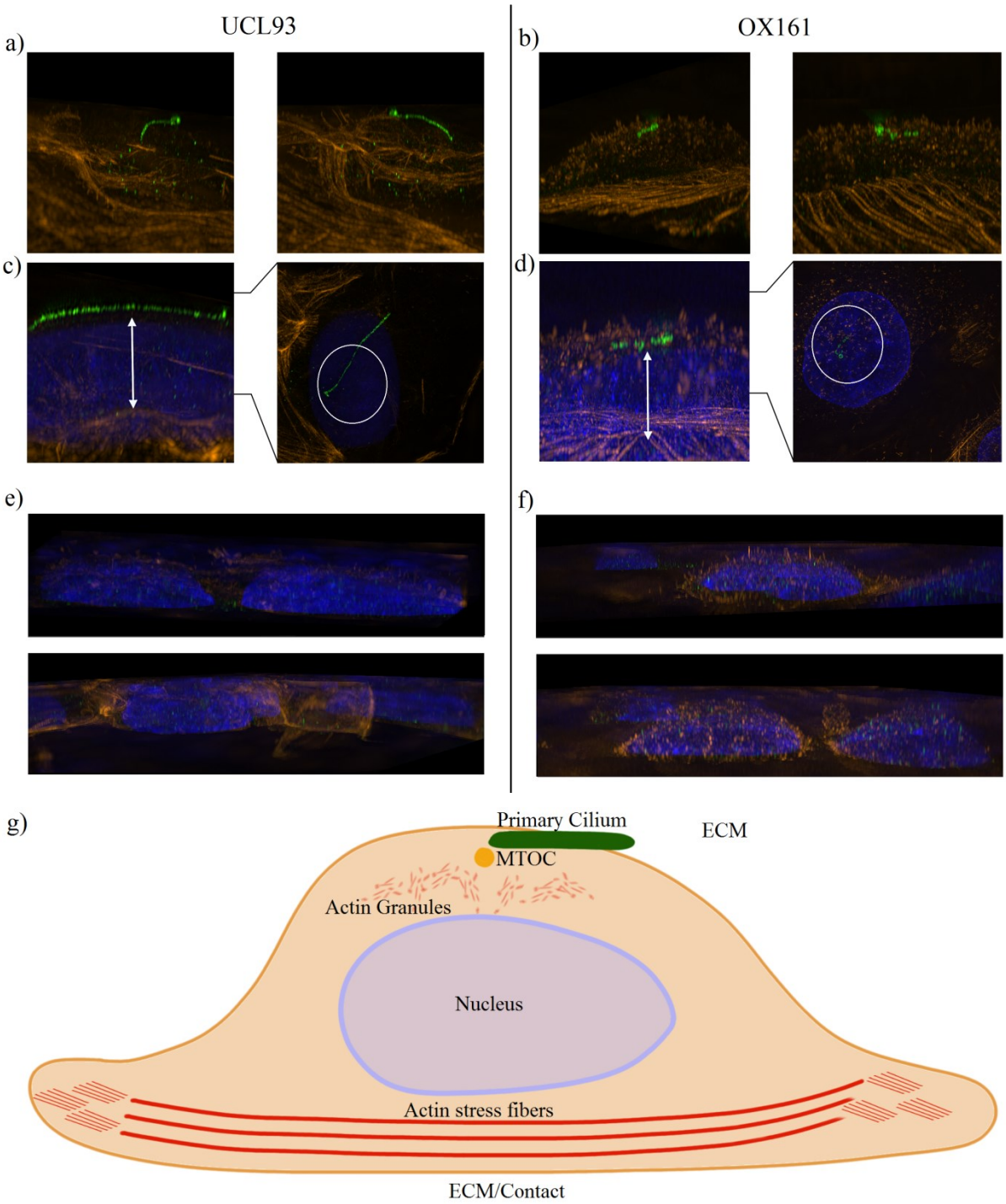

Figure 4.6. SIM 3D images of primary cilia and actin structures. Representative 3 dimensional images of high-resolution light microscope SIM (Structured Illumination Microscopy) of normal and ADPKD cells. **a**, **b)** primary cilia (ARL13b: Green) and actin structures (Phalloidin: Yellow) are shown in two representative images from two angles of a three dimensional surpass image. **c**, **d) Left:** Increased magnification of a region located above the bottom actin plane near the primary cilium and on the edge of the nucleus, (Arrow represents actin structures distance from the bottom) **Right:** corresponding aerial view of the cut section for the investigation of micro actin structures near the originating primary cilium. **e**, **f)** Representative images of micro actin arrangements above and on the perinuclear area. **g)** Model representation.

4.3 Microtubules

4.3.1 Introduction

The evidence of crosstalk between microtubules and the actin cytoskeleton which is emerging in recent studies in migration of cells, points to closely interconnected regulatory mechanism for these two structural proteins (Akhshi et al, 2014; Etienne-Manneville et al, 2004).

4.3.2 Microtubule stability affects primary cilia formation

To investigate the potential role of microtubule organization in cilia formation, nocodazole was used as a tubulin depolymerizing agent and taxol as a tubulin stabilizing agent. Nocodazole is an antineoplastic agent which exerts its effect in cells by interfering with the polymerization of microtubules and is commonly used to synchronise the cell cycle. The mechanism of nocodazole in regulating microtubule stabilization are not fully understood, but is thought to promote the formation of nocodazole-tubulin dimers and induce tubulin GTPase activity thus leading to microtubule depolymerisation (Vasquez et al, 1997).

After treatment with nocodazole, an increase in ciliary length in the normal cells was observed, confirming a previous report (Yoder et al, 2011). Conversely in ADPKD cells, only a small increase in ciliary length was observed even after prolonged incubation (24h) (**Figure 4.7**).

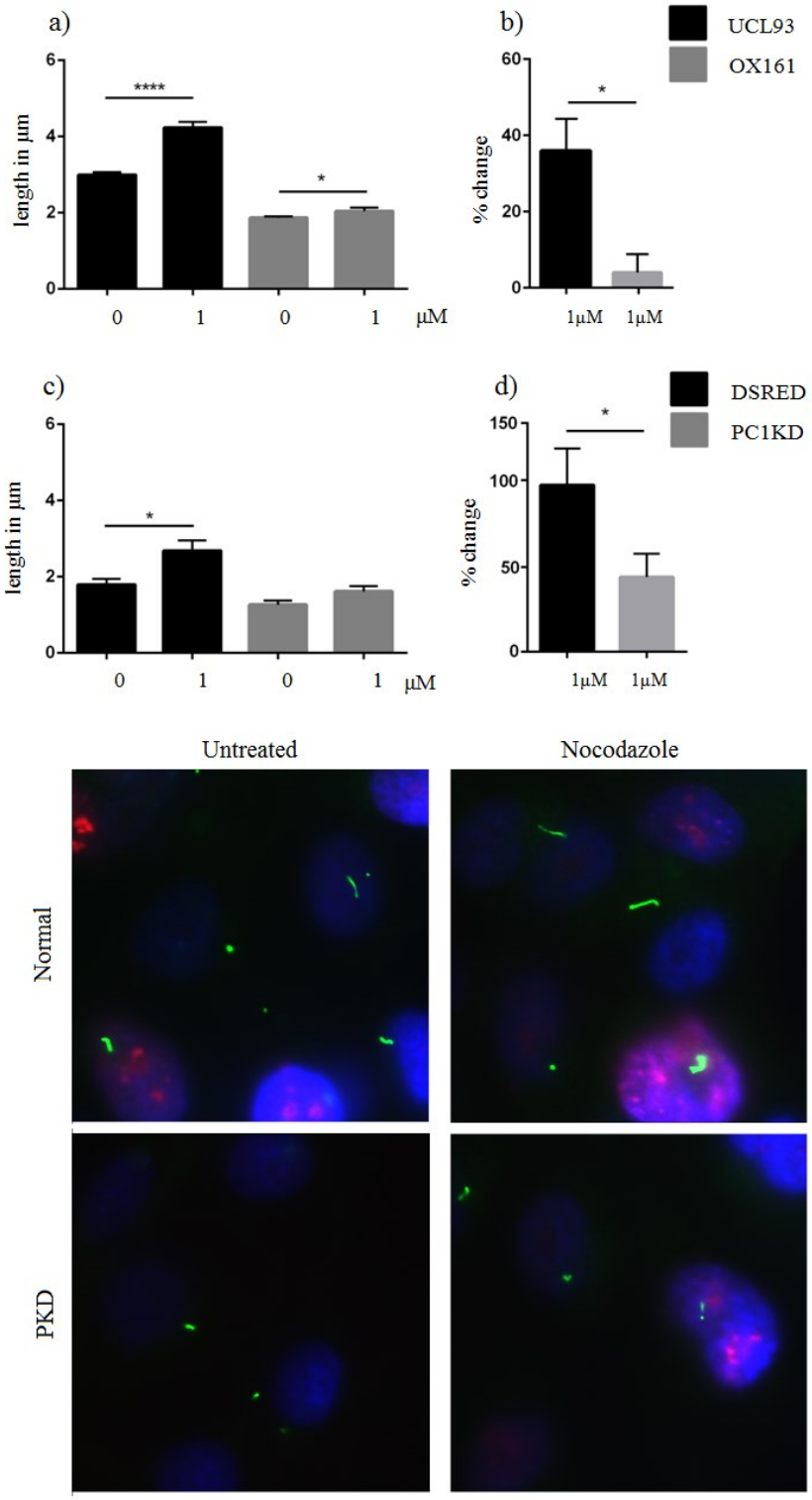

Figure 4.7 Effect of Microtubule depolymerisation. Treatment with nocodazole induced MT depolymerisation and induces a significant ciliary length increase in normal **a)** and only marginal in **b)** PKD cells. Comparison of % change after treatment shows a significant impaired/reduced cilium elongation effect in ADPKD models **b)**, **d)** suggesting that the latter are more resistant to nocodazole induced cilium elongation. (n=3, Statistical test:paired t -test (* = p≤ 0.05), Error bars indicate mean ± S.E.M). Antibody used: DAPI-stained nuclei (Blue), ARL13b stained primary cilia (Green) Magnification 60 X.

4.3.3 ADPKD cells have increased microtubule stability

The reduced response of ADPKD cells to nocodazole suggested that they might have increased microtubule polymerisation. The reversed experiment i.e. the effect of tubulin stabilisation on primary cilium formation was next studied using taxol.

Stabilization of microtubules via taxol had little effect on cilia length in formed primary cilia of normal and ADPKD cells **Figure 4.8 (a-d**). As expected, taxol completely prevented nocodazole induced cilium elongation in normal cells while in the ADPKD models this effect was marginal. Taxol did not prevent cAMP dependent cilium elongation in normal and ADPKD cells suggesting that both effects were independent. Strikingly, nocodazole had an additive effect to db-cAMP in normal cells but not in ADPKD cells.

The minor effect of nocodazole on cilia length in ADPKD cells implied an increase in microtubule stability. To quantify this more accurately, a nocodazole resistance assay was performed. Comparison of the normal PTEC DS RED cell line and the PTEC PC1 KD showed that a significant increased amount of cells with persistent acetylated a-tubulin structures after nocodazole in the ADPKD model compared to controls (**e, f**). Some of the nocodazole-resistant microtubules could be found in the region between the nucleus and the leading edge, confirming the polarized formation of stabilized microtubules reported by (Gundersen & Bulinski et al, 1988). Unfortunately it was not possible to perform the same analysis in patient derived cystic lines due to inability of these cells to remain adherent after the intensive 1% Triton washes required for the nocodazole resistance assay.

Analysis of microtubules posttranslational modifications showed no obvious differences in Glutamylation (**g**) and Glycylation (**h**) of α tubulin between normal and ADPKD models.

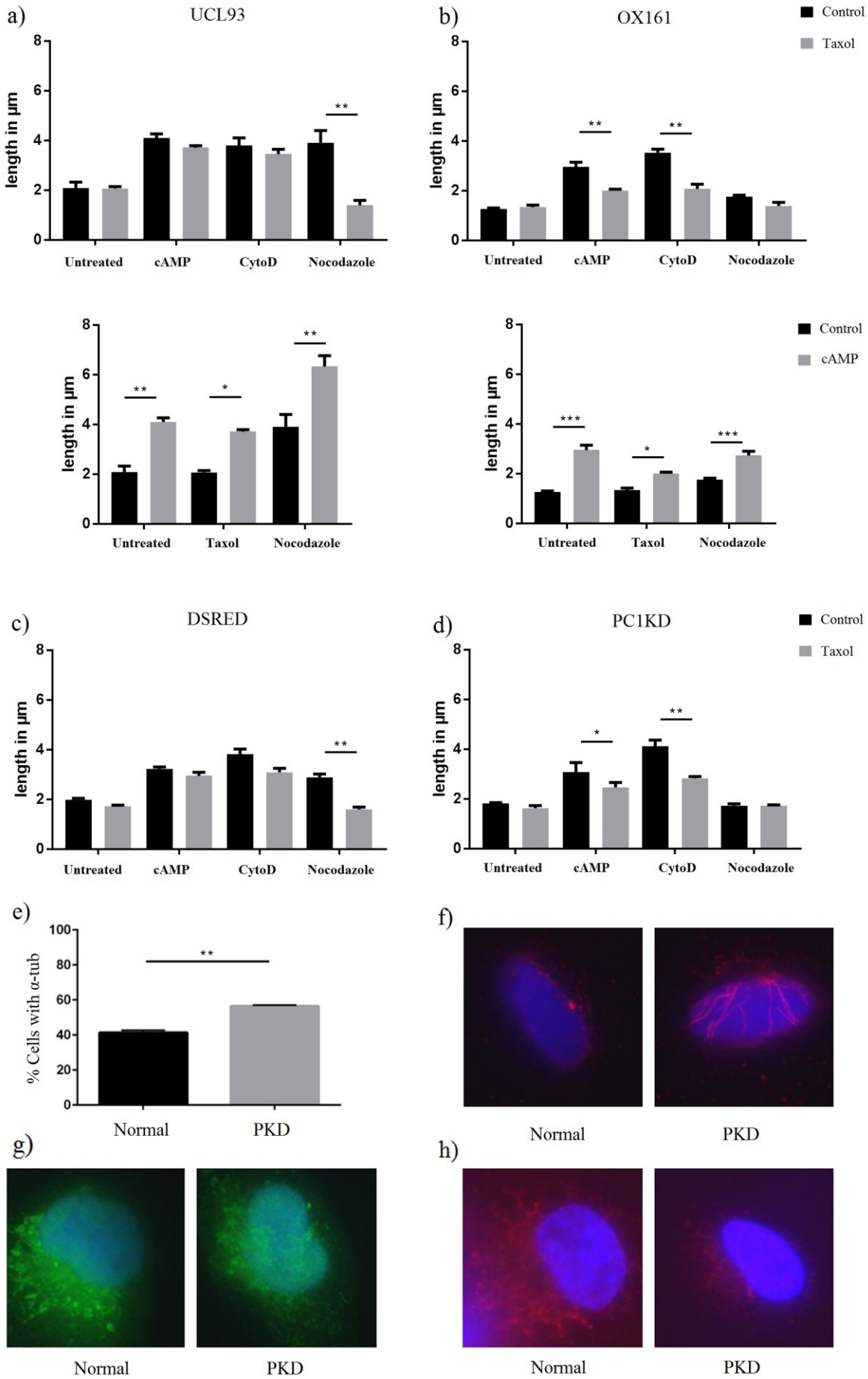
a)
UCL93
b)
OX161
Control
Taxol
length in µm
Untreated
cAMP
CytoD
Nocodazole
Taxol
Control
cAMP
c)
DSRED
d)
PC1KD
e)
% Cells with α-tub
Normal
PKD
f)
g)
h)

Figure 4.8 Microtubule stabilization affects cilium elongation. In all tested cells, db-cAMP induced cilium elongation is independent of the effect of nocodazole (amount of free tubulin) in all tested cell lines. cAMP elongation was additive to nocodazole treatment in tested cell lines **(a**, **b).** Stabilization of tubulin via taxol had no significant effect on cytochalasin-D induced cilium elongation in normal cells. In the ADPKD model, a significant reduction of the cytochalasin-D effect was detected. Stabilization of tubulin via taxol in the nocodazole treatment has as expected a reducing effect in the normal cell lines, while in the ADPKD model there is almost no effect, (n=3, Statistical test:two way anova + multiple comparison test (* = $p \leq 0.05$), Error bars indicate mean ± S.E.M).
e) Nocodazole resistance assay graph showing amount of cells with α-tubulin left in %. **f)** Representative image of normal and ADPKD cells after nocodazole resistance assay. **g)** Representative image of normal and ADPKD cells after GLU-rich tubulin and **f)** Beta tubulin.

4.3.4 Microtubule/Actin organization controls cilia independently of cAMP/PKA

cAMP/PKA has been reported to have effects on actin filaments in other cell types, especially in the field of cell migration (McKenzie et al, 2011). The striking effects of cytochalasin D and nocodazole on cilia length described above led to the analysis, whether they were independent of cAMP/PKA regulation. As shown, PKA inhibition did not prevent the elongation of the primary cilium in response to either agent, while it was able to fully block db-cAMP dependent cilium elongation **(Figure 4.9)**. These results indicated that the changes in cilia length due to actin and microtubule organization were independent of cAMP/PKA signalling.

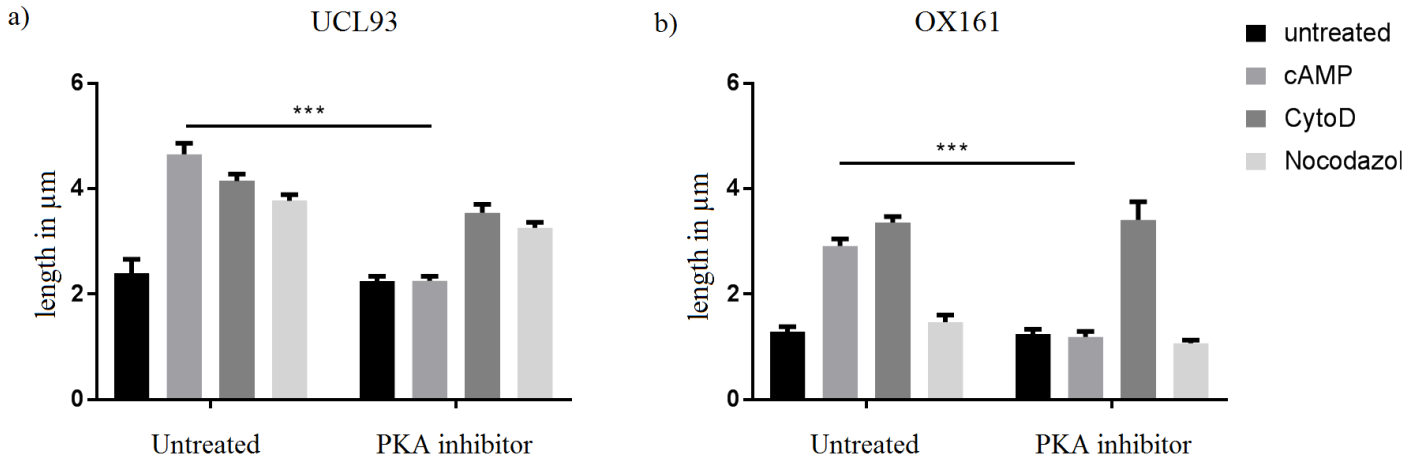

Figure 4.9 PKA inhibition and microtubule/actin modulation on cilia length

Inhibition of PKA prior to db-cAMP treatment prevents cilium elongation in **a)** normal and **b)** ADPKD cells. Neither cytochalasin D nor nocodazole prevented db-cAMP induced cilium elongation in **a)** normal and **b)** ADPKD cells (n=3, Statistical test:two way anova + multiple comparison test (* = $p \leq 0.05$), Error bars indicate mean ± S.E.M).

4.4 PI3K is important in ciliogenesis

Next, the potential role of the PI3K pathway in regulating cilia length through actin and microtubule stability was tested. The PI3K inhibitor LY294002 reduced primary cilia disassembly in response to serum reintroduction in serum starved normal and ADPKD cells (**Figure 4.10 b)**. There were no significant differences between normal and cystic models at 6 and 24 h, suggesting that the effect of PI3K on the cilia disassembly or the cell cycle is not defective in PKD (**Figure 4.10 c)**.

The next step was to investigate whether inhibition of PI3K could influence actin depolymerisation and induce ciliary length increase. As seen in (**Figure 4.11 e**), PI3K inhibition led to actin filament shortening and increased stress fibres in normal cells. In the ADPKD models, no further changes could be seen in the already disorganized actin structures. PI3K inhibition resulted in significant cilium elongation in normal cells but had little effect in ADPKD cells (**Figure 4.11 a-d)**. Treatment with LY294002 and db-cAMP resulted in an additive cilium elongation effect only in normal cells. Likewise, the combination of LY294002 with nocodazole was additive only in normal cells. In normal cells, LY294002 had no additive effect to cytochalasin-D suggesting that they could both be acting via actin depolymerisation.

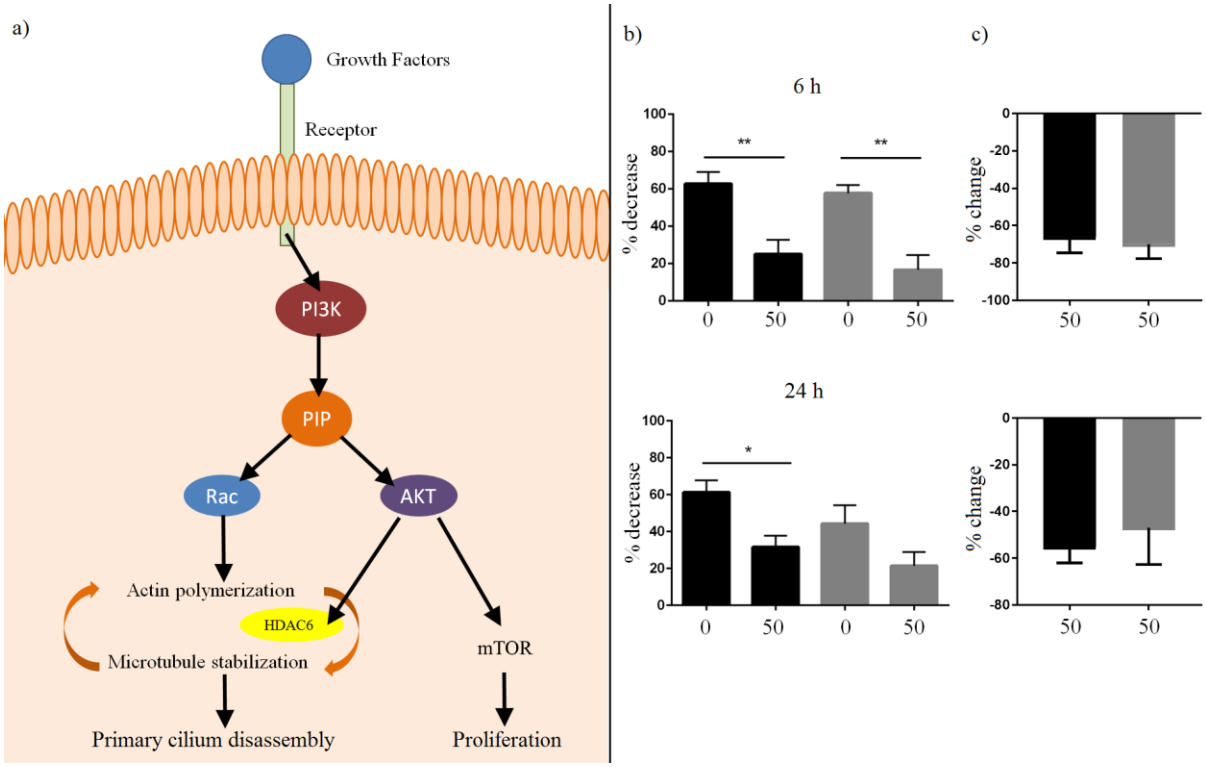

Figure 4.10 PI3K in ciliogenesis **a)** Representative signalling model of PI3K activation, influncing proliferation and cytoskeletal organization. **b)** After starvation, serum was reintroduced in untreated and PI3K inhibited normal and ADPKD cells and the percentage decrease is shown in the graph. PI3K inhibition significantly prevents serum reintroduction dependent decrease in percentage of ciliated cells. **c)** Percentange change comparison between the normal (UCL93) and ADPKD model (OX161). (n=3, Statistical test:paired t -test (* = p≤ 0.05), Error bars indicate mean ± S.E.M).

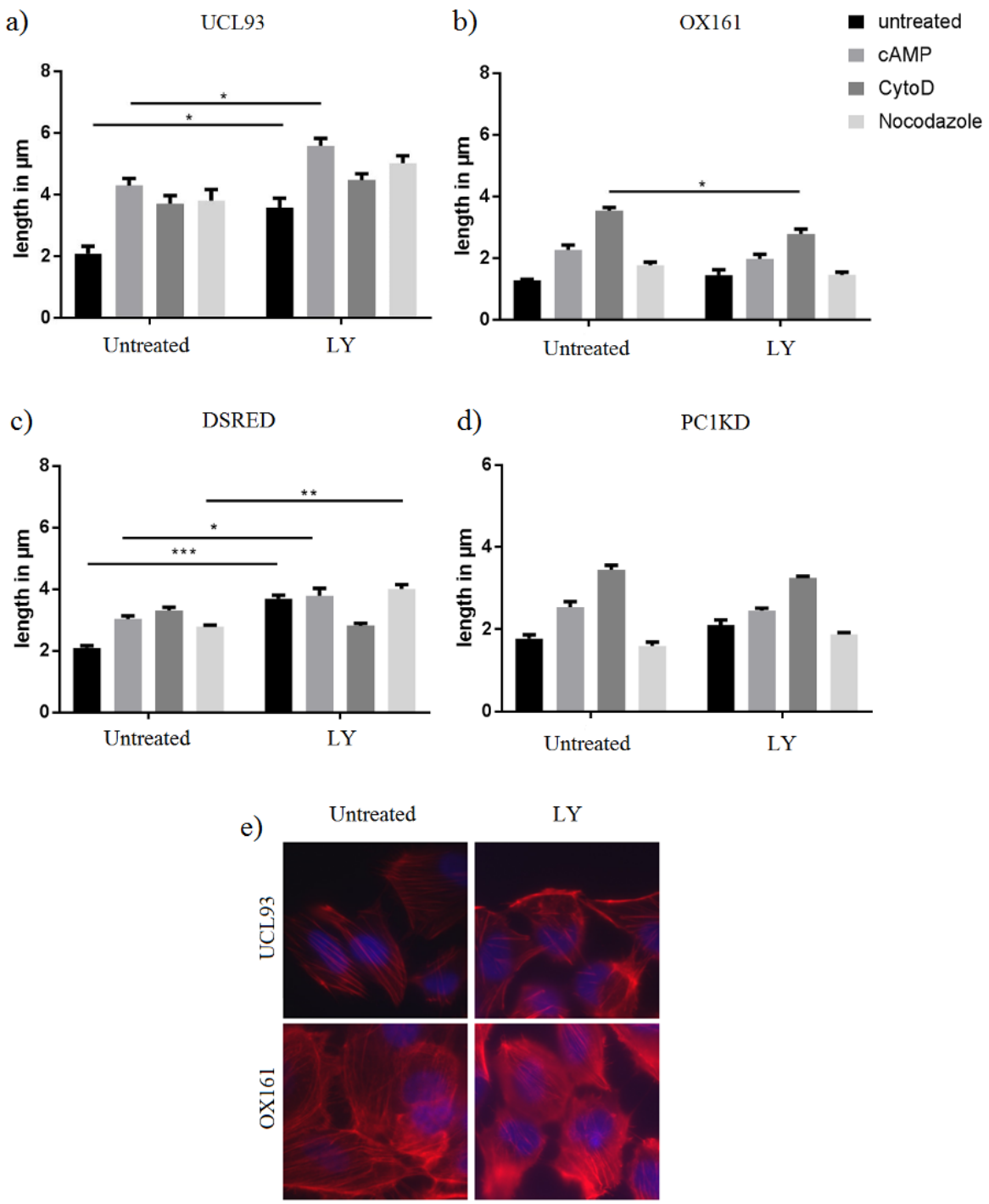

Figure 4.11 PI3K is involved in primary cilia length regulation a, c) PI3K inhibitor LY at 50 µM induces primary cilium elongation in normal cells. dbcAMP treatment in combination with LY induces an additive primary cilium elongation in normal cells. Nocodazole and Cytochalasin D treatment in combination with LY does not have an additive effect on primary cilium elongation in normal cells. PI3K inhibitor LY at 50 µM does not induce primary cilium elongation in ADPKD models; also the effect of Cytochalasin D is reduced in OX161. **e)** PI3K inhibitor LY at 50 µM induces Actin filaments depolymerisation and shortening in normal cells. Antibody used: Actin (Phalloidin: Red), nuclei (DAPI: Blue). n=3, Statistical test: Two Way Anova + Multiple comparison test (* = $p \leq 0.05$), Error bars indicate mean ± S.E.M).

To exclude the possibility that reduced effect of PI3K inhibition on primary cilium regulation in ADPKD cells was related to dose, higher doses up to 500 μM were also tested. An increase in cilia length was observed in ADPKD cells at 250μM (**Figure 4.12 a**). However, there was evidence of cell toxicity at this concentration and the effect on other kinases cannot be ruled out. It has been reported that LY-294002 used at maximum of 50 μM is sufficient to abolish PI3 kinase activity (IC50=0.43 μg/ml; 1.40 μM) without affecting other lipid or protein kinases such as PI4 kinase, PKC, MAP kinase or c-Src (Vlahos et al, 1994), thus suggesting a specific defect in normal PI3K inhibition mechanism in ADPKD models.

Taken together, these results show that PI3K inhibition induces actin filament depolymerisation and shortening in normal cells leading to significant primary cilium elongation. No effect was however observed in ADPKD models suggesting that it is unable to overcome the pre-existing increase in actin polymerisation, unlike the effect of cytochalasin D. Finally, it was also observed that the PI3K inhibition had an additive effect to cAMP/PKA dependent primary cilium elongation in normal cells, (**Figure 4.12 b**) confirming that PI3K cilia regulation mechanism are independent of cAMP related signals.

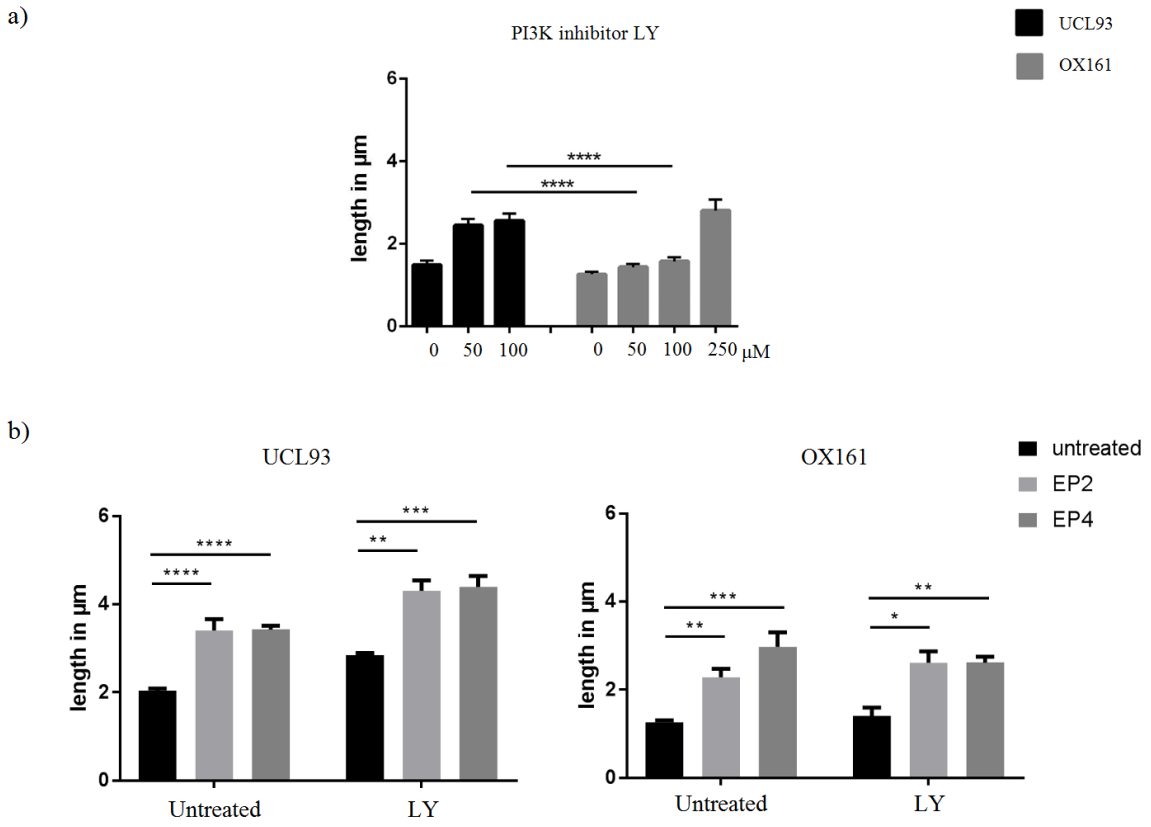

Figure 4.12 a) ADPKD cells are more resistant to PI3K inhibition induced cilia elongation

The PI3K inhibitor LY294002 resulted in a comparable cilium elongation level in OX161 cells to the UCL93 cell line at 250µM. **b) PI3K inhibitor and EP receptors agonists** PI3K inhibition has an additive effect on the EP2, EP4 receptor agonist dependent cilium elongation. Statistical test: Two Way Anova + Multiple comparison test (* = $p \leq 0.05$), Error bars indicate mean ± S.E.M).

4.5 Rho GTPases modulate primary cilia length

4.5.1 Introduction

The ability of cytochalasin D to normalise cilia length in disease cells suggested a primary defect in actin organisation. The Rho family of GTPases (classically RhoA, Rac and cdc42) are known to primarily regulate actin organisation (Nobes et al, 1995). To assess the contribution of these 3 regulators in actin and primary cilium dynamics, selective Rho kinase inhibitors were tested for their ability to influence ciliary length in normal and ADPKD models.

4.5.2 Rac-1 inhibition causes increased cilia elongation in ADPKD models

The well characterized inhibitor NSC23766 was used to block Rac-1 activation (Gao et al, 2004). Although blocking Rac-1 had no significant effect on the number of formed cilia compared to untreated controls (**Figure 4.19**), a significant increase in ciliary length was observed in both normal and ADPKD models, with a more pronounced percentage increase in the ADPKD model (**Figure 4.13 a, c**).

These results indicate the potential role of increased Rac-1 activation in ADPKD cells. As with the other two Rho family members of interest, Rac-1 signalling is involved in a variety of signalling cascades (**Figure 4.13 e**), any of which could be defective in ADPKD leading to abnormal microtubule or actin organization.

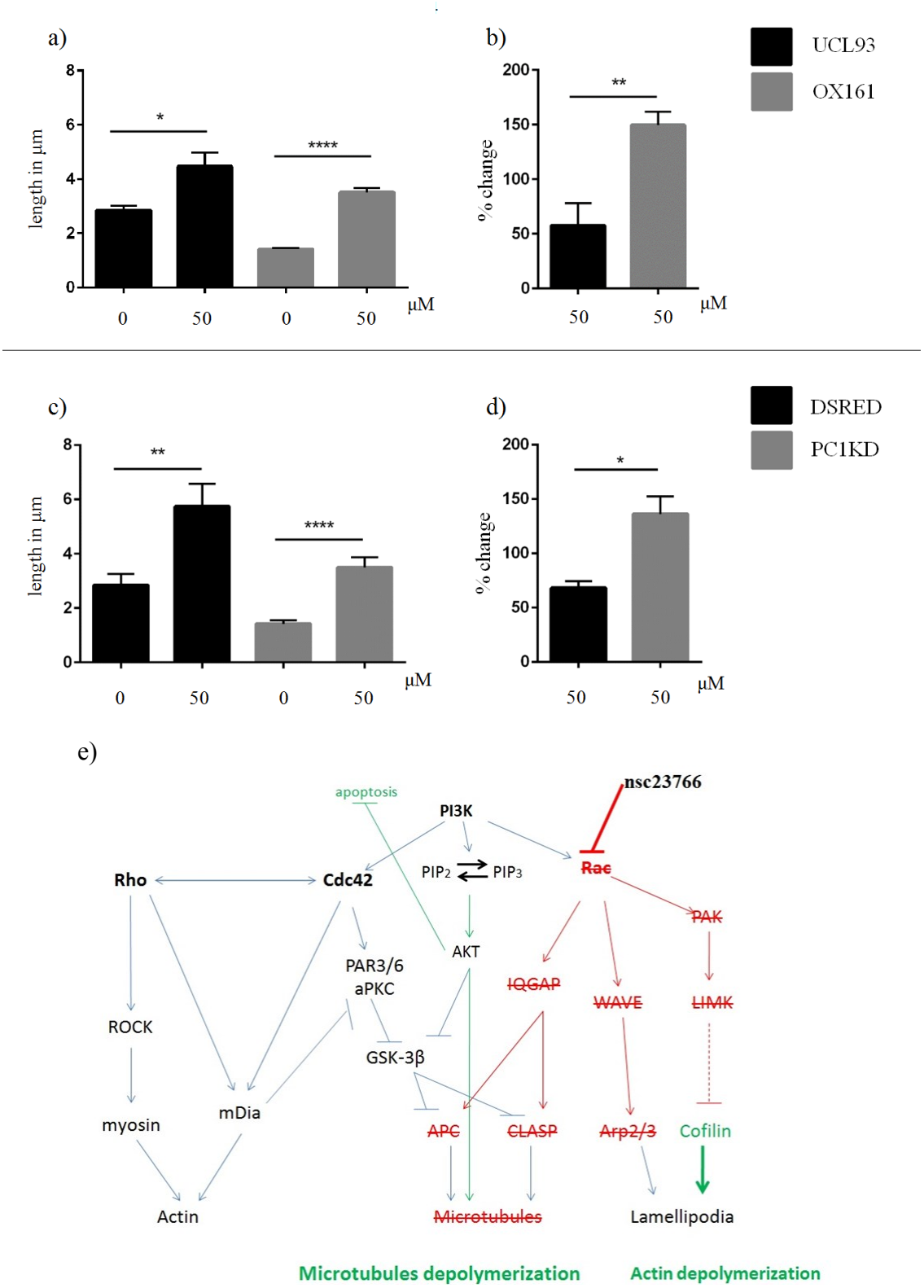

Figure 4.13 Rac-1 and cilia regulation Treatment with Rac-1 inhibitor nsc23766 for 4 h induces a significant ciliary length increase in normal and ADPKD cells **a**, **c)**. Comparison of percentage change shows a significant increased cilium elongation effect in ADPKD models **b)**, **d)**. (n=6, 100 cells/N. Statistical test:paired t- test (* = $p \leq 0.05$), Error bars indicate mean ± S.E.M). **e)** Pathway model of Rac-1 inhibition.

4.5.3 ROCK inhibition normalizes ciliary length in ADPKD models

The effect of the Rho kinase (ROCK) inhibitor Y-27632 on primary cilium formation was next tested. In contrast to Rac-1, ROCK 1/2 inhibition led to the restoration of normal ciliary length in ADPKD cells to that of normal cells**.** Surprisingly, there was little cilium elongation effect in normal cells **Figure 4.14 (a, c)**. The effect of the ROCK inhibitor seemed to be limited almost exclusively to ADPKD cells, with a significant fold change increase in ciliary length (**b, d)**.

Taxol did not prevent ROCK inhibition-dependent primary cilium elongation in ADPKD cells indicating a microtubule–independent effect (**Figure 4.14 f, g)**. Treatment with phalloidin to stabilize actin prior to ROCK inhibition to prevent actin depolymerisation had a lethal effect. On the other hand, phalloidin treatment itself was not toxic in either normal or ADPKD cells and did not alter cilia length except in one line (PTEC-DSRED).

740 Y-P, a PI3K activator had a cilia shortening effect in normal but not ADPKD cells, the exact opposite effect to that observed with LY294002 (**Figure 4.11**). However it reduced the increase in cilia length in ADPKD cells after ROCK inhibition (**Figure 4.14 f, g,)** possibly by inducing actin polymerization and antagonising the actin depolymerisation induced by ROCK inhibition (**Figure 4.14 e**).

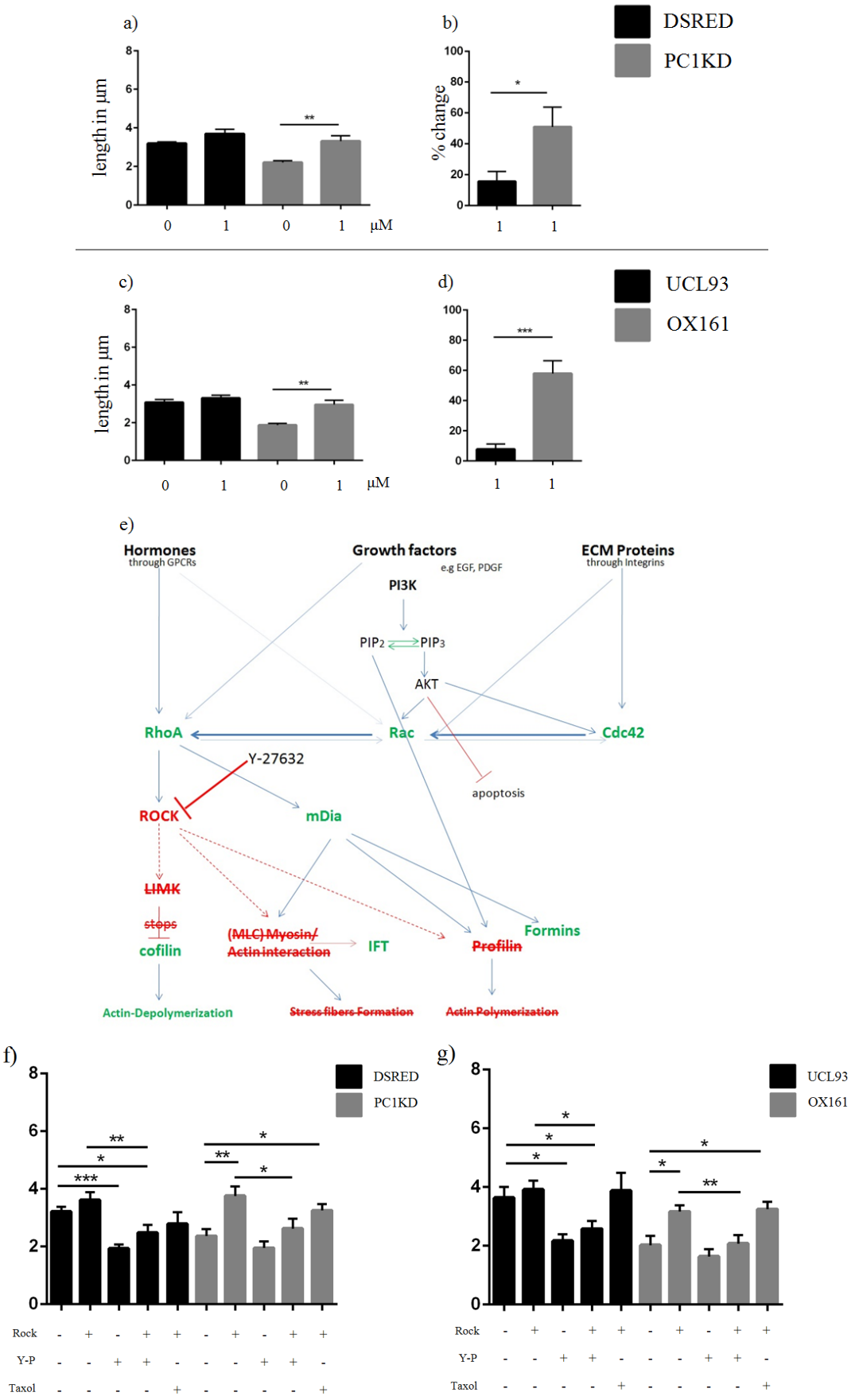
a)
b)
DSRED
PC1KD
length in µm
% change
µM
c)
d)
UCL93
OX161
e)
Hormones
through GPCRs
Growth factors
e.g EGF, PDGF
ECM Proteins
through Integrins
PI3K
PIP2
PIP3
AKT
RhoA
Rac
Cdc42
Y-27632
apoptosis
ROCK
mDia
LIMK
stops
cofilin
(MLC) Myosin/
Actin Interaction
IFT
Formins
Profilin
Actin-Depolymerization
Stress fibers Formation
Actin Polymerization
f)
g)
Rock
Y-P
Taxol

Figure 4.14 ROCK and cilia regulation. a, **c)** Treatment with ROCK inhibitor Y-27632 for 4h normalizes primary cilium length of ADPKD models to basal levels, and has no significant effect on normal cells **b)**, **d)**. Comparison of percentage change shows a significant increased cilium elongation effect in ADPKD models. (n=4, 100 cells/N. Statistical test:paired t- test (* = $p \leq 0.05$), Error bars indicate mean ± S.E.M). **e)** Pathway model of ROCK inhibition: The influence of hormones, growth factors or extracellular stimuli could induce defective signalling in form of an aberrant hyper-activation of ROCK1/2, thus increase in downstream activation of LIMK and mDia resulting in increased stress fiber formation and actin polymerization **f-g)** Pre-treatment with taxol had no significant effect on ROCK inhibition effect. Pre-treatment with PI3K activator Y-P had no effect on ADPKD cells while ciliary length was decreased in normal cells. (n=4, 100 cells/N. Statistical test:paired t- test (* = $p \leq 0.05$), Error bars indicate mean ± S.E.M)

4.5.4 Cdc42 inhibition causes increased cilia elongation in ADPKD models

Using the same protocol, growth arrested cells following Cdc42 inhibition using ML141 were analysed. Surprisingly in non-disease models, Cdc42 inhibition had no effect on primary cilium regulation in the PTEC while in the UCL93 cell line, a significant increase in cilia length was observed. In comparison, Cdc42 inhibition in the ADPKD models resulted in a greater increase in cilia length **(Figure 4.15)**.

Similar to the results of Rac-1 inhibition, the percentage increase analysis revealed that there was significant increase responsiveness to the cilia elongation compound in the ADPKD models (**b, d**). This could be due to the known effects of Cdc42 and Rac-1 on both the microtubule and actin cytoskeleton, unlike Rho which acts only on actin (**Figure. 4.13 e** and **4.15 e**).

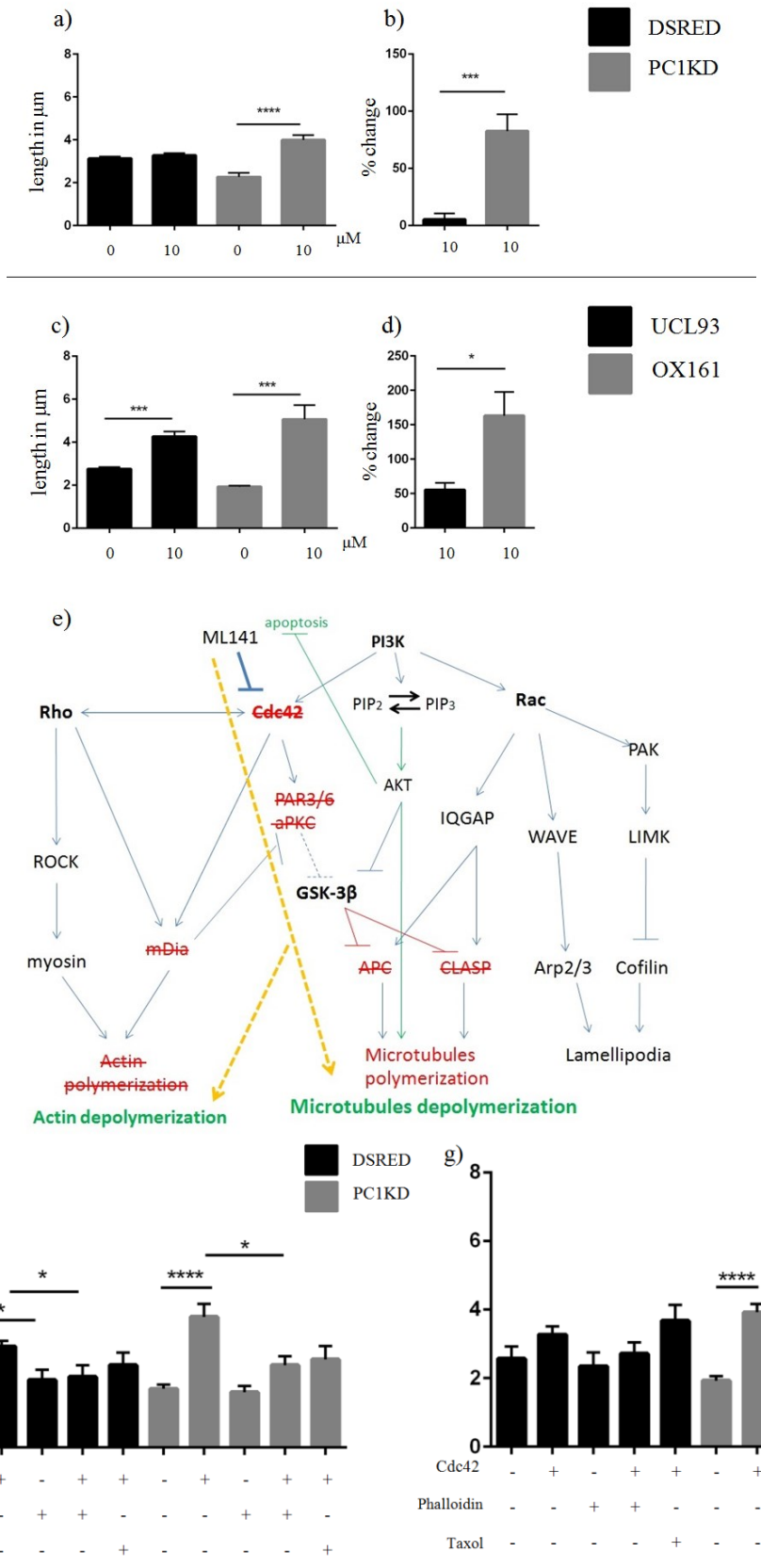
a)
b)
DSRED
PC1KD
length in µm
% change
µM
c)
d)
UCL93
OX161
e)
ML141
apoptosis
PI3K
Rho
Cdc42
PIP2
PIP3
Rac
PAK
AKT
PAR3/6
aPKC
IQGAP
WAVE
LIMK
ROCK
GSK-3β
myosin
mDia
APC
CLASP
Arp2/3
Cofilin
Actin polymerization
Microtubules polymerization
Lamellipodia
Actin depolymerization
Microtubules depolymerization
f)
g)
Cdc42
Phalloidin
Taxol

Figure 4.15 CDC42 inhibition and cilia length Treatment with Cdc42 inhibitor ML141 for 4 h normalizes primary cilium length of ADPKD models to basal levels, and has no significant effect in one normal cell line **a)**, but increased ciliary length in the other **c)**. Comparison of percentage change shows a significant increased cilium elongation effect in ADPKD models **b**) **d**). (n=6, 100 cells/N. Statistical test:paired t- test (* = $p \leq 0.05$), Error bars indicate mean ± S.E.M).
e) Pathway model of Cdc42 inhibition **f-g)** Treatment with phalloidin alone decreased ciliary length in the PTEC normal cell line. Phalloidin or taxol reduced Cdc42-dependent cilium elongation in ADPKD cells.

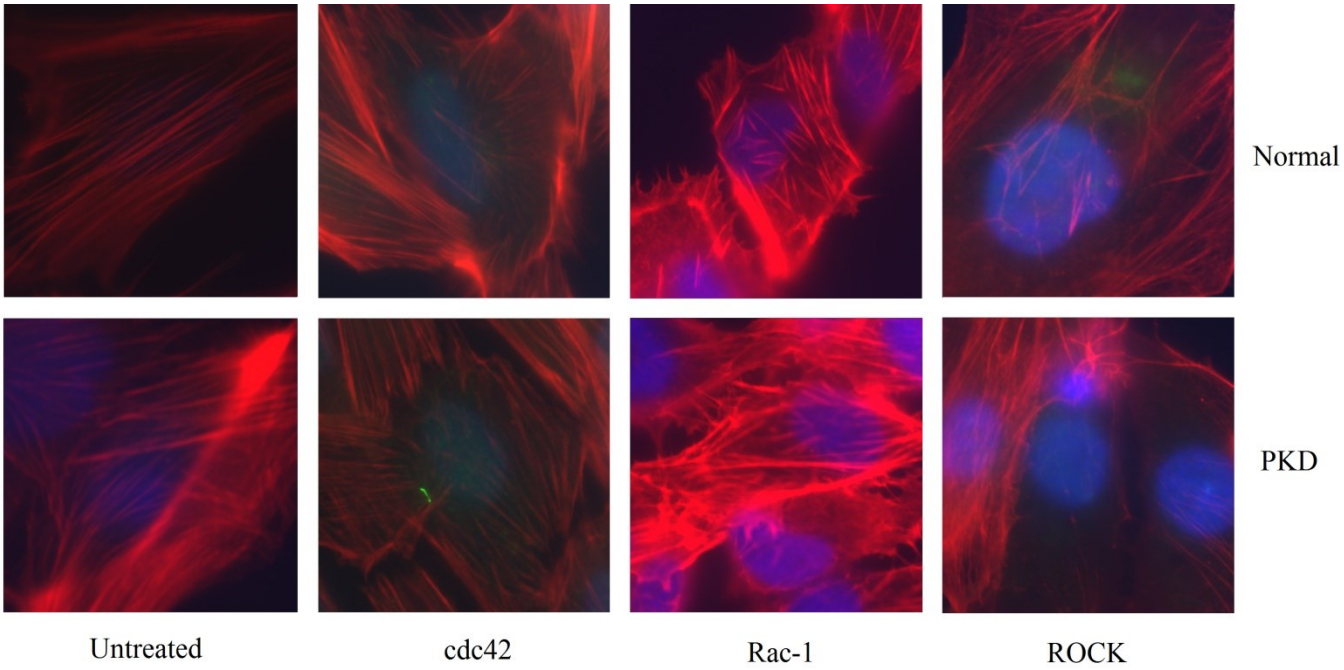

Figure 4.16. Effect of Rho GTPases inhibition on actin structures in normal and ADPKD models.
In untreated cells, stress fibers can clearly been seen extending throughout the cytoplasm while other actin structures are arranged in dense bands around the cell periphery. In the ADPKD model stress fibers appear enlarged or entangled in some areas and actin staining appears also increased compared with the normal long parallel and defined filaments in the normal model. Upon inhibition of any of the Rho GTPases, actin structures and filaments are broken down to different degrees depending on the compound used. The effect on normal and ADPKD cells after treatment appears very similar with minimal differences in the ADPKD models in form of irregular structures. The Rac-1 effect on actin structures seems to be concomitant with cell contraction and concentrated filaments while in the Cdc42 cells and filaments retain a normal appearance after filament fragmentation. The effect of ROCK kinase inhibition also results in a decrease of actin structures and fibers which appear very similar in normal and ADPKD cells. Antibody used: Actin (Phalloidin: Red), nuclei (DAPI: Blue).

Next, the effect of microtubule or actin polymerisation on Cdc42 dependent cilium elongation effect was studied. In ADPKD cells, Cdc42 inhibition resulted in a significant increase in cilia length which was reduced by either tubulin (taxol) or actin (phalloidin) stabilization. This suggests that Cdc42 regulation of cilia length depends on both tubulin and actin depolymerisation (**Figure 4.15 f, g**).

In summary, these results show that all three actin modulators were able to rescue ciliary length in ADPKD cells. Their effect in normal cells was much more varied but usually less or absent compared to the ADPKD lines.

Different Rho GTPases are known to have distinct effectors: in fibroblasts, Cdc42 is reported to affect filopodia, Rac-1 affect lamellipodia while RhoA preferably affect stress fibres formation (Dubois et al, 2005). Our results show that inhibition of Cdc42, Rac-1 or ROCK kinase results to different degrees in actin depolymerization and that the effect of these compounds on normal and ADPKD cells is comparable in regards to actin reduction and morphological appearance by fluorescence microscopy analysis (**Figure 4.16**).

4.5.5 Influence of cytoskeleton agents on primary cilia number

Finally, the effect of these agents on the number of ciliated cells was studied. A short treatment (3 h) with these compounds did not alter the percentage of ciliated cells in normal controls (**Figure 4.17. a**, **b**). In ADPKD models however, there was a consistent increase in ciliated cell number observed with cytochalasin D and the ROCK inhibitor. Cdc42 inhibition increased cilia number in one ADPKD line (OX161) but not in another (PC1-KD).

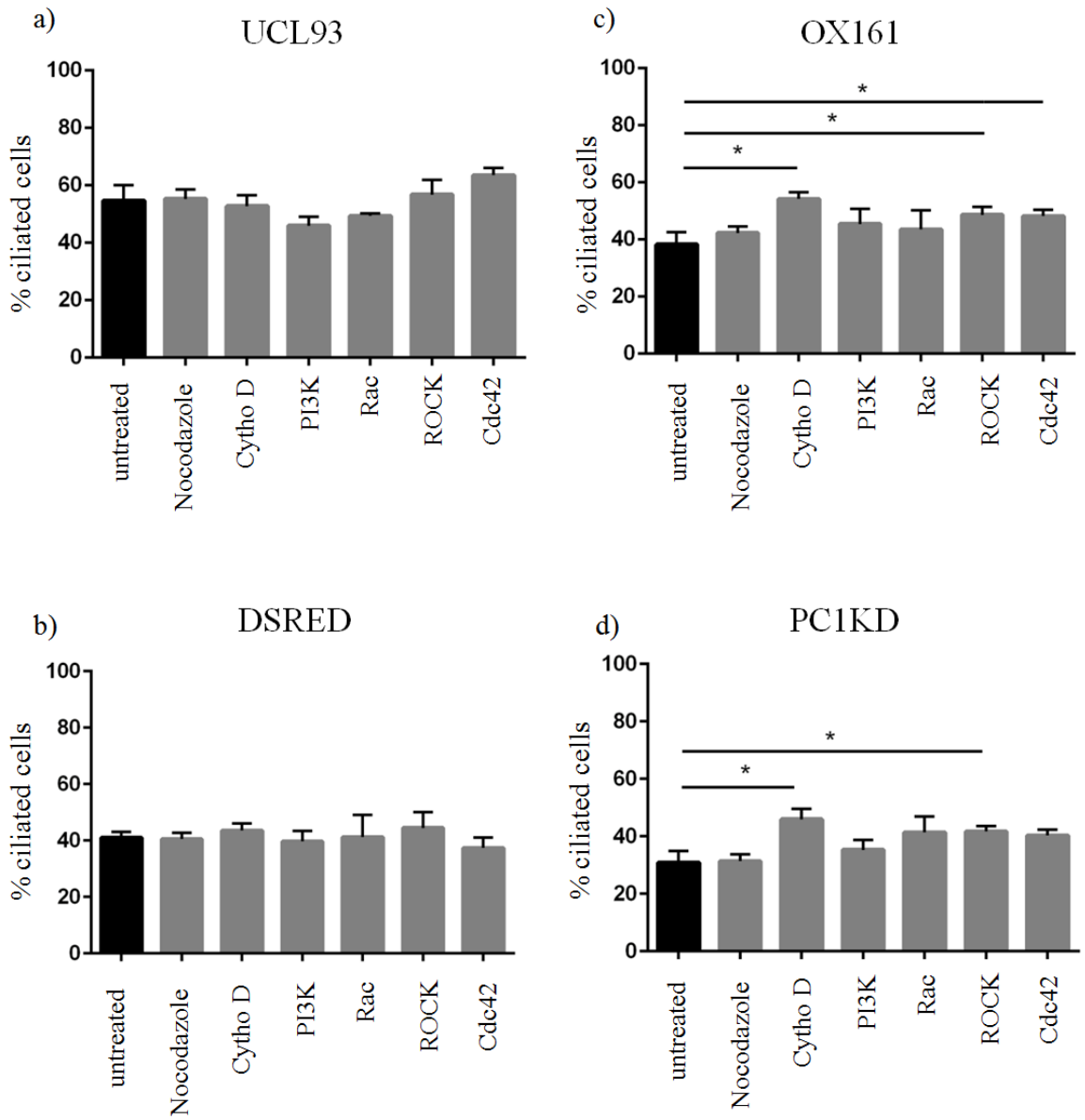

Figure 4.17 Effect of Rho GTPases in ciliogenesis a, **b**) No significant change in numbers ciliated cells could be detected in normal growth arrested cells after treatment with different compounds of interest. **c)** In ADPKD cystic model, significant increase in numbers ciliated cells could be detected with the Cdc42 or ROCK inhibitors and cytochalasin D and to the same degree in the PC1KD model **d**) but without the Cdc42 effect. (n=3, 100 cells/N. Statistical test:paired t- test (* = $p \leq 0.05$), Error bars indicate mean ± S.E.M).

4.6 Sphingolipids affect ciliary length

Sphingolipids, or glycosylceramides belong to a class of lipids containing a backbone of sphingoid bases characterized by an eighteen carbon amino-alcohol complex which is synthesized in the ER from nonsphingolipid precursors (Gault et al, 2010).
The multitude of the different sphingolipid family variants is ultimately based on the modifications to this simple basic structure, which confers distinct roles in membrane biology and cell regulation. Despite their diversity of function and structure, the regulatory mechanism involved in the synthetization and breaking down of sphingolipids follows a common synthetic and catabolic pathways. The molecules defined as ceramides are produced by the action of ceramide synthases, which induce sphingosine acylation with one of several possible acyl CoA molecules. Depending on the produced acyl chain, different variants with again specialized functions of ceramides can be synthetized (Kitatani et al, 2008; Gault et al, 2010).

A pathogenic link between sphingolipid metabolism and ADPKD was recently described (Natoli et al, 2010). In particular, glycosphingolipids membrane levels were found to be abnormally enriched in cystic cells and increased synthesis of glucosylceramide correlated with increased cell proliferation and apoptosis. An important study showed that reduction of glucosylceramide by treatment with the SK1 inhibitor Genz-123346 inhibited cystogenesis in several mouse PKD models (Natoli et al, 2010).
Sphingosine kinases (SphK) are conserved lipid kinases and the functional role of the cytosolic Sphingosine kinase 1 (SphK1 or SK1) involves its ability to phosphorylate sphingosine to sphingosine-1-phosphates (S1P). It has been shown that accumulation of intracellular ceramide could be prevented with sphingosine kinase 1 (SK1) by promoting its metabolism into S1P (**Figure 4.18**) (Bruce et al, 2012). Previous studies also showed that SK1 activators were associated with increased proliferation and activation of the PI3K/AKT pathway (Song et al, 2011), while SK1 inhibition was conversely associated with decreased proliferation and PI3K/AKT activation (Kapitonov et al, 2009). Interestingly, a recent study hints to a possible role of TORC2 upstream of sphingolipid biosynthesis, on top of its ability to regulate actin organization and endocytosis (Rispal et al, 2015).

a)

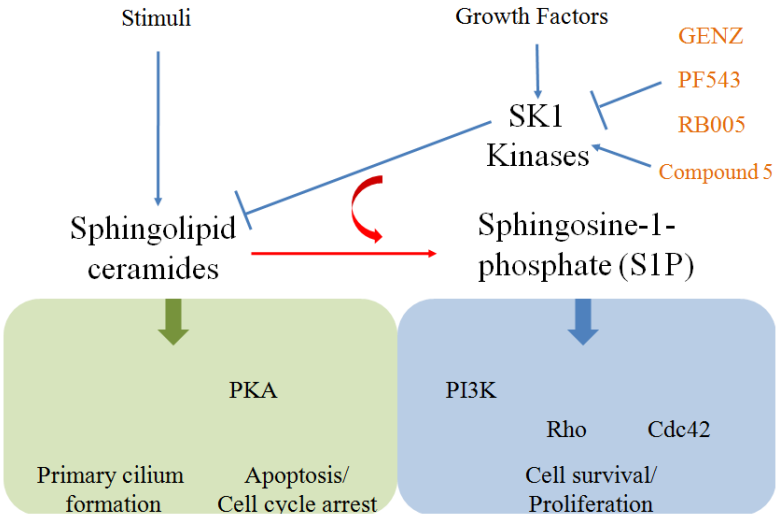

b)

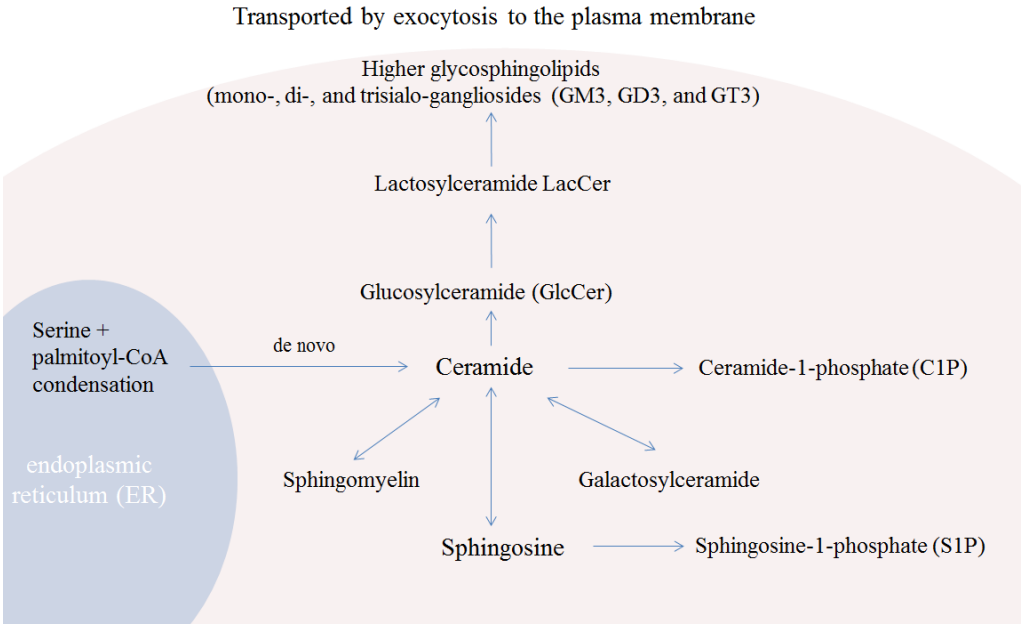

Figure 4.18 Ceramide-sphingosines a) Ceramide-sphingosine-sphingosine 1- model. Sphingolipids and ceramides are situated in a balance with sphingosine 1-phosphates (S1P) responsible for tissue homeostasis. The balance regulates basic cellular functions, aiding to proliferation and cell survival in the presence of abundant S1P levels or shifting to proliferation arrest and apoptosis with increasing sphingolipid and ceramide levels. **b)** deNovo synthesis of ceramide occurs in the ER, and represents the metabolic precursor of complex sphingolipids and Glycosphingolipids as shown in the diagram

To study the role of sphingolipid ceramides in primary cilium development in normal and ADPKD models, a range of different Sphingosine kinase 1 (SK) inhibitors (Genz-123346, RB005, PF543) and an activator (Compound 5) were tested in our cellular models. PF-543 is a SK1 selective inhibitor and RB-005 is a SK1/ceramide synthase inhibitor (MacRitchie et al, 2016). By blocking both SK1 and ceramide synthase, RB-005 may prevent back-conversion of sphingosines to ceramide in the presence of SKI inhibition alone (MacRitchie et al, 2016).

Treatment with SK1 inhibitors lead to an increase in cilia length in normal cells but this effect was impaired or absent in the ADPKD models **Figure 4.19 (a, b**). The strongest effect was detected with RB005. Treatment with a SK1 activator (compound 5) slightly decreased cilia length in one normal cell line (DSRED), but had no significant effect in the other lines. The effect of RB005 was not altered in the presence of taxol or phalloidin suggesting that this was likely to be an effect independent of actin or microtubule organization.

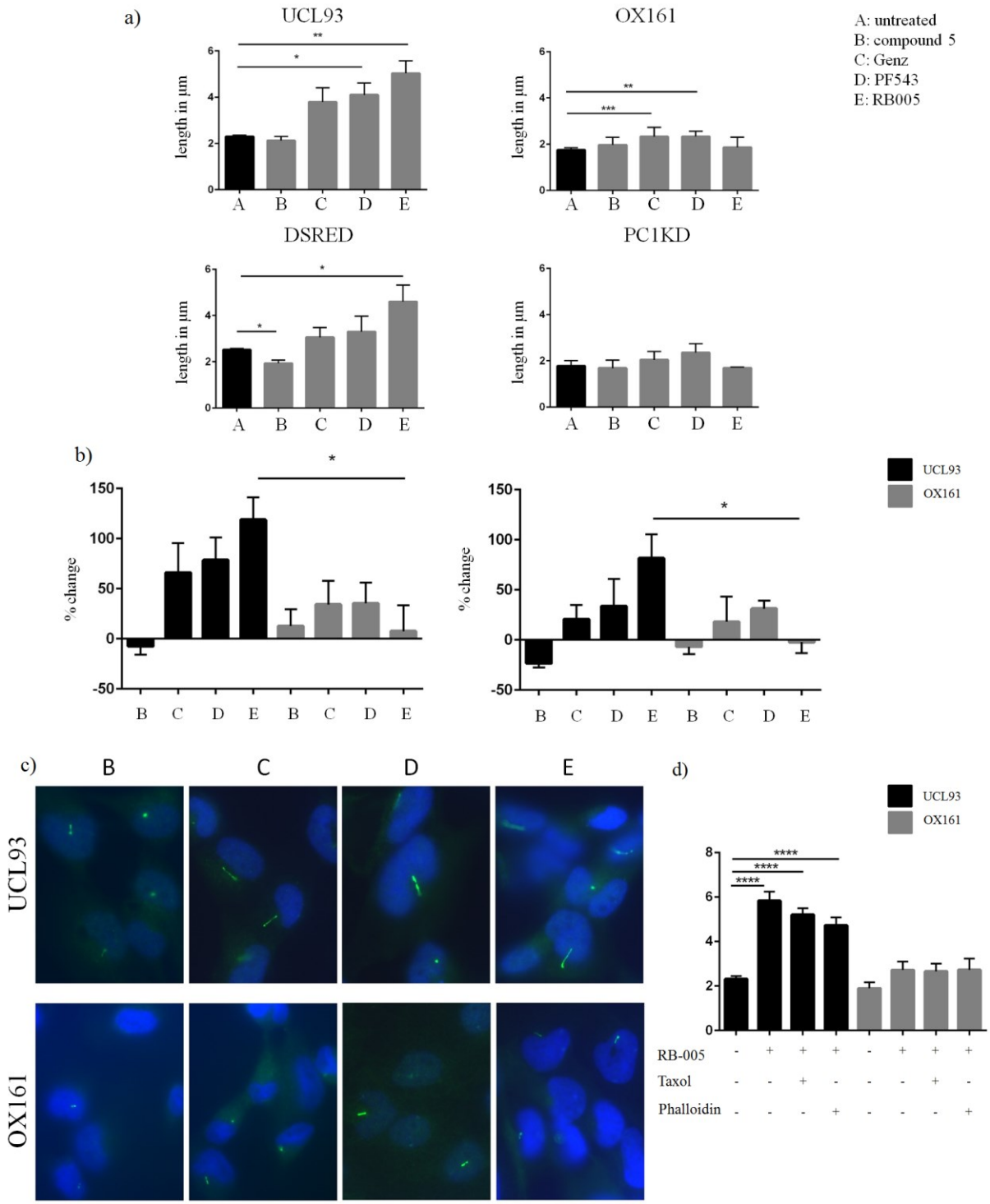

Figure 4.19 SK1 inhibitors or activators in normal and PKD primary cilium formation

a) Effect on primary cilium elongation of SK1 activator: Compound 5. SK1 inhibitors: GENZ, PF-543, RB005

b) Percentage change in ciliary length between treatments and comparison between normal and PKD models

c) Representative image and comparison of ciliary length appearance after treatment with SK1 inhibitors/activators in normal and PKD cells **d) Ceramide cilium regulation and actin/microtubules organization.** Stabilizing actin or tubulin prior and during ceramide inhibition does not prevent cilium elongation, suggesting an actin and tubulin independent pathway of cilium regulation. Antibody used: primary cilia (ARL13b: Green), cell nuclei (DAPI: Blue).

4.7 Summary and Discussion

The apparent defect in cilia reorientation in wounding assays (Result Chapter 3.16) stimulated further study into the role of the actin cytoskeleton in cilia assembly. Further clues came from a study showing that cell spatial confinement appeared to regulate primary cilium formation, possibly through cytoskeletal alterations which influenced changes in cell geometry, polarity and basal body positioning in human retinal pigment epithelial (RPE1) cells (Pitaval et al, 2010).

4.7.1 Actin organisation in normal and ADPKD cells

The main finding of this chapter was that actin depolymerisation using cytochalasin D could restore cilia length in ADPKD models. Although the primary cilium does not contain actin, there is a sub-apical actin network and a specialised compartment around the cilia base which appears essential for normal cilia assembly (Keeling et al, 2016).

A recent siRNA screen to identify proteins that could regulate cilia length identified several proteins involved in actin organization such as Gelsolin family proteins gelsolin (GSN) and Advillin (AVIL), which regulate cytoskeletal actin organization by severing actin filaments. They further showed that inhibition of actin polymerization, via cytochalasin-D treatment resulted in cilia elongation and an increased accumulation of a vesicular structure called the pre-ciliary compartment (PCC) at the basal body (Kim et al, 2010). The link between perturbation of the actin cytoskeleton and cilia length control (Bershteyn et al, 2010; Sharma et al, 2011) has been confirmed in several other cell types including hTERT-RPE1, IMCD and mouse embryonic fibroblasts (MEFs). These findings suggest that an organised and dynamic actin network is essential for accurate basal body docking at the cilia base and for correct trafficking of ciliary vesicles for cilia formation (Bershteyn et al, 2010; Hernandez et al, 2013; Kim et al, 2010, 2015; Rao et al, 2014; Yan et al, 2013). These structures are likely to be transient and highly dynamic as suggested by findings that less than 10% population of normal cells had detectable actin near the base of an originating primary cilium (Quarmby et al, 2014).

In ADPKD cells, the actin network was highly disorganised and showed increased polymerisation. These findings suggest that polycystin-1 may function to inhibit actin polymerisation or stimulate actin depolymerisation in normal cells. ADPKD cells may become more 'stiff' or rigid as suggested by studies in RPE-1 cells (Pivatal et al, 2010). A recent paper has reported associations between polycystin-1 and actin stabilization through a novel polycystin-1-Pacsin 2-N-Wasp complex (Yao et al, 2014). Moreover, the ability of polycystin-1 to regulate the actin cytoskeleton, cell migration and microtubule stability has been reported with polycystin-1 overexpression in MDCK cells resulting in dynamic actin protrusion (Castelli et al, 2007 & 2015). Notably, the effect of cytochalasin D on cilia length was independent of cAMP/PKA activation (Chapter 4.3.4), but not of PI3K inhibition. It has also been reported that other cystoproteins including polycystin-2/TRPP2 can interact with cytoskeletal proteins which may regulate its function (Chen et al, 2008). The exact mechanism linking cytoskeletal actin remodelling in controlling ciliogenesis are still not clear. However, new studies are uncovering interesting candidates such as actin remodelling factors LIMK2 and TESK1 which are part of the YAP/TAZ and directional vesicle trafficking mechanism, which on its own have shown to modulate primary cilia dynamics (Kim et al, 2015). Interesting, in the context of actin organization is the finding that the activity of YAP/TAZ was shown to require Rho GTPase and tension of the actin cytoskeleton to transduce mechanical signals exerted by ECM rigidity and cell shape, thus suggesting that defects in actin organization would result in defective YAP/TAZ function or vice-versa (Dupont et al, 2011).

4.7.2 The role of microtubules in primary cilium regulation

In this study, microtubule depolymerisation using nocodazole had differential effects on cilia length in normal and ADPKD cells. Current models suggest that GTPase activity is induced by nocodazole followed by nocodazole-tubulin dimer formation, which prevents addition and growth of the tubulin chain (Mejillano, 1996).

The lack of effect in ADPKD suggested increased microtubule stability or polymerisation which was confirmed using a nocodazole resistance assay. The effect of nocodazole was completely blocked by taxol confirming the importance of microtubule dynamics for normal cilia assembly. Taxol itself had no effects on preformed cilia and did not inhibit cAMP

induced cilia elongation indicating that cAMP effect is independent of microtubule stability. Likewise, the nocodazole effect was independent of that of cAMP in normal cells.

Previous studies have reported short or stunned cilia when katanin, a microtubule-severing protein was disrupted in *Tetrahymena* (Sharma et al, 2007) or defects in cilia formation when the activity of CrKinesin-13-a microtubule depolymerizing kinesin was decreased (Piao et al, 2009). These observations confirm that the ability of microtubules to depolymerize into free soluble tubulin is critical for cilia formation. Consequently, in addition to IFT regulation, the cell may be able to indirectly influence the ability of primary cilia to elongate or retract by controlling the levels of soluble tubulin ultimately needed to build the cilia axoneme. The first examples of microtubule and flagella dynamics in the model organism *Chlamydomonas* showed that tubulin levels increased in response to deflagellation or amputation (Silflow et al, 1981). The increase in microtubule stability in ADPKD cells suggests that similar to actin, polycystin-1 may inhibit microtubule polymerisation or stimulate its depolymerisation in normal cells. Labelling of polycystin-1 on β-tubulin positive microtubules has been reported (Beaulieu et al, 2010) and interestingly, one group has reported that polycystin-1 can decrease the stability of microtubules, as well as regulate the organization of the actin cytoskeleton (Castelli et al, 2015). Although not examined, it is of interest to note that Ca^{2+} promotes the disassembly of microtubules by specifically promoting the catastrophe reaction (O'Brien et al, 1997) and directly destabilizing growing microtubule ends without any significant change in the detected concentration of free tubulin. Potentially, a lowering of intracellular Ca^{2+} at the growing ends could lead to more stable microtubules in ADPKD (O'Brien et al, 1997).

4.7.3 The link between actin and microtubules

Studies of other ciliopathy proteins have suggested regulation of actin and microtubules as critical factors influencing ciliogenesis, For instance, BBS4 localizes to the centriolar satellites and basal bodies of primary cilia and is crucial for targeting cargo to the pericentriolar region, microtubule anchoring and cell cycle progression (Kim et al, 2004). In this study, BBS4 acted as an adaptor of p150 dynactin which then recruited the pericentriolar material protein 1 (PCM1) to the centriolar satellites. In mutant cells, PCM1 was mislocalized resulting in microtubule disorganization and longer cilia. The Meckel-Gruber syndrome (MKS) proteins MKS1 and Meckelin (MKS3) have been showed to regulate nesprin-2, a scaffold protein involved in microtubule and actin cytoskeleton maintenance

(Dawe et al, 2009). Reduction of meckelin directly correlated with the ability to reorganize actin resulting in defects of centriole/basal body migration and/or docking at the cell membrane prior to ciliogenesis (Dawe et al, 2009).

A clear hierarchical regulation of microtubules and actin interaction has proved difficult to define although many studies have tried to identify which of these two factors is in control. In migration, the actin cytoskeleton is thought to provide the major driving force with protrusion of actin structures at the leading edge and by the arrangement and contraction of actin stress fibers in the cell body and trailing edge (Etienne-Manneville 2004). Other studies however suggest that even in the case of migration, microtubules could be the primary regulators of actin dynamics, acting as generators for the protrusion activity at the leading edge. This is supported by data showing that the growing plus ends of microtubules can generate enough force to deform the cell wall lipid bilayer (Howard & Hyman 2003). In other studies such as during intrinsic cell polarization, microtubules and not actin appear to be the key elements (Palazzo & Gundersen 2002). In most systems however, the organization of microtubule and actin appears to be similarly polarized, and studies suggest that these two polymers must be able to interact through some still unknown intermediate proteins or signalling molecules, as shown by studies where microtubules were able to participate in actin rearrangements (Etienne-Manneville 2004). In addition, RhoGTPases whose main assigned role are as regulators of the actin cytoskeleton, are also able to regulate microtubule organization thus promoting a coordinated mechanism of these structural elements (Wojnacki et al, 2014). Conversely, microtubule modulation has been reported to alter the ratio of Rho GTPase activity (Togawa et al, 1999; Etienne-Manneville 2004).

Potential candidates linking actin and microtubules are formins, shown to move within the growing ends of actin filaments and which are then able to stabilize microtubules as a means of assisting directed steering in cell migration (Chesarone et al, 2010). Another potential candidate is tau, a neuronal microtubule-associated protein, which has been shown to bind to actin and microtubules simultaneously, resulting in a coordinated extension of both networks. Specifically, this coupled mechanism showed actin filaments which polymerised along pre-established microtubule tracks and single microtubules which grew along actin filament bundles (Elie et al, 2015). Alternatively, if we consider the plain mechanical and physical arrangement of these proteins in a cellular system, it has been shown that dense regions of

microtubules networks limit actin polymerization while actin-rich regions barely contain any microtubules during cell migration. Microtubules would then simply be excluded from actin-rich networks, by a physical steric obstruction of microtubule elongation, and studies supporting this show that depolymerisation of actin resulted in elongation of microtubules towards the leading edge in migrating cells (Pierini et al, 2002).

In this study, depolymerisation of actin (but not microtubules) was able to normalise cilia length in ADPKD cells suggesting that this is likely to be the primary abnormality. However, in ADPKD cells taxol partially inhibited the effect of cytochalasin D suggesting that its effect in disease may be two-fold i.e. to increase the levels of free tubulin as well as depolymerise actin. A previous study in htRPE and IMCD3 cells found that cytochalasin D resulted in an increase in the levels of free tubulin which was prevented by taxol pre-treatment (Sharma et al, 2011). In our study however, taxol did not prevent cytochalasin D induced cilium elongation in normal cells suggesting that the level of free tubulin was not a rate-limiting factor under normal conditions. However, since a dense microtubule network could prevent normal actin organization (Etienne-Manneville 2004), it seems likely that there is a functional interaction between both actin and microtubules in regulating cilia length.

4.7.4 Polycystin-1 is involved in cytoskeletal organization

In cell adhesion and migration it was shown that over-expression of polycystin-1 induced actin protrusion (Boca et al, 2007; Castelli et al, 2013), while polycystin-1 silenced models had less actin and microtubule-based protrusions at the leading edge in wounding assays, bigger and more randomly localized focal adhesions and a reduced ability of adherence. The authors suggest that focal adhesion kinase (FAK) is a potential target regulated by polycystin-1 with focal adhesion disassembly positively regulated by polycystin-1 and that the latter also regulated microtubule elongation and stabilization (Castelli et al, 2015).

In polycystin-1 over-expressing cells, actin rearrangements were also mediated by the PI-3 kinase cascade (Castelli et al, 2015) suggesting a critical role of PI3K in polycystin-1 mediated actin regulation. Other studies have also shown that polycystin-1 is able to interact with different GTPases and GTPase-activating proteins, a family of proteins which have been shown to be involved in a variety of cellular process (Arnould et al, 1998; Ward et al, 2011),

including the regulation of the Actin Cytoskeleton via an Arf GTPase-activating protein of the centaurin β family named ASAP1 (Randazzo et al, 2000).

4.7.5 PI3K is a ciliary length regulator

Phosphatidylinositol-4,5-bisphosphate 3-kinase (PI3Ks) are a large family of enzymes subcategorized in different classes and involved in a variety of different cellular functions (Liu et al, 2009). These enzymes have been shown to have multiple roles in cell behaviour, especially in cell migration, cell survival and cell division but also in differentiation, motility, and intracellular trafficking (Liu et al, 2009; Franco et al, 2014).

PI3K is activated in response to a variety of growth factors and has long been known to be involved in cell migration through regulating the actin cytoskeleton e.g. PDGF-induced lamellipodium formation (Wennström et al, 1994). Phosphorylated Akt, which is activated downstream of PI3K after PDGF stimulation, can be localized to the leading edge in migrating cells, thus providing one of the many hints which seem to highlight the importance of this pathway in cell migration (Higuchi et al, 2001). Other studies have shown that that the PI3K-Akt signalling pathway is involved in the stabilization of microtubules oriented toward the leading edge of wound-edge cells. In addition the PI3K-Akt pathway was suggested to stabilize microtubules in migrating fibroblasts which acted as tracks for the transfer of membrane vesicles to the leading edge (Onishi et al, 2007).

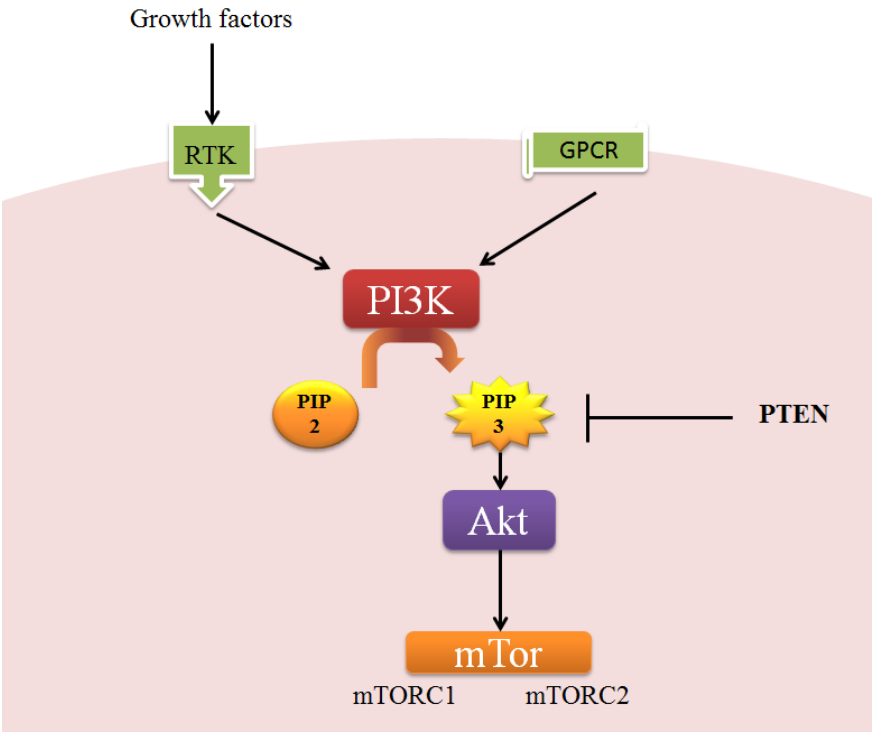

Figure 4.20 PI3K pathway Key function of PI3K is the regulation of a membrane lipid called phosphatidylinositol-3,4,5-trisphosphate (PIP3) from its Phosphatidylinositol 4,5-bisphosphate precursor (PIP2). PI3K signalling can be activated via different means, such as G protein–coupled receptors (GPCRs) or receptor tyrosine kinases (RTKs). The levels of PIP3 are regulated by several lipid phosphatases such as Phosphatase and tensin homolog (PTEN). PIP3 is involved in the activation of different pathways, most importantly the serine/ threonine kinase Akt (or protein kinase B) which results in a variety of PI3K/Akt downstream signalling activation, such as the well-known mTOR pathway.

The PI3K pathway is also involved in microtubule dependent membrane transport for neuronal growth cone guidance, downstream of Ca^{2+} which locally acted as axon turning potentials in oriented cone growth. Interestingly, PI3K inhibition attenuated microtubule advance, while exogenous phosphatidylinositol 3,4,5-trisphosphate (PIP3) had the opposite effect in promoting microtubule advance (Akiyama &, Kamiguchi 2010). These studies implicate PI3K in directional cell migration and demonstrate the potential importance of PtdIns(3,4)P2 and PtdIns(3,4,5)P3 in activating downstream signalling components, including Rac-1 GTPases. This in turn activates the polymerization of F-actin and membrane protrusion at the leading edge and further activation of PI3K through Rac-1 as a positive feedback loop to enhance cell polarity and oriented cell migration (Qing et al, 2012; Kölsch, et al, 2008). The link between actin dynamics, the PI3K signalling pathway and migration offers an important clue to the specific cell mechanics involved in cell movement and orientation.

To our knowledge a detailed role of PI3K in cilia assembly had not been previously examined in ADPKD. PI3K inhibition via LY-294002 induced primary cilium elongation in normal cells. This effect on cilium elongation was independent of cAMP/PKA and microtubule stability but was dependent on actin polymerisation (**Figure 4.11-12**).

Surprisingly, PI3K inhibition had no effect in ADPKD models. The effect of the latter in normal cells is therefore likely to be via actin depolymerisation whereas the effect of PGE2/cAMP may be via stimulating anterograde IFT velocity (Jin et al, 2014). While cAMP had similar effects in control and ADPKD cells, the lack of effect of PI3K inhibition in the latter was surprising given that PI3K inhibition could inhibit cilia disassembly in response to serum similarly in starved control and disease cells (**Figure 4.10**). One explanation could be that there is mislocalisation of a distinct PI3K isoform (PI3K Class II α) from the basal body or pre-cilia compartment in disease that specifically regulates cilia assembly (Franco et al, 2014). Alternatively, there could be a disconnection between PI3K and its downstream effectors acting on actin to stabilise cilia formation. These possibilities need to be tested in future studies.

4.7.6 Rho GTPases modulate primary cilia length

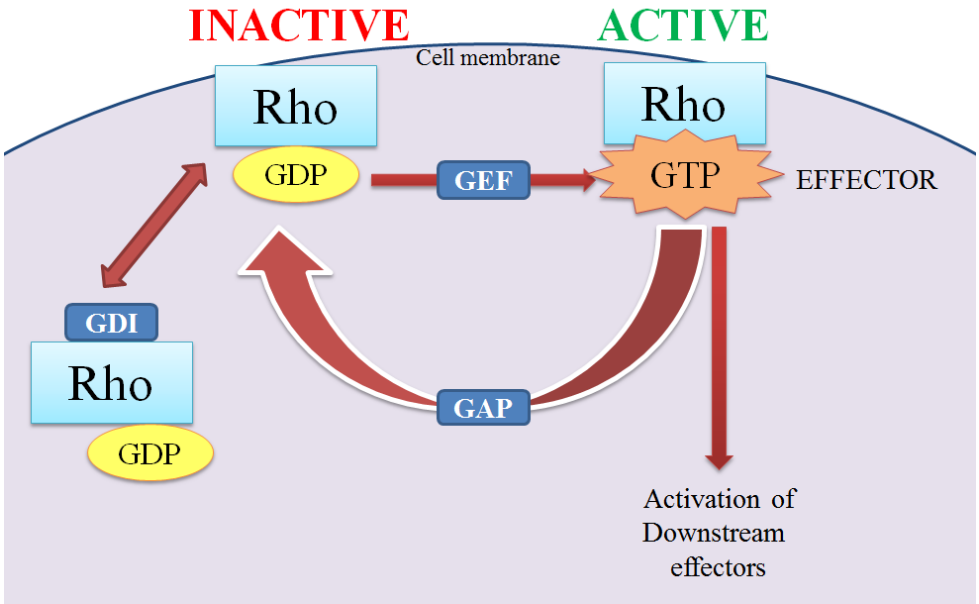

Figure 4.21 Rho GTPase regulation The activation cycle of Rho-GTPases at the plasma membrane, is regulated by GEFs that promote GTP loading resulting in activation of Rho-GTPases as an active effector involved in the activation of different downstream effectors. The inactivation of Rho-GTPases is mediated by GAPs by GTP hydrolysis to GDP. Rho-GTPases are deactivated via Rho-GDP dissociation inhibitors (Rho-GDIs) which transport and seclude inactive GDP-bound Rho-GTPases in the cytoplasm (Huveneers and Danen 2009).

The downstream effect of cytochalasin D was studied using selective Rho GTPase inhibitors. Although inhibition of all three major effectors (Rac-1, ROCK, Cdc42) resulted in increased cilia length, the most selective effect for ADPKD cells was seen with ROCK inhibition which restored cilia length (**Figure 4.14**). The link between Rho GTPase expression or activation *in vivo* with renal cyst formation and reduced cilia length or number is supported by previous reports from mouse mutants.

First, a mouse Rho GDIα mutant was found to develop various degrees of cystic distal and collecting renal tubular dilatation (Togawa et al, 1999). Rho GDIs bind to and interact with variety of Rho family members, including RhoA, Rac-1 and cdc42 (Tapon et al, 1997) keeping them in the GDP-bound inactive state; thus mutation would result in Rho activation. In this model, cilia were not examined.

A second study reported that a mouse mutant p190A RhoGAP (*Arhgap35*) developed glomerular cysts, accompanied by a drastic reduction of ciliated cells and average ciliary length in the proximal tubules. Loss of this GAP led to persistent activation of Rac-1 and ROCK. Of relevance, ciliogenesis in Rho GTPase Activating Protein 35 (Arhgap35) mutant cells could be rescued by inhibition of Rac1 or ROCK1/2 suggesting a direct pathogenic link between ciliogenesis and Rho activation (Stewart et al, 2016).

Finally, kidney-specific inactivation of Cdc42 in mice using a specific Cre recombinase (Ksp-Cre) resulted in the development of cysts in distal tubules and collecting ducts with associated ciliary defects, increased tubular cell proliferation and apoptosis (Choi et al, 2013). Here, the loss of Cdc42 rather than its increased activation resulted in structural cilia abnormalities and cyst formation. Although cilia were described as 'disordered' in cyst areas, surprisingly changes in length were not detected. Conversely, it has been shown that pre-cystic kidneys have high up-regulation of Cdc42 protein levels, suggesting that it is deregulated very early in ADPKD pathogenesis (Luyten et al, 2010).

4.7.7 Sphingolipids (ceramides) and primary cilium formation

A possible role in lipid signaling in the pathogenesis of ADPKD was first reported several decades ago, linking ceramide lipids with altered signalling role in PKD epithelial cells (Deshmukh et al, 1994).

Ceramides are molecules present in the lipid cell membrane of cells and are a mixed composite of sphingosine and fatty acids. A ceramide synthesis and deriving complex sphingolipid model is shown in the diagram (**Figure 4.18 b**) Pioneering studies on sphingolipids showed that they could be divided into two main categories, the family of ceramide sphingoid bases, which are involved in modulation of protein kinases and phosphatases, ion transporters, and signal transduction processes and the family of complex sphingolipids defined by an carbohydrate or phosphor-choline head group which interact with the extracellular matrix and growth factor receptors (Spiegel et al, 1996). Recent studies suggest that glycosphingolipids levels are abnormally enriched in cystic cell membranes and that increased synthesis of glucosylceramide correlated with increased cell proliferation and apoptosis (Natoli et al, 2010). Glucosylceramide and ganglioside GM3 levels were markedly increased in PKD tissues from human and several mouse models independent of the causative mutation. Importantly, the authors showed that treatment with the SK1 inhibitor Genz-123346 inhibited cystogenesis in *Pkd1*, *jck* and *pcy* mice (Natoli et al, 2010). The effects on primary cilia were not examined in this study.

In this study, a striking difference between normal and disease cells on cilia length following inhibition of Sphingosine-1-phosphate synthesis using SK1 inhibitors was observed. In normal cells, the effect on cilia length was independent of actin and microtubule polymerization (**Figure 4.19**). A previous study reported that ceramide is required for ciliogenesis and was co-localized to centrosomes with Cdc42 and atypical protein kinase Cζ/λ (aPKC) (Wang et al, 2009; He et al, 2012). The increased effect of RB-005 that we observed in normal cells may imply that apart from ceramide, sphingosines could be important mediators of cilia length. The lack of effect with the SK1 inhibitors on cilia length in disease cells was unexpected but is similar to the lack of effect of PI3K inhibitors observed in the same assay. These negative results could indicate that the pericentriolar recycling endocytic compartment is also disrupted in ADPKD (He et al, 2012).

Summary

- There was significant disorganisation of the actin cytoskeleton in ADPKD models.
- Actin depolymerisation (cytochalasin D) restored cilia length in ADPKD models to control levels.
- Microtubule polymerisation and stability was increased in ADPKD models compared to control cells.
- Microtubule modulation depolymerisation (nocodazole) increased ciliary length only in normal, but not ADPKD models.
- Microtubule/actin depolymerisation dependent cilium elongation was independent of cAMP or PKA activation.
- PI3K inhibition reduced cilia disassembly in response to serum reintroduction similarly in serum starved control and ADPKD models
- PI3K inhibition increased cilia length in control but not ADPKD cells. This effect was independent of cAMP and microtubule depolymerisation.
- Rac-1, ROCK and Cdc42 inhibition causes primary cilium elongation in normal and ADPKD cells to different degrees.
- The effect of ROCK inhibition in ADPKD cells was independent of microtubule polymerisation but not of PI3K activation.
- The effect of cdc42 inhibition was dependent on both microtubule and actin depolymerisation.
- There was an increase in the number of ciliated cells in the ADPKD models with cytochalasin D and ROCK inhibitors.
- Inhibition of sphingosine kinase 1 increased cilia length in normal but not ADPKD cells. This effect was independent of actin and microtubule depolymerisation.

Results Chapter V

Cystoproteins interacting proteins involved in primary cilium regulation

5.1 Introduction

In this chapter, the potential role of two ciliary proteins in primary cilium regulation was studied. Preliminary studies in our laboratory (unpublished) had identified INPP5E and NPHP3 as potential binding partners of polycystin-1 and polycystin-2 respectively. Both these proteins have been identified as playing roles in regulating primary cilia structure and function (Jacoby et al, 2009; Zhou et al, 2010).

5.1.1 Inositol-polyphosphate 5-phosphatase (INPP5E)

The first part of the study was concentrated on the interacting partners of the polycystin-1 protein. Because of the difficulties associated with the study of full-length polycystin-1 in biochemical assays, the study was concentrated on the intracellular domain of polycystin-1 called PLAT (polycystin lipoxygenase α-toxin). Previously, the PLAT domain has been shown in our laboratory to be able to bind lipids (Xu et al, 2015).

PLAT is the abbreviation for an evolutionary conserved polycystin/lipoxygenase/α-toxin domain found in all Polycystin-1 family members and in some lipid-associated proteins. It is suggested that this domain, which is located in the first cytoplasmic loop between TM1 and TM2 of PC-1, is involved in protein or membrane protein interactions (Bateman and Sandford 1999) and that its primary role might be as an evolutionary conserved mediator of intracellular signalling pathways of PC1 (Hu and Barr 2005).

A potential interacting candidate of the PLAT domain based on its ability to bind lipids (Xu, et al, 2015), is the lipid phosphatase, inositol polyphosphate 5-phosphatase, INPP5E. Preliminary work in our laboratory showed that the Polycystin-1 was able to bind to phosphoinositol (PI-4P) and the lipid kinase PI-4P-5Kinase via PLAT domain possibly acting as a protein scaffold involved in the regulation of PIP2 and PIP3 synthesis. INPP5E has been localized to the primary cilium and plays a critical role in the conversion of phosphatidyl-inositol-4,5-bisphosphate [PI(4,5)P2] to PI4P regulating PIP2 and PIP3 levels. A potential link between the PLAT domain and INPP5E was investigated in this chapter. The INPP5E

signalling pathway had been shown to be involved in primary cilium stability and cell proliferation in recent studies (Jacoby et al, 2009; Garcia-Gonzalo et al, 2015). The *INPP5E* gene on human chromosome 9q34.3 encodes for a 72kDa protein (Jacoby et al, 2009). *Inpp5e* mutant mice developed several ciliopathy phenotypes such as renal cysts, defects in neural tube closure and developmental problems including absence of eyes and polydactyly (Jacoby et al, 2009).

5.1.2 NPHPs, Gatekeepers of the ciliary compartment

The contribution of polycystin-2 to ADPKD is obvious but another important function of this protein is in left-right axis determination (Pennekamp et al, 2002). Polycystin-2 and a number of other cystoproteins are associated both with the formation of kidney cysts and laterality defects when disrupted in the mouse models. Two examples of these proteins are the nephrocystins (NPHP), NPHP2 or Inversin (INVS) (Otto et al, 2003) and NPHP3 (Olbrich et al, 2003).

The nephrocystins are mutated in Nephronophthisis (NPHP), an autosomal recessive kidney disease and one of the most frequent genetic causes of end-stage renal disease up to the third decade of life. Today more than 20 genes have been identified (Wolf 2015), which are involved in a wide variety of cellular processes. Recent studies have suggested that most of the nephrocystins localize to the primary cilium or centrosomes. These observations have lent support to a common ciliary hypothesis of cyst formation (Wolf et al, 2005; Jauregui et al, 2008). The current view is that many of the NPHP proteins act as gatekeepers of the ciliary compartment and as such are able to control the influx or aid the transition of proteins from the cellular compartment to the primary cilium.

In the case of NPHP2 (INVS), NPHP3 and NPHP9 (NEK8), it has been demonstrated that these proteins localized to the proximal cilia shaft in ciliated cells – the so-called 'Invs compartment' (Wolf et al, 2010). Recently, another cystoprotein named ANKS6 has been shown to interact with NPHP3, INVS and NPHP9 and co-localize to this region (Hoff et al, 2013). This localization is determined specifically by INVS, which may function to anchor the complex to this compartment (Shiba et al, 2010). Interestingly, another paper has linked *NPHP3* with *NPHP9* and identified a mutation in the latter, which was associated with a

decreased expression of polycystin-1 and 2 in cultured fibroblasts (Frank et al, 2013), suggesting that NPHP9 could be important for normal polycystin function or localization. In this context, *nphp9* mutations were shown to cause juvenile cystic kidney (jck) disease in a mouse model (Liu et al, 2002). Another study pointed out, that the appearance of renal cysts, laterality defects and the defective response to fluid shear and reduced calcium response to flow in the Nek8-null phenotype strongly resembled that of the polycystin-2-null mice, suggesting a strong functional link between these two proteins. Interestingly, this study found aberrant phosphorylation of polycystin-2 in jck mice beside the ability of polycystin-2 to co-immunoprecipitate both w.t. and disease *Nphp9* (Sohara et al, 2008). In the same study, ciliogenesis was reported to be normal in *nphp9*-null kidney cells, suggesting that a loss of polycystin-2 cilia localization might be the primary defect (Manning et al, 2013).

A MS analysis of the polycystin-2 interactome in our laboratory using a stable MDCK cell line expressing epitope-tagged polycystin-2 identified NPHP3 as a potential interacting partner. This study tested the hypothesis that NPHP3 interacts with polycystin-2 and in a complex with other known NPHP proteins, regulates polycystin-2 entry into the primary cilium.

5.2 INPP5E

5.2.1 INPP5E binds to polycystin-1 PLAT domain

To investigate a possible interaction between these two proteins, HA-tagged *INPP5E* and YFP-tagged *PLAT* domain were co-expressed in HEK cells followed by co-immunoprecipitation with specific HA and YFP epitope tag antibodies. Controls in this study were a positive control GFP and a negative control empty vector PCDNA3.
The epitope-tagged *INPP5E* and PLAT proteins were pulled down and detected by immunoblotting with rat HA and mouse GFP antibody respectively. The pull down experiment showed that HA-*INPP5E* (78kDa) was able to co-immunoprecipitate with YFP-*PLAT* (42kDa) in both directions (**Figure 5.1A**).

Next, a FLAG tagged polycystin-1 construct (PC1-FLAG) was used to confirm the interaction capability of INPP5E with full-length polycystin-1 (**Figure 5.1B**). Again, both full

length polycystin-1 (460kDa) and INPP5E (78kDa) were shown to co-immunoprecipitate.

The interaction capability of INPP5E with several PLAT mutants was next tested. These mutations included a *PKD1* patient mutation YFP-PLAT (R3162C) and two mutants created in our laboratory. The YFP-PLAT (S3164A) phosphodefective mutant prevents phosphorylation by endogenous PKA at serine 3164 and a phosphomimetic YFP-PLAT (S3164D) mutant. This residue at Ser3164 has been shown to be phosphorylated by PKA, a cAMP activated protein kinase (Xu et al, 2015). The consensus binding domain for PKA at S3164 includes the residue R3162 which has been shown to be a pathogenic mutation (R3162>C) giving rise to ADPKD, highlighting the functional significance of phosphorylation at this site. Work in our laboratory showed that this phosphorylation site might be important in regulating trafficking of PLAT to the plasma membrane. YFP-PLAT was able to localize to the plasma membrane, while the S3164D mutation was characterized by a complete loss of surface localization. However, none of these mutations affected the interaction between these two proteins *in vitro* (**Figure 5.2**).

In conclusion, the study showed that INPP5E was able to interact with polycystin-1, specifically through the PLAT intracellular domain, suggesting that this interaction might play an important role in the function of this enzyme which had been shown to regulate cilium dynamics.

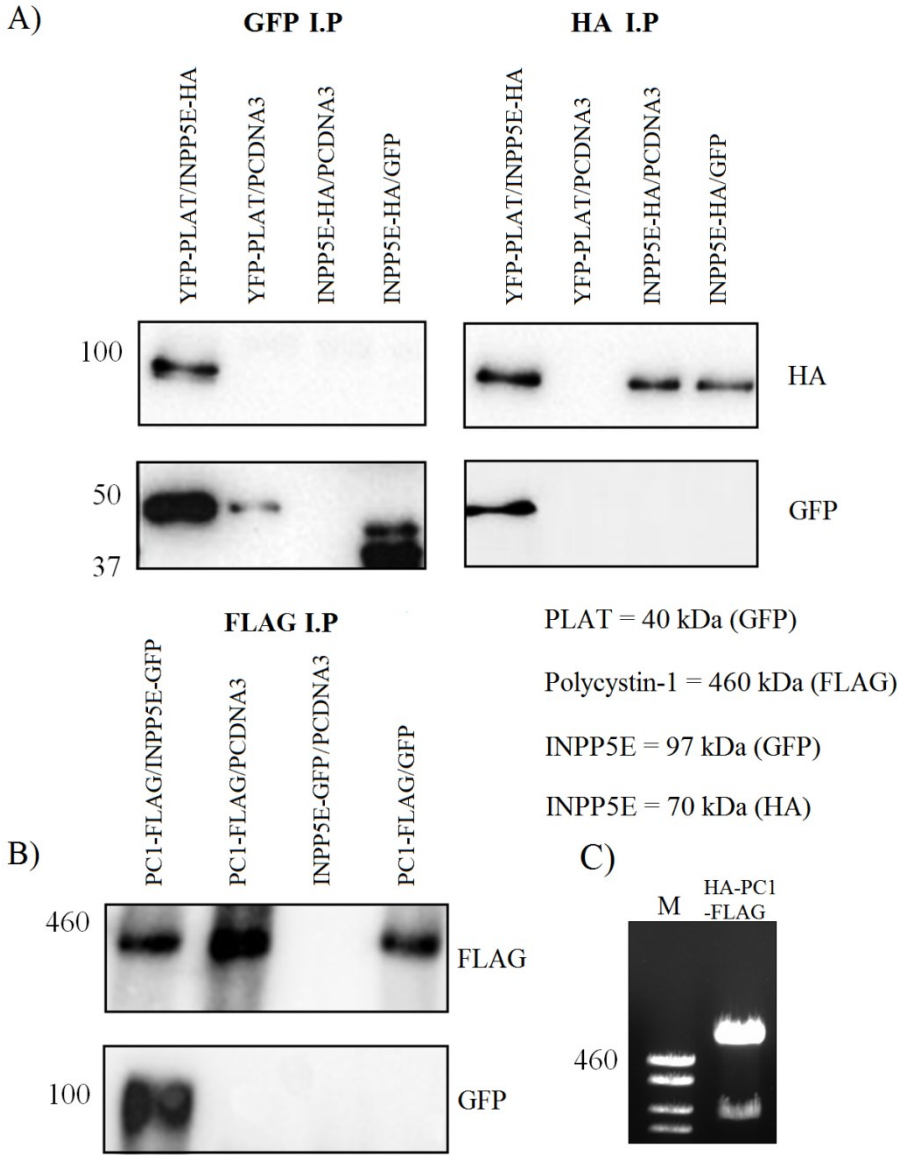

Figure 5.1 PLAT/INPP5E interaction: A) I.P GFP: Blot HA shows co-immunoprecipitation of INPP5E-HA protein which can be detected as a band at 78 KDa (Predicted Molecular Weight of INPP5E 72 kDa). **I.P HA**: Blot HA shows direct pull down of INPP5E-HA appearing at 80 KDa. Controls (INPP5E-HA + PCDNA3), (GFP + INPP5E-HA). **I.P GFP**: Blot GFP shows direct pull down of YFP-PLAT appearing at 42KDa. **I.P HA**: Blot Mouse GFP shows coimmunoprecipitation of YFP-PLAT which can be detected at 44 KDa. **B) PC1 I.P**: Blot FLAG shows direct pull down of PC1-FLAG. Blot HA shows co-immunoprecipitation of INPP5E-HA protein which can be detected as a band at 78 KDa (Predicted Molecular Weight of INPP5E 72 kDa).**C)** Generation and verification of HA-PC1-FLAG plasmid. Representative experiments of 3 repeats

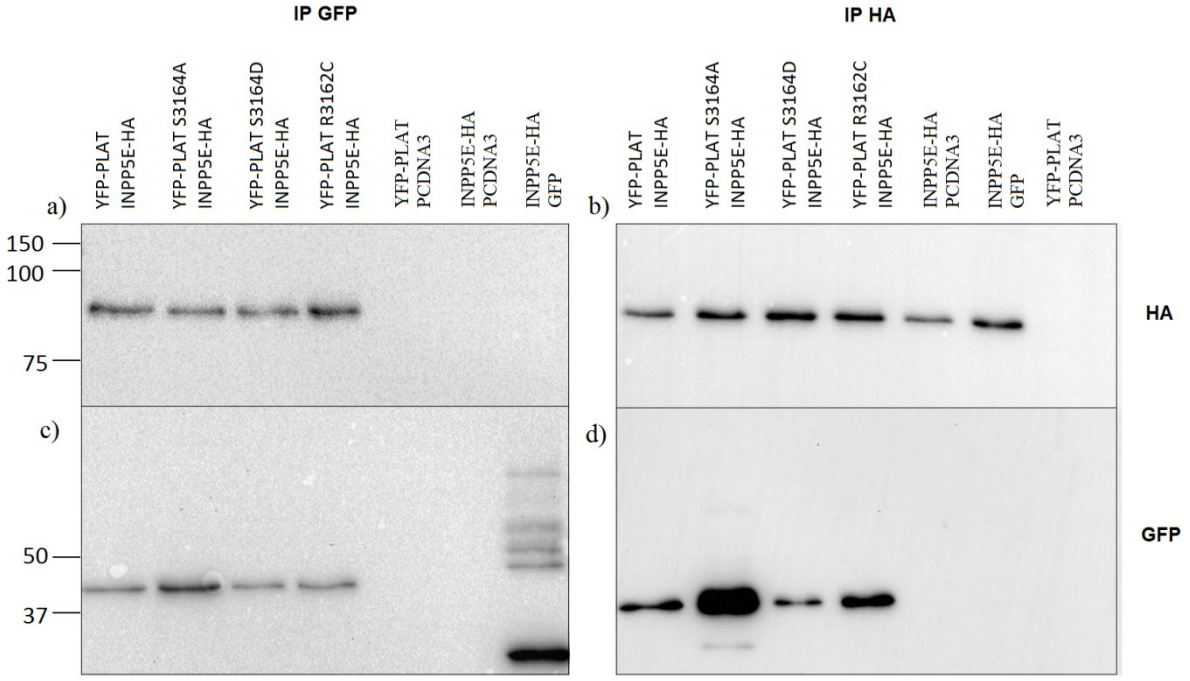

Figure 5.2 PLAT Mutants/INPP5E interaction: a) I.P with rabbit GFP isolates YFP-PLAT protein complexes, blot with Rat HA shows INPP5E-HA Co-Immunoprecipitation in YFP-PLAT and YFP-PLAT (S3164A, S3164D, R3162C) mutants. **b)** Direct I.P with Rabbit HA and blot with Rat HA shows pull down of INPP5E. **c)** I was able to directly I.P with rabbit GFP and detect YFP-PLAT and YFP-PLAT Mutants via Mouse GFP blot. **d)** I.P via Rabbit HA isolates INPP5E-HA protein complexes, blot with mouse GFP shows YFP-PLAT Co-Immunoprecipitation in YFP-PLAT and YFP-PLAT (S3164A, S3164D, R3162C) mutants.

5.2.2 INPP5E localization in normal and ADPKD cells

In view of the interaction between INPP5E and polycystin-1, the hypothesis that INPP5E cilia localization was altered in polycystin-1 deficient cells was next tested.

The INPP5E antibody used in this study was an anti-mouse Inpp5e antibody (Jacoby et al, 2009). Sequence alignment showed that this antibody was able to detect INPP5E specifically in mouse kidney cells and probably canine kidney cells.

INPP5E was shown to localize to the primary cilium of different normal mouse cell lines and MDCKII, as shown in (**Figure 5.3**). INPP5E was detected along the cilia of IMCD3 and polycystin-1 knocked down IMCD3 (**Figure 5.3 a**) which showed significant reduction of expressed polycystin-1 (**Figure 5.3 b)**. INPP5E appeared to localize uniquely to the primary cilium in growth arrested IMCD3, and this localization was not impaired in polycystin-1 knock down cells. Similar results were confirmed in the MEK PC1 null cells and the WT control lines, with uniform co-localization of INPP5E staining with the α-acetylated tubulin at the primary cilia (**Figure 5.3 c**). An interesting observation showed that a distinct small percentage around 10% of primary cilia was characterized by a non-uniform Inpp5e localization to the primary cilium in different models, which concentrated predominantly at the ciliary base or was not able to fully extent to the ciliary tip. In addition in extensive elongated cilia such as in MDCKII, some degree of INPP5E localization extends towards the ciliary tip and is evident as punctuated green patches (**Figure 5.3 d**).

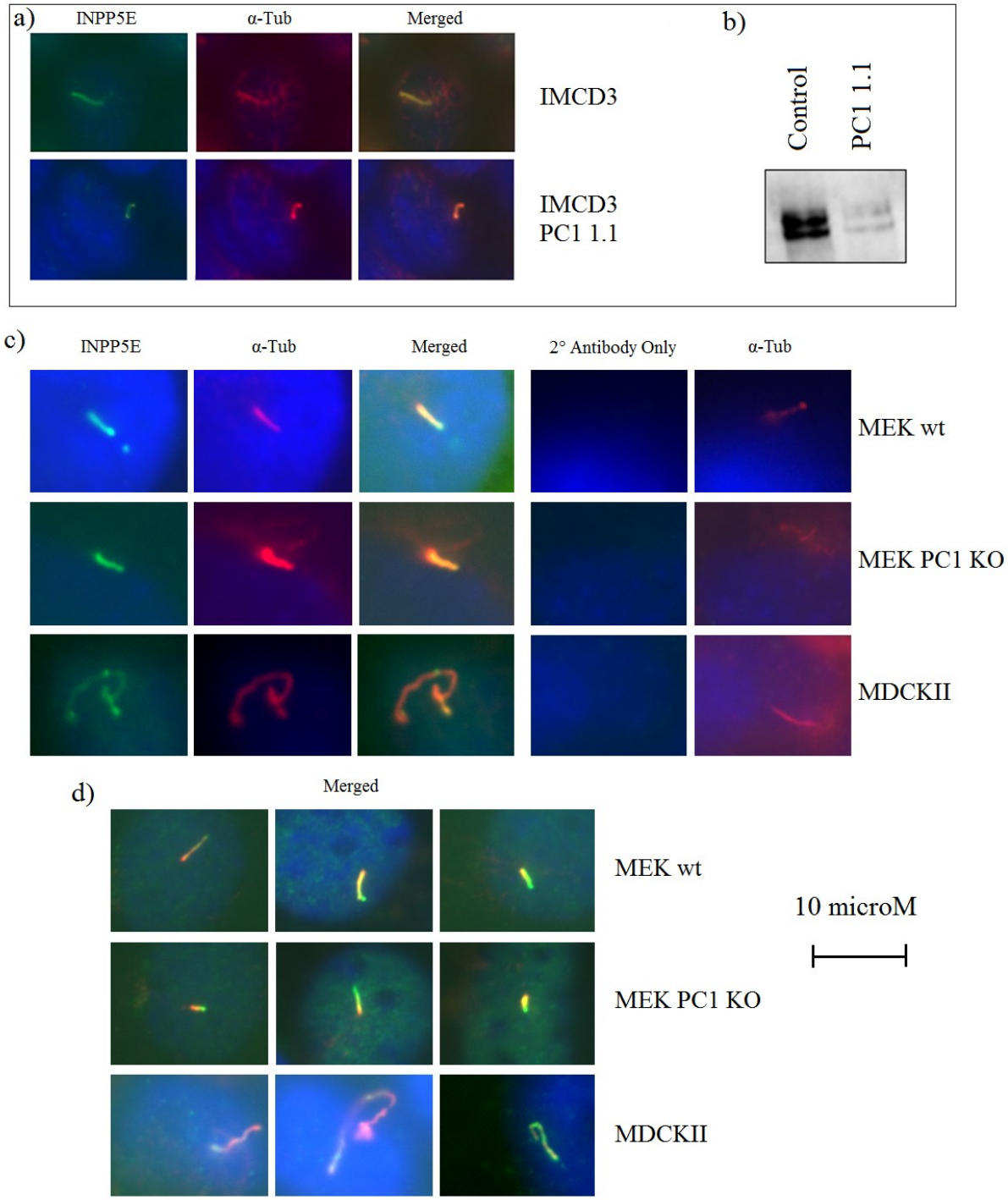

Figure 5.3 INPP5E localization in different cell lines. INPP5E staining (green) localize to primary cilia stained with α-Tub (Red) **a)** w.t and PC1 KD IMCD3. **b)** Blot showing expression of PC1 in KD IMCD3 cells. INPP5E (Green), α-Tub (Red). **c)** w.t and PC1 null MEK cells and MDCKII cells.

d) Localization of Inpp5e to the cilium is limited to the proximal region in a reduced number of cells.

Antibody used: primary cilia (INPP5E: Green) (acetylated tubulin: Red), cell nuclei (DAPI: Blue).

5.2.3 INPP5E siRNA reduces ciliary length

In the previous chapters, it was shown that polycystin-1 deficiency appeared to be associated with a defect in primary cilium formation rather than cilium stability. For this purpose, a specific siRNA against mouse *INPP5E* was used to analyse the effect of *INPP5E* knock down in two baseline mouse models, IMCD3 and NIH3T3.

Treatment with *INPP5E* siRNA at 10 and 50 μM concentrations significantly decreased INPP5E expression in mouse IMCD3 cells by qPCR with a fold change in *INPP5E* mRNA of 0.5 (**Figure 5.4 a, b**). Interestingly, *INPP5E* knockdown was associated with a significant dose dependent reduction in cilia length in IMCD3 and NIH3T3 cells **(Figure 5.4c)**.

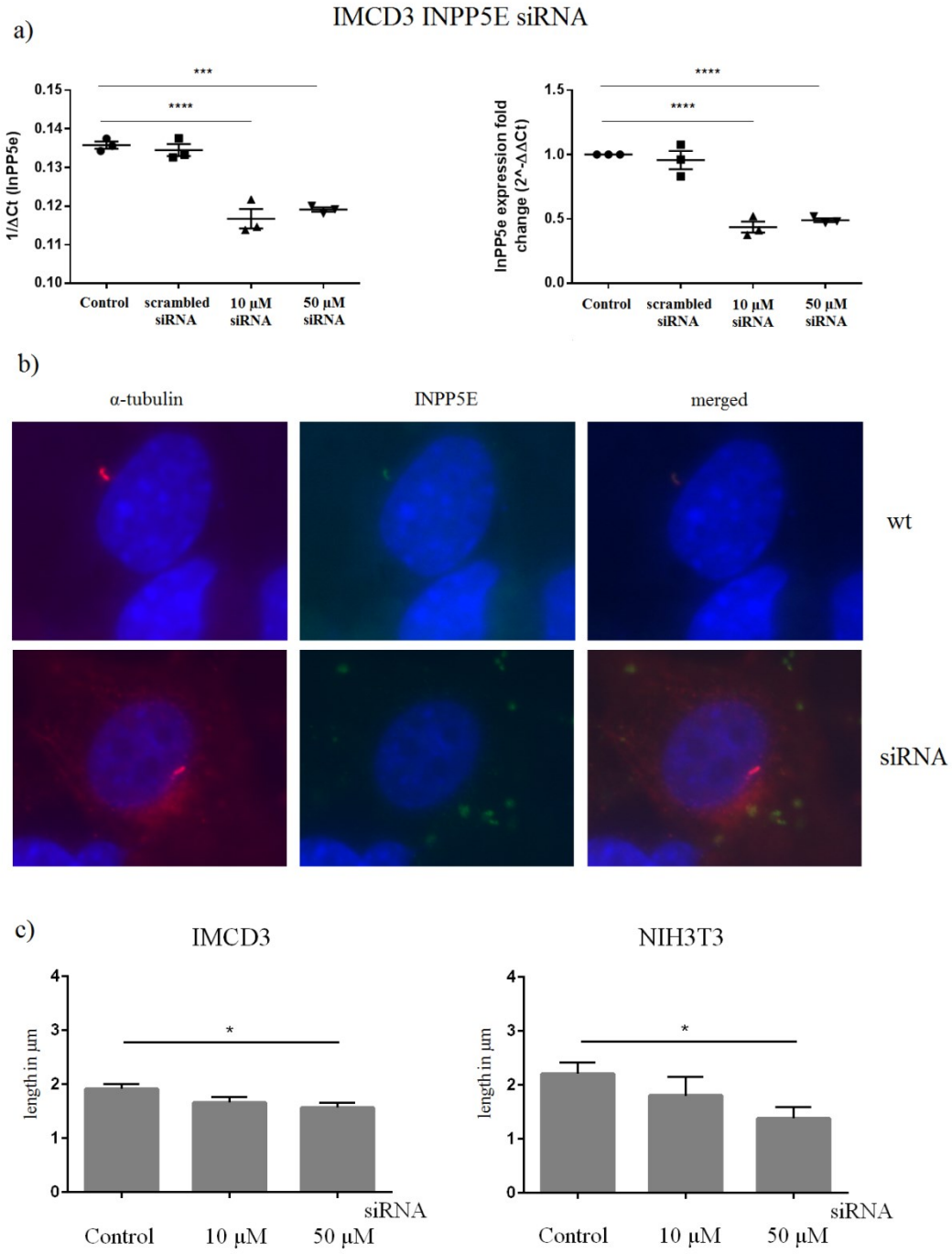

Figure 5.4 *INPP5E* siRNA treatment and ciliary length. a) *INPP5E* expression in CT and fold change after siRNA treatment at different concentrations. **b)** Representative image of *INPP5E* reduction after siRNA treatment under fluorescent microscopy analysis. **c)** Length of primary cilia after treatment with *INPP5E* siRNA at different concentrations in IMCD3 and NIH3T3 and scrambled control. Antibody used: primary cilia (INPP5E: Green) (acetylated tubulin: Red), cell nuclei (DAPI: Blue).

5.3 Polycystin-2 interacts with NPHPs

5.3.1 Polycystin-2 interacts with NPHP3 and NPHP9

Since NPHP3 and NPHP9 are known to interact (Frank et al, 2013), this was confirmed first by co-expression in HEK293 cells followed by co-immunoprecipitation (**Figure 5.5 A**). Interestingly, the NPHP3 protein appeared to have a stronger ability to co-immunoprecipitate the NPHP9 than the reverse.

Next, the ability of polycystin-2 to interact with both NPHP proteins was tested. For these experiments, the FLAG tagged NPHP proteins were used and tested for their co-immunoprecipitation ability of PKTAG tagged polycystin-2 (PC2-PKTAG) (**Figure 5.5 B**). Blotting for PKTAG or a polycystin-2 antibody (G20) showed a possible interaction although binding was weak in this direction. A reverse IP using a HA tagged polycystin-2 construct however showed a stronger interaction **(Figure 5.6)**.

5.3.2 NPHP2/INVS binds to the polycystin-2/nephrocystins complex

To study a potential interaction between inversin and polycystin-2, co-immunoprecipitation of GFP tagged INVS and HA tagged polycystin-2 constructs were used. Pull-down of HA-PC2 using HA affinity beads or HA antibody showed that INVS-GFP could be detected. (**Figure 5.7 a, b**). The reverse pull down with INVS-GFP protein resulted in co-immunoprecipitation of the HA-PC2 **(Figure 5.7 c)**.

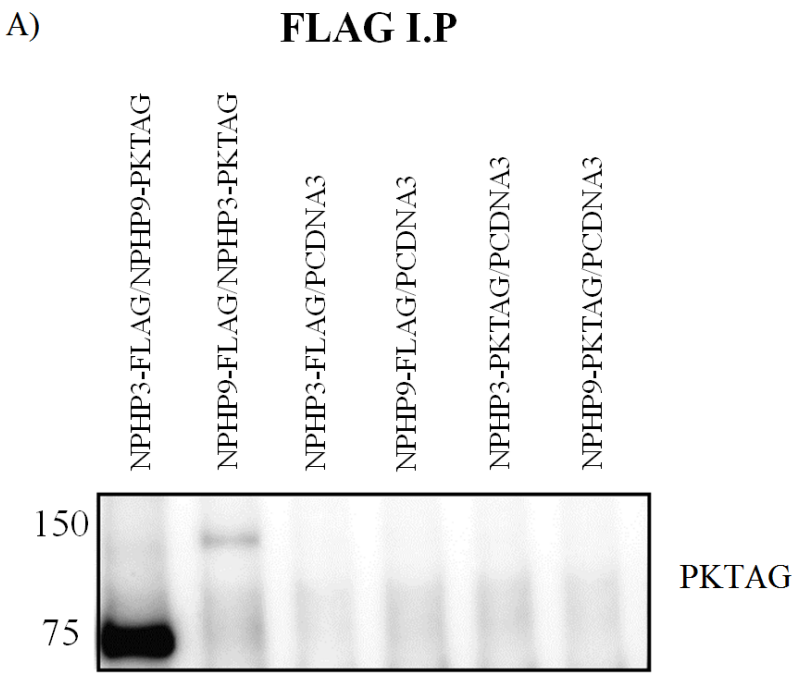

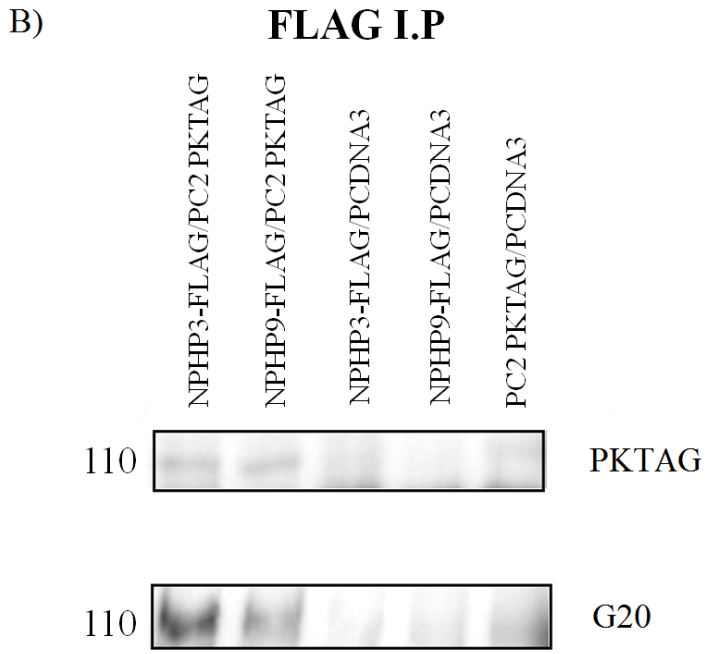

Figure 5.5 A) NPHP3/NPHP9 interaction FLAG tagged NPHP3 and NPHP9, PKTAG Tagged NPHP3 and NPHP9, NPHP3 (148 KDa), NPHP9 (74.9 kDa). NPHP3 pulls down NPHP9 and reversely NPHP9 pulls down NPHP3, suggesting that this two proteins interact **B) NPHP3/NPHP9 and PC2 interaction**. NPHPs pulls down Polycystin-2. NPHP3 and NPHP9 were able to immune-precipitate PC2 and be detected with two different antibodies, mouse PKTAG and G20. Representative experiments of 3 repeats

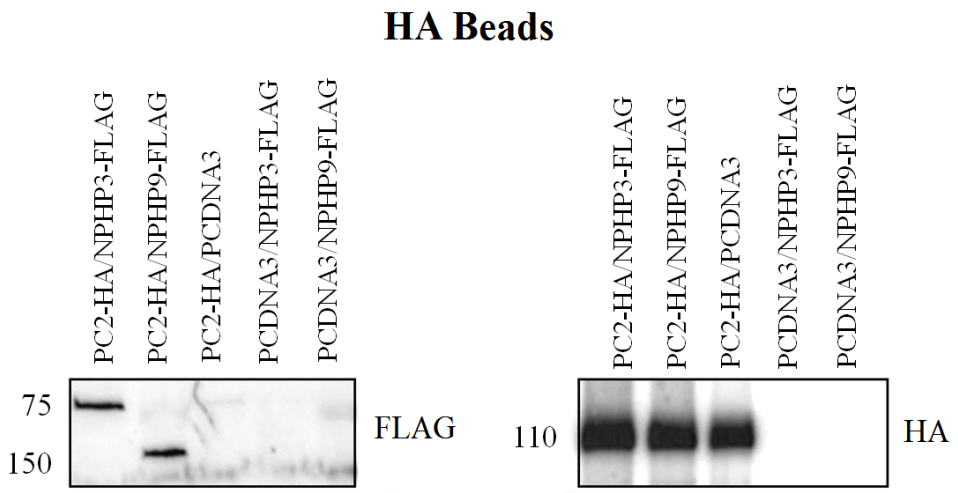

Figure 5.6 Polycystin 2 pulls down both NPHP3 and NPHP9. Polycystin-2 immuno-precipitates NPHP3 and NPHP9 at comparable levels. Representative experiments of 3 repeats.

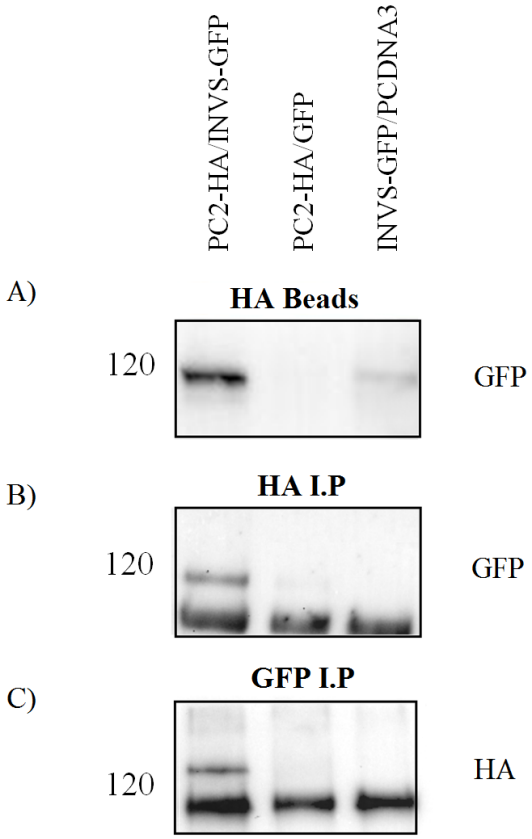

Figure 5.7 INVS/PC2 interaction A) HA Beads affinity beads were used to pull down INVS-GFP which was detected as a co-immunoprecipitate band at the correct molecular weight via GFP blot. **B)** Standard immunoprecipitation was used to confirm that INVS-GFP co-immunoprecipitated with polycystin-2 protein. **C)** In reverse, pull down of INVS results in co-immunoprecipitation of polycystin-2 detected at the correct molecular weight marker via HA blot. PC2 (HA) = 110 kDa, INVS (GFP) = 117 kDa. Representative experiments of 3 repeats.

5.3.3 Localization of cystoproteins to the primary cilium

Of the NPHP proteins in our study, NPHP2/Inversin retains the most important role of the entire complex, by possibly overseeing and localizing various parts of the complex to the correct cellular compartment (Shiba et al, 2010). Thus, the requirement of NPHP2 for the correct localization of endogenous polycystin-2 to the primary cilium was tested. Preliminary experiments showed that polycystin-2 could be detected at the primary cilium (**Figure 5.8 A**). Next, all our cell lines were tested for polycystin-2 localization (G20) in combination with the ciliary protein ARL13b. The results show that polycystin-2 can be detected almost uniformly along the entire length of the primary cilium in all normal cells as previously reported (Pazour et al, 2002). However, no difference was detected in polycystin-1 defective cell lines, though ciliary polycystin-2 localization in normal cells appeared to be increased towards the ciliary tip (**Figure 5.8 A-C**). The specificity of these findings was confirmed by the absence of polycystin-2 localization to the primary cilium in *PKD2* KD cells (**Figure 5.8 D**).

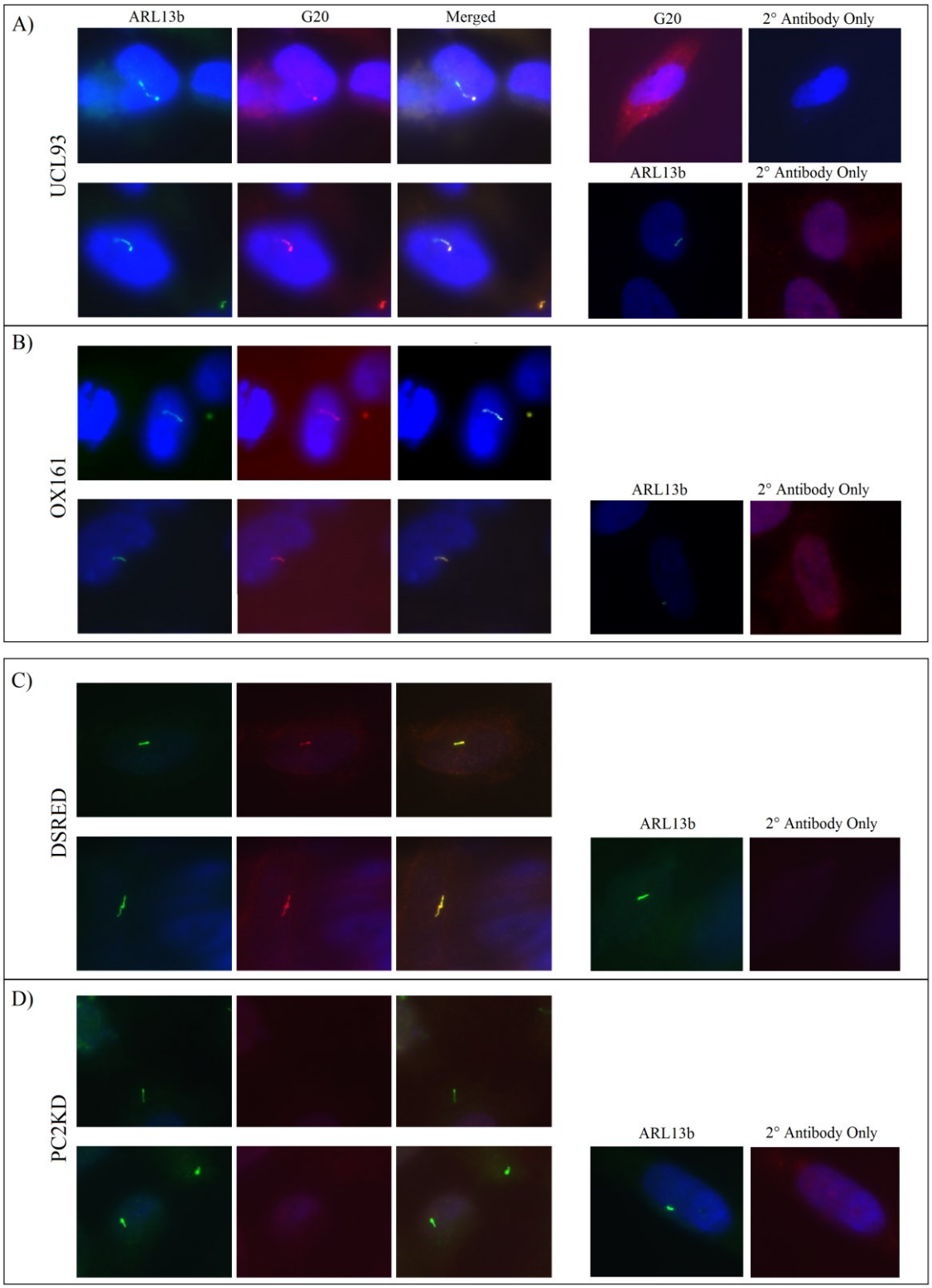

Figure 5.8 A-D (left) Endogenous polyscytin-2 localization study in primary cilia. Representative images of co-localization of polycystin-2 via G20 (Red) antibody with the ciliary antibody ARL13b in (green) growth arrested normal and ADPKD cell lines. **A (right)** G20 on its own stains the primary cilium. **A-D (right)** Control samples with ARL13b antibody and secondary G20 antibody. Magnification 60X.

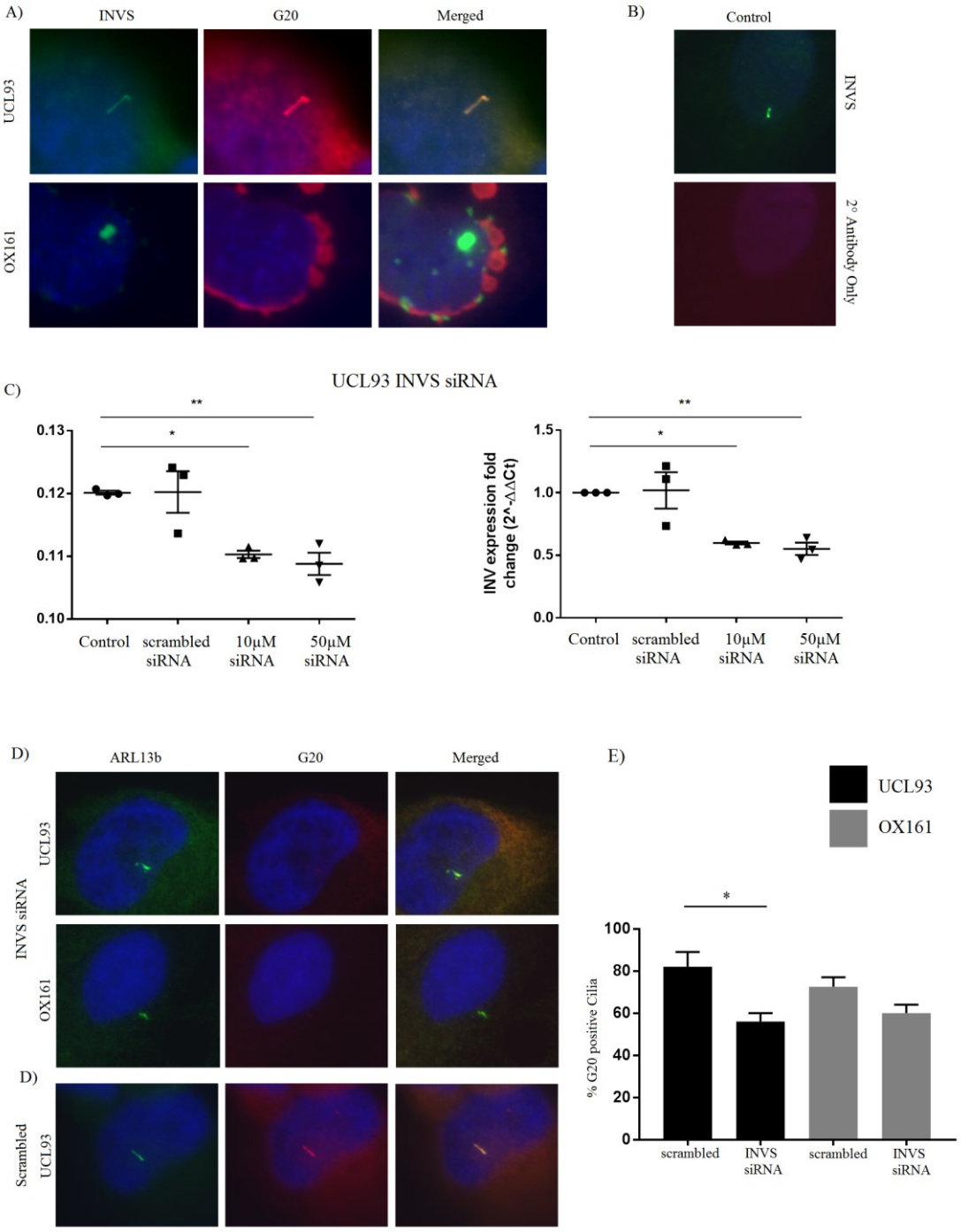

Figure 5.9 INVS in primary cilia **A)** Representative images of INVS localization to primary cilia in normal and ADPKD models via transfection of INVS-GFP construct for INVS detection and endogenous G20 antibody for polycystin-2. **B**) Control, INVS GFP detection alone. **C**) INVS expression CT and fold change after siRNA treatment at different concentrations. **D**) Representative images of polycystin-2 localization to primary cilia after knock down for Inversin via siRNA shows a reducing trend with a number of cells negative for G20 (polycystin-2) staining to the cilia, quantified in **E**).

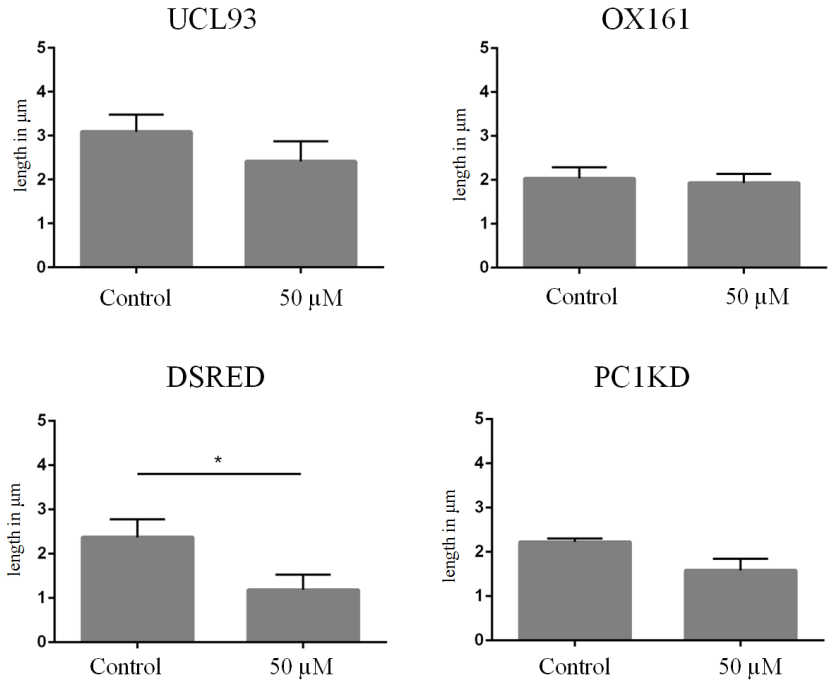

Figure 5.10 INVS and primary cilium regulation Primary cilium length measurement in normal (UCL93/PTEC DSRED) and ADPKD models (OX161/ PTEC PC1KD) after reduction of INVS via siRNA in growth arrested cells. KD of INVS partially reduces ciliary length in normal, but not PKD models.

Following the identification of an interaction complex between INVS and polycystin-2, the importance of this interaction for cilia localization of polycystin-2 was examined.

Over-expression of INVS-GFP in normal and PKD models showed accumulation of INVS protein along the entire length of the primary cilium in normal cells, but surprisingly this localization was impaired in the ADPKD cells (**Figure 5.9 A**).

To study the localization of polycystin-2 in Inversin deficient models, expression of INVS was reduced using INV-siRNA. Treatment with INVS siRNA at 10 and 50 μM concentrations significantly decreased INVS mRNA expression in human UCL93 cells (**Figure 5.9 C**). In normal cells, the cilia localization of polycystin-2 was significantly reduced (**Figure 5.9 D**). A non-significant trend was also observed in ADPKD cells (**Figure 5.9 E**). Cilia length was not significantly reduced by INVS knockdown in normal and PKD models except in one normal line (DSRED) (**Figure 5.10**).

5.4 Discussion

In this study, a number of candidate cystoproteins involved in primary cilium regulation were analysed for their ability to interact with polycystin-1 or polycystin-2 and tested for their effect on cilia length and polycystin-2 cilia localisation.

5.4.1 INPP5E interacts with the PLAT domain of polycystin-1

In recent years, research has focused on the role of different enzymes involved in lipid signalling associated with possible roles in the ciliopathies. INPP5E is one of the most investigated and its main pathogenic role has been associated with Joubert syndrome. Although rare, it is possible that the function of this enzyme may shed light on ADPKD pathogenesis due to a common cilia pathway. Defects in INPP5E have been shown to lead to a variety of ciliopathy related features such as polydactyly, retinitis pigmentosa, cerebellar changes and renal cysts (Jacoby et al, 2009; Luo et al, 2012). INPP5E is widely expressed in the cytosol and accumulates at the perinuclear/TGN via its N-terminal proline rich domain (Kong et al, 2000) while in non-proliferating cells, it has been localized to the primary cilium possibly via an N-terminal CAAX motif (Jacoby et al, 2009). INPP5E is shown to specifically inactivate PI(4,5)P2, (PIP2) and at higher rates PI(3,4,5)P3 (PIP3) by hydrolysis, showing no activity towards soluble inositol phosphates compared with other phospoinositide 5 -phosphatase family members (Kisseleva et al, 2000; Kong et al, 2000). These two types of membrane phospholipids play a crucial role in a variety of key cellular processes including primary and second messenger signalling, membrane trafficking and regulation of proteins involved in phospholipid metabolism. Growth factor stimulation directly activates the PI3K/AKT/mTOR pathway via PIP3 synthesis generated by phosphorylation of PIP2 (Lieberthal and Levine 2009). PI3K/AKT/mTOR pathway starts at the plasma membrane via external growth factor stimulation. Usually, the binding of the growth factor causes phosphorylation of the intracellular region of the receptor which will now be able to bind PI3K. Subsequently PI3K shifts to the PIP2 protein on the membrane which is phosphorylated to generate the second messenger PIP3. PIP3 will then activate Akt which will result in downstream effects Rheb and mTor activation, leading to translation and cell

growth or apoptosis. Both PIP2 and PIP3 are most likely connected to pathways that inhibit PI3K activation (Lieberthal and Levine 2009) and so responses to growth factor stimulation. It is suggested that INPP5E inactivation of PIP cause inhibition of Akt phosphorylation by platelet-derived growth factor (PDGF) and insulin-like growth factor-1 (IGF-1) stimulation resulting in the sensitization of cells to Fas induced apoptosis (Kisseleva et al, 2002).

Previous studies have shown an involvement of the INPP5E protein in primary cilium regulation, but this study shows for the first time a potential link to polycystin-1 through the intracellular PLAT domain. A cilia localisation for INPP5E was confirmed but showed that it does not change in the absence of polycystin-1. *INPP5E* knockdown however resulted in shorter cilia in both normal and ADPKD cells. In the original study by Jacoby et al, INPP5E inactivation did not prevent the formation of normal primary cilia, but rather affected the rate of cilium disassembly after serum reintroduction. Ciliary stability was restored by either PI3K or PDGF-R alpha blockade suggesting a clear involvement of INPP5E as a controller of the PDGF/PDGF-R/ PI3K kinase signalling pathway, primary cilium stability and cell proliferation (Jacoby et al, 2009). However, a recent study challenges these results, showing that INPP5E was also associated with shortened and decreased cilia formation in zebrafish (Luo et al, 2012).

5.4.2 NPHP2, 3 and 9 form a complex with polycystin-2

In this study, it was shown that NPHP3 and NPHP9 are able to interact with each other and that both interact with polycystin-2 to different degrees. NPHP3 appeared to bind more strongly to polycystin-2 than NPHP9 suggesting a possible direct interaction. To my knowledge, an interaction between INVS and polycystin-2 was also shown for the first time. Other groups have shown that INVS has a controlling role over many nephrocystins (Fukui et al, 2012) and may act as a molecular anchor for the NPHP3/ NPHP9 complex and possibly others at the cilium base (Dai Shiba et al, 2010). Together, the nephrocystins are thought to act as gatekeepers for different ciliary proteins (Omran et al, 2010). Results from this suggest that the function/or trafficking of polycystin-2 in or out of the cilium could be influenced by the integrity of this complex.

Although some studies had suggested that the *nphp9* mouse mutant (*Nek8* Null) had a more similar phenotype to polycystin-2 than Inversin Null phenotypes, it was also shown that Nek8 reduction did not correlate to a failed expression or localization and Ca^{2+} channel function of polycystin-2 in tissues and cells (Manning et al, 2013). Thus NPHP9 might be involved indirectly in regulating polycystin-2 function through other proteins such as the transcriptional regulator TAZ which binds to NPHP9 and has shown to promote the stability of the polycystin-2 protein via direct binding to its C-terminal domain (Habbig et al, 2012; Tian et al, 2007).

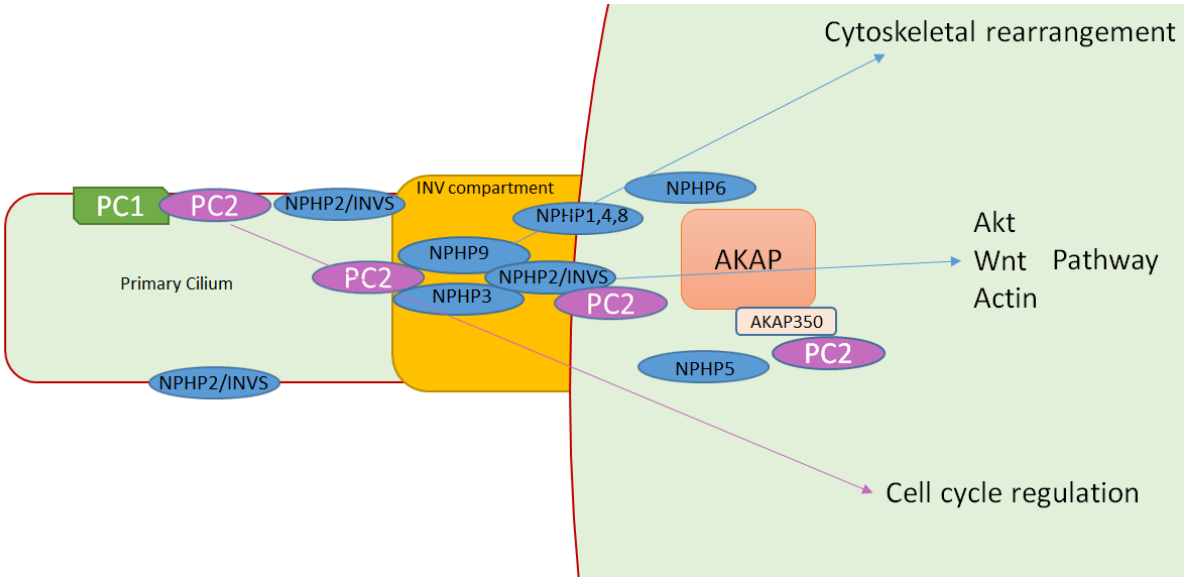

Figure 5.11 Polycystin-2/NPHP complex. Schematic representation of the theorized arrangement of the polycystin-2/NPHP complex at the base of the cilium. Polycystin-2 in the primary cilium is involved in different functions including cell cycle regulation and homeostasis. The trafficking in and out of the cilium is regulated at the INVS compartment at the base of the cilium, where the INVS protein forms anchors different cystoproteins such as NPHPs and polycystin-2, regulating its function.

5.4.3 INVS siRNA influences polycystin-2 localization

Treatment of normal cells with INVS siRNA resulted in a reduction in ciliary polycystin-2 localization, suggesting that INVS could be regulating its cilia localization, one of the hypotheses of this study. Further studies will have to be performed in additional cell lines to confirm this finding. There was also a trend towards ciliary length reduction in reduced INVS samples, which did not however reach statistical significance except in one line. Variability in the efficiency of knockdown could have led to the biological variability. Of interest, a previous report showed that Inversin was able to modulate the cortical actin network during mitosis (Werner et al, 2013). In this study, Inversin was required for proper spindle positioning and resulted in an increase of multinucleated cells; notably, Inversin knockdown also resulted in extensive filopodia (actin-based) formation in human HeLa or HEK-293 cells (Werner et al, 2013). An effect on the cortical actin network could imply a role for INVS in stabilizing the actin network at the ciliary base although this needs to be formally tested.

Summary

- INPP5E was able to bind to the polycystin-1 PLAT domain.
- INPP5E was localized to the primary cilium in both normal and ADPKD cells.
- Knockdown of *INPP5E* reduced ciliary length.
- Polycystin-2 interacts with NPHP3, NPHP9 and NPHP2/INV.
- NPHP2/INVS knockdown reduced polycystin-2 cilia localization without a consistent effect on cilia length.

Chapter VI

Conclusion

The pathogenesis of ADPKD is associated with germ line mutations in *PKD1* or *PKD2*. However, the molecular basis that leads to cyst formation remains elusive. The localisation of polycystin-1 and polycystin-2 to primary cilia and their putative role as a flow-activated mechanosensory receptor-cilia channel complex has been the dominant hypothesis over the past decade, although recent results have cast doubt on this idea. In this study, the potential role of the polycystins in regulating the dynamics of primary cilia assembly were examined. Two consistent characteristics were identified in ADPKD cells when compared to normal cells. First, defects in primary cilia formation with a lower number of ciliated cells and a shorter average primary cilium length and secondly, structural alterations in actin polymerisation and organization. Treatment with actin depolymerizing compounds was able to rescue cilia length, suggesting that the changes in actin prevent normal cilium development in ADPKD cells. Previous studies have shown that polycystin-1 may play a key role in actin remodelling, a conclusion confirmed by these results.

The incomplete or defective primary cilium formation in ADPKD models tested in this study was remarkable discovery. The development of functional primary cilia seems to be a conserved and essential feature of many cells and accordingly, partial or even complete loss of primary cilia development is shown to ultimately facilitate the growth of hyperplastic epithelia in various organs, including liver, kidney and pancreas as a result of failure to detect flow through the tubules of these organs (Moyer, et al 1994). This leads to a diverse spectrum of clinical phenotypes characterized by cystic dilatation of renal tubules as found in ADPKD (Zalli, et al 2012).

A fully formed functional primary cilium could be a needed requirement for both, proliferation control and maintenance of planar cell polarity, which are important in the regulation of tubular diameter in the nephron. Studies on a PKD mouse model support this, showing that wound healing following acute kidney injury modulated cilia length and modulated cell cycle processes. Conversely, the removal of normal cilium surveillance mechanisms promoted the uncontrolled proliferation of cells and ultimately increased the overall cystogenic potential and expansion of cysts (Happe, et al 2009; Patel, et al 2009; Verghese, et al 2008 & 2009). The primary cilium in kidney epithelial cells might be required to balance and hold proliferative and anti-proliferative signals in a stable state which ensures

enduring tissue homeostasis, while alterations of this balance would gradually shift this homeostasis in an inability to inhibit growth.

The original cilia hypothesis suggested that the ciliary polycystin-1/2 complex acted to regulate flow-activated Ca^{2+} entry upon primary cilium bending in the apical lumen of renal epithelial cells (Nauli et al, 2003). However, this model has recently been challenged by evidence that cilia bending did not elicit a rapid Ca^{2+} response (Delling et al, 2016). These new insights indicate that the function of the cilia polycystin-1/2 complex remains unresolved. It is possible that the polycystins might have other mechanosensitive polycystin-2 independent roles in cilia or even mechanosensory roles in other cell substructures, including cell junctions with relevant roles in cytoskeletal organization (Bhoonderowa et al, 2016). Our study showed that deficiency in polycystin-1 affected the organization of actin structures and the primary cilium orientation capability during migration, supporting a primary role in directing cytoskeletal organization and cellular morphology and resulting functions such as directional migration, orientated cell division and proper cilia formation.

This study supports that the two major elements of the cytoskeleton, actin and tubulin are able to influence primary cilium formation. Normal actin and microtubule organization ability could represent the basic matrix upon which a smooth dynamic regulation of primary cilium and its signals is possible.

Disorganization or stabilization of one of these two processes is then likely to result in a defected or impaired extension or maintenance of the primary cilium as supported by studies which suggested that the elongation of cilia caused by actin depolymerisation excreted its effect on vesicular structures around a vesicle docking site named PCC which functions as a temporary reservoir for ciliary membrane and associated proteins, and that destabilization of this site resulted in an increased membrane transport into the cilium (Kim et al, 2004 2010).

So far not only cystoproteins have been found to interact with several cytoskeletal components (Chen, et al 2008) but also many promising candidates for the mediation of structural interactions between microtubules and actin filament have been identified in mammalian cells (Mandato et al 2003). Although further investigation is needed to elucidate all the mechanisms and effectors of these interactions, it is reasonable to assume that any of the cystoproteins involved in ADPKD or its effectors might directly or directly be involved in tubulin/actin interaction, thus worth a detailed investigation in future work.

A large genomic screen strongly supports a coupling between the actin cytoskeleton and cilia elongation (Kim, et al 2010) thus underlining the importance of the significant effect in

ADPKD cells of actin depolymerizing agents. It is possible that increased actin polymerization or simple disorganization in ADPKD cells could affect normal primary cilia development, with nodes and lumps of entangled actin filaments preventing normal organization of the cytoskeletal matrix. Drastic treatments with acting depolymerizing agents, which aim to release these entangled structures and restore normal cytostructural mechanism, could be responsible for restoring maximum primary cilia elongation to levels seen in the normal cells. Actin structural analysis performed in this study showed that the primary cilia itself are actin free organelle, suggests that the actin modulatory effects on primary cilium length modulation are indirectly governed from within the cell, probably in structures near the primary cilia like the basal bodies. The growing number of reports underlining the influence of filamentous versus soluble actin in ciliogenesis plus the ability of the actin cytoskeleton as some studies suggest to directly regulate and promote the correct docking of the basal bodies at the base of the cilium, enabling in the first place the normal trafficking of ciliary vesicles, offers a valuable target for a more precise cellular localization of possible defective actin organization in ADPKD cells (Bershteyn , et al 2010; Hernandez, et al 2013; Kim, et al 2010, 2015; Rao, et al 2014; Yan, et al 2013). In our study, high resolution analysis of actin structures near the basal body area, revealed an increase or accumulation of what appeared as partially unpolymerized actin residues or structured in ADPKD cells compared to normal cells. One hypothesis could be that this debris at the basal body area of ADPKD cells could represent leftovers of partially unpolymerized actin structures, which in turn could sterically hinder normal ciliation processes or pathways involved in this regulation. This hypothesis would also assume that polycystin-1 is required to organize and prevent the uncompleted depolymerisation of these structures. In support of this, it was shown that overexpression of polycystin-1 in MDCK cells induced actin reorganization and cell scattering which was directly proportional to an increase in migratory ability and decrease in cell-cell adhesion (Boca et al, 2007). I have shown that in polycystin-1 deficient cells, there is increased disorganisation and polymerisation of actin leading to shortened cilia and impaired cilia reorientation in response to wound healing. A primary role for polycystin-1 in regulating the actin cytoskeleton, either in the cortical apical membrane or at the cilia base seems highly likely.

Previous studies have shown localization of polycystin-1 to tight junctions and adherens junctions. In renal tissue, it had been shown that polycystin-1 interacted with intermediate

filaments, assembling in a complex containing α -, β - γ –catenins and E-cadherin (Huan and Adelsberg 1999). Interestingly, the latter has been shown to be abnormally secluded in intracellular pools in ADPKD models (Charron et al, 2000). Furthermore, polycystin-1 is found in a complex with α2β1 integrin, tropomyosin, troponin 1, vinculin, α-actinin and other cytoskeletal proteins, reinforcing a cytoskeletal organizing role of polycystin-1 (Wilson 2001). Polycystin-1 may also sense mechanosensory stimuli between cells via its extracellular domains through homophilic interactions (Streets et al, 2009) and transduce these signals through its cytoskeletal connections such as actin and intermediate filaments to regulate cellular shape, adhesion, movement and cytoskeletal organization.

Similarly, some studies have shown that polycystin-2 localizes at intercellular contacts, together with polycystin-1 (Newby et al, 2002; Scheffers et al, 2002; Bhoonderowa 2016). Specifically, a link between α –actinin, which binds F-actin, and polycystin-2 has been shown with data suggesting that α –actinin regulates polycystin-2 channel function (Li et al, 2005). Recent studies even suggested that the primary role of polycystin-2 in mechanotransduction was in cytoskeleton recruitment independent of its channel function (Bhoonderowa et al, 2016). Interestingly in mitotic spindles of dividing cells, polycystin-2 was shown to interact with mDia1, a Rho GTPase effector protein, which accelerates actin nucleation and elongation by interacting with its barbed ends (Rundle et al, 2004). The binding of several actin-binding proteins to polycystin-2 could imply potential reciprocal functional regulation between F-actin and polycystin-2. To support this is data suggesting a link between polycystin-2 and the actin cytoskeleton, with polycystin-2 directly interacting with Hax-1 (Gallagher et al, 2000).

This study found that the inhibition of different actin effectors i.e. Rho GTPases were able to restore primary cilium length to different degrees. Thus polycystin-1 could specifically regulate the activation of Rho GTPases including RhoA, Rac1 and Cdc42, which are important factors enabling the cell to dynamically organize the actin and microtubule cytoskeleton. Changes in the cytoskeletal organization in disease also negatively influenced primary cilium reorientation towards the leading edge during migration following wound healing. These results suggest that polycystin-1 is an important regulator of cytoskeletal organization and that deficiency in this protein affect other mechanisms requiring dynamic and flexible changes in cell morphology including migration, division or primary cilium formation. Potential future treatments for the restoration of primary cilia and/or normalization

of cytoskeletal organization through targeting of specific pathways involved in these processes such as ROCK could be tested.

Finally, data showing that the nephrocystins (NPHP 2, 3, 9) can interact with polycystin-2 and may regulate its cilia localisation supports a functional interaction between two different cystic kidney diseases, nephronopthisis (NPHP) and ADPKD. This finding suggests that polycystin-2 may be the common link in both diseases and therefore further studies of its role in cilia is indicated.

In **Figure 6,** the main findings from this study are summarised. Is is shown that the formation and organisation of the primary cilium is complex. Trafficking of different ciliary proteins including GPCRs and RTK receptors and calcium channels such as polycystin-2 is regulated at the ciliary base at the transition zone, where key proteins such as INVS exert a gatekeeping role. The mother centriole which develops into the basal body as well as the MTOC plays a key role in cilia formation and could be influenced by different signalling pathways such as Ca^{2+} and cAMP/PKA; PKA also has an effect on intraflagellar transport (IFT). The core of the cilium comprises microtubules and their polymerisation and stabilisation is an important determinant of cilia assembly and disassembly. Finally, the organisation of actin in the cortical membrane and at the cilia base seem to be key in maintaining normal cilia length. Changes in actin and microtubule polymerisation appear to be processes dependent on normal polycystin-1 and polycystin-2 function.

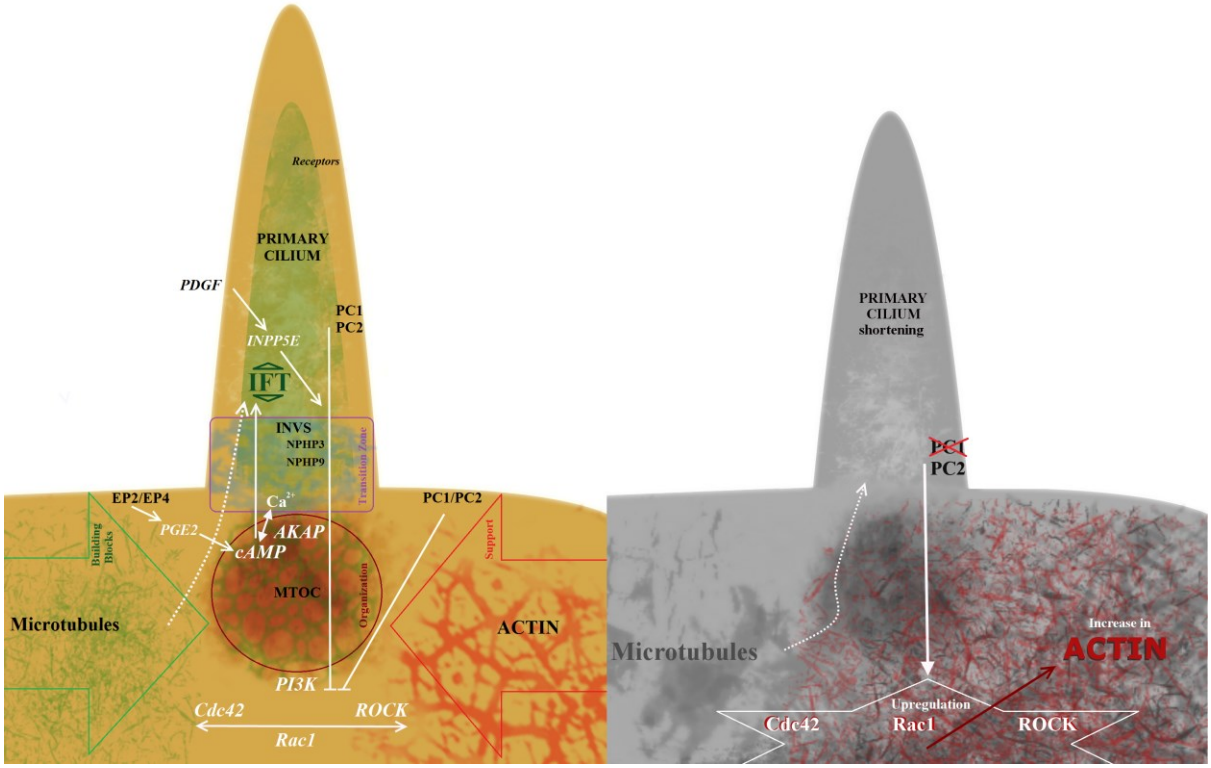

Figure 6. **Role of cystoproteins in primary cilia/cytoskeletal regulation**.

Left: The regulation of primary cilia is dependent on different specialized sections, each of which when disturbed affect normal ciliogenesis. The polycystin-1/2 complex and other cystoproteins are able to modulate cytoskeletal organization and different RhoGTPases. This in turn creates permissible conditions for normal primary cilium development and cellular functions. Right: In ADPKD, polycystin-1 deficiency results in an increase in RhoGTPase signalling, actin disorganization and a resulting impairment of normal ciliogenesis mechanisms.

Implications and Further Research

ADPKD has long been categorized as a class of incurable diseases, which from the categorization itself is a high burden for patients newly diagnosed with this disease.

In every disease, hope and a mind-set oriented towards a positive outcome plays important psychological role in the disease development of the afflicted patient. Providing a therapeutic approach in ADPKD, which is not only aimed at managing the symptomatic journey towards kidney replacement and instead influences or greatly reduces disease progression, is a critically important step in the fight against this disease. Recently a promising potential treatment based on the vasopressin-2 receptor antagonist Tovalptan has emerged. Clinical trials showed some success of this drug at slowing down ADPKD progression (Torres, et al 2012). Tovalptan or OTSUKA'S JINARC® has been approved by the European Commission for treatment of ADPKD patients in February 2015 and can be prescribed to patients with advanced chronic kidney disease (stages 4-5). Another potential treatment is a synthetic somatostatin analogue named octreotide, which in recent clinical trials has shown an encouraging effect on decreasing kidney volume in ADPKD patients, however these results are limited by a short one year follow up and need more validation in the long term (Caroli, et al 2013). In this study we have identified an underlying defect in normal ciliogenesis in ADPKD cell models and tissue samples, suggesting that the regulation of normal primary cilia structure and potentially its normal function is disrupted during ADPKD pathogenesis. Primary cilia are key regulators of many important signalling pathways, thus abnormal regulation and formation is likely to result in disease development such as cyst formation, which is associated with most ciliopathies. Future therapeutic treatments aimed at rescuing normal ciliogenesis e.g. ROCK inhibitors, hence allowing the normal transduction of ciliogenic signals, or treatments replacing the underlining intact signalling pathways will be promising novel approaches, with the potential to add to or improve the current limited number of ADPKD therapeutic treatments.

Critical future work deriving from my work, will be to test the hypothesis that an abnormal increase of RhoGTPase levels in ADPKD models is the main cause for the primary cilium

and cytoskeletal defects described in this thesis. Detailed localisation and activation studies of Rho kinases in the cell, i.e. at the cilia are warranted. This idea is supported by findings in another ciliopathy, in which RhoA-GTPs were found to modulate ciliary length through regulation of actin polymerization in Bardet–Biedl syndrome. In addition RhoA-GTP levels were found to be highly upregulated in the absence of Bbs protein (Hernandez et al, 2013).

Deriving from this, RhoGTPase inhibitors could be tested to rescue the primary cilia formation, length and orientation defects additional ADPKD model cell lines as well as other ciliopathies before moving into *in-vivo* models such as zebrafish.

Bibliography

af Forselles, K.J., Root, J., Clarke, T., Davey, D., Aughton, K., Dack, K. & Pullen, N., 2011. In vitro and in vivo characterization of PF-04418948, a novel, potent and selective prostaglandin EP_2 receptor antagonist. *British journal of pharmacology*, 164(7), pp.1847–56.

Akhshi, T.K., Wernike, D. & Piekny, A., 2014. Microtubules and actin crosstalk in cell migration and division. *Cytoskeleton*, 71(1), pp.1–23.

Akiyama, H. & Kamiguchi, H., 2010. Phosphatidylinositol 3-kinase facilitates microtubule-dependent membrane transport for neuronal growth cone guidance. *Journal of Biological Chemistry*, 285(53), pp.41740–41748.

Albert, D.A., Nodzenski, E., Cruz, G.H., Kuchibholtla, J. & Kowalski, J., 1991. Deoxyadenosine- and cyclic AMP-induced cell cycle arrest and cytotoxicity. *Experimental Cell Research*, 197(1), pp.75–81.

Albrecht-Buehler, G., 1977. Phagokinetic tracks of 3T3 cells: Parallels between the orientation of track segments and of cellular structures which contain actin or tubulin. *Cell*, 12(2), pp.333–339.

Alieva, I.B., Gorgidze, L. a, Komarova, Y. a, Chernobelskaya, O. a & Vorobjev, I. a, 1999. Experimental model for studying the primary cilia in tissue culture cells. *Membrane & cell biology*, 12(6), pp.895–905.

Amin, N. & Vincan, E., 2012. The Wnt signaling pathways and cell adhesion. *Frontiers in bioscience : a journal and virtual library*, 17, pp.784–804.

Amos, L.A. & Schlieper, D., 2005. Microtubules and maps. *Advances in Protein Chemistry*, 71, pp.257–298.

Anyatonwu, G.I., Estrada, M., Tian, X., Somlo, S. & Ehrlich, B.E., 2007. Regulation of ryanodine receptor-dependent calcium signaling by polycystin-2. *Proceedings of the National Academy of Sciences of the United States of America*, 104(15), pp.6454–9.

Archer, F.L. & Wheatley, D.N., 1971. Cilia in cell-cultured fibroblasts. II. Incidence in mitotic and post-mitotic BHK 21-C13 fibroblasts. *Journal of anatomy*, 109(Pt 2), pp.277–292.

Arnould, T., 1998. The Polycystic Kidney Disease 1 Gene Product Mediates Protein Kinase C alpha -dependent and c-Jun N-terminal Kinase-dependent Activation of the Transcription Factor AP-1. *Journal of Biological Chemistry*, 273(11), pp.6013–6018.

Arnould, T., Kim, E., Tsiokas, L., Jochimsen, F., Grüning, W., Chang, J.D. & Walz, G., 1998. The polycystic kidney disease 1 gene product mediates protein kinase C alpha-dependent and c-Jun N-terminal kinase-dependent activation of the transcription factor AP-1. *The Journal of biological chemistry*, 273(11), pp.6013–8.

Badano, J.L., Mitsuma, N., Beales, P.L. & Katsanis, N., 2006. The ciliopathies: an emerging class of human genetic disorders. *Annual review of genomics and human genetics*, 7(May), pp.125–148.

Bai,CX,. Kim,S., Li, W,. Streets, AJ,. Ong, ACM,. Tsiokas, L,. 2008 Activation of TRPP2 through mDia1-dependent voltage gating. EMBO J. 2008 May 7; 27(9): 1345–1356.

Barter, M.J., Pybus, L., Litherland, G.J., Rowan, A.D., Clark, I.M., Edwards, D.R., Cawston, T.E. & Young, D.A., 2010. HDAC-mediated control of ERK- and PI3K-dependent TGF-??-induced extracellular matrix-regulating genes. *Matrix Biology*, 29(7), pp.602–612.

Basten, S.G. & Giles, R.H., 2013. Functional aspects of primary cilia in signaling, cell cycle and tumorigenesis. *Cilia*, 2(1), p.6.

Bateman, A., and Sandford, R. (1999). The PLAT domain: a new piece in the PKD1 puzzle. *Curr. Biol*. 9, R588-R590.

Battini, L., Macip, S., Fedorova, E., Dikman, S., Somlo, S., Montagna, C. & Gusella, G.L., 2008. Loss of polycystin-1 causes centrosome amplification and genomic instability. *Human Molecular Genetics*, 17(18), pp.2819–2833.

Berbari, N.F., O'Connor, A.K., Haycraft, C.J. & Yoder, B.K., 2009. The Primary Cilium as a Complex Signaling Center. *Current Biology*, 19(13).

Bershteyn, M., Atwood, S.X., Woo, W.M., Li, M. & Oro, A.E., 2010. MIM and cortactin antagonism regulates ciliogenesis and hedgehog signaling. *Developmental Cell*, 19(2), pp.270–283.

Bertuccio, C. a & Caplan, M.J., 2013. Polycystin-1C terminus cleavage and its relation with polycystin-2, two proteins involved in polycystic kidney disease. *Medicina*, 73(2), pp.155–62.

Besschetnova, T.Y., Kolpakova-Hart, E., Guan, Y., Zhou, J., Olsen, B.R. & Shah, J. V., 2010. Identification of Signaling Pathways Regulating Primary Cilium Length and Flow-Mediated Adaptation. *Current Biology*, 20(2), pp.182–187.

Bhattacharyya, S., Rainey, M.A., Arya, P., Dutta, S., George, M., Storck, M.D., McComb, R.D., Muirhead, D., Todd, G.L., Gould, K., Datta, K., Waes, J.G., Band, V. & Band, H., 2016. Endocytic recycling protein EHD1 regulates primary cilia morphogenesis and SHH signaling during neural tube development. *Scientific reports*, 6, p.20727.

Bhoonderowa, L,. Hameurlaine, F,. Arbabian, A,. Faqir, F,. Amblard, F,. Coscoy, S. 2016. Polycystins and intercellular mechanotransduction: A precise dosage of polycystin 2 is necessary for alpha-actinin reinforcement of junctions upon mechanical

stimulation. Exp Cell Res 15;348(1):23-35.

Bhunia, A.K., Piontek, K., Boletta, A., Liu, L., Qian, F., Xu, P.N., Germino, F.J. & Germino, G.G., 2002. PKD1 induces p21waf1 and regulation of the cell cycle via direct activation of the JAK-STAT signaling pathway in a process requiring PKD2. *Cell*, 109(2), pp.157–168.

Bielas, S.L., Silhavy, J.L., Brancati, F., Kisseleva, M. V, Al-Gazali, L., Sztriha, L., Bayoumi, R.A., Zaki, M.S., Abdel-Aleem, A., Rosti, R.O., Kayserili, H., Swistun, D., Scott, L.C., Bertini, E., Boltshauser, E., Fazzi, E., Travaglini, L., Field, S.J., Gayral, S., Jacoby, M., Schurmans, S., Dallapiccola, B., Majerus, P.W., Valente, E.M. & Gleeson, J.G., 2009. Mutations in INPP5E, encoding inositol polyphosphate-5-phosphatase E, link phosphatidyl inositol signaling to the ciliopathies. *Nature genetics*, 41(9), pp.1032–6.

Bisceglia, M., Galliani, C.A., Senger, C., Stallone, C. & Sessa, A., 2006. Renal cystic diseases: a review. *Advances in anatomic pathology*, 13(1), pp.26–56.

Bisel, B., Calamai, M., Vanzi, F. & Pavone, F.S., 2013. Decoupling polarization of the Golgi apparatus and GM1 in the plasma membrane. *PLoS ONE*, 8(12).

Bisel, B., Wang, Y., Wei, J.H., Xiang, Y., Tang, D., Miron-Mendoza, M., Yoshimura, S.I., Nakamura, N. & Seemann, J., 2008. ERK regulates Golgi and centrosome orientation towards the leading edge through GRASP65. *Journal of Cell Biology*, 182(5), pp.837–843.

Blitzer, A.L., Panagis, L., Gusella, G.L., Danias, J., Mlodzik, M. & Iomini, C., 2011. Primary cilia dynamics instruct tissue patterning and repair of corneal endothelium. *Proceedings of the National Academy of Sciences of the United States of America*, 108(7), pp.2819–24.

Boca, M., D'Amato, L., Distefano, G., Polishchuk, R.S., Germino, G.G. & Boletta, A., 2007. Polycystin-1 induces cell migration by regulating phosphatidylinositol 3-kinase-dependent cytoskeletal rearrangements and GSK3beta-dependent cell cell mechanical adhesion. *Molecular biology of the cell*, 18(10), pp.4050–61.

Bodle, J.C., Rubenstein, C.D., Phillips, M.E., Bernacki, S.H., Qi, J., Banes, A.J. & Loboa, E.G., 2013. Primary Cilia: The Chemical Antenna Regulating Human Adipose-Derived Stem Cell Osteogenesis. *PLoS ONE*, 8(5).

Boehlke, C., Kotsis, F., Patel, V., Braeg, S., Voelker, H., Bredt, S., Beyer, T., Janusch, H., Hamann, C., Gödel, M., Müller, K., Herbst, M., Hornung, M., Doerken, M., Köttgen, M., Nitschke, R., Igarashi, P., Walz, G. & Kuehn, E.W., 2010. Primary cilia regulate mTORC1 activity and cell size through Lkb1. *Nature cell biology*, 12(11), pp.1115–1122.

Braun, W.E., 2009. Autosomal dominant polycystic kidney disease: Emerging concepts of pathogenesis and new treatments. *Cleveland Clinic Journal of Medicine*, 76(2), pp.97–104.

Bruce, C.R., Risis, S., Babb, J.R., Yang, C., Kowalski, G.M., Selathurai, A., Lee-Young, R.S., Weir, J.M., Yoshioka, K., Takuwa, Y., Meikle, P.J., Pitson, S.M. & Febbraio, M.A., 2012. Overexpression of sphingosine kinase 1 prevents ceramide accumulation and ameliorates muscle insulin resistance in high-fat diet-fed mice. *Diabetes*, 61(12), pp.3148–3155.

Burtey, S., Riera, M., Ribe, ??milie, Pennenkamp, P., Rance, R., Luciani, J., Dworniczak, B., Mattei, M.G. & Font??s, M., 2008. Centrosome overduplication and mitotic instability in PKD2 transgenic lines. *Cell Biology International*, 32(10), pp.1193–1198.

Busson, S., Dujardin, D., Moreau, A., Dompierre, J. & Mey, J.R.D., 1998. Dynein and dynactin are localized to astral microtubules and at cortical sites in mitotic epithelial cells. *Current Biology*, 8(9), pp.541–544.

Cao, M., Li, G. & Pan, J., 2009. Regulation of cilia assembly, disassembly, and length by protein phosphorylation. *Methods in cell biology*, 94, pp.333–346.

Caretta, A. & Mucignat-Caretta, C., 2011. Protein kinase a in cancer. *Cancers*, 3(1), pp.913–926.

Carnegie, G.K., Means, C.K. & Scott, J.D., 2009. A-kinase anchoring proteins: From protein complexes to physiology and disease. *IUBMB Life*, 61(4), pp.394–406.

Caroli, A., Perico, N., Perna, A., Antiga, L., Brambilla, P., Pisani, A., Visciano, B., Imbriaco, M., Messa, P., Cerutti, R., Dugo, M., Cancian, L., Buongiorno, E., De Pascalis, A., Gaspari, F., Carrara, F., Rubis, N., Prandini, S., Remuzzi, A., Remuzzi, G. & Ruggenenti, P., 2013. Effect of longacting somatostatin analogue on kidney and cyst growth in autosomal dominant polycystic kidney disease (ALADIN): A randomised, placebo-controlled, multicentre trial. *The Lancet*, 382(9903), pp.1485–1495.

Castelli, M., De Pascalis, C., Distefano, G., Ducano, N., Oldani, A., Lanzetti, L. & Boletta, A., 2015. Regulation of the microtubular cytoskeleton by Polycystin-1 favors focal adhesions turnover to modulate cell adhesion and migration. *BMC cell biology*, 16, p.15.

Cattoretti, G., Becker, M.H.G., Key, G., Duchrow, M., Schluter, C., Galle, J. & Gerdes, J., 1992. Monoclonal antibodies against recombinant parts of the Ki-67 antigen (MIB 1 and MIB 3) detect proliferating cells in microwave-processed formalin-fixed paraffin sections. *Journal of Pathology*, 168(4), pp.357–363.

Chaki, M., Airik, R., Ghosh, A.K., Giles, R.H., Chen, R., Hildebrandt, F., et al., 2012. Exome capture reveals ZNF423 and CEP164 mutations, linking renal ciliopathies to DNA damage response signaling. *Cell*, 150(3), pp.533–548.

Charron, AJ,. Nakamura, S,. Bacallao, R,. Wandinger-Ness, A.. 2000 Compromised cytoarchitecture and polarized trafficking in autosomal dominant polycystic kidney disease cells, J. Cell Biol. 149 (1) 111–124.

Chauvet, V., Tian, X., Husson, H., Grimm, D.H., Wang, T., Hieseberger, T., Igarashi, P., Bennett, A.M., Ibraghimov-Beskrovnaya, O., Somlo, S. & Caplan, M.J., 2004. Mechanical

stimuli induce cleavage and nuclear translocation of the polycystin-1 C terminus. *Journal of Clinical Investigation*, 114(10), pp.1433–1443.

Chen, T.C., Hinton, D.R., Zidovetzki, R. & Hofman, F.M., 1998. Up-regulation of the cAMP/PKA pathway inhibits proliferation, induces differentiation, and leads to apoptosis in malignant gliomas. *Lab Invest*, 78(2), pp.165–174.

Chen, X.Z., Li, Q., Wu, Y., Liang, G., Lara, C.J. & Cantiello, H.F., 2008. Submembraneous microtubule cytoskeleton: Interaction of TRPP2 with the cell cytoskeleton. *FEBS Journal*, 275(19), pp.4675–4683.

Chesarone, M. a, DuPage, A.G. & Goode, B.L., 2010. Unleashing formins to remodel the actin and microtubule cytoskeletons. *Nature reviews. Molecular cell biology*, 11(1), pp.62–74.

Choi, S.Y., Chacon-Heszele, M.F., Huang, L., McKenna, S., Wilson, F.P., Zuo, X. & Lipschutz, J.H., 2013. Cdc42 deficiency causes ciliary abnormalities and cystic kidneys. *Journal of the American Society of Nephrology : JASN*, 24(9), pp.1435–50.

Choi, Y.-H., Suzuki, A., Hajarnis, S., Ma, Z., Chapin, H.C., Caplan, M.J., Pontoglio, M., Somlo, S. & Igarashi, P., 2011. Polycystin-2 and phosphodiesterase 4C are components of a ciliary A-kinase anchoring protein complex that is disrupted in cystic kidney diseases. *Proceedings of the National Academy of Sciences of the United States of America*, 108(26), pp.10679–84.

Christensen, S.T., Clement, C.A., Satir, P. & Pedersen, L.B., 2012. Primary cilia and coordination of receptor tyrosine kinase (RTK) signalling. *Journal of Pathology*, 226(2), pp.172–184.

Christensen, S.T., Pedersen, S.F., Satir, P., Veland, I.R. & Schneider, L., 2008. The primary cilium coordinates signaling pathways in cell cycle control and migration during development and tissue repair. *Current topics in developmental biology*, 85(08), pp.261–301.

Christensen, S.T., Veland, I.R., Schwab, A., Cammer, M. & Satir, P., 2013. Analysis of primary cilia in directional cell migration in fibroblasts. *Methods in Enzymology*, 525, pp.45–58.

Cooper, D.M., Mons, N. & Karpen, J.W., 1995. Adenylyl cyclases and the interaction between calcium and cAMP signalling. *Nature*, 374(6521), pp.421–424.

Corbit, K.C., Shyer, A.E., Dowdle, W.E., Gaulden, J., Singla, V., Chen, M.-H., Chuang, P.-T. & Reiter, J.F., 2008. Kif3a constrains beta-catenin-dependent Wnt signalling through dual ciliary and non-ciliary mechanisms. *Nature cell biology*, 10(1), pp.70–76.

Cordeiro, J. V & Jacinto, A., 2013. The role of transcription-independent damage signals in the initiation of epithelial wound healing. *Nature reviews. Molecular cell biology*, 14(4), pp.249–62.

daCosta, C.J.B. & Baenziger, J.E., 2009. A lipid-dependent uncoupled conformation of the acetylcholine receptor. *Journal of Biological Chemistry*, 284(26), pp.17819–17825.

Dawe, H.R., Adams, M., Wheway, G., Szymanska, K., Logan, C. V, Noegel, A. a, Gull, K. &

Johnson, C. a, 2009. Nesprin-2 interacts with meckelin and mediates ciliogenesis via remodelling of the actin cytoskeleton. *Journal of cell science*, 122(Pt 15), pp.2716–2726.

De Brabander, MJ., Van de Veire, RM., Aerts, FE., Borgers, M., Janssen, P.A,. 1976. The effects of methyl (5-(2-thienylcarbonyl)-1H-benzimidazol-2-yl) carbamate (R 17934; NSC 238159), a new synthetic antitumoral drug interfering with microtubules, on mammalian cells cultured in vitro. Cancer Res. 36:905–916.

Dedkova, E.N., Sigova, A.A. & Zinchenko, V.P., 2000. Mechanism of action of calcium ionophores on intact cells: ionophore-resistant cells. *Membrane & cell biology*, 13(3), pp.357–68.

Dell'Acqua, M.L., Faux, M.C., Thorburn, J., Thorburn, A. & Scott, J.D., 1998. Membrane-targeting sequences on AKAP79 bind phosphatidylinositol-4,5-bisphosphate. *EMBO Journal*, 17(8), pp.2246–2260.

Delling, M., Indzhykulian, A.A., Liu, X., Xie, T., Clapham, D.E., Ca, T., Ca, C., Figs, E.D., Fig, E.D., Video, S. & Information, S., 2016. Primary cilia are not calcium-responsive mechanosensors. *Nature*, 531, pp.656–660.

Delmas, P., Nomura, H., Li, X., Lakkis, M., Luo, Y., Segal, Y., Fernandez-Fernandez, J.M., Harris, P., Frischauf, A.M., Brown, D.A. & Zhou, J., 2002. Constitutive activation of G-proteins by polycystin-1 is antagonized by polycystin-2. *Journal of Biological Chemistry*, 277(13), pp.11276–11283.

Dempsey, G.T., Vaughan, J.C., Chen, K.H., Bates, M. & Zhuang, X., 2011. Evaluation of fluorophores for optimal performance in localization-based super-resolution imaging. *Nature Methods*, 8(12), pp.1027–1036.

Deng, Q. & Huttenlocher, a., 2012. Leukocyte migration from a fish eye's view. *Journal of Cell Science*, 125, pp.3949–3956.

Denker, S.P. & Barber, D.L., 2002. Cell migration requires both ion translocation and cytoskeletal anchoring by the Na-H exchanger NHE1. *Journal of Cell Biology*, 159(6), pp.1087–1096.

Desai, A. & Mitchison, T.J., 1997. Microtubule polymerization dynamics. *Annual review of cell and developmental biology*, 13, pp.83–117.

Deshmukh, G.D., Radin, N.S., Gattone, V.H. & Shayman, J. a, 1994. Abnormalities of glycosphingolipid, sulfatide, and ceramide in the polycystic (cpk/cpk) mouse. *Journal of lipid research*, 35, pp.1611–1618.

El Din El Homasany, B.S., Volkov, Y., Takahashi, M., Ono, Y., Keryer, G., Delouvée, A., Looby, E., Long, A. & Kelleher, D., 2005. The scaffolding protein CG-NAP/AKAP450 is a critical integrating component of the LFA-1-induced signaling complex in migratory T cells. *Journal of immunology (Baltimore, Md. : 1950)*, 175(12), pp.7811–8.

Distefano, G., Boca, M., Rowe, I., Wodarczyk, C., Ma, L., Piontek, K.B., Germino, G.G., Pandolfi,

P.P. & Boletta, A., 2009. Polycystin-1 regulates extracellular signal-regulated kinase-dependent phosphorylation of tuberin to control cell size through mTOR and its downstream effectors S6K and 4EBP1. *Molecular and cellular biology*, 29(9), pp.2359–71.

Diviani, D., Langeberg, L.K., Doxsey, S.J. & Scott, J.D., 2000. Pericentrin anchors protein kinase A at the centrosome through a newly identified RII-binding domain. *Current Biology*, 10(7), pp.417–420.

Diviani, D., Soderling, J. & Scott, J.D., 2001. AKAP-Lbc Anchors Protein Kinase A and Nucleates G?? 12-selective Rho-mediated Stress Fiber Formation. *Journal of Biological Chemistry*, 276(47), pp.44247–44257.

Dodge, K.L., Khouangsathiene, S., Kapiloff, M.S., Mouton, R., Hill, E. V., Houslay, M.D., Langeberg, L.K. & Scott, J.D., 2001. mAKAP assembles a protein kinase A/PDE4 phosphodiesterase cAMP signaling module. *EMBO Journal*, 20(8), pp.1921–1930.

Dubois, T., Paléotti, O., Mironov, A. a, Fraisier, V., Stradal, T.E.B., De Matteis, M.A., Franco, M. & Chavrier, P., 2005. Golgi-localized GAP for Cdc42 functions downstream of ARF1 to control Arp2/3 complex and F-actin dynamics. *Nature cell biology*, 7(4), pp.353–364.

Dumont, J.E., Jauniaux, J.C. & Roger, P.P., 1989. The cyclic AMP-mediated stimulation of cell proliferation. *Trends in Biochemical Sciences*, 14(2), pp.67–71.

Dupont, S., Morsut, L., Aragona, M., Enzo, E., Giulitti, S., Cordenonsi, M., Zanconato, F., Le Digabel, J., Forcato, M., Bicciato, S., Elvassore, N. & Piccolo, S., 2011. Role of YAP/TAZ in mechanotransduction. *Nature*, 474(7350), pp.179–183.

Dutertre, S., Descamps, S. & Prigent, C., 2002. On the role of aurora-A in centrosome function. *Oncogene*, 21(40), pp.6175–6183.

Eddy, R.J., Pierini, L.M. & Maxfield, F.R., 2002. Microtubule asymmetry during neutrophil polarization and migration. *Molecular Biology of the Cell*, 13(12), pp.4470–83.

Elberg, G., Elberg, D., Lewis, T. V, Guruswamy, S., Chen, L., Logan, C.J., Chan, M.D. & Turman, M.A., 2007. EP2 receptor mediates PGE2-induced cystogenesis of human renal epithelial cells. *American journal of physiology. Renal physiology*, 293(5), pp.F1622–32.

Elie, A., Prezel, E., Guérin, C., Denarier, E., Ramirez-Rios, S., Serre, L., Andrieux, A., Fourest-Lieuvin, A., Blanchoin, L. & Arnal, I., 2015. Tau Co-Organizes Dynamic Microtubule and Actin Networks. *Scientific Reports*, 5, p.9964.

Etienne-Manneville, S., 2004. Actin and microtubules in cell motility: Which one is in control? *Traffic*, 5(7), pp.470–477.

Etienne-Manneville, S., 2012. Adherens junctions during cell migration. *Sub-cellular biochemistry*, 60, pp.225–49.

Etienne-Manneville, S., 2013. Microtubules in cell migration. *Annual review of cell and*

developmental biology, 29, pp.471–99.

Ezratty, E.J., Stokes, N., Chai, S., Shah, A.S., Williams, S.E. & Fuchs, E., 2011. A role for the primary cilium in notch signaling and epidermal differentiation during skin development. *Cell*, 145(7), pp.1129–1141.

Farrow, B., Rychahou, P., Murillo, C., O'Connor K, L., Iwamura, T. & Evers, B.M., 2003. Inhibition of pancreatic cancer cell growth and induction of apoptosis with novel therapies directed against protein kinase A. *Surgery*, 134(2), pp.197–205.

Fedeles, S. V., Gallagher, A.R. & Somlo, S., 2014. Polycystin-1: A master regulator of intersecting cystic pathways. *Trends in Molecular Medicine*, 20(5), pp.251–260.

Feil, S., Valtcheva, N. & Feil, R., 2009. Inducible cre mice. *Methods in Molecular Biology*, 530, pp.343–363.

Fliegauf, M., Benzing, T. & Omran, H., 2007. When cilia go bad: cilia defects and ciliopathies. *Nature reviews. Molecular cell biology*, 8(11), pp.880–93.

Fonte, V.G., Searls, R.L. & Hilfer, S.R. 1971 relationship of cilia with cell division and differentiation. *J Cell Biol.* 1971 49(1):226-9.

Forman, J.R., Qamar, S., Paci, E., Sandford, R.N. & Clarke, J., 2005. The remarkable mechanical strength of polycystin-1 supports a direct role in mechanotransduction. *Journal of Molecular Biology*, 349(4), pp.861–871.

Forselles KJ1, Root J, Clarke T, Davey D, Aughton K, Dack K, Pullen N. 2011 In vitro and in vivo characterization of PF-04418948, a novel, potent and selective prostaglandin EP_2 receptor antagonist. Br J Pharmacol. 2011 Dec;164(7):1847-56.

Forte, M., Satow, Y., Nelson, D. & Kung, C., 1981. Mutational alteration of membrane phospholipid composition and voltage-sensitive ion channel function in paramecium. *Proceedings of the National Academy of Sciences of the United States of America*, 78(11), pp.7195–7199.

Franco, I., Gulluni, F., Campa, C.C., Costa, C., Margaria, J., Ciraolo, E., Martini, M., Monteyne, D., De Luca, E., Germena, G., Posor, Y., Maffucci, T., Marengo, S., Haucke, V., Falasca, M., Perez-Morga, D., Boletta, A., Merlo, G.R. & Hirsch, E., 2014. PI3K class II ?? controls spatially restricted endosomal PtdIns3P and Rab11 activation to promote primary cilium function. *Developmental Cell*, 28(6), pp.647–658.

Franco, I., Margaria, J.P., De Santis, M.C., Ranghino, A., Monteyne, D., Chiaravalli, M., Pema, M., Campa, C.C., Ratto, E., Gulluni, F., Perez-Morga, D., Somlo, S., Merlo, G.R., Boletta, A. & Hirsch, E., 2015. Phosphoinositide 3-Kinase-C2 Regulates Polycystin-2 Ciliary Entry and Protects against Kidney Cyst Formation. *Journal of the American Society of Nephrology*, pp.1–10.

Frank, V., Habbig, S., Bartram, M.P., Eisenberger, T., Veenstra-Knol, H.E., Decker, C., Boorsma, R.A.C., G??bel, H., N??rnberg, G., Griessmann, A., Franke, M., Borgal, L., Kohli, P.,

V??lker, L.A., D??tsch, J., N??rnberg, P., Benzing, T., Bolz, H.J., Johnson, C., Gerkes, E.H., Schermer, B. & Bergmann, C., 2013. Mutations in NEK8 link multiple organ dysplasia with altered Hippo signalling and increased c-MYC expression. *Human Molecular Genetics*, 22(11), pp.2177–2185.

Fukui, H., Shiba, D., Asakawa, K., Kawakami, K. & Yokoyama, T., 2012. The ciliary protein Nek8/Nphp9 acts downstream of Inv/Nphp2 during pronephros morphogenesis and left-right establishment in zebrafish. *FEBS Letters*, 586(16), pp.2273–2279.

Fukumoto, S., Koyama, H., Hosoi, M., Yamakawa, K., Tanaka, S., Morii, H., Nishizawa, S., 1999. Distinct Role of cAMP and cGMP in the Cell Cycle Control of Vascular Smooth Muscle Cells cGMP Delays Cell Cycle Transition Through Suppression of Cyclin D1 and Cyclin-Dependent Kinase 4 Activation Circulation Research. 85: 985-991

Gallagher, a R., Cedzich, a, Gretz, N., Somlo, S. & Witzgall, R., 2000. The polycystic kidney disease protein PKD2 interacts with Hax-1, a protein associated with the actin cytoskeleton. *Proceedings of the National Academy of Sciences of the United States of America*, 97(8), pp.4017–4022.

Gallagher, A.R., Hoffmann, S., Brown, N., Cedzich, A., Meruvu, S., Podlich, D., Feng, Y., Könecke, V., de Vries, U., Hammes, H.-P., Gretz, N. & Witzgall, R., 2006. A truncated polycystin-2 protein causes polycystic kidney disease and retinal degeneration in transgenic rats. *Journal of the American Society of Nephrology : JASN*, 17(10), pp.2719–2730.

Gao, C. & Chen, Y.G., 2010. Dishevelled: The hub of Wnt signaling. *Cellular Signalling*, 22(5), pp.717–727.

Gao, Y., Dickerson, J.B., Guo, F., Zheng, J. & Zheng, Y., 2004. Rational design and characterization of a Rac GTPase-specific small molecule inhibitor. *Proceedings of the National Academy of Sciences of the United States of America*, 101(20), pp.7618–23.

Garcia-Gonzalo, F.R., Phua, S.C., Roberson, E.C., Garcia, G., Abedin, M., Schurmans, S., Inoue, T. & Reiter, J.F., 2015. Phosphoinositides Regulate Ciliary Protein Trafficking to Modulate Hedgehog Signaling. *Developmental Cell*, 34(4), pp.400–409.

Gattone, V.H., Wang, X., Harris, P.C. & Torres, V.E., 2003. Inhibition of renal cystic disease development and progression by a vasopressin V2 receptor antagonist. *Nature medicine*, 9(10), pp.1323–1326.

Gault, C.R., Obeid, L.M. & Hannun, Y.A., 2010. An overview of sphingolipid metabolism: From synthesis to breakdown. *Advances in Experimental Medicine and Biology*, 688, pp.1–23.

Gerdes, J.M., Liu, Y., Zaghloul, N. a, Leitch, C.C., Lawson, S.S., Kato, M., Beachy, P. a, Beales, P.L., DeMartino, G.N., Fisher, S., Badano, J.L. & Katsanis, N., 2007. Disruption of

the basal body compromises proteasomal function and perturbs intracellular Wnt response. *Nature genetics*, 39(11), pp.1350–1360.

Gillingham, A.K. & Munro, S., 2000. The PACT domain, a conserved centrosomal targeting motif in the coiled-coil proteins AKAP450 and pericentrin. *EMBO reports*, 1(6), pp.524–529.

Goetz, S.C. & Anderson, K. V, 2010. The primary cilium: a signalling centre during vertebrate development. *Nature reviews. Genetics*, 11(5), pp.331–44.

Goto, H., Inoko, A. & Inagaki, M., 2013. Cell cycle progression by the repression of primary cilia formation in proliferating cells. *Cellular and Molecular Life Sciences*, 70(20), pp.3893–3905.

Graser, S., Stierhof, Y.D., Lavoie, S.B., Gassner, O.S., Lamla, S., Le Clech, M. & Nigg, E.A., 2007. Cep164, a novel centriole appendage protein required for primary cilium formation. *Journal of Cell Biology*, 179(2), pp.321–330.

Grayson, C., Bartolini, F., Chapple, J.P., Willison, K.R., Bhamidipati, A., Lewis, S.A., Luthert, P.J., Hardcastle, A.J., Cowan, N.J. & Cheetham, M.E., 2002. Localization in the human retina of the X-linked retinitis pigmentosa protein RP2, its homologue cofactor C and the RP2 interacting protein Arl3. *Hum Mol Genet*, 11(24), pp.3065–3074.

Grimm, D.H., Cai, Y., Chauvet, V., Rajendran, V., Zeltner, R., Geng, L., Avner, E.D., Sweeney, W., Somlo, S. & Caplan, M.J., 2003. Polycystin-1 distribution is modulated by polycystin-2 expression in mammalian cells. *Journal of Biological Chemistry*, 278(38), pp.36786–36793.

Gundersen, G.G. & Bulinski, J.C., 1988. Selective stabilization of microtubules oriented toward the direction of cell migration. *Proceedings of the National Academy of Sciences of the United States of America*, 85(16), pp.5946–50.

Gundersen, G.G., Wen, Y., Eng, C.H., Schmoranzer, J., Cabrera-Poch, N., Morris, E.J.S., Chen, M. & Gomes, E.R., 2005. Regulation of microtubules by Rho GTPases in migrating cells. *Novartis Foundation symposium*, 269, pp.106–116; discussion 116–126, 223–230.

Habbig, S., Bartram, M.P., Sägmüller, J.G., Griessmann, A., Franke, M., Müller, R.U., Schwarz, R., Hoehne, M., Bergmann, C., Tessmer, C., Reinhardt, H.C., Burst, V., Benzing, T. & Schermer, B., 2012. The ciliopathy disease protein NPHP9 promotes nuclear delivery and activation of the oncogenic transcriptional regulator TAZ. *Human Molecular Genetics*, 21(26), pp.5528–5538.

Hammond, J.W., Huang, C.-F., Kaech, S., Jacobson, C., Banker, G. & Verhey, K.J., 2010. Posttranslational modifications of tubulin and the polarized transport of kinesin-1 in neurons. *Molecular biology of the cell*, 21(4), pp.572–583.

Hanaoka, K. & Guggino, W.B., 2000. cAMP regulates cell proliferation and cyst formation in autosomal polycystic kidney disease cells. *Journal of the American Society of Nephrology : JASN*, 11(7), pp.1179–1187.

Hanaoka, K., Qian, F., Boletta, a, Bhunia, a K., Piontek, K., Tsiokas, L., Sukhatme, V.P., Guggino, W.B. & Germino, G.G., 2000. Co-assembly of polycystin-1 and -2 produces unique cation-permeable currents. *Nature*, 408(6815), pp.990–994.

Hansen, C.G., Ng, Y.L.D., Lam, W.-L.M., Plouffe, S.W. & Guan, K.-L., 2015. The Hippo pathway effectors YAP and TAZ promote cell growth by modulating amino acid signaling to mTORC1. *Cell research*, 25(12), pp.1299–313.

Happé, H., Leonhard, W.N., van der Wal, A., van de Water, B., Lantinga-van Leeuwen, I.S., Breuning, M.H., de Heer, E. & Peters, D.J.M., 2009. Toxic tubular injury in kidneys from Pkd1-deletion mice accelerates cystogenesis accompanied by dysregulated planar cell polarity and canonical Wnt signaling pathways. *Human Molecular Genetics*, 18(14), pp.2532–2542.

Happé, H. & Peters, D.J.M., 2014. Translational research in ADPKD: lessons from animal models. *Nature reviews. Nephrology*, 10(10), pp.587–601.

Harris, P.C. & Torres, V.E., 2014. Genetic mechanisms and signaling pathways in autosomal dominant polycystic kidney disease. *The Journal of clinical investigation*, 124(6), pp.2315–24.

Haycraft, C.J., Swoboda, P., Taulman, P.D., Thomas, J.H. & Yoder, B.K., 2001. The C. elegans homolog of the murine cystic kidney disease gene Tg737 functions in a ciliogenic pathway and is disrupted in osm-5 mutant worms. *Development (Cambridge, England)*, 128, pp.1493–1505.

He, Q., Wang, G., Dasgupta, S., Dinkins, M., Zhu, G. & Bieberich, E., 2012. Characterization of an apical ceramide-enriched compartment regulating ciliogenesis. *Molecular Biology of the Cell*, 23(Cv), pp.3156–3166.

Heggo, O., 1966. A microdissection study of cystic disease of the kidneys in adults *J. Pathol. Bacteriol.*, 91 pp. 311–315.

Heidebrecht, H.J., Buck, F., Haas, K., Wacker, H.H. & Parwaresch, R., 1996. Monoclonal antibodies Ki-S3 and Ki-S5 yield new data on the “Ki-67” proteins. *Cell proliferation*, 29(7), pp.413–25.

Hernandez-Hernandez, V., Pravincumar, P., Diaz-Font, A., May-Simera, H., Jenkins, D., Knight, M. & Beales, P.L., 2013. Bardet-biedl syndrome proteins control the cilia length through regulation of actin polymerization. *Human Molecular Genetics*, 22(19), pp.3858–3868.

Higuchi, M., Masuyama, N., Fukui, Y., Suzuki, A. & Gotoh, Y., 2001. Akt mediates Rac/Cdc42-regulated cell motility in growth factor-stimulated cells and in invasive PTEN knockout cells. *Current Biology*, 11(24), pp.1958–1962.

Hildebrandt, F., Attanasio, M. & Otto, E., 2009. Nephronophthisis: disease mechanisms of a ciliopathy. *Journal of the American Society of Nephrology : JASN*, 20(1), pp.23–35.

Hino, S., Tanji, C., Nakayama, K.I. & Kikuchi, A., 2005. Phosphorylation of beta-catenin by cyclic AMP-dependent protein kinase stabilizes beta-catenin through inhibition of its ubiquitination. *Molecular and cellular biology*, 25(20), pp.9063–72.

Hoch, R. V & Soriano, P., 2003. Roles of PDGF in animal development. *Development (Cambridge, England)*, 130(20), pp.4769–4784.

Hoff, S., Halbritter, J., Epting, D., Frank, V., Nguyen, T.-M.T., van Reeuwijk, J., Boehlke, C., Schell, C., Yasunaga, T., Helmstädter, M., Mergen, M., Filhol, E., Boldt, K., Horn, N., Ueffing, M., Otto, E.A., Eisenberger, T., Elting, M.W., van Wijk, J.A.E., Bockenhauer, D., Sebire, N.J., Rittig, S., Vyberg, M., Ring, T., Pohl, M., Pape, L., Neuhaus, T.J., Elshakhs, N.A.S., Koon, S.J., Harris, P.C., Grahammer, F., Huber, T.B., Kuehn, E.W., Kramer-Zucker, A., Bolz, H.J., Roepman, R., Saunier, S., Walz, G., Hildebrandt, F., Bergmann, C. & Lienkamp, S.S., 2013. ANKS6 is a central component of a nephronophthisis module linking NEK8 to INVS and NPHP3. *Nature genetics*, 45(8), pp.951–6.

Hong, J.H., Youm, J.-K., Kwon, M.J., Park, B.D., Lee, Y.-M., Lee, S.-I., Shin, D.M. & Lee, S.H., 2008. K6PC-5, a direct activator of sphingosine kinase 1, promotes epidermal differentiation through intracellular Ca2+ signaling. *The Journal of investigative dermatology*, 128(9), pp.2166–78.

Hopp, K., Ward, C.J., Hommerding, C.J., Nasr, S.H., Tuan, H.-F., Gainullin, V.G., Rossetti, S., Torres, V.E. & Harris, P.C., 2012. Functional polycystin-1 dosage governs autosomal dominant polycystic kidney disease severity. *The Journal of clinical investigation*, 122(11), pp.4257–73.

Houslay, M.D. & Milligan, G., 1997. Tailoring cAMP-signalling responses through isoform multiplicity. *Trends in Biochemical Sciences*, 22(6), pp.217–224.

Howard, J. & Hyman, A.A., 2003. Dynamics and mechanics of the microtubule plus end. *Nature*, 422(6933), pp.753–758.

Hu, J. & Barr, M.M., 2005. ATP-2 interacts with the PLAT domain of LOV-1 and is involved in Caenorhabditis elegans polycystin signaling. *Molecular biology of the cell*, 16(2), pp.458–69.

Huan, Y. & van Adelsberg, J., 1999. Polycystin-1, the PKD1 gene product, is in a complex containing E-cadherin and the catenins. *The Journal of clinical investigation*, 104(10), pp.1459–68.

Huet, D., Blisnick, T., Perrot, S. & Bastin, P., 2014. The GTPase IFT27 is involved in both anterograde and retrograde intraflagellar transport. *eLife*, 2014(3).

Hundsrucker, C. & Klussmann, E., 2008. Direct AKAP-mediated protein-protein interactions as potential drug targets. *Handbook of Experimental Pharmacology*, 186, pp.483–503.

Huveneers, S. & Danen, E.H.J., 2009. Adhesion signaling - crosstalk between integrins, Src and Rho.

Journal of cell science, 122, pp.1059–1069.

Ibraghimov-Beskrovnaya, O., Bukanov, N.O., Donohue, L.C., Dackowski, W.R., Klinger, K.W. & Landes, G.M., 2000. Strong homophilic interactions of the Ig-like domains of polycystin-1, the protein product of an autosomal dominant polycystic kidney disease gene, PKD1. *Human molecular genetics*, 9(11), pp.1641–9.

Irigoín, F. & Badano, J.L., 2011. Keeping the balance between proliferation and differentiation: the primary cilium. *Current genomics*, 12(4), pp.285–97.

Ishikawa, H., Kubo, A., Tsukita, S. & Tsukita, S., 2005. Odf2-deficient mother centrioles lack distal/subdistal appendages and the ability to generate primary cilia. *Nature cell biology*, 7(5), pp.517–24.

Ishikawa, H., Thompson, J., Yates, J.R. & Marshall, W.F., 2012. Proteomic analysis of mammalian primary cilia. *Current biology : CB*, 22(5), pp.414–9.

Jacoby, M., Cox, J.J., Gayral, S., Hampshire, D.J., Ayub, M., Blockmans, M., Pernot, E., Kisseleva, M. V, Compère, P., Schiffmann, S.N., Gergely, F., Riley, J.H., Pérez-Morga, D., Woods, C.G. & Schurmans, S., 2009. INPP5E mutations cause primary cilium signaling defects, ciliary instability and ciliopathies in human and mouse. *Nature genetics*, 41(9), pp.1027–31.

James, T.T., Aroor, A.R., Lim, R.W. & Shukla, S.D., 2012. Histone H3 phosphorylation (Ser10, Ser28) and phosphoacetylation (K9S10) are differentially associated with gene expression in liver of rats treated in vivo with acute ethanol. *The Journal of pharmacology and experimental therapeutics*, 340(2), pp.237–47.

Jauregui, A.R., Nguyen, K.C.Q., Hall, D.H. & Barr, M.M., 2008. The Caenorhabditis elegans nephrocystins act as global modifiers of cilium structure. *Journal of Cell Biology*, 180(5), pp.973–988.

Jensen, C.G., Davison, E. a, Bowser, S.S. & Rieder, C.L., 1987. Primary cilia cycle in PtK1 cells: effects of colcemid and taxol on cilia formation and resorption. *Cell motility and the cytoskeleton*, 7(3), pp.187–97.

Jin, D., Ni, T.T., Sun, J., Wan, H., Amack, J.D., Yu, G., Fleming, J., Chiang, C., Li, W., Papierniak, A., Cheepala, S., Conseil, G., Cole, S.P.C., Zhou, B., Drummond, I.A., Schuetz, J.D., Malicki, J. & Zhong, T.P., 2014. Prostaglandin signalling regulates ciliogenesis by modulating intraflagellar transport. *Nature cell biology*, 16(9), pp.841–51.

Jordan, M.A. & Kamath, K., 2007. How do microtubule-targeted drugs work? An overview. *Current cancer drug targets*, 7(8), pp.730–742.

Kapitonov, D., Allegood, J.C., Mitchell, C., Hait, N.C., Almenara, J.A., Adams, J.K., Zipkin, R.E., Dent, P., Kordula, T., Milstien, S. & Spiegel, S., 2009. Targeting sphingosine kinase 1 inhibits Akt signaling, induces apoptosis, and suppresses growth of human glioblastoma cells and xenografts. *Cancer Research*, 69(17), pp.6915–6923.

Kathem, S.H., Mohieldin, A.M. & Nauli, S.M., 2015. The Roles of Primary cilia in Polycystic Kidney Disease. *AIMS molecular science*, 1(1), pp.27–46.

Keeling, J., Tsiokas, L. & Maskey, D., 2016. Cellular Mechanisms of Ciliary Length Control. *Cells*, 5(1), p.6.

Khan, N.A., Willemarck, N., Talebi, A., Marchand, A., Binda, M.M., Dehairs, J., Rueda-Rincon, N., Daniels, V.W., Bagadi, M., Raj, D.B.T.G., Vanderhoydonc, F., Munck, S., Chaltin, P. & Swinnen, J. V, 2016. Identification of drugs that restore primary cilium expression in cancer cells. *Oncotarget*.

Kim, J., Jo, H., Hong, H., Kim, M.H., Kim, J.M., Lee, J.-K., Heo, W. Do & Kim, J., 2015. Actin remodelling factors control ciliogenesis by regulating YAP/TAZ activity and vesicle trafficking (Supplementary). *Nat Commun*, 6(22), p.6781.

Kim, J., Lee, J.E., Heynen-Genel, S., Suyama, E., Ono, K., Lee, K., Ideker, T., Aza-Blanc, P. & Gleeson, J.G., 2010. Functional genomic screen for modulators of ciliogenesis and cilium length. *Nature*, 464(7291), pp.1048–51.

Kim, J.C., Badano, J.L., Sibold, S., Esmail, M. a, Hill, J., Hoskins, B.E., Leitch, C.C., Venner, K., Ansley, S.J., Ross, A.J., Leroux, M.R., Katsanis, N. & Beales, P.L., 2004. The Bardet-Biedl protein BBS4 targets cargo to the pericentriolar region and is required for microtubule anchoring and cell cycle progression. *Nature genetics*, 36(5), pp.462–470.

Kitatani, K., Idkowiak-Baldys, J. & Hannun, Y.A., 2008. The sphingolipid salvage pathway in ceramide metabolism and signaling. *Cellular Signalling*, 20(6), pp.1010–1018.

Kölsch, V., Charest, P.G. & Firtel, R.A., 2008. The regulation of cell motility and chemotaxis by phospholipid signaling. *Journal of cell science*, 121(Pt 5), pp.551–9.

Kong, A.M., Speed, C.J., O'Malley, C.J., Layton, M.J., Meehan, T., Loveland, K.L., Cheema, S., Ooms, L.M. & Mitchell, C.A., 2000. Cloning and characterization of a 72-kDa inositol-polyphosphate 5-phosphatase localized to the Golgi network. *Journal of Biological Chemistry*, 275(31), pp.24052–24064.

Konishi, Y. & Setou, M., 2009. Tubulin tyrosination navigates the kinesin-1 motor domain to axons. *Nature neuroscience*, 12(5), pp.559–567.

Koulen, P., Cai, Y., Geng, L., Maeda, Y., Nishimura, S., Witzgall, R., Ehrlich, B.E. & Somlo, S., 2002. Polycystin-2 is an intracellular calcium release channel. *Nature cell biology*, 4(3), pp.191–197.

Kuehn, E.W., Park, K.M., Somlo, S. & Bonventre, J. V, 2002. Kidney injury molecule-1 expression in murine polycystic kidney disease. *American journal of physiology. Renal physiology*, 283(6), pp.F1326–36.

Kurbegovic, A., Côté, O., Couillard, M., Ward, C.J., Harris, P.C. & Trudel, M., 2010. Pkd1 transgenic mice: Adult model of polycystic kidney disease with extrarenal and renal phenotypes.

Human Molecular Genetics, 19(7), pp.1174–1189.

Lacroix, B., Van Dijk, J., Gold, N.D., Guizetti, J., Aldrian-Herrada, G., Rogowski, K., Gerlich, D.W. & Janke, C., 2010. Tubulin polyglutamylation stimulates spastin-mediated microtubule severing. *Journal of Cell Biology*, 189(6), pp.945–954.

Lal, M. & Caplan, M., 2011. Regulated intramembrane proteolysis: signaling pathways and biological functions. *Physiology (Bethesda)*, 26(1), pp.34–44.

Landsverk, H.B., Carlson, C.R., Steen, R.L., Vossebein, L., Herberg, F.W., Tasken, K. & Collas, P., 2001. Regulation of anchoring of the RII{alpha} regulatory subunit of PKA to AKAP95 by threonine phosphorylation of RII{alpha}: implications for chromosome dynamics at mitosis. *J. Cell Sci.*, 114(18), pp.3255–3264.

Larsson, O., Zetterberg, a & Engström, W., 1985. Consequences of parental exposure to serum-free medium for progeny cell division. *Journal of cell science*, 75, pp.259–68.

Lee, K., Battini, L. & Gusella, G.L., 2011. Cilium, centrosome and cell cycle regulation in polycystic kidney disease. *Biochimica et biophysica acta*, 1812(10), pp.1263–71.

Lee K, Hoey D and Jacobs C (2010) Primary Cilia-Mediated Mechanotransduction in Bone *Clinic Rev Bone Miner Metab* 8:201–212

Li, J.B., Gerdes, J.M., Haycraft, C.J., Fan, Y., Teslovich, T.M., May-Simera, H., Li, H., Blacque, O.E., Li, L., Leitch, C.C., Lewis, R.A., Green, J.S., Parfrey, P.S., Leroux, M.R., Davidson, W.S., Beales, P.L., Guay-Woodford, L.M., Yoder, B.K., Stormo, G.D., Katsanis, N. & Dutcher, S.K., 2004. Comparative genomics identifies a flagellar and basal body proteome that includes the BBS5 human disease gene. *Cell*, 117(4), pp.541–552.

Li, Q., Dai, Y., Guo, L., Liu, Y., Hao, C., Wu, G., Basora, N., Michalak, M. & Chen, X.Z., 2003. Polycystin-2 associates with tropomyosin-1, an actin microfilament component. *Journal of Molecular Biology*, 325(5), pp.949–962.

Li, Q., Montalbetti, N., Shen, P.Y., Dai, X.Q., Cheeseman, C.I., Karpinski, E., Wu, G., Cantiello, H.F. & Chen, X.Z., 2005. Alpha-actinin associates with polycystin-2 and regulates its channel activity. *Human Molecular Genetics*, 14(12), pp.1587–1603.

Li, Q., Montalbetti, N., Wu, Y., Ramos, A., Raychowdhury, M.K., Chen, X.-Z. & Cantiello, H.F., 2006. Polycystin-2 cation channel function is under the control of microtubular structures in primary cilia of renal epithelial cells. *The Journal of biological chemistry*, 281(49), pp.37566–75.

Li, X., Luo, Y., Starremans, P.G., McNamara, C. a, Pei, Y. & Zhou, J., 2005. Polycystin-1 and polycystin-2 regulate the cell cycle through the helix-loop-helix inhibitor Id2. *Nature cell biology*, 7(12), pp.1202–1212.

Lian, P., Li, A., Li, Y., Liu, H., Liang, D., Hu, B., Lin, D., Jiang, T., Moeckel, G., Qin, D. & Wu, G., 2014. Loss of polycystin-1 inhibits Bicc1 expression during mouse development.

PLoS ONE, 9(3).

Liang, A.H., Ruiz, F., Heckmann, K., Klotz, C., Tollon, Y., Beisson, J. & Wright, M., 1996. γ-tubulin is permanently associated with basal bodies in ciliates. *European Journal of Cell Biology*, 70(N4), pp.331–338.

Lieberthal, W. & Levine, J.S., 2009. The role of the mammalian target of rapamycin (mTOR) in renal disease. *Journal of the American Society of Nephrology : JASN*, 20(12), pp.2493–2502.

Liu, P., Cheng, H., Roberts, T.M. & Zhao, J.J., 2009. Targeting the phosphoinositide 3-kinase pathway in cancer. *Nature reviews. Drug discovery*, 8(8), pp.627–44.

Liu, S., Lu, W., Obara, T., Kuida, S., Lehoczky, J., Dewar, K., Drummond, I. a & Beier, D.R., 2002. A defect in a novel Nek-family kinase causes cystic kidney disease in the mouse and in zebrafish. *Development (Cambridge, England)*, 129(24), pp.5839–5846.

Liu, Y., Zhu, M., Nishida, K., Hirano, T. & Zhang, W., 2007. An essential role for RasGRP1 in mast cell function and IgE-mediated allergic response. *The Journal of experimental medicine*, 204(1), pp.93–103.

Low, S.H., Vasanth, S., Larson, C.H., Mukherjee, S., Sharma, N., Kinter, M.T., Kane, M.E., Obara, T. & Weimbs, T., 2006. Polycystin-1, STAT6, and P100 function in a pathway that transduces ciliary mechanosensation and is activated in polycystic kidney disease. *Developmental Cell*, 10(1), pp.57–69.

Lu, C.J., Du, H., Wu, J., Jansen, D.A., Jordan, K.L., Xu, N., Sieck, G.C. & Qian, Q., 2008. Non-random distribution and sensory functions of primary cilia in vascular smooth muscle cells. *Kidney and Blood Pressure Research*, 31(3), pp.171–184.

Luciano, A.M., Pocar, P., Milanesi, E., Modina, S., Rieger, D., Lauria, A. & Gandolfi, F., 1999. Effect of different levels of intracellular cAMP on the in vitro maturation of cattle oocytes and their subsequent development following in vitro fertilization. *Molecular Reproduction and Development*, 54(1), pp.86–91.

Ludueña, R.F. & Banerjee, A., 2008. The isotypes of tubulin- distribution and functional significance. In *Cancer Drug Discovery and Development: The Role of Microtubules in Cell Biology, Neurobiology, and Oncology*. pp. 123–175.

Luo, N., Lu, J. & Sun, Y., 2012. Evidence of a role of inositol polyphosphate 5-phosphatase INPP5E in cilia formation in zebrafish. *Vision Research*, 75, pp.98–107.

Luo, Y., Vassilev, P.M., Li, X., Kawanabe, Y. & Zhou, J., 2003. Native polycystin 2 functions as a plasma membrane Ca2+-permeable cation channel in renal epithelia. *Molecular and cellular biology*, 23(7), pp.2600–7.

Luyten, A., Su, X., Gondela, S., Chen, Y., Rompani, S., Takakura, A. & Zhou, J., 2010. Aberrant regulation of planar cell polarity in polycystic kidney disease. *Journal of the American Society of Nephrology : JASN*, 21(9), pp.1521–1532.

Ma, M., Tian, X., Igarashi, P., Pazour, G,J., Somlo, S. 2013. Loss of cilia suppresses cyst growth in genetic models of autosomal dominant polycystic kidney disease. Nat Genet. 2013 Sep; 45(9): 1004–1012.

Mac Ritchie, N., Volpert, G., Al Washih, M., Watson, DG., Futerman, AH., Kennedy, S., Pyne, S., Pyne, NJ., 2016. Effect of the sphingosine kinase 1 selective inhibitor, PF-543 on arterial and cardiac remodelling in a hypoxic model of pulmonary arterial hypertension. *Cell Signal.*28(8):946-55.

Maddala, R., Reddy, V.N., Epstein, D.L. & Rao, V., 2003. Growth factor induced activation of Rho and Rac GTPases and actin cytoskeletal reorganization in human lens epithelial cells. *Molecular vision*, 9(February), pp.329–336.

Mahjoub, M.R., Trapp, M.L. & Quarmby, L.M., 2005. NIMA-Related Kinases Defective in Murine Models of Polycystic Kidney Diseases Localize to Primary Cilia and Centrosomes. *Journal of the American Society of Nephrology*, 16(12), pp.3485–3489.

Majeed, S., Moloney, B.C. & Nauli, S.M., 2012. Mechanisms regulating cilia growth and cilia function in endothelial cells. *Cellular and Molecular Life Sciences*, 69(1), pp.165–173.

Mandato, C.A., Bement, W.M., 2003. Actomyosin transports microtubules and microtubules control actomyosin recruitment during Xenopus oocyte wound healing. Curr Biol. 1;13(13):1096-105.

Mangolini, A., de Stephanis, L. & Aguiari, G., 2016. Role of calcium in polycystic kidney disease: From signaling to pathology. *World journal of nephrology*, 5(1), pp.76–83.

Manning, D.K., Sergeev, M., van Heesbeen, R.G., Wong, M.D., Oh, J.-H., Liu, Y., Henkelman, R.M., Drummond, I., Shah, J. V & Beier, D.R., 2013. Loss of the ciliary kinase Nek8 causes left-right asymmetry defects. *Journal of the American Society of Nephrology : JASN*, 24(1), pp.100–12.

Marshall, W.F. & Nonaka, S., 2006. Cilia: Tuning in to the Cell's Antenna. *Current Biology*, 16(15).

May, J. a, Ratan, H., Glenn, J.R., Lösche, W., Spangenberg, P. & Heptinstall, S., 1998. GPIIb-IIIa antagonists cause rapid disaggregation of platelets pre-treated with cytochalasin D. Evidence that the stability of platelet aggregates depends on normal cytoskeletal assembly. *Platelets*, 9(3-4), pp.227–32.

McGowan, S.E. & McCoy, D.M., 2013. Platelet-derived growth factor-A and sonic hedgehog signaling direct lung fibroblast precursors during alveolar septal formation. *American journal of physiology. Lung cellular and molecular physiology*, 305(3), pp.L229–39.

McKenzie, A.J., Campbell, S.L. & Howe, A.K., 2011. Protein kinase a activity and anchoring are required for ovarian cancer cell migration and invasion. *PLoS ONE*, 6(10).

Mejillano, M.R., Shivanna, B.D. & Himes, R.H., 1996. Studies on the nocodazole-induced GTPase

activity of tubulin. *Archives of biochemistry and biophysics*, 336(1), pp.130–8.

Mekahli, D., Decuypere, J.P., Sammels, E., Welkenhuyzen, K., Schoeber, J., Audrezet, M.P., Corvelyn, A., Dechênes, G., Ong, A.C.M., Wilmer, M.J., Van Den Heuvel, L., Bultynck, G., Parys, J.B., Missiaen, L., Levtchenko, E. & De Smedt, H., 2014. Polycystin-1 but not polycystin-2 deficiency causes upregulation of the mTOR pathway and can be synergistically targeted with rapamycin and metformin. *Pflugers Archiv European Journal of Physiology*, 466(8), pp.1591–1604.

Mekahli, D., Sammels, E., Luyten, T., Welkenhuyzen, K., van den Heuvel, L.P., Levtchenko, E.N., Gijsbers, R., Bultynck, G., Parys, J.B., De Smedt, H. & Missiaen, L., 2012. Polycystin-1 and polycystin-2 are both required to amplify inositol-trisphosphate-induced Ca 2+ release. *Cell Calcium*, 51(6), pp.452–458.

Meraldi, P., Honda, R. & Nigg, E.A., 2002. Aurora-A overexpression reveals tetraploidization as a major route to centrosome amplification in p53-/- cells. *EMBO Journal*, 21(4), pp.483–492.

Messner, M.C. & Cabot, M.C., 2010. Glucosylceramide in humans. *Advances in Experimental Medicine and Biology*, 688, pp.156–164.

Michaud, E.J. & Yoder, B.K., 2006. The primary cilium in cell signaling and cancer. *Cancer Research*, 66(13), pp.6463–6467.

Mitchison, T. & Kirschner, M., 1984. Dynamic instability of microtubule growth. *Nature*, 312(5991), pp.237–42.

Miyamoto, T., Hosoba, K., Ochiai, H., Royba, E., Izumi, H., Sakuma, T., Yamamoto, T., Dynlacht, B. & Matsuura, S., 2015. The Microtubule-Depolymerizing activity of a mitotic kinesin protein KIF2A drives primary cilia disassembly coupled with cell proliferation. *Cell Reports*, 10(5), pp.664–673.

Miyoshi, K., Kasahara, K., Miyazaki, I. & Asanuma, M., 2011. Factors that influence primary cilium length. *Acta Medica Okayama*, 65(5), pp.279–285.

Mochizuki T1, Wu G, Hayashi T, Xenophontos SL, Veldhuisen B, Saris JJ, Reynolds DM, Cai Y, Gabow PA, Pierides A, Kimberling WJ, Breuning MH, Deltas CC, Peters DJ, Somlo S. 1996. PKD2, a gene for polycystic kidney disease that encodes an integral membrane protein. Science. 31;272(5266):1339-42.

Montalbetti, N., Li, Q., Wu, Y., Chen, X.-Z. & Cantiello, H.F., 2007. Polycystin-2 cation channel function in the human syncytiotrophoblast is regulated by microtubular structures. *The Journal of physiology*, 579(Pt 3), pp.717–28.

Moyer, J.H., Lee-Tischler, M.J., Kwon, H.Y., Schrick, J.J., Avner, E.D., Sweeney, W.E., Godfrey, V.L., Cacheiro, N.L., Wilkinson, J.E. & Woychik, R.P., 1994. Candidate gene associated with a mutation causing recessive polycystic kidney disease in mice. *Science (New York, N.Y.)*, 264(5163), pp.1329–1333.

Nakakura, T., Asano-Hoshino, A., Suzuki, T., Arisawa, K., Tanaka, H., Sekino, Y., Kiuchi, Y., Kawai, K. & Hagiwara, H., 2015. The elongation of primary cilia via the acetylation of ??-tubulin by the treatment with lithium chloride in human fibroblast KD cells. *Medical Molecular Morphology*, 48(1), pp.44–53.

Natoli, T. a, Smith, L. a, Rogers, K. a, Wang, B., Komarnitsky, S., Budman, Y., Belenky, A., Bukanov, N.O., Dackowski, W.R., Husson, H., Russo, R.J., Shayman, J. a, Ledbetter, S.R., Leonard, J.P. & Ibraghimov-Beskrovnaya, O., 2010. Inhibition of glucosylceramide accumulation results in effective blockade of polycystic kidney disease in mouse models. *Nature medicine*, 16(7), pp.788–792.

Nauli, S.M., Alenghat, F.J., Luo, Y., Williams, E., Vassilev, P., Li, X., Elia, A.E.H., Lu, W., Brown, E.M., Quinn, S.J., Ingber, D.E. & Zhou, J., 2003. Polycystins 1 and 2 mediate mechanosensation in the primary cilium of kidney cells. *Nature genetics*, 33(2), pp.129–37.

Nauli, S.M., Kawanabe, Y., Kaminski, J.J., Pearce, W.J., Ingber, D.E. & Zhou, J., 2008. Endothelial cilia are fluid shear sensors that regulate calcium signaling and nitric oxide production through polycystin-1. *Circulation*, 117(9), pp.1161–1171.

Nauli, S.M. & Zhou, J., 2004. Polycystins and mechanosensation in renal and nodal cilia. *BioEssays*, 26(8), pp.844–856.

Newby, L.J., Streets, A.J., Zhao, Y., Harris, P.C., Ward, C.J. & Ong, A.C.M., 2002. Identification, characterization, and localization of a novel kidney polycystin-1-polycystin-2 complex. *Journal of Biological Chemistry*, 277(23), pp.20763–20773.

Newlon, M.G., Roy, M., Morikis, D., Carr, D.W., Westphal, R., Scott, J.D. & Jennings, P.A., 2001. A novel mechanism of PKA anchoring revealed by solution structures of anchoring complexes. *EMBO Journal*, 20(7), pp.1651–1662.

Nigg, E.A. & Raff, J.W., 2009. Centrioles, Centrosomes, and Cilia in Health and Disease. *Cell*, 139(4), pp.663–678.

Nikonova, A.S., Plotnikova, O. V, Serzhanova, V., Efimov, A., Bogush, I., Cai, K.Q., Hensley, H.H., Egleston, B.L., Klein-Szanto, A., Seeger-Nukpezah, T. & Golemis, E. a, 2014. Nedd9 restrains renal cystogenesis in Pkd1-/- mice. *Proceedings of the National Academy of Sciences of the United States of America*, 111(35), pp.12859–64.

Nobes, C.D. & Hall, A., 1995. Rho, Rac, and Cdc42 GTPases regulate the assembly of multimolecular focal complexes associated with actin stress fibers, lamellipodia, and filopodia. *Cell*, 81(1), pp.53–62.

Nogales, E., 2001. Structural Insights into Microtubule Function. *Annual Review of Biophysics and Biomolecular Structure*, 30(1), pp.397–420.

Nogales, E. & Wang, H.W., 2006. Structural mechanisms underlying nucleotide-dependent self-assembly of tubulin and its relatives. *Current Opinion in Structural Biology*, 16(2),

pp.221–229.

Nogales, E., Wolf, S.G. & Downing, K.H., 1998. Structure of the alpha beta tubulin dimer by electron crystallography. *Nature*, 391, pp.199–203.

O Bukanov, N., Husson, H., Dackowski, W.R., Lawrence, B.D., Clow, P. a, Roberts, B.L., Klinger, K.W. & Ibraghimov-Beskrovnaya, O., 2002. Functional polycystin-1 expression is developmentally regulated during epithelial morphogenesis in vitro: downregulation and loss of membrane localization during cystogenesis. *Human molecular genetics*, 11(8), pp.923–936.

O'Brien, E.T., Salmon, E.D. & Erickson, H.P., 1997. How calcium causes microtubule depolymerization. *Cell Motility and the Cytoskeleton*, 36(2), pp.125–135.

Oakley, C.E. & Oakley, B.R., 1989. Identification of gamma-tubulin, a new member of the tubulin superfamily encoded by mipA gene of Aspergillus nidulans. *Nature*, 338(6217), pp.662–664.

Olbrich, H., Fliegauf, M., Hoefele, J., Kispert, A., Otto, E., Volz, A., Wolf, M.T., Sasmaz, G., Trauer, U., Reinhardt, R., Sudbrak, R., Antignac, C., Gretz, N., Walz, G., Schermer, B., Benzing, T., Hildebrandt, F. & Omran, H., 2003. Mutations in a novel gene, NPHP3, cause adolescent nephronophthisis, tapeto-retinal degeneration and hepatic fibrosis. *Nature genetics*, 34(4), pp.455–459.

Omran, H., 2010. NPHP proteins: Gatekeepers of the ciliary compartment. *Journal of Cell Biology*, 190(5), pp.715–717.

Ong, A.C.M., 2000 Polycystin expression in the kidney and other tissues: complexity, consensus and controversy. *Exp Nephrol*. 2000;8(4-5):208-14

Ong, A.C.M., 2013. Primary cilia and renal cysts: does length matter? *Nephrol Dial Transplant.* 2013 Nov;28(11):2661-3.

Ong, A.C.M., Devuyst, O., Knebelmann, B. & Walz, G., 2015. Autosomal dominant polycystic kidney disease: The changing face of clinical management. *The Lancet*, 385(9981), pp.1993–2002.

Ong, A.C.M. & Harris, P.C., 2005. Molecular pathogenesis of ADPKD: The polycystin complex gets complex. *Kidney International*, 67(4), pp.1234–1247.

Ong, A.C.M. & Wheatley, D.N., 2003. Polycystic kidney disease--the ciliary connection. *Lancet*, 361(9359), pp.774–6.

Onishi, K., Higuchi, M., Asakura, T., Masuyama, N. & Gotoh, Y., 2007. The PI3K-Akt pathway promotes microtubule stabilization in migrating fibroblasts. *Genes to Cells*, 12(4), pp.535–546.

Otto, E. a, Schermer, B., Obara, T., O'Toole, J.F., Hiller, K.S., Mueller, A.M., Ruf, R.G., Hoefele, J., Beekmann, F., Landau, D., Foreman, J.W., Goodship, J. a, Strachan, T., Kispert, A., Wolf, M.T., Gagnadoux, M.F., Nivet, H., Antignac, C., Walz, G., Drummond, I.A.,

Benzing, T., Hildebrandt, F. & Toole, J.F.O., 2003. Mutations in INVS encoding inversin cause nephronophthisis type 2, linking renal cystic disease to the function of primary cilia and left-right axis determination. *Nature genetics*, 34(4), pp.413–420.

Otto, E. a, Trapp, M.L., Schultheiss, U.T., Helou, J., Quarmby, L.M. & Hildebrandt, F., 2008. NEK8 mutations affect ciliary and centrosomal localization and may cause nephronophthisis. *Journal of the American Society of Nephrology : JASN*, 19(3), pp.587–592.

Palazzo, A.F. & Gundersen, G.G., 2002. Microtubule-actin cross-talk at focal adhesions. *Science's STKE : signal transduction knowledge environment*, 2002(139), p.pe31.

Pampliega, O., Orhon, I., Patel, B., Sridhar, S., Díaz-Carretero, A., Beau, I., Codogno, P., Satir, B.H., Satir, P. & Cuervo, A.M., 2013. Functional interaction between autophagy and ciliogenesis. *Nature*, 502(7470), pp.194–200.

Pan, J. & Snell, W.J., 2005. Chlamydomonas shortens its flagella by activating axonemal disassembly, stimulating IFT particle trafficking, and blocking anterograde cargo loading. *Developmental Cell*, 9(3), pp.431–438.

Pardee, a B., 1974. A restriction point for control of normal animal cell proliferation. *Proceedings of the National Academy of Sciences of the United States of America*, 71(4), pp.1286–90.

Paridaen, J.T.M.L., Wilsch-Bräuninger, M. & Huttner, W.B., 2013. XAsymmetric inheritance of centrosome-associated primary cilium membrane directs ciliogenesis after cell division. *Cell*, 155(2).

Parker, E., Newby, L., Sharpe, C., Rossetti, S., Streets, A., Harris, P., O 'hare, M. & Ong, A., 2007. Hyperproliferation of PKD1 cystic cells is induced by insulin-like growth factor-1 activation of the Ras/Raf signalling system. *Kidney International*, 72, pp.157–165.

Parnell, S.C., Magenheimer, B.S., Maser, R.L., Rankin, C. a, Smine, A., Okamoto, T. & Calvet, J.P., 1998. The polycystic kidney disease-1 protein, polycystin-1, binds and activates heterotrimeric G-proteins in vitro. *Biochemical and biophysical research communications*, 251(2), pp.625–631.

Parnell, S.C., Magenheimer, B.S., Maser, R.L., Zien, C.A., Frischauf, A.-M. & Calvet, J.P., 2002. Polycystin-1 activation of c-Jun N-terminal kinase and AP-1 is mediated by heterotrimeric G proteins. *J Biol Chem*, 277(22), pp.19566–19572.

Patel, V., Chowdhury, R. & Igarashi, P., 2009. Advances in the pathogenesis and treatment of polycystic kidney disease. *Current opinion in nephrology and hypertension*, 18(2), pp.99–106.

Patel, V., Li, L., Cobo-stark, P., Shao, X., Somlo, S., Lin, F. & Igarashi, P., 2008. Acute kidney injury and aberrant planar cell polarity induce cyst formation in mice lacking renal cilia. *Human Molecular Genetics*, 17(11), pp.1578–1590.

Paul, B.M. & Vanden Heuvel, G.B., 2014. Kidney: Polycystic kidney disease. *Wiley Interdisciplinary Reviews: Developmental Biology*, 3(6), pp.465–487.

Pazour, G.J., Agrin, N., Leszyk, J. & Witman, G.B., 2005. Proteomic analysis of a eukaryotic cilium. *Journal of Cell Biology*, 170(1), pp.103–113.

Pazour, G.J., Agustina, J., Follita, JA., Rosenbaumb, JL., Witman, GB., 2002. Polycystin-2 localizes to kidney cilia and the ciliary level is elevated in orpk mice with polycystic kidney disease. *Curr Biol*. 2002 Jun 4;12(11):R378-80.

Pedersen, L.B., Veland, I.R., Schrøder, J.M. & Christensen, S.T., 2008. Assembly of primary cilia. *Developmental Dynamics*, 237(8), pp.1993–2006.

Pei, Y., 2001. A "two-hit" model of cystogenesis in autosomal dominant polycystic kidney disease? *Trends in Molecular Medicine*, 7(4), pp.151–156.

Pennekamp, P., Karcher, C., Fischer, A., Schweickert, A., Skryabin, B., Horst, J., Blum, M. & Dworniczak, B., 2002. The ion channel polycystin-2 is required for left-right axis determination in mice. *Current Biology*, 12(11), pp.938–943.

Perico, N., Antiga, L., Caroli, A., Ruggenenti, P., Fasolini, G., Cafaro, M., Ondei, P., Rubis, N., Diadei, O., Gherardi, G., Prandini, S., Panozo, A., Bravo, R.F., Carminati, S., De Leon, F.R., Gaspari, F., Cortinovis, M., Motterlini, N., Ene-Iordache, B., Remuzzi, A. & Remuzzi, G., 2010. Sirolimus therapy to halt the progression of ADPKD. *Journal of the American Society of Nephrology : JASN*, 21(6), pp.1031–40.

Peters DJ1, van de Wal A, Spruit L, Saris JJ, Breuning MH, Bruijn JA, de Heer E. 1999. Cellular localization and tissue distribution of polycystin-1. J Pathol. Aug;188(4):439-46.

Piao, T., Luo, M., Wang, L., Guo, Y., Li, D., Li, P., Snell, W.J. & Pan, J., 2009. A microtubule depolymerizing kinesin functions during both flagellar disassembly and flagellar assembly in Chlamydomonas. *Proceedings of the National Academy of Sciences of the United States of America*, 106(12), pp.4713–8.

Piel, M., Meyer, P., Khodjakov, A., Rieder, C.L. & Bornens, M., 2000. The respective contributions of the mother and daughter centrioles to centrosome activity and behavior in vertebrate cells. *Journal of Cell Biology*, 149(2), pp.317–329.

Pinton, P., Ferrari, D., Rapizzi, E., Di Virgilio, F., Pozzan, T. & Rizzuto, R., 2001. The Ca2+ concentration of the endoplasmic reticulum is a key determinant of ceramide-induced apoptosis: Significance for the molecular mechanism of Bcl-2 action. *EMBO Journal*, 20(11), pp.2690–2701.

Pitaval, A., Tseng, Q., Bornens, M. & Théry, M., 2010. Cell shape and contractility regulate ciliogenesis in cell cycle-arrested cells. *Journal of Cell Biology*, 191(2), pp.303–312.

Plotnikova, O. V., Pugacheva, E.N. & Golemis, E.A., 2009. Primary cilia and the cell cycle. *Methods in cell biology*, 94, pp.137–160.

Pollard, T.D. & Borisy, G.G., 2003. Cellular motility driven by assembly and disassembly of actin

filaments. *Cell*, 112(4), pp.453–465.

Praetorius, H.A. & Spring, K.R., 2001. Bending the MDCK cell primary cilium increases intracellular calcium. *Journal of Membrane Biology*, 184(1), pp.71–79.

Praetorius, H.A. & Spring, K.R., 2003. Removal of the MDCK cell primary cilium abolishes flow sensing. *Journal of Membrane Biology*, 191(1), pp.69–76.

Pugacheva, E.N. & Golemis, E.A., 2005. The focal adhesion scaffolding protein HEF1 regulates activation of the Aurora-A and Nek2 kinases at the centrosome. *Nature cell biology*, 7(10), pp.937–46.

Pugacheva, E.N., Jablonski, S.A., Hartman, T.R., Henske, E.P. & Golemis, E.A., 2007. HEF1-Dependent Aurora A Activation Induces Disassembly of the Primary Cilium. *Cell*, 129(7), pp.1351–1363.

Qian, F., Boletta, A., Bhunia, A.K., Xu, H., Liu, L., Ahrabi, A.K., Watnick, T.J., Zhou, F. & Germino, G.G., 2002. Cleavage of polycystin-1 requires the receptor for egg jelly domain and is disrupted by human autosomal-dominant polycystic kidney disease 1-associated mutations. *Proceedings of the National Academy of Sciences*, 99(26), pp.16981–16986.

Qian, F., Germino, F.J., Cai, Y., Zhang, X., Somlo, S. & Germino, G.G., 1997. PKD1 interacts with PKD2 through a probable coiled-coil domain. *Nature Genetics*, 16(2), pp.179–183.

Qian, Q., Du, H., King, B.F., Kumar, S., Dean, P.G., Cosio, F.G. & Torres, V.E., 2008. Sirolimus reduces polycystic liver volume in ADPKD patients. *Journal of the American Society of Nephrology : JASN*, 19(3), pp.631–638.

Qian, Y., Corum, L., Meng, Q., Blenis, J., Zheng, J.Z., Shi, X., Flynn, D.C. & Jiang, B.-H., 2004. PI3K induced actin filament remodeling through Akt and p70S6K1: implication of essential role in cell migration. *American journal of physiology. Cell physiology*, 286(1), pp.C153–C163.

Qin, H., Wang, Z., Diener, D. & Rosenbaum, J., 2007. Intraflagellar Transport Protein 27 Is a Small G Protein Involved in Cell-Cycle Control. *Current Biology*, 17(3), pp.193–202.

Quarmby, L., 2014. Cilia assembly: A role for F-actin in IFT recruitment. *Current Biology*, 24(17), pp.R796–R798.

Ran, J., Yang, Y., Li, D., Liu, M. & Zhou, J., 2015. Deacetylation of α-tubulin and cortactin is required for HDAC6 to trigger ciliary disassembly. *Scientific reports*, 5, p.12917.

Randazzo, P.A., Andrade, J., Miura, K., Brown, M.T., Long, Y.Q., Stauffer, S., Roller, P. & Cooper, J.A., 2000. The Arf GTPase-activating protein ASAP1 regulates the actin cytoskeleton. *Proceedings of the National Academy of Sciences of the United States of America*, 97(8), pp.4011–6.

Rao, Y., Hao, R., Wang, B. & Yao, T.P., 2014. A Mec17-Myosin II effector axis coordinates microtubule acetylation and actin dynamics to control primary cilium biogenesis.

PLoS ONE, 9(12).

Resnick, A. & Hopfer, U., 2007. Force-response considerations in ciliary mechanosensation. *Biophysical journal*, 93(4), pp.1380–90.

Rieder, C.L., Jensen, C.G. & Jensen, L.C.W., 1979. The resorption of primary cilia during mitosis in a vertebrate (PtK1) cell line. *Journal of Ultrasructure Research*, 68(2), pp.173–185.

Riparbelli, M.G., Callaini, G. & Megraw, T.L., 2012. Assembly and Persistence of Primary Cilia in Dividing Drosophila Spermatocytes. *Developmental Cell*, 23(2), pp.425–432.

Rispal, D., Eltschinger, S., Stahl, M., Vaga, S., Bodenmiller, B., Abraham, Y., Filipuzzi, I., Movva, N.R., Aebersold, R., Helliwell, S.B. & Loewith, R., 2015. Target of rapamycin complex 2 regulates actin polarization and endocytosis via multiple pathways. *Journal of Biological Chemistry*, 290(24), pp.14963–14978.

Rizk, D. & Chapman, A.B. (2003) Cystic and inherited kidney diseases. *American Journal of Kidney Diseases,* Volume 42, Issue 6, Pages 1305–1317

Rocha, C., Papon, L., Cacheux, W., Marques Sousa, P., Lascano, V., Tort, O., Giordano, T., Vacher, S., Lemmers, B., Mariani, P., Meseure, D., Medema, J.P., Bièche, I., Hahne, M. & Janke, C., 2014. Tubulin glycylases are required for primary cilia, control of cell proliferation and tumor development in colon. *The EMBO journal*, 33(19), pp.2247–60.

Rodova, M., Islam, M.R., Maser, R.L. & Calvet, J.P., 2002. The polycystic kidney disease-1 promoter is a target of the beta-catenin/T-cell factor pathway. *J Biol Chem*, 277(33), pp.29577–29583.

Rodriguez, O.C., Schaefer, A.W., Mandato, C. a, Forscher, P., Bement, W.M. & Waterman-Storer, C.M., 2003. Conserved microtubule-actin interactions in cell movement and morphogenesis. *Nature cell biology*, 5(7), pp.599–609.

Rodriguez-Collazo, P., Snyder, S.K., Chiffer, R.C., Bressler, E.A., Voss, T.C., Anderson, E.P., Genieser, H.G. & Smith, C.L., 2008. cAMP signaling regulates histone H3 phosphorylation and mitotic entry through a disruption of G2 progression. *Experimental Cell Research*, 314(15), pp.2855–2869.

Rosenbaum, J.L. & Witman, G.B., 2002. Intraflagellar transport. *Nature reviews. Molecular cell biology*, 3(11), pp.813–825.

Rundle DR,. Gorbsky, G,. Tsiokas, L,. 2004 PKD2 Interacts and Co-localizes with mDia1 to Mitotic Spindles of Dividing Cells: role of mDia1 IN PKD2 localization to mitotic spindles. J. Biol. Chem. 279 (28) (2004) 29728–29739

Saadi-Kheddouci, S., Berrebi, D., Romagnolo, B., Cluzeaud, F., Peuchmaur, M., Kahn, a, Vandewalle, a & Perret, C., 2001. Early development of polycystic kidney disease in transgenic mice expressing an activated mutant of the beta-catenin gene. *Oncogene*, 20(42), pp.5972–81.

Saggese, T., Young, A., Huang, C., Braeckmans, K., McGlashan, S,R., 2012. Development of a method for the measurement of primary cilia length in 3D. Cilia; 1: 11.

Sammels, E., Devogelaere, B., Mekahli, D., Bultynck, G., Missiaen, L., Parys, J.B., Cai, Y., Somlo, S. & De Smedt, H., 2010. Polycystin-2 activation by inositol 1,4,5-trisphosphate-induced Ca 2+ release requires its direct association with the inositol 1,4,5-trisphosphate receptor in a signaling microdomain. *Journal of Biological Chemistry*, 285(24), pp.18794–18805.

Sánchez de Diego, A., Alonso Guerrero, A., Martínez-A, C. & van Wely, K.H.M., 2014. Dido3-dependent HDAC6 targeting controls cilium size. *Nature communications*, 5, p.3500.

Sánchez, S., Jiménez, C., Carrera, A.C., Diaz-Nido, J., Avila, J. & Wandosell, F., 2004. A cAMP-activated pathway, including PKA and PI3K, regulates neuronal differentiation. *Neurochemistry International*, 44(4), pp.231–242.

Sandford, R., Mulroy, S. & Foggensteiner, L., 1999. The polycystins: A novel class of membrane-associated proteins involved in renal cystic disease. *Cellular and Molecular Life Sciences*, 56(7-8), pp.567–579.

Satir, P. & Christensen, S.T., 2007. Overview of structure and function of mammalian cilia. *Annual review of physiology*, 69, pp.377–400.

Scheffers, M.S., van der Bent, P., Prins, F., Spruit, L., Breuning, M.H., Litvinov, S. V, de Heer, E. & Peters, D.J., 2000. Polycystin-1, the product of the polycystic kidney disease 1 gene, co-localizes with desmosomes in MDCK cells. *Human molecular genetics*, 9(18), pp.2743–2750.

Scheffers, M.S., Le, H., van der Bent, P., Leonhard, W., Prins, F., Spruit, L., Breuning, M.H., de Heer, E. & Peters, D.J.M., 2002. Distinct subcellular expression of endogenous polycystin-2 in the plasma membrane and Golgi apparatus of MDCK cells. *Human molecular genetics*, 11(1), pp.59–67.

Schmidt, D., Jiang, Q.-X. & MacKinnon, R., 2006. Phospholipids and the origin of cationic gating charges in voltage sensors. *Nature*, 444(7120), pp.775–779.

Schmidt, P.H., Dransfield, D.T., Claudio, J.O., Hawley, R.G., Trotter, K.W., Milgram, S.L. & Goldenring, J.R., 1999. AKAP350, a multiply spliced protein kinase A-anchoring protein associated with centrosomes. *Journal of Biological Chemistry*, 274(5), pp.3055–3066.

Schneider, L., Cammer, M., Lehman, J., Nielsen, S.K., Guerra, C.F., Veland, I.R., Stock, C., Hoffmann, E.K., Yoder, B.K., Schwab, A., Satir, P. & Christensen, S.T., 2010. Directional cell migration and chemotaxis in wound healing response to PDGF-AA are coordinated by the primary cilium in fibroblasts. *Cellular Physiology and Biochemistry*, 25(2-3), pp.279–292.

Schneider, L., Clement, C.A., Teilmann, S.C., Pazour, G.J., Hoffmann, E.K., Satir, P. & Christensen,

S.T., 2005. PDGFRαα signaling is regulated through the primary cilium in fibroblasts. *Current Biology*, 15(20), pp.1861–1866.

Seeley, E.S., Carri??re, C., Goetze, T., Longnecker, D.S. & Korc, M., 2009. Pancreatic cancer and precursor pancreatic intraepithelial neoplasia lesions are devoid of primary cilia. *Cancer Research*, 69(2), pp.422–430.

Sen, S., Katayama, H., Sasai, K., 2008 Functional Significance of Aurora Kinase A in Centrosome Amplification and Genomic Instability. *Hormonal Carcinogenesis*., Vol 617 pp 99-108

Shanks, R.A., Cecilia Larocca, M., Berryman, M., Edwards, J.C., Urushidani, T., Navarre, J. & Goldenring, J.R., 2002. AKAP350 at the golgi apparatus: II. Association of AKAP350 with a novel chloride intracellular channel (CLIC) family member. *Journal of Biological Chemistry*, 277(43), pp.40973–40980.

Sharif-Naeini, R., Folgering, J.H.A., Bichet, D., Duprat, F., Lauritzen, I., Arhatte, M., Jodar, M., Dedman, A., Chatelain, F.C., Schulte, U., Retailleau, K., Loufrani, L., Patel, A., Sachs, F., Delmas, P., Peters, D.J.M. & Honoré, E., 2009. Polycystin-1 and -2 Dosage Regulates Pressure Sensing. *Cell*, 139(3), pp.587–596.

Sharma, N., Bryant, J., Wloga, D., Donaldson, R., Davis, R.C., Jerka-Dziadosz, M. & Gaertig, J., 2007. Katanin regulates dynamics of microtubules and biogenesis of motile cilia. *Journal of Cell Biology*, 178(6), pp.1065–1079.

Sharma, N., Kosan, Z.A., Stallworth, J.E., Berbari, N.F. & Yoder, B.K., 2011. Soluble levels of cytosolic tubulin regulate ciliary length control. *Molecular biology of the cell*, 22(6), pp.806–16.

Shiba, D., Manning, D.K., Koga, H., Beier, D.R. & Yokoyama, T., 2010. Inv acts as a molecular anchor for Nphp3 and Nek8 in the proximal segment of primary cilia. *Cytoskeleton*, 67(2), pp.112–119.

Shiba, D., Yamaoka, Y., Hagiwara, H., Takamatsu, T., Hamada, H. & Yokoyama, T., 2009. Localization of Inv in a distinctive intraciliary compartment requires the C-terminal ninein-homolog-containing region. *Journal of cell science*, 122(Pt 1), pp.44–54.

Shillingford, J.M., Murcia, N.S., Larson, C.H., Low, S.H., Hedgepeth, R., Brown, N., Flask, C.A., Novick, A.C., Goldfarb, D.A., Kramer-Zucker, A., Walz, G., Piontek, K.B., Germino, G.G. & Weimbs, T., 2006. The mTOR pathway is regulated by polycystin-1, and its inhibition reverses renal cystogenesis in polycystic kidney disease. *Proceedings of the National Academy of Sciences of the United States of America*, 103(14), pp.5466–71.

Silflow, C.D. & Rosenbaum, J.L., 1981. Multiple ??- and ??-tubulin genes in chlamydomonas and regulation of tubulin mRNA levels after deflagellation. *Cell*, 24(1), pp.81–88.

Sillibourne, J.E., Milne, D.M., Takahashi, M., Ono, Y. & Meek, D.W., 2002. Centrosomal anchoring of the protein kinase CK1?? mediated by attachment to the large, coiled-coil

scaffolding protein CG-NAP/AKAP450. *Journal of Molecular Biology*, 322(4), pp.785–797.

Simons, M., Gloy, J., Ganner, A., Bullerkotte, A., Bashkurov, M., Krönig, C., Schermer, B., Benzing, T., Cabello, O.A., Jenny, A., Mlodzik, M., Polok, B., Driever, W., Obara, T. & Walz, G., 2005. Inversin, the gene product mutated in nephronophthisis type II, functions as a molecular switch between Wnt signaling pathways. *Nature genetics*, 37(5), pp.537–43.

Singh, M.K., Cowell, L., Seo, S., O'Neill, G.M. & Golemis, E.A., 2007. Molecular basis for HEF1/NEDD9/Cas-L action as a multifunctional co-ordinator of invasion, apoptosis and cell cycle. *Cell Biochemistry and Biophysics*, 48(1), pp.54–72.

Slaats, G.G., Ghosh, A.K., Falke, L.L., Le Corre, S., Shaltiel, I.A., van de Hoek, G., Klasson, T.D., Stokman, M.F., Logister, I., Verhaar, M.C., Goldschmeding, R., Nguyen, T.Q., Drummond, I.A., Hildebrandt, F. & Giles, R.H., 2014. Nephronophthisis-Associated CEP164 Regulates Cell Cycle Progression, Apoptosis and Epithelial-to-Mesenchymal Transition. *PLoS Genetics*, 10(10).

Sohara, E., Luo, Y., Zhang, J., Manning, D.K., Beier, D.R. & Zhou, J., 2008. Nek8 regulates the expression and localization of polycystin-1 and polycystin-2. *Journal of the American Society of Nephrology : JASN*, 19(3), pp.469–476.

Song, L., Xiong, H., Li, J., Liao, W., Wang, L., Wu, J. & Li, M., 2011. Sphingosine kinase-1 enhances resistance to apoptosis through activation of PI3K/Akt/NF-κB pathway in human non-small cell lung cancer. *Clinical cancer research : an official journal of the American Association for Cancer Research*, 17(7), pp.1839–49.

Song, Y. & Brady, S.T., 2015. Post-translational modifications of tubulin: Pathways to functional diversity of microtubules. *Trends in Cell Biology*, 25(3), pp.125–136.

Spektor, A., Tsang, W.Y., Khoo, D. & Dynlacht, B.D., 2007. Cep97 and CP110 Suppress a Cilia Assembly Program. *Cell*, 130(4), pp.678–690.

Spiegel, S. & Merrill, A.H., 1996. Sphingolipid metabolism and cell growth regulation. *FASEB journal : official publication of the Federation of American Societies for Experimental Biology*, 10(12), pp.1388–97.

Stallone, G., Infante, B., Grandaliano, G., Bristogiannis, C., Macarini, L., Mezzopane, D., Bruno, F., Montemurno, E., Schirinzi, A., Sabbatini, M., Pisani, A., Tataranni, T., Schena, F.P. & Gesualdo, L., 2012. Rapamycin for treatment of type I autosomal dominant polycystic kidney disease (RAPYD-study): a randomized, controlled study. *Nephrology, dialysis, transplantation : official publication of the European Dialysis and Transplant Association - European Renal Association*, 27(9), pp.3560–7.

Stefan, E., Wiesner, B., Baillie, G.S., Mollajew, R., Henn, V., Lorenz, D., Furkert, J., Santamaria, K., Nedvetsky, P., Hundsrucker, C., Beyermann, M., Krause, E., Pohl, P., Gall, I.,

MacIntyre, A.N., Bachmann, S., Houslay, M.D., Rosenthal, W. & Klussmann, E., 2007. Compartmentalization of cAMP-dependent signaling by phosphodiesterase-4D is involved in the regulation of vasopressin-mediated water reabsorption in renal principal cells. *Journal of the American Society of Nephrology : JASN*, 18(1), pp.199–212.

Steinwall, M., Åkerlund, M., Bossmar, T., Nishii, M. & Wright, M., 2004. ONO-8815Ly, an EP2 agonist that markedly inhibits uterine contractions in women. *BJOG: An International Journal of Obstetrics and Gynaecology*, 111(2), pp.120–124.

Stewart, K., Gaitan, Y., Shafer, M.E.R., Aoudjit, L., Hu, D., Sharma, R., Tremblay, M., Ishii, H., Marcotte, M., Stanga, D., Tang, Y.C., Boualia, S.K., Nguyen, A.H.T., Takano, T., Lamarche-Vane, N., Vidal, S. & Bouchard, M., 2016. A Point Mutation in p190A RhoGAP Affects Ciliogenesis and Leads to Glomerulocystic Kidney Defects. *PLoS Genetics*, 12(2).

Streets, A.J., Newby, L.J., O'Hare, M.J., Bukanov, N.O., Ibraghimov-Beskrovnaya, O. & Ong, A.C.M., 2003. Functional analysis of PKD1 transgenic lines reveals a direct role for polycystin-1 in mediating cell-cell adhesion. *Journal of the American Society of Nephrology : JASN*, 14(5), pp.1804–1815.

Streets, A.J,. Wagner, B.E,. Harris, P.C. , Ward, C.J., Ong, A.C,. 2009 Homophilic and heterophilic polycystin 1 interactions regulate E-cadherin recruitment and junction assembly in MDCK cells, J. Cell Sci. 122 (Pt 9) 1410–1417

Surendran, K., Selassie, M., Liapis, H., Krigman, H. & Kopan, R., 2010. Reduced Notch signaling leads to renal cysts and papillary microadenomas. *Journal of the American Society of Nephrology*, 21(5), pp.819–32.

Takahashi, M., Shibata, H., Shimakawa, M., Miyamoto, M., Mukai, H. & Yoshitaka, O., 1999. Characterization of a novel giant scaffolding protein, CG-NAP, that anchors multiple signaling enzymes to centrosome and the Golgi apparatus. *Journal of Biological Chemistry*, 274(24), pp.17267–17274.

Takahashi, M., Yamagiwa, A., Nishimura, T., Mukai, H. & Ono, Y., 2002. Centrosomal proteins CG-NAP and kendrin provide microtubule nucleation sites by anchoring gamma-tubulin ring complex. *Molecular biology of the cell*, 13(9), pp.3235–45.

Takakura, A., Contrino, L., Zhou, X., Bonventre, J. V., Sun, Y., Humphreys, B.D. & Zhou, J., 2009. Renal injury is a third hit promoting rapid development of adult polycystic kidney disease. *Human Molecular Genetics*, 18(14), pp.2523–2531.

Takiar, V. & Caplan, M.J., 2010. Telling kidneys to cease and decyst. *Nature medicine*, 16(7), pp.751–752.

Tapon, N. & Hall, A., 1997. Rho, Rac and Cdc42 GTPases regulate the organization of the actin cytoskeleton. *Current Opinion in Cell Biology*, 9(1), pp.86–92.

Taskén, K.A., Collas, P., Kemmner, W.A., Witczak, O., Conti, M. & Taskén, K., 2001. Phosphodiesterase 4D and Protein Kinase A Type II Constitute a Signaling Unit in the Centrosomal Area. *Journal of Biological Chemistry*, 276(25), pp.21999–22002.

Taulman, P.D., Haycraft, C.J., Balkovetz, D.F. & Yoder, B.K., 2001. Polaris, a protein involved in left-right axis patterning, localizes to basal bodies and cilia. *Molecular biology of the cell*, 12(3), pp.589–99.

Teixidó-Travesa, N., Roig, J. & Lüders, J., 2012. The where, when and how of microtubule nucleation - one ring to rule them all. *Journal of cell science*, 125(Pt 19), pp.4445–56.

Terrin, A., Monterisi, S., Stangherlin, A., Zoccarato, A., Koschinski, A., Surdo, N.C., Mongillo, M., Sawa, A., Jordanides, N.E., Mountford, J.C. & Zaccolo, M., 2012. PKA and PDE4D3 anchoring to AKAP9 provides distinct regulation of cAMP signals at the centrosome. *Journal of Cell Biology*, 198(4), pp.607–621.

Tian, Y., Kolb, R., Hong, J.-H.H., Carroll, J., Li, D., You, J., Bronson, R., Yaffe, M.B., Zhou, J. & Benjamin, T., 2007. TAZ promotes PC2 degradation through a SCFbeta-Trcp E3 ligase complex. *Mol.Cell Biol.*, 27(18), pp.6383–6395.

Togawa, a, Miyoshi, J., Ishizaki, H., Tanaka, M., Takakura, A., Nishioka, H., Yoshida, H., Doi, T., Mizoguchi, A., Matsuura, N., Niho, Y., Nishimune, Y., Nishikawa, S.I. & Takai, Y., 1999. Progressive impairment of kidneys and reproductive organs in mice lacking Rho GDIalpha. *Oncogene*, 18(39), pp.5373–80.

Torres, V.E., Boletta, a, Chapman, a, Gattone, V., Pei, Y., Qi, Q. a, Wallace, D.P., Weimbs, T. & Wuethrich, R.P., 2010. Prospects for mTOR Inhibitor Use in Patients with Polycystic Kidney Disease and Hamartomatous Diseases. *Clinical Journal of the American Society of Nephrology*, 5(7), pp.1312–1329.

Torres, V.E., Chapman, A.B., Devuyst, O., Gansevoort, R.T., Grantham, J.J., Higashihara, E., Perrone, R.D., Krasa, H.B., Ouyang, J. & Czerwiec, F.S., 2012. Tolvaptan in patients with autosomal dominant polycystic kidney disease. *The New England journal of medicine*, 367(25), pp.2407–18.

Torres, V.E. & Harris, P.C., 2009. Autosomal dominant polycystic kidney disease: the last 3 years. *Kidney international*, 76(2), pp.149–68.

Torres, V.E., Harris, P.C. & Pirson, Y., 2007. Autosomal dominant polycystic kidney disease. *Lancet*, 369(9569), pp.1287–1301.

Torres, V.E., Higashihara, E., Devuyst, O., Chapman, A.B., Gansevoort, R.T., Grantham, J.J., Perrone, R.D., Ouyang, J., Blais, J.D. & Czerwiec, F.S., 2016. Effect of Tolvaptan in Autosomal Dominant Polycystic Kidney Disease by CKD Stage: Results from the TEMPO 3:4 Trial. *Clinical Journal of the American Society of Nephrology*, (February 2015), pp.1–9.

Tran, P. V, Talbott, G.C., Turbe-Doan, A., Jacobs, D.T., Schonfeld, M.P., Silva, L.M., Chatterjee, A.,

Prysak, M., Allard, B.A. & Beier, D.R., 2014. Downregulating hedgehog signaling reduces renal cystogenic potential of mouse models. *Journal of the American Society of Nephrology : JASN*, 25(10), pp.2201–12.

Tran, U., Zakin, L., Schweickert, A., Agrawal, R., Döger, R., Blum, M., De Robertis, E.M. & Wessely, O., 2010. The RNA-binding protein bicaudal C regulates polycystin 2 in the kidney by antagonizing miR-17 activity. *Development (Cambridge, England)*, 137(7), pp.1107–1116.

Trapp, M.L., Galtseva, A., Manning, D.K., Beier, D.R., Rosenblum, N.D. & Quarmby, L.M., 2008. Defects in ciliary localization of Nek8 is associated with cystogenesis. *Pediatric Nephrology*, 23(3), pp.377–387.

Tsang, W.Y., Bossard, C., Khanna, H., Per??nen, J., Swaroop, A., Malhotra, V. & Dynlacht, B.D., 2008. CP110 Suppresses Primary Cilia Formation through Its Interaction with CEP290, a Protein Deficient in Human Ciliary Disease. *Developmental Cell*, 15(2), pp.187–197.

Tsiokas, L., Kim, E., Arnould, T., Sukhatme, V.P. & Walz, G., 1997. Homo- and heterodimeric interactions between the gene products of PKD1 and PKD2. *Proceedings of the National Academy of Sciences of the United States of America*, 94(13), pp.6965–70.

Tucker, R.W. & Scher, C.D., 1979. Centriole deciliation associated with the early response of 3T3 cells to growth factors but not to SV40. *Cell*.

Uetake, Y., Lon??arek, J., Nordberg, J.J., English, C.N., La Terra, S., Khodjakov, A. & Sluder, G., 2007. Cell cycle progression and de novo centriole assembly after centrosomal removal in untransformed human cells. *Journal of Cell Biology*, 176(2), pp.173–182.

Ulloa, F. & Martí, E., 2010. Wnt won the war: Antagonistic role of Wnt over Shh controls dorso-ventral patterning of the vertebrate neural tube. *Developmental Dynamics*, 239(1), pp.69–76.

Uzman, A., Lodish, H., Berk, A., Zipursky, L. & Baltimore, D., 2000. Molecular Cell Biology (4th edition) New York, NY, 2000, ISBN 0-7167-3136-3. *Biochemistry and Molecular Biology Education*, 29, p.Section 1.2The Molecules of Life.

Valente, E.M., Rosti, R.O., Gibbs, E. & Gleeson, J.G., 2014. Primary cilia in neurodevelopmental disorders. *Nature reviews. Neurology*, 10(1), pp.27–36.

Vasquez, R.J., Howell, B., Yvon, A.M., Wadsworth, P. & Cassimeris, L., 1997. Nanomolar concentrations of nocodazole alter microtubule dynamic instability in vivo and in vitro. *Molecular biology of the cell*, 8(6), pp.973–85.

Velagapudi, C., Bhandari, B.S., Abboud-Werner, S., Simone, S., Abboud, H.E. & Habib, S.L., 2011. The tuberin/mTOR pathway promotes apoptosis of tubular epithelial cells in diabetes. *Journal of the American Society of Nephrology : JASN*, 22(2), pp.262–73.

Veland, I.R., Lindb??k, L. & Christensen, S.T., 2014. Linking the primary cilium to cell migration in

tissue repair and brain development. *BioScience*, 64(12), pp.1115–1125.

Veland, I.R., Montjean, R., Eley, L., Pedersen, L.B., Schwab, A., Goodship, J., Kristiansen, K., Pedersen, S.F., Saunier, S. & Christensen, S.T., 2013. Inversin/Nephrocystin-2 Is Required for Fibroblast Polarity and Directional Cell Migration. *PLoS ONE*, 8(4).

Verbalis, J.G., 2002. Vasopressin V2 receptor antagonists. *Journal of Molecular Endocrinology*, 29(1), pp.1–9.

Verghese, E., Ricardo, S.D., Weidenfeld, R., Zhuang, J., Hill, P. a, Langham, R.G. & Deane, J. a, 2009. Renal primary cilia lengthen after acute tubular necrosis. *Journal of the American Society of Nephrology : JASN*, 20(10), pp.2147–2153.

Verghese, E., Weidenfeld, R., Bertram, J.F., Ricardo, S.D. & Deane, J.A., 2008. Renal cilia display length alterations following tubular injury and are present early in epithelial repair. *Nephrology Dialysis Transplantation*, 23(3), pp.834–841.

Verghese, E., Zhuang, J., Saiti, D., Ricardo, S.D. & Deane, J. a, 2011. In vitro investigation of renal epithelial injury suggests that primary cilium length is regulated by hypoxia-inducible mechanisms. *Cell biology international*, 35(9), pp.909–913.

Verhey, K.J. & Gaertig, J., 2007. The tubulin code. *Cell Cycle*, 6(17), pp.2152–2160.

Vlahos, C.J., Matter, W.F., Hui, K.Y. & Brown, R.F., 1994. A specific inhibitor of phosphatidylinositol 3-kinase, 2-(4-morpholinyl)-8-phenyl-4H-1-benzopyran-4-one (LY294002). *Journal of Biological Chemistry*, 269(7), pp.5241–8.

Wallace, D.P., 2011. Cyclic AMP-mediated cyst expansion. *Biochimica et Biophysica Acta - Molecular Basis of Disease*, 1812(10), pp.1291–1300.

Walz, G., Budde, K., Mannaa, M., Nürnberger, J., Wanner, C., Sommerer, C., Kunzendorf, U., Banas, B., Hörl, W.H., Obermüller, N., Arns, W., Pavenstädt, H., Gaedeke, J., Büchert, M., May, C., Gschaidmeier, H., Kramer, S. & Eckardt, K.-U., 2010. Everolimus in patients with autosomal dominant polycystic kidney disease. *The New England journal of medicine*, 363(9), pp.830–840.

Wang, G., Krishnamurthy, K. & Bieberich, E., 2009. Regulation of primary cilia formation by ceramide. *Journal of lipid research*, 50(10), pp.2103–2110.

Wang, X., Gattone, V., Harris, P.C. & Torres, V.E., 2005. Effectiveness of vasopressin V2 receptor antagonists OPC-31260 and OPC-41061 on polycystic kidney disease development in the PCK rat. *Journal of the American Society of Nephrology : JASN*, 16(4), pp.846–51.

Wang, X., Wu, Y., Ward, C.J., Harris, P.C. & Torres, V.E., 2008. Vasopressin directly regulates cyst growth in polycystic kidney disease. *Journal of the American Society of Nephrology : JASN*, 19(1), pp.102–108.

Wann, A.K.T. & Knight, M.M., 2012. Primary cilia elongation in response to interleukin-1 mediates the inflammatory response. *Cellular and Molecular Life Sciences*, 69(17), pp.2967–

2977.

Ward, H.H., Brown-Glaberman, U., Wang, J., Morita, Y., Alper, S.L., Bedrick, E.J., Gattone, V.H., Deretic, D. & Wandinger-Ness, A., 2011. A conserved signal and GTPase complex are required for the ciliary transport of polycystin-1. *Molecular biology of the cell*, 22(18), pp.3289–305.

Waschek, J.A., Dicicco-Bloom, E., Nicot, A. & Lelievre, V., 2006. Hedgehog signaling: New targets for GPCRs coupled to cAMP and protein kinase A. In *Annals of the New York Academy of Sciences*. pp. 120–128.

Washburn, M.P., Wolters, D. & Yates, J.R., 2001. Large-scale analysis of the yeast proteome by multidimensional protein identification technology. *Nature biotechnology*, 19(3), pp.242–7.

Webster, D.R., Gundersen, G.G., Bulinski, J.C. & Borisy, G.G., 1987. Assembly and turnover of detyrosinated tubulin in vivo. *Journal of Cell Biology*, 105(1), pp.265–276.

Wegner, A. & Isenberg, G., 1983. 12-fold difference between the critical monomer concentrations of the two ends of actin filaments in physiological salt conditions. *Proceedings of the National Academy of Sciences of the United States of America*, 80(16), pp.4922–5.

Weimbs, T., 2007. Polycystic kidney disease and renal injury repair: common pathways, fluid flow, and the function of polycystin-1. *American journal of physiology. Renal physiology*, 293(5), pp.F1423–F1432.

Weiner, O.D., 2002. Regulation of cell polarity during eukaryotic chemotaxis: The chemotactic compass. *Current Opinion in Cell Biology*, 14(2), pp.196–202.

Weiner, O.D., Neilsen, P.O., Prestwich, G.D., Kirschner, M.W., Cantley, L.C. & Bourne, H.R., 2002. A PtdInsP(3)- and Rho GTPase-mediated positive feedback loop regulates neutrophil polarity. *Nature cell biology*, 4(7), pp.509–513.

Wennström, S., Hawkins, P., Cooke, F., Hara, K., Yonezawa, K., Kasuga, M., Jackson, T., Claesson-Welsh, L. & Stephens, L., 1994. Activation of phosphoinositide 3-kinase is required for PDGF-stimulated membrane ruffling. *Current Biology*, 4(5), pp.385–393.

Werner, M.E., Ward, H.H., Phillips, C.L., Miller, C., Gattone, V.H. & Bacallao, R.L., 2013. Inversin modulates the cortical actin network during mitosis. *American journal of physiology. Cell physiology*, 305(1), pp.C36–47.

Wheatley, D., 1995. Primary cilia in normal and pathological tissues. *Pathobiology*, 63(4), pp.222–238.

Wheway, G., Schmidts, M., Mans, D.A., Szymanska, K., Nguyen, T.-M.T., Johnson, C.A., et al., 2015. An siRNA-based functional genomics screen for the identification of regulators of ciliogenesis and ciliopathy genes. *Nature Cell Biology*, 17(8), pp.1074–1087.

White, M.C. & Quarmby, L.M., 2008. The NIMA-family kinase, Nek1 affects the stability of centrosomes and ciliogenesis. *BMC Cell Biology*, 9(1), p.29.

Williamson, S.M., Silva, D.A., Richey, E. & Qin, H., 2012. Probing the role of IFT particle complex A and B in flagellar entry and exit of IFT-dynein in Chlamydomonas. *Protoplasma*, 249(3), pp.851–856.

Wilson, P.D., 2001. Polycystin: new aspects of structure, function, and regulation. *Journal of the American Society of Nephrology : JASN*, 12(4), pp.834–845.

Wodarczyk, C., Distefano, G., Rowe, I., Gaetani, M., Bricoli, B., Muorah, M., Spitaleri, A., Mannella, V., Ricchiuto, P., Pema, M., Castelli, M., Casanova, A.E., Mollica, L., Banzi, M., Boca, M., Antignac, C., Saunier, S., Musco, G. & Boletta, A., 2010. Nephrocystin-1 forms a complex with polycystin-1 via a polyproline Motif/SH3 domain interaction and regulates the apoptotic response in mammals. *PLoS ONE*, 5(9).

Wojnacki, J., Quassollo, G., Marzolo, M.-P. & Cáceres, A., 2014. Rho GTPases at the crossroad of signaling networks in mammals: Impact of Rho-GTPases on microtubule organization and dynamics. *Small GTPases*, 5(March), p.e28430.

Wolf, M.T.F., 2015. Nephronophthisis and related syndromes. *Current Opinion in Pediatrics*, 27(2), pp.201–211.

Wolf, M.T.F. & Hildebrandt, F., 2011. Nephronophthisis. *Pediatric nephrology (Berlin, Germany)*, 26(2), pp.181–94.

Wolf, M.T.F., Lee, J., Panther, F., Otto, E.A., Guan, K.-L. & Hildebrandt, F., 2005. Expression and phenotype analysis of the nephrocystin-1 and nephrocystin-4 homologs in Caenorhabditis elegans. *Journal of the American Society of Nephrology : JASN*, 16(3), pp.676–87.

Wynshaw-Boris, A., 2012. Dishevelled: In Vivo Roles of a Multifunctional Gene Family During Development. *Current Topics in Developmental Biology*, 101, pp.213–235.

Xu, C., Rossetti, S., Jiang, L., Harris, P.C., Brown-Glaberman, U., Wandinger-Ness, A., Bacallao, R. & Alper, S.L., 2007. Human ADPKD primary cyst epithelial cells with a novel, single codon deletion in the PKD1 gene exhibit defective ciliary polycystin localization and loss of flow-induced Ca2+ signaling. *American journal of physiology. Renal physiology*, 292(3), pp.F930–45.

Xu, G.M., Sikaneta, T., Sullivan, B.M., Zhang, Q., Andreucci, M., Stehle, T., Drummond, I. & Arnaout, M.A., 2001. Polycystin-1 Interacts with Intermediate Filaments. *Journal of Biological Chemistry*, 276(49), pp.46544–46552.

Xu, S., Zhang, Z., Ogawa, O., Yoshikawa, T., Sakamoto, H., Shibasaki, N., Goto, T., Wang, L. & Terada, N., 2014. An EP4 Antagonist ONO-AE3-208 Suppresses Cell Invasion, Migration, and Metastasis of Prostate Cancer. *Cell Biochemistry and Biophysics*, 70(1), pp.521–527.

Xu, Y., Streets, A.J., Hounslow, A.M., Tran, U., Jean-Alphonse, F., Needham, A.J., Vilardaga, J.-P., Wessely, O., Williamson, M.P. & Ong, A.C.M., 2015. The Polycystin-1,

Lipoxygenase, and α-Toxin Domain Regulates Polycystin-1 Trafficking. *Journal of the American Society of Nephrology : JASN*, pp.1–15.

Yamaguchi, T., Hempson, S.J., Reif, G.A., Hedge, A.-M. & Wallace, D.P., 2006. Calcium restores a normal proliferation phenotype in human polycystic kidney disease epithelial cells. *Journal of the American Society of Nephrology : JASN*, 17(1), pp.178–87.

Yamaguchi, T., Pelling, J.C., Ramaswamy, N.T., Eppler, J.W., Wallace, D.P., Nagao, S., Rome, L. a, Sullivan, L.P. & Grantham, J.J., 2000. cAMP stimulates the in vitro proliferation of renal cyst epithelial cells by activating the extracellular signal-regulated kinase pathway. *Kidney international*, 57(4), pp.1460–1471.

Yamaguchi, T., Wallace, D.P., Magenheimer, B.S., Hempson, S.J., Grantham, J.J. & Calvet, J.P., 2004. Calcium restriction allows cAMP activation of the B-Raf/ERK pathway, switching cells to a cAMP-dependent growth-stimulated phenotype. *Journal of Biological Chemistry*, 279(39), pp.40419–40430.

Yan, X. & Zhu, X., 2013. Branched F-actin as a negative regulator of cilia formation. *Experimental Cell Research*, 319(2), pp.147–151.

Yao, G., Su, X., Nguyen, V., Roberts, K., Li, X., Takakura, A., Plomann, M. & Zhou, J., 2014. Polycystin-1 regulates actin cytoskeleton organization and directional cell migration through a novel PC1-pacsin 2-N-wasp complex. *Human Molecular Genetics*, 23(10), pp.2769–2779.

Yoder, B.K., 2007. Role of primary cilia in the pathogenesis of polycystic kidney disease. *Journal of the American Society of Nephrology : JASN*, 18(5), pp.1381–1388.

Yoder, B.K., Tousson, A., Millican, L., Wu, J.H., Bugg, C.E., Schafer, J. a & Balkovetz, D.F., 2002. Polaris, a protein disrupted in orpk mutant mice, is required for assembly of renal cilium. *American journal of physiology. Renal physiology*, 282(3), pp.F541–52.

Yoshiba, S., Shiratori, H., Kuo, I.Y., Kawasumi, A., Shinohara, K., Nonaka, S., Asai, Y., Sasaki, G., Belo, J.A., Sasaki, H., Nakai, J., Dworniczak, B., Ehrlich, B.E., Pennekamp, P. & Hamada, H., 2012. Cilia at the node of mouse embryos sense fluid flow for left-right determination via Pkd2. *Science (New York, N.Y.)*, 338(6104), pp.226–31.

Yoshimura, S.I., Egerer, J., Fuchs, E., Haas, A.K. & Barr, F.A., 2007. Functional dissection of Rab GTPases involved in primary cilium formation. *Journal of Cell Biology*, 178(3), pp.363–369.

Yu, F., Ran, J. & Zhou, J., 2016. Ciliopathies: Does HDAC6 Represent a New Therapeutic Target? *Trends in Pharmacological Sciences*, 37(2), pp.114–119.

Yuan, S., Li, J., Diener, D., Choma, M., Rosenbaum, J., Suna, Z. 2012. Target-of-rapamycin complex 1 (Torc1) signalling modulates cilia size and function through protein synthesis regulation. Proc Natl Acad Sci U S A; 109(6): 2021–2026.

Zalli, D., Bayliss, R. & Fry, A.M., 2012. The Nek8 protein kinase, mutated in the human cystic

kidney disease nephronophthisis, is both activated and degraded during ciliogenesis. *Human Molecular Genetics*, 21(5), pp.1155–1171.

Zatti, A., Chauvet, V., Rajendran, V., Kimura, T., Pagel, P. & Caplan, M.J., 2005. The C-terminal tail of the polycystin-1 protein interacts with the Na,K-ATPase alpha-subunit. *Mol.Biol.Cell*, 16(1059-1524 (Print)), pp.5087–5093.

Zhang, J. & Wang, J.H.C., 2014. Prostaglandin E2 (PGE2) exerts biphasic effects on human tendon stem cells. *PLoS ONE*, 9(2).

Zheleznova, N.N., Wilson, P.D. & Staruschenko, A., 2011. Epidermal growth factor-mediated proliferation and sodium transport in normal and PKD epithelial cells. *Biochimica et Biophysica Acta - Molecular Basis of Disease*, 1812(10), pp.1301–1313.

Zhou, J., 2009. Polycystins and primary cilia: primers for cell cycle progression. *Annual review of physiology*, 71, pp.83–113.

Zhou, W., Dai, J., Attanasio, M. & Hildebrandt, F., 2010. Nephrocystin-3 is required for ciliary function in zebrafish embryos. *American journal of physiology. Renal physiology*, 299(1), pp.F55–62.